University of Southampton Research Repository

UNIVERSITY OF SOUTHAMPTON

Faculty of Medicine

Bone and Joint Research Group

The use of synthetic clay to enhance fracture healing and bone regeneration

by

David Mark Richard Gibbs

Thesis for the degree of Doctor of Philosophy

March 2016

UNIVERSITY OF SOUTHAMPTON

<u>ABSTRACT</u>

FACULTY OF MEDICINE

<u>Doctor of Philosophy</u>

Thesis for the degree of Doctor of Philosophy

THE USE OF SYNTHETIC CLAY TO ENHANCE FRACTURE HEALING AND BONE REGENERATION

David Mark Richard Gibbs

Fractures are extremely common and can take months to heal. Bone graft material is used to stimulate healing and fill voids in reconstructive surgery. Bone Morphogenetic Protein (BMP) has been used clinically to stimulate fracture healing and arthrodesis; however inefficient delivery methods necessitated the use of high doses which resulted in significant side effects. Materials currently used for bone grafting such as: autograft, allograft and synthetic bone products all have significant limitations. These studies have investigated the ability of Laponite, a synthetic clay, to facilitate growth factor delivery to enhance fracture healing and improve the osteogenicity of graft material produced using additive manufacture. Initial studies culturing cells with Laponite demonstrated the biocompatibility of this material. Subsequently, the ability of Laponite to deliver and localise active growth factor was shown using Human Umbilical Vein Endothelial Cells and Myoblast cell cultures. Feasibility of combining Laponite with Additive Manufacturing techniques to produce bone graft material was assessed *in vitro*. In murine studies Laponite was observed to enhance the osteogenic effect of BMP applied to allograft and, furthermore, reduce the dose of BMP required to mediate ectopic bone formation within collagen sponge. Finally, in an ovine femoral defect Laponite was observed to convey active BMP. The *in vitro* and *in vivo* evidence for the ability of Laponite to deliver BMP presented in this thesis demonstrates the exciting potential of Laponite to accelerate fracture healing and enhance the osteogenicity of graft material.

Table of Contents

List of Tables

List of Figures

List of Accompanying Materials

DECLARATION OF AUTHORSHIP

I, David Mark Richard Gibbs declare that this thesis and the work presented in it are my own and has been generated by me as the result of my own original research.

The use of synthetic clay to enhance fracture healing and bone regeneration.

I confirm that:

1. This work was done wholly or mainly while in candidature for a research degree at this University;

2. Where any part of this thesis has previously been submitted for a degree or any other qualification at this University or any other institution, this has been clearly stated;

3. Where I have consulted the published work of others, this is always clearly attributed;

4. Where I have quoted from the work of others, the source is always given. With the exception of such quotations, this thesis is entirely my own work;

5. I have acknowledged all main sources of help;

6. Where the thesis is based on work done by myself jointly with others, I have made clear exactly what was done by others and what I have contributed myself;

7. Parts of this work have been published as:

    Gibbs, D. M., Black, C. R., Dawson, J. I. & Oreffo, R. O. (2014a). A review of hydrogel use in fracture healing and bone regeneration. Journal of Tissue Engineering and Regenerative Medicine.

    Gibbs, D. M. R., Vaezi, M., Yang, S. & Oreffo, Richard O. (2014b). Hope versus hype: what can additive manufacturing realistically offer trauma and orthopaedic surgery? Regenerative Medicine, 9, 535-549.

Signed...

Date:...

Acknowledgements

I am extremely grateful to my supervisors Richard Oreffo and Jonathon Dawson.

I wish to acknowledge some specific technical assistance, in particular: Help with Cell Profiler software from Jonathon Dawson, and assistance with the *in vivo* studies from Dr Janos Kanczler and Cameron Black. I also wish to acknowledge the critical help I was given with the micro CT work from Gry Hulsart-Billstrom. Some of the microscopy of the histological sections was performed by Julia Wells.

I am very grateful for training in tissue culture from Kate White, Julia Wells and Steph Inglis.

I also wish to thank my wife Lucy Bailey for her continuing support.

Definitions and Abbreviations

AM	Additive Manufacture (encompassing all types of 3D printing)
ALP	Alkaline Phosphatase
A/S	Alcian Blue and Sirius Red Staining
BMP	Bone Morphogenetic Protein
BRF	Biomedical Research Facility
CPC	Calcium phosphate cement
DBM	Demineralised bone matrix
DMSO	Dimethyl sulfoxide
ECM	Extracellular matrix
FDM	Fused deposition modelling
FGFR	Fibroblast Growth Factor Receptor
GF	Growth factor
HA	Hydroxyapatite
HBMSC	Human Bone Marrow Stromal Cells
HUVEC	Human Umbilical Vein Endothelial Cell
IGF-1	Insulin like Growth Factor -1
IHH	Indian Hedgehog
IL	Interleukin
Megagen	Synthetic bone product derived from biphasic Calcium Phosphate,
OPG	Osteoprotegerin
PEG	Polyethylene glycol
PDGF	Platelet Derived Growth Factor
PHA	Precipitated Hydroxyapatite
PLA	Poly (lactic-co-glycolic acid)
PRP	Platelet Rich Plasma
PTHrP	Parathyroid hormone-related protein
RANKL	Receptor activator of nuclear factor kappa-B ligand
RUNX2	Runt-related transcription factor 2
ROI	Regions of Interest (Area selected on CT images for quantitative analysis)
SMAD	Intracellular mediator of cell surface serine/threonine kinase receptors
Smo	Membrane protein smoothened
SDF	Sideroblastic Growth Factor
TGF	Transforming Growth Factor Beta
TNF	Tumour Necrosis Factor

TRAP   Tartrate-resistant acid phosphatase

UoS   University of Southampton

VEGF   Vascular Endothelial Derived Growth Factor

Chapter 1: Introduction

Portions of this chapter have been published previously in:

Gibbs, D. M., Black, C. R., Dawson, J. I. & Oreffo, R. O. (2014a). A review of hydrogel use in fracture healing and bone regeneration. Journal of Tissue Engineering and Regenerative Medicine.

Gibbs, D. M. R., Vaezi, M., Yang, S. & Oreffo, Richard O. (2014b). Hope versus hype: what can additive manufacturing realistically offer trauma and orthopaedic surgery? Regenerative Medicine, 9, 535-549.

Black, C.R., Goriainov V., Gibbs D., Kanczler J., Tare R.S., Oreffo R.O.
Bone Tissue Engineering. Current Molecular Bology Reports,

2015;1(3):132-140.

1.1   Fractures and bone grafting: clinical need

Every year over 2 million people in the UK suffer a fracture (van Staa et al., 2001). While the majority of fractures heal uneventfully, patients typically require a minimum of 7 and 16 weeks off work following ankle and tibial fractures respectively (Egol et al., 2000, Hooper et al., 1991). In high energy tibial fractures up to 40% will not heal (Lack et al., 2014). Worldwide over 2.2 million bone graft procedures are performed annually (Van der Stok et al., 2011). Bone grafting is applied to fulfil distinct clinical requirements, in a wide range of procedures which include:

> i) Application at the site of non-union to stimulate healing
>
> ii) As a void filler to facilitate reconstruction in the case of peri-articular fracture
>
> ii) To stimulate fusion in spinal or joint arthrodesis
>
> iv) As a mechanical and biological construct in regeneration of segmental bone
> defects arising from trauma, neoplasia, or infection.

The ideal or indeed essential properties of graft material are entirely dependent upon the clinical situation in which the graft material is deployed.
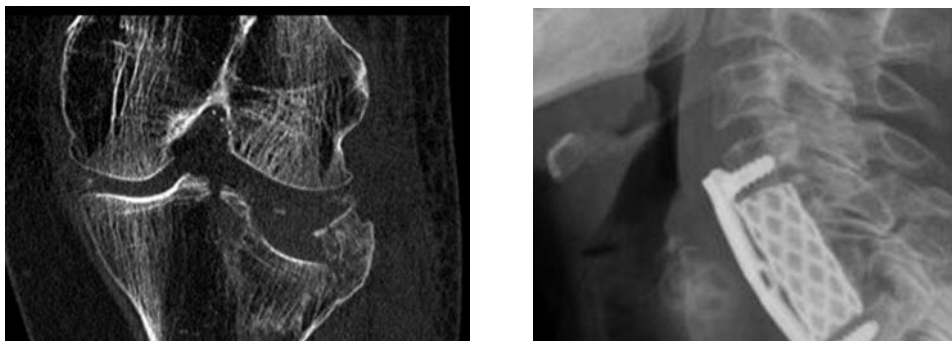
Figure 1-1 Images of clinical scenarios requiring treatment with bone graft

(Left) Coronal CT image of the proximal tibia demonstrating a fracture likely to require bone graft. (Right) Lateral radiograph of the cervical spine showing a cage fusion device containing autologous bone graft, taken from (Coughlin and Klezl 2013).

1.2 Functions of bone

Bone has mechanical, metabolic, and haematopoietic functions (Oryan et al., 2015). The biomechanical properties of bone provide protection from trauma to other organ systems, and in combination with muscles permit locomotion. The vast majority of the body's available calcium is stored in bone. Bone cells are able to respond to endocrine signalling and sequester or release calcium as required. This process is able to achieve tight control of intravascular calcium, which is vital to all cellular functions. Red bone marrow, which resides inside the bone, is responsible for the production of erythrocytes, leukocytes, and platelets, with the surrounding bone providing protection, and facilitating controlled access to the vascular compartment.

1.3 Structure of bone

The term bone refers to a range of materials (cancellous, cortical and woven bone), which share in common the same repeating unit, the mineralised collagen fibre, which, through multiple hierarchical levels of organisation, gives rise to diverse structures and correspondingly diverse biomechanical properties as shown in Figure 1-2 (Weiner and Wagner, 1998). Type 1 collagen is a triple helix arrangement of $2\alpha_1$ and $1\alpha_2$ which produces a fibril 1.5nm thick, with adjacent fibres packed together in a staggered arrangement. Carbonated apatite ($Ca_5 PO_4 CO_3)_3(OH)$ crystals form in layers on the fibrils. In addition to collagen and apatite, water also constitutes a major component of bone, and mechanical properties of wet bone differ substantially from those of dry bone. It is noteworthy that composite materials are commonly used in the field of engineering, for example; steel reinforced concrete, in which compressive and tensile strength are provided by the concrete and steel respectively. Thus bone can be described as a highly specialised composite material in which collagen and mineral components provide tensile and compressive strength respectively. Bones are surrounded by fibrous tissue, periosteum, which is composed of an outer fibrous layer, contributing to structural integrity, and an inner cambium layer that possesses osteogenic potential.
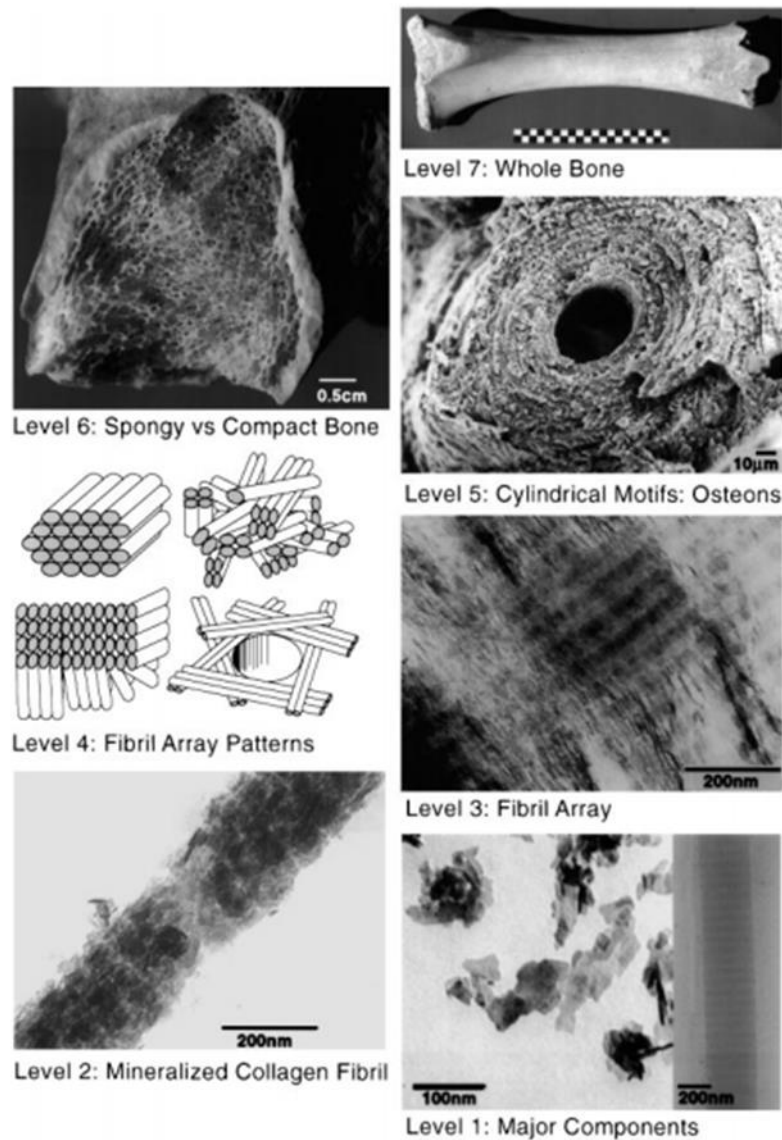
Figure 1-2 Multiple hierarchical levels of organisation observed in bone

(Weiner and Wagner, 1998)

Level 1: Un-mineralised collagen fibrils and isolated crystals under light microscopy.

Level 2: Electron microscopy of a mineralised collagen fibril from a Turkey tendon

Level 3: Electron microscopy of mineralised Turkey tendon, demonstrating array of fibrils.

Level 4: Diagram of the variety of fibril array patterns.

Level 5: Electron microscopy of a single osteon from human bone

Level: 6: Light microscopy of a fossilised human femur demonstrating cortical and cancellous bone.

Level 7: Arrangement of cortical and cancellous bone to produce an entire bovine femur.

Lamellae bone comprises groups of parallel fibres, lamellae. Fibres in adjacent lamellae run at oblique angles to each other, and apatite crystals in between the lamellae are sequentially rotated (Weiner and Wagner, 1998). In cortical bone, these lamellae are arranged in concentric rings, parallel to the long axis of the bone, around a central vascular channel, known as the Haversian canal, with the entire unit referred to as an osteon or Haversian system. Cancellous bone is found in the metaphysis and epiphyses of long bones, and centrally in cuboid bones, cancellous bone is composed of parallel sheets of lamellae, but lacks a Haversian system.

In common with other organs, the vast majority of bone comprises matrix (90%) combined with a minority of cells (10%). Type 1 collagen represents the most abundant protein in bone, however a number of other proteins such as: osteocalcin, osteonectin, osteopontin, bone sialoprotein 2, decorin, bioglycan and fibronectin are also present (Sroga et al., 2011). While the exact function of these non-collagenous proteins is not completely understood, these proteins are likely to contribute both directly to the mechanical properties of the bone, and to modulate growth factor activity through various binding sites. As Hynes described: "The Extracellular matrix is not just pretty fibrils" (Hynes, 2009), this is clearly the case in bone, where, for example, deficiency of osteopontin was observed to result in a 30% decrease in toughness (Thurner et al., 2010), and decorin has been shown to bind TGF-ß and enhance its activity (Takeuchi et al., 1994).
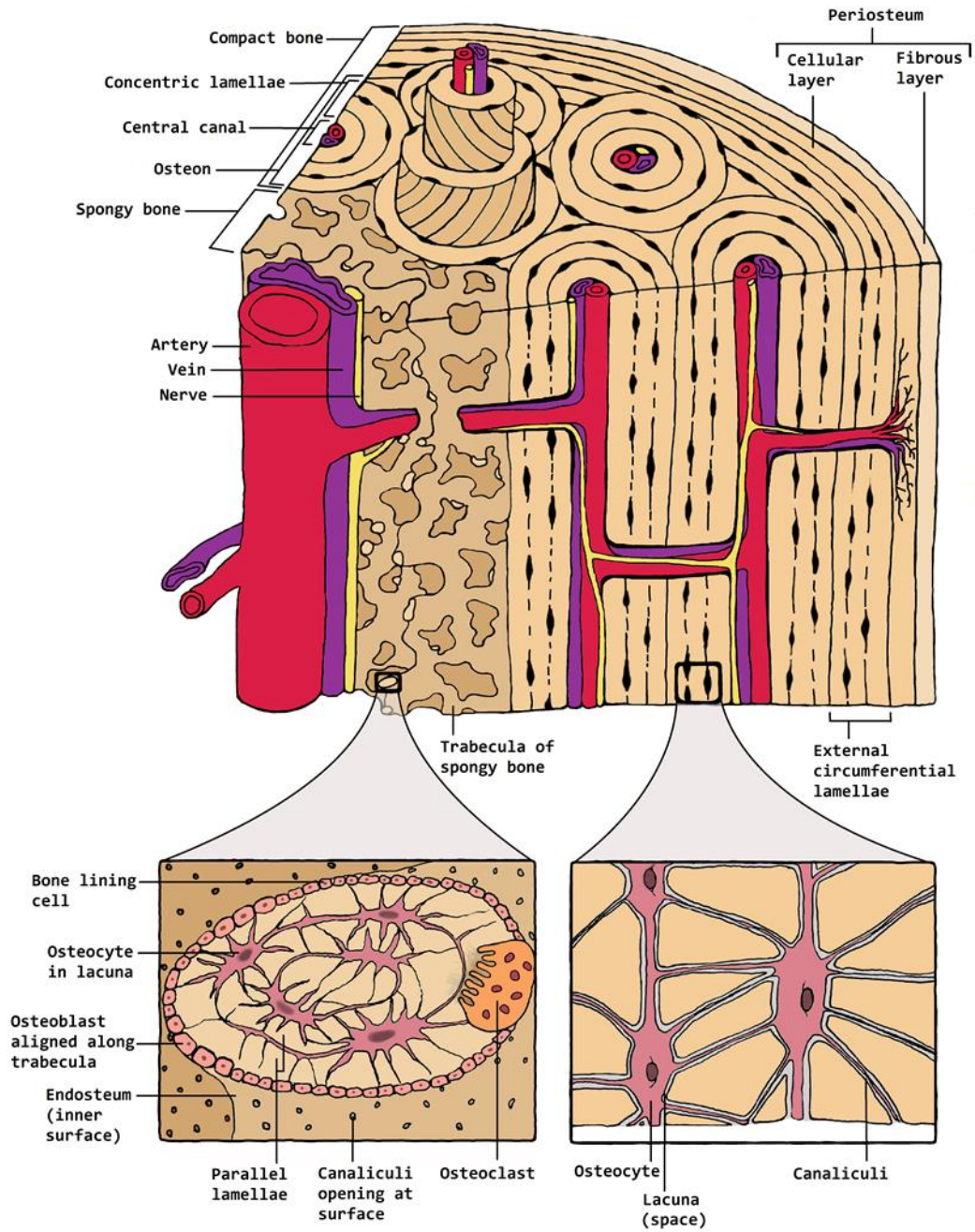
Figure 1-3 Structure of bone

(Courtesy of Gry Hulsart-Billstrom; Bone and Joint Research Group, UoS)

Arrangement of lamellae in spongy (cancellous) bone and compact (cortical) bone is shown. Osteons are present only in cortical bone cell biology.

1.4   Bone cell biology

Bone marrow refers to the tissue found in the medulla of bones. This specialised tissue is categorised into red marrow parenchyma, from which haemocytoblast cells (haematopoietic stem cells) are produced, and stroma from which bone cells are derived. Within the red marrow, the haemocytoblasts produce pro-erythroblasts, myloblasts, lymphoblasts, monoblasts, and megakaryocytes, which subsequently, produce the red cells, white cells and platelets found in blood as shown in Figure 1-4.
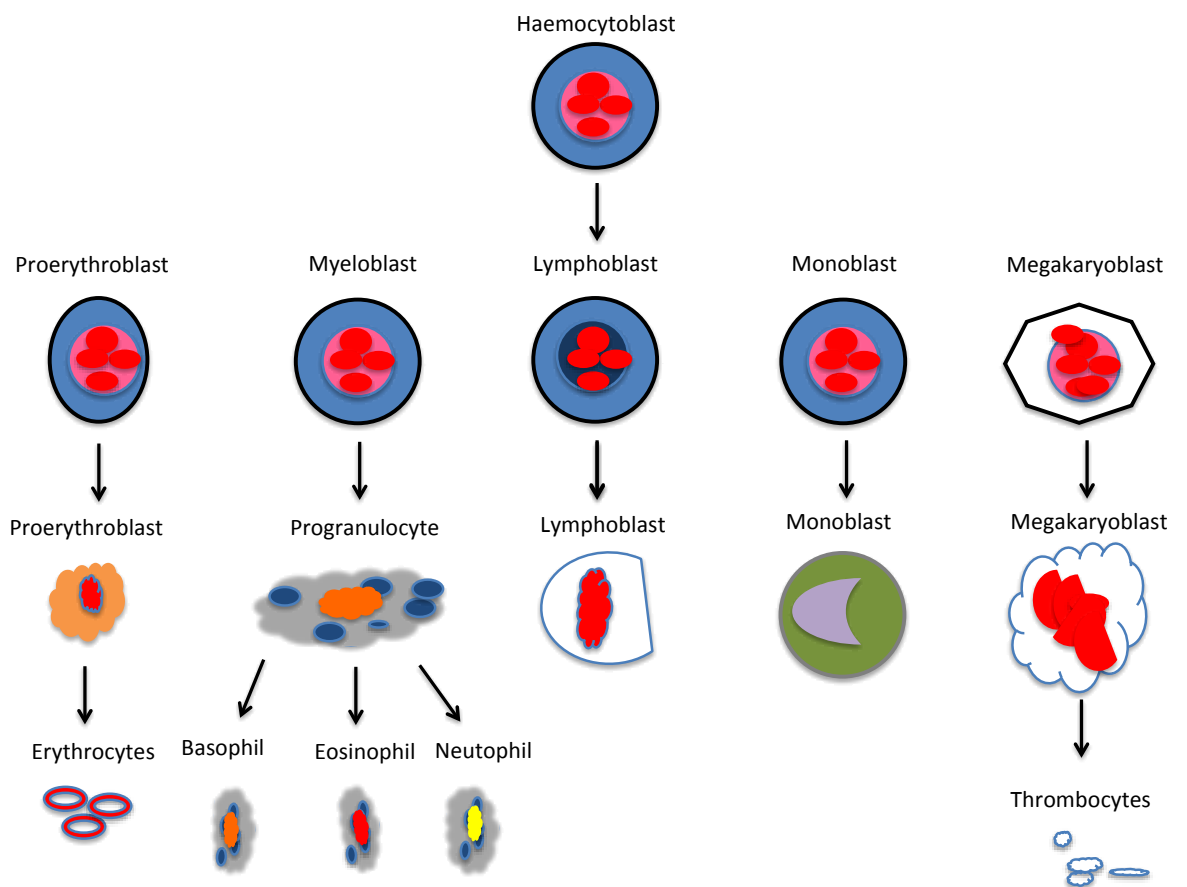
Figure 1-4 Haematopoiesis

Mesenchymal stem cells, from which bone cells are derived, are included in the heterogeneous fraction of cells separated from haematopoietic cells by their capacity to adhere to plastic. This was first described almost four decades ago in the former USSR by Friedenstein, as described by Bianco (Bianco et al., 2008). Friedenstein observed that a group of cells, derived from bone marrow,

adhered to filter material in a diffusion chamber, and subsequently formed osteogenic tissue. Following these early findings, the use of plastic adherence to select a population of cells from marrow, within which a subset were capable of maintaining a normal karyotype, and telomerase activity even up to passage 12 has been described (Pittenger et al., 1999). Furthermore, this subset of cells were capable of adipogenic, chondrogenic and osteogenic differentiation (stromal lineages) upon exposure to lineage specific culture conditions (Pittenger et al., 1999). Given the properties of clonal expansion, and multi-lineage capacity, this sub population of plastic adherent cells were termed mesenchymal stem cells by Caplan (Caplan, 1991). Simmons (Simmons and Torok-Storb, 1991) demonstrated that the subpopulation of stromal cell precursors could be enriched with the use of murine IgM monoclonal antibody STRO-1. The nature of the STRO-1 antigen remains undetermined, furthermore, the sub group of cells exhibiting STRO-1 remains heterogeneous, including non-mesenchymal stem cells such as fibroblasts, smooth muscle cells, and some cells incapable of clonal expansion. The ability to select a more homogenous population of mesenchymal stem cells has improved with selection of cells expressing greater quantities of STRO-1, termed STRO bright, and expression of Vascular Cell Adhesion Molecule (VCAM) (Gronthos et al., 2003).

For a number of decades the general perception was that osteogenic precursor cells were derived from a component of the bone marrow stroma, more recently some have speculated (Medici et al., 2010, Sacchetti et al., 2007) that the osteogenic precursors cells may originate from perivascular cells within the bone marrow stroma.

The use of the term mesenchymal stem cell implies that the cell is capable of differentiation into all cells derived from the mesenchyme, i.e. not just adipocytes, chondrocytes and osteoblasts, but also tenocytes, cardiac and smooth muscle myocytes. Such multi-lineage capacity has never been demonstrated *in vivo*, from this cell population, hence it has been suggested that the term bone marrow stromal cells (HBMSC) would be more appropriate (Bianco et al., 2008), and therefore is the term used in this thesis.

Osteoblasts are the cells that make bone and are responsible for the synthesis and secretion of the extracellular matrix of bone; this consists predominantly of type 1 collagen, and smaller quantities of osteocalcin, matrix gla protein, osteopontin, and bone sialoprotein (Huang et al., 2007). In addition to the matrix, osteoblasts also secrete growth factors, including Bone Morphogenetic Protein (BMP) and Transforming Growth Factor Beta (TGF-ß). Early markers of osteoblastogenesis include

expression of: Alkaline Phosphatase (ALP), type 1 collagen, osteopontin, and bone sialoprotein; while osteocalcin and parathyroid protein receptor represent late markers. Formation of osteoblasts, osteoblastogenesis, is governed by the interaction of the stimulatory factors TGF- ß, BMP-2, 4 and 7, and the presence of their inhibitors noggin, chordin, gremlin and sclerostin. Deficiency of sclerostin of is manifested clinically as sclerosteosis, a rare autosomal dominant disease in which progressive bone thickening is seen. Transcription factors which are critical for osteoblast differentiation and thus function include Runt-related transcription factor 2 (RUNX 2), osterix, and activated transcription factor 4. Osteoblasts may become encased in matrix and become Osteocytes. These cells are thought to pivotal in transducing the effect of mechanical stimulation on bone formation, a phenomenon described by Julius Wolff in 1892, and confirmed by recent *in vivo* work (Barak et al., 2011).

Osteoclasts are derived from myeloid progenitor cells under the influence of factors such as macrophage colony stimulating factor and Receptor activator nuclear factor kappa-B (RANKL) (Boyce, 2013) as depicted in figure 1-7. Signalling pathways governing osteoclast activation and inhibition are complex, with mediators including Osteoprotegerin and RANKL (Boyce, 2013) which are discussed in 1-6. Upon stimulation osteoclasts become polarised, a ruffled membrane is directed towards the bone matrix forming a compartment, which is acidified by ATPase proton pumps located within the membrane (Mattsson et al., 1997). This acidified environment dissolves Hydroxyapatite, the inorganic component of bone, subsequently proteolytic enzymes breakdown the organic bone matrix.

Chondrocytes are derived from bone marrow stromal cells; they are responsible for the secretion of various components of the extracellular matrix of cartilage, such as type 2 collagen, aggregan, glyconaminoglycan, hyaluronan, and growth factors such as Indian Hedgehog, BMP and FGF. The process of endochondral ossification is primarily orchestrated by chondrocytes.

1.5   Bone embryogenesis

During embryogenesis, limbs are derived from buds, which consist of a layer of ectoderm covering an underlying mesoderm, which form somite and the lateral mesodermal plate. Somite material later forms skeletal muscle, while the lateral mesodermal plate forms bone and connective tissue. Bone is derived from the mesoderm through a transitional process of: condensation, chondrofication, segmentation, and finally ossification, resulting in the bones of the limb; a process known as endochondral ossification. Formation of bones such as the skull and clavicle is achieved directly from transformation of mesenchymal condensation to bone, referred to as intramembranous ossification.

Ossification of the cartilage analogue of the long bones results from a primary ossification centre in the diaphysis, and secondary ossification centres in the epiphysis (Figure 1-5). Within the primary ossification centre a ring of periosteum undergoes intramembranous ossification to produce bone. At the epiphysis the secondary ossification centres undergo endochondral ossification to produce bone, and is it this process at the physis which results in longitudinal limb growth (Mackie et al., 2008). At skeletal maturity the cartilaginous growth plate between the ossification centres are replaced by bone, leaving only articular cartilage at the bone ends.
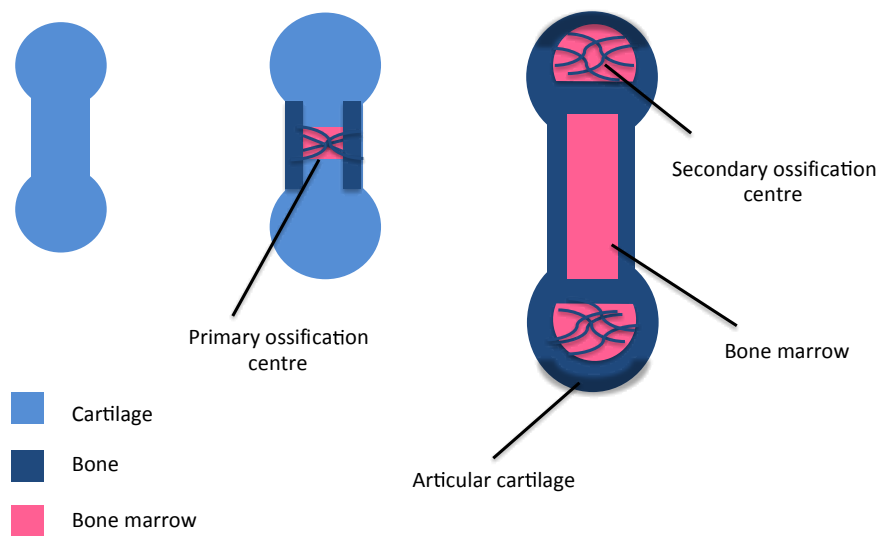
Figure 1-5 Endochondral bone formation

1.6   Signalling pathways in musculoskeletal tissue formation

Bone and cartilage formation in the embryo, and following birth, arises as a consequence of the controlled differentiation of bone marrow stromal cells, and the regulated temporal and spatial activity of the resulting progeny. The interaction involves at least six signalling pathways: Wnt, TGF-ß family, FGF, Indian hedgehog, Ephrin, and the Sympathetic system, with each other, and with components of the extracellular matrix, to determine if uncommitted progenitor cells become osteoblasts or chondrocytes, and the subsequent activity of the cells (Figure 1-6).
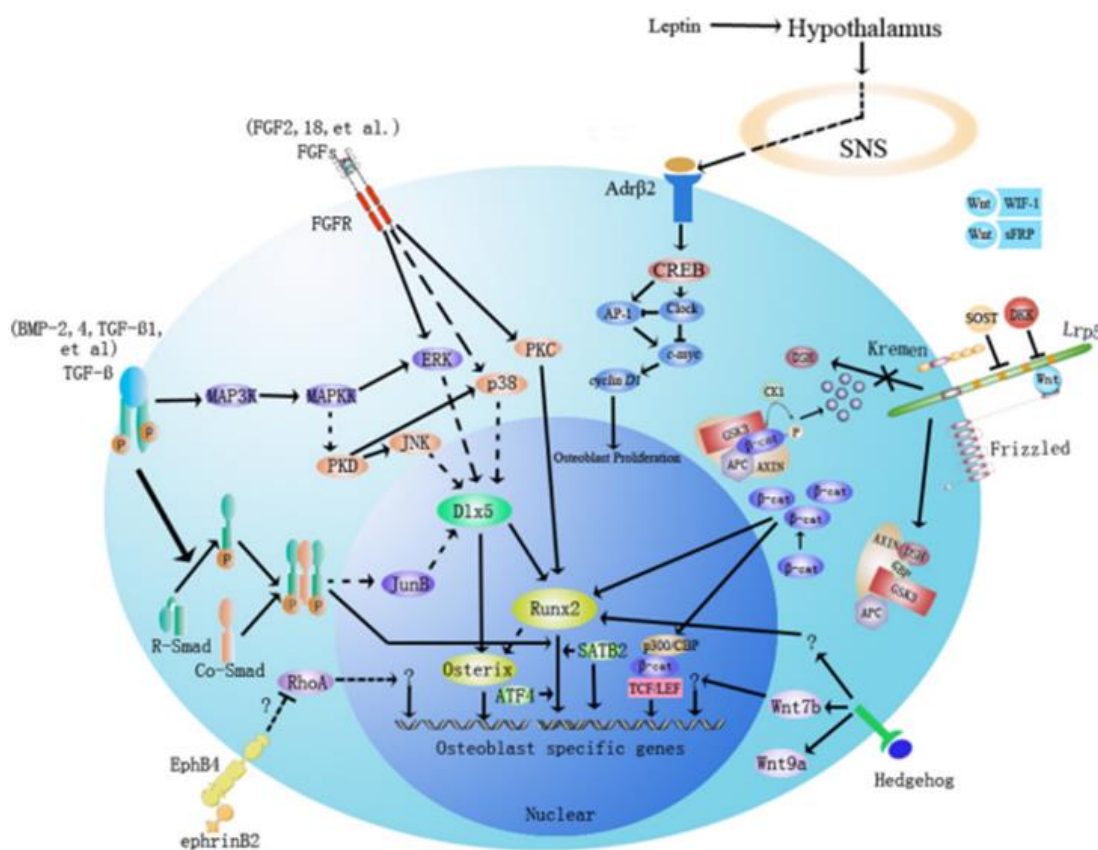
Figure 1-6 Signalling pathways determining osteoblast differentiation.

(Huang et al., 2007)

Wnt

Wnt refers to a family of 19 secreted proteins which bind to frizzled, a G-protein coupled receptor which is associated with low density lipoprotein receptors (LRP) 5 and 6. Sclerostin exerts an inhibitory effect on osteoblasts through an effect on the LRP 5 receptor. Wnt binding may result in an increase or decrease of ß-catenin depending on the interaction with the co-receptors. The

subsequent activation of transcription factors by ß-catenin induces osteoblastogenesis, and suppresses chondrogenesis in early osteochondroprogenitors (Day et al., 2005) as depicted in figure 1-7; and increases production of Osteoprotegerin (OPG), an inhibitor of osteoclast formation. In addition to ß-catenin signalling, referred to as canonical, Wnt also acts via an alternative, ß-catenin independent (non-canonical pathway) (Veeman et al., 2003). Wnt is known to be capable of stimulating chondrogenesis, although the exact mechanism through which this is achieved is uncertain (Mackie et al., 2008).
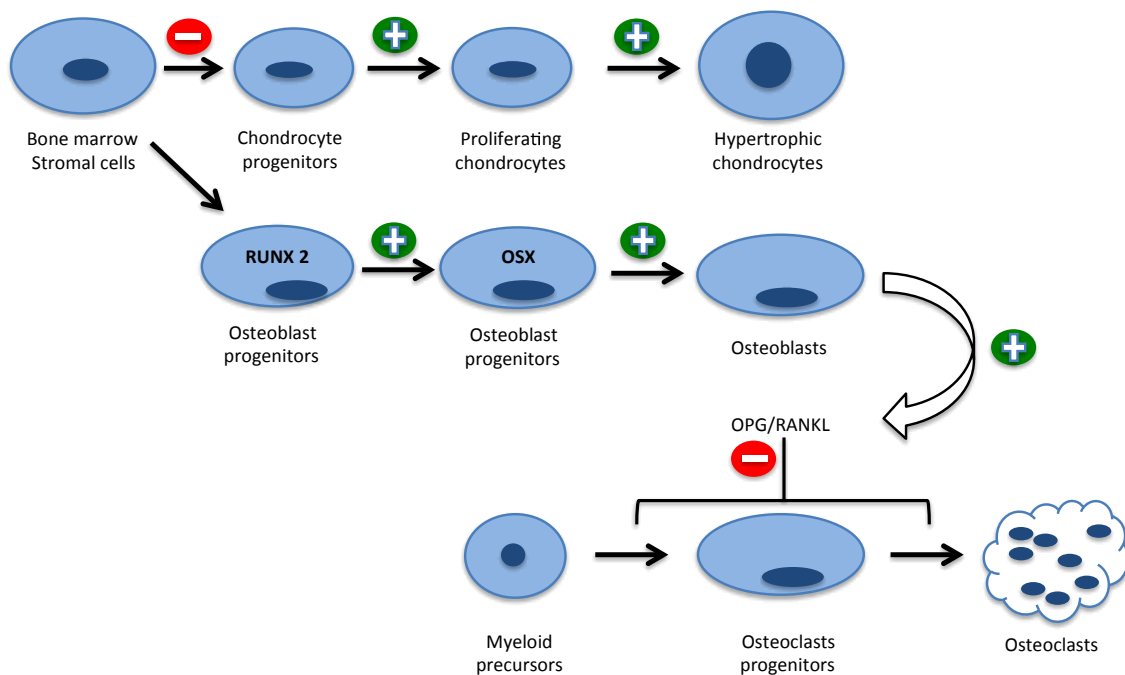
Figure 1-7 Effects of Wnt on differentiation of chondrocytes and osteoblasts

Adapted from (Liu et al., 2008). OPG = Osteoprotegerin, RANKL =Receptor activator of nuclear factor kappa-B ligand, OSX = Osterix. Green and red denote positive and inhibitory effects of WNT

TGF-ß

The TGF-ß superfamily includes at least twenty human types of BMP, of which eight (BMP-1-BMP8a) and TGF- ß have a known osteochondral function (Even et al., 2012). This family of growth factors has been shown to bind to serine/threonine kinase receptors, which activate a group of transcription factors known as SMAD and RUNX2. Of the more than twenty BMPs identified, only two (BMP-2 and BMP-7), are commercially available for clinical use in spinal arthrodesis and tibial non-union

respectively (Garrison et al., 2007). BMP-2 and BMP-7 have not been demonstrated to exhibit different effects in human studies; their application in different therapies is driven by commercial reasons and intellectual property.

Indian Hedgehog

Indian Hedgehog (IHH) is a protein which exerts its effects by binding to patched-1, a cell surface receptor which normally suppresses the membrane protein smoothened (Smo). Binding by IHH removes this inhibition, resulting in transcription of target genes.

FGF, Ephrin, and Sympathetic signalling

Fibroblast growth factors (FGF) are a family of polypeptides which exert their effect through four tyrosine kinase receptors, FGFR1-4, and are critical in the process of endochondral and intramembranous ossification. Ephrins mediate bidirectional signalling between osteoclasts and osteoblasts via Ephrin receptors and ligands. Little is known about the role of sympathetic signalling in osteogenesis; however osteoblasts express receptors for a number of neuropeptides, suggesting the ability to integrate neuronal signals.

1.7   Bone growth

At the physis, chondrocytes and matrix are organised into four specialised layers (resting, proliferative, hypertrophic, and zone of provisional calcification) and act in concert to achieve longitudinal growth (Figure 1-8).

Resting chondrocytes reside adjacent to the epiphysis, upon stimulation these cells proliferate, following proliferation, their secretory activity increases, and the cells separate as they secrete ECM around themselves. Proliferation is controlled by the balance of stimulatory factors such as Growth hormone, acting via Insulin like Growth Factor -1 (IGF-1), BMPs, and inhibitory factors mediated by FGF receptors. The dysfunction of these signalling systems are clinically manifest in gigantism and acromegaly seen in GH excess pre and post ossification respectively, and in achondroplasia, which results from a mutation in FGFR3. Critically, activity of signalling pathways such as IHH and FGF are modulated by components within the ECM, glycosaminoglycans. This is illustrated by dwarfism

observed in mice lacking the ability to desulphinate glycosaminoglycan, a state which can be rescued by crossing such mice with FGF18 null mice (Settembre et al., 2008).

Thyroid hormone appears to be critical in the regulation of chondrocyte hypertrophy, with hypothyroidism resulting in abnormalities in this process, the exact mechanism through which thyroid hormone exerts the effect remains uncertain. Following hypertrophy, the chondrocytes undergo cell death, and blood vessels, osteoclasts, and osteoblast invade, transform, and mineralise the tissue. This process mediated by the release of growth factors such as IHH, VEGF, as well as High-mobility group box protein 1 from the chondrocytes themselves.
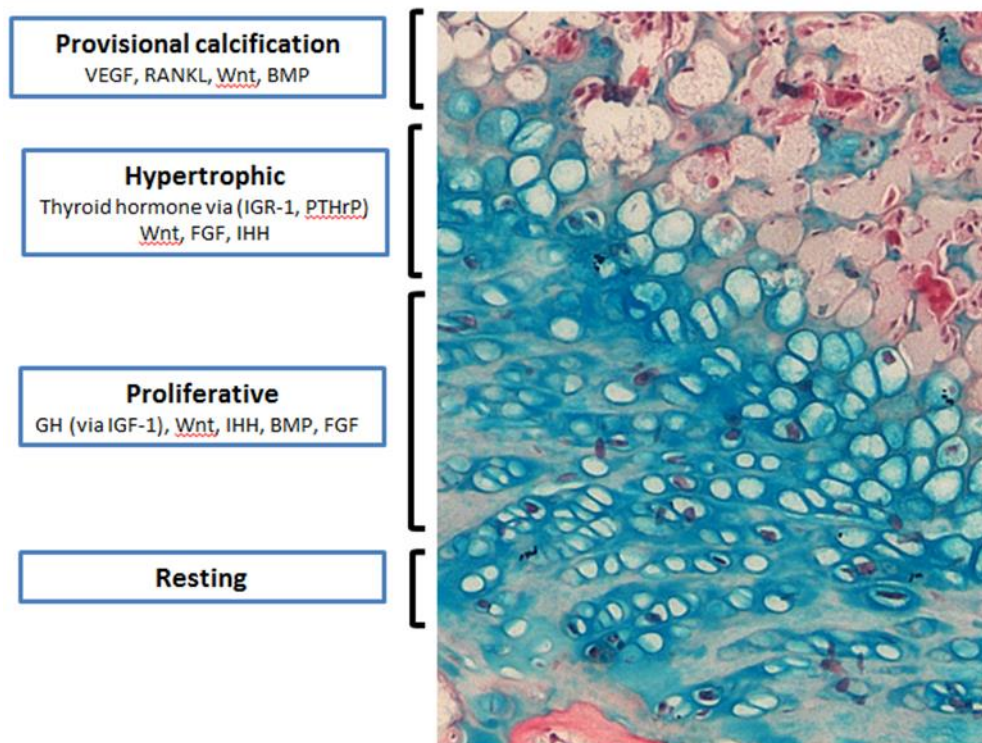
Figure 1-8 Physis

 (Courtesy of Dr Janos Kanczler, Bone and Joint Research Group, UoS)

 Histological section of physis from an 8 week old rat which stained with Tartrate-resistant acid phosphatase/Alcian blue/Haematoxylin. Annotations demonstrate on which layers of the physis hormones and cytokines exert their effect.   RANKL =Receptor activator of nuclear factor kappa-B ligand, PTHrP = Parathyroid hormone-related protein. IGR-1 =Insulin Growth Factor Receptor-1.

1.8   Fracture Healing

Fractures in which bone fragments are reduced anatomically and rigidly held may heal via primary healing, while secondary healing takes place when inter fragmentary motion is present.

Primary Fracture healing

Primary fracture healing, which is also referred to as direct cortical, osteonal or Haversian bone healing occurs only in conditions of absolute stability, typically following open reduction and internal fixation. Primary fracture healing maybe categorised into contact healing, in which the gap between bone fragments is 0.01mm and strain <2% (Shapiro, 1988), or gap healing in which the gap is less than 1mm (Kaderly, 1991). During contact healing cutting cones are formed, the tips of which comprise of osteoclasts, which cross the fracture line and generate longitudinal cavities. These cavities are later filled by bone produced from following osteoblasts. This process simultaneously results in bony union, and axially orientated Haversian systems (Kaderly, 1991). Gap healing differs from contact healing in that the initial lamellae formed are perpendicular to the longitudinal axis of the bone, requiring a secondary remodelling process to produce longitudinally orientated Haversian systems which are required to restore the mechanical properties of the bone.

Secondary fracture healing

Secondary fracture healing (healing via callus formation) occurs following treatment in a cast, or less rigid forms of operative management such as intra-medullary nailing or external fixation, and involves both endochondral and intramembranous ossification (Marsell and Einhorn, 2011). In secondary healing the quantity of movement between the bone fragments is critical, with excessive or absent movement resulting in hyper-tropic or atrophic non-union respectively (Green et al., 2004). Secondary fracture healing is a single continuous process, although, it may be conceptualised into four stages (see Figure 1-9):

> i) Acute inflammation with haematoma formation
>
> ii) Soft callus formation
>
> iii) Hard callus formation
>
> iv) Remodelling

Stage four, remodelling is analogous to primary fracture healing.

Immediately following fracture an acute inflammatory response is initiated which lasts for approximately one week, during this time a fibrin rich haematoma forms at the bone ends (Figure 1-9), and chemotactic and angiogenic factors such as TNF-α, IL: (1, 6, 11, 18), SDF-1 and BMP mediate angiogenesis and recruitment of bone marrow stromal cells. Whether these osteochondroprogenitors originate from local tissue, or a distant systemic site, and the exact function of the growth factors implicated, is incompletely understood (Granero-Moltó et al., 2009, Marsell and Einhorn, 2011).

Following the haematoma formation chondrocyte progenitors migrate, differentiate, and secrete type 2 procollagen and proteoglycan, this process peaks at approximately 7-10 days (Einhorn, 1998). Simultaneously, while this soft callus is formed, intra-membranous ossification occurs subperiosteally adjacent to the bone ends, resulting in formation of some hard callus.
After formation of a cartilage analogue at the fracture site, in a process analogous to endochondral bone formation in foetal development, the chondrocytes undergo hypertrophy, and cell death, whilst through the release of factors such as Wnt, they mediate osteoblast migration and mineralisation, resulting in woven bone (hard callus), as shown in Figure 1-9.

Bone remodelling commences some 3-4 weeks following fracture and may take years to complete. Axial loading stimulates the action of osteoclasts and osteoblasts to replace the isotropic woven bone with anisotropic lamellae bone.
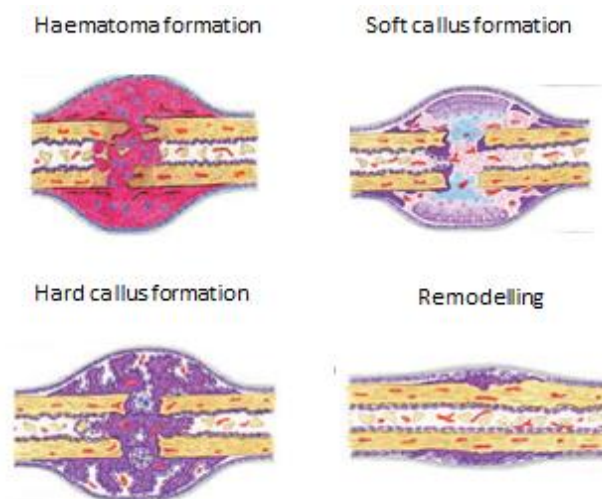
Figure 1-1-9 the four stages of secondary fracture healing

Illustration adapted from (Nunamaker, 1998)

1.9   Bone graft

Three types of graft are used clinically, **Autograft** (patient's own bone), **Allograft** (donor bone) and **synthetic bone products**. Autograft is described as the gold standard for the stimulation of fracture healing and arthrodesis, and holds intrinsic osteogenic activity, containing viable osteogenic cells, growth factors, and bone structural proteins.

1.9.1.1   Autograft

Autograft is typically harvested from the iliac crest. Risks of this procedure include pain and infection (Younger and Chapman, 1989), volume available is strictly limited, and with an estimated financial cost of around £400, is not cheap (Kurien et al., 2013b). Iliac crest Autograft contains non-vascularized segments of cancellous and cortical bone; vascularised grafts can be harvested through preservation of a vascular pedicle, such as in a vascularized fibula graft. This technically complex procedure is not routinely performed, and understandably involves sacrifice of a significant quantity of bone from the donor site.

1.9.1.2   Allograft

Allograft is usually derived from donated femoral heads of patients undergoing total hip arthroplasty. Patients are tested for transmittable viruses, and the donated bone is processed in a variety of steps which involve some form of sterilisation, such as gamma irradiation, and processes to permit storage such as freezing or freeze-drying. Immuno-rejection reaction to transplanted allograft material has been described (Delloye et al., 2007), and there is a postulated risk of prion transmission as current screening processes are not able to detect prions. Allograft is more expensive than autograft, with a single femoral head of 40-60g costing approximately £700 in the UK (Kurien et al., 2013b) as of 2013.

Demineralised bone matrix (DBM), is derived from Allograft, and consists of bone minus the mineral component, which is removed via an acid based treatment. DBM contains osteoconductive, collagenous and non-collagenous proteins, many of which modulate growth factor function as described previously. In addition to these structural proteins, DBM contains variable amounts of

growth factors including BMP. Major limitations with DBM use clinically include poor mechanical strength, and batch to batch variability, rendering the clinical effect unpredictable.

Integration of Autograft and Allograft

The two major determinants of clinical outcome following Autograft transplantation are the volume of graft retained, and the biological behaviour of the graft. The final volume of graft material is the net result of both osteogenesis, produced by osteoblasts resident within the graft and surrounding bone, and osteolysis, resulting from the action of osteoclasts (Rogers and Greene, 2012). The biological behaviour of the graft is the result of a variety of events such as mechanical loading of the graft, ability of the graft to integrate with surrounding tissue, presence of infection, and the survival of osteoblasts and osteocytes residing within the graft material. In non-vascularised grafts, resident osteoblasts and osteocytes must receive sufficient nutrients solely from passive diffusion until angiogenesis is complete. Cell death deprives the graft of potential osteoblastic activity, and may also precipitate inflammation and osteolysis. Following transplantation, osteoclasts cut channels into the graft; angiogenesis and bone formation subsequently take place within these channels, a process referred to as creeping substitution. The microarchitecture of the transplanted graft, in particular the surface area to volume ratio of graft material determines both the quantity of cells able to receive adequate nutrients via passive diffusion, and also the rate at which angiogenesis takes place (Rogers and Greene, 2012). Allograft and DBM also undergo osteo-integration via creeping substitution; however, this process is accompanied by a variable degree of inflammation due to the presence of immunogenic material residing within the allogeneic material. In contrast to bone formation within the embryo, both fracture healing, and integration of Auto and Allograft involve an acute inflammatory reaction.

1.9.1.3   Synthetic bone substitutes

The limitations of auto and allograft use have stimulated the development of a variety of synthetic bone substitutes. 59 products are currently available for clinical use in the UK (Kurein 2013). These products are derived from calcium sulphate, calcium phosphate, and bioactive glass. In order to optimise biomechanical properties these materials are often used in combination with each other, and are also combined with additional biomaterials such as hydrogels.

Figure 1-10 Classification of synthetic bone products

Within each box chemical derivatives of manufacturing processes are given, examples of these materials in current clinical practice is given underneath. TCP = Tricalcium Phosphate, HA = Hydroxyapatite.
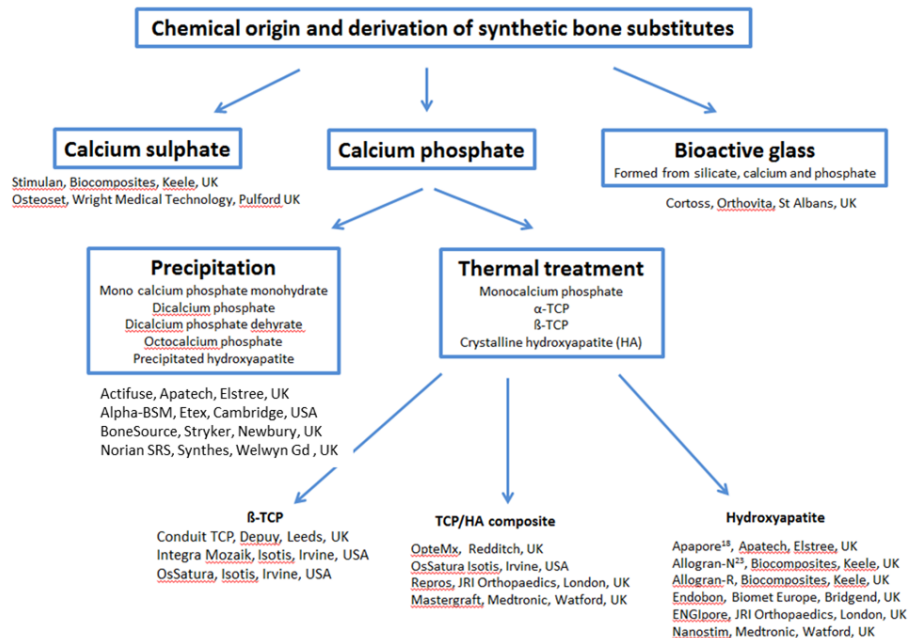
Synthetic bone substitutes can be classified according to the process of manufacture (Figure 1-10). Calcium phosphate based compounds maybe formed by precipitation reactions which occur around room temperature, or through thermal treatment giving rise to ceramics. Bioactive glass is based on silicate and thus categorised separately.

Calcium sulphate, the hydrated form of which is plaster of Paris degrades rapidly and thus is of limited clinical use as the material is likely to bio resorb prior to provision of adequate stability by the healing fracture (Peters et al., 2006). The process of manufacture of synthetic bone results in products which differ significantly in biomechanical properties, and consequently vary greatly in their clinical properties. For example, products derived from precipitation reactions can be used without resulting in thermal damage to adjacent tissue, and variation in crystalline structure can determine rates of biodegradation. For this reason the chemistry of derivation of synthetic bone products is explored in detail.

A variety of Calcium compounds, containing the orthophosphate group (PO_4^{3-}) have been used in production of synthetic bone substitutes, and it is noteworthy that subtle differences in structure of

these compounds may have profound effects upon *in vivo* behaviour. In general terms biodegradability of Calcium Phosphate compounds may be predicted by comparison of their solubility in water with the mineral phase of bone. Compounds of greater solubility biodegrade, while those of less solubility than the mineral phase of bone in water biodegrade very slowly, if at all. It is important to acknowledge that biodegradation is also affected by porosity, and degradation maybe delayed by the formation of another, less soluble Calcium Phosphate compound on the surface of the original mineral (Bohner, 2000). Calcium Phosphate based bone substitutes can be categorised into 2 groups, those resulting from precipitation reactions occurring around room temperatures, and those formed by thermal treatment.

Calcium Phosphate based compounds formed via precipitation include Calcium Phosphate based cements (CPCs). The process of formation of these compounds was patented by Brown and Chow over 20 years ago (Brown and Chow, 1986). CPC result from addition of Calcium Phosphate compounds to water which results in precipitation of Calcium Phosphate crystals, which grow and interlock. This precipitation reaction is predominantly isothermic, and therefore of greater biocompatibility than the exothermic reactions seen in polymerization, e.g. formation of polymethylmethacrylate. Compounds resulting from CPC formation vary and include: mono calcium phosphate monohydrate $Ca(H_2PO_4)_2H_2O$, dicalcium phosphate $CaHPO_4$, dicalcium phosphate dehydrate $CaHPO_42H_2O$, octocalcium phosphate $Ca_8H_2(PO_4)_65H_2O$ and precipitated hydroxyapatite (PHA) $Ca_{10-x}(HPO_4)_x(PO_4)6(OH)_{2-x}$. PHA formed may have a Ca/P ratio from 1.5-1.67, with PHA formed with Ca/P ratio of 1.5 referred to as calcium deficient hydroxyapatite, or tri-Calcium phosphate. PHA crystals are poorly crystalline and of submicron dimensions, with solubility increasing as CaP ratio decreases (Bohner, 2000).

Calcium phosphate compounds resulting from thermal treatment include: monocalcium phosphate $Ca(H2PO_4)_2$, ß-TCP; $ß-Ca_3(PO_4)_2$; α-TCP, α $Ca_3(PO_4)_2$, and hydroxyapatite, HA, $Ca_5(PO_4)_3OH$). HA formed in this case is stoichiometric and highly crystalline, it biodegrades very slowly, if at all. In order to improve biodegradation Daculsi and colleagues developed the concept of biphasic calcium phosphates, combining ß-TCP and HA in a variety of ratios (Daculsi et al., 2010). The rate of biodegradation can be accelerated by increasing the content of ß-TCP. Most commercial products contain 60% HA and 40% ß-TCP, e.g. Triosite (Zimmer) and BCP (Sofamor). Calcium phosphate biomaterials have been combined with hydrogels in an attempt to optimise rheological properties and facilitate injection (Daculsi et al., 2010, D'Este and Eglin, 2013).

Bioactive glass describes materials formed from Silicate, Calcium and Phosphates which have been reported to bond to bone (Nuss et al., 2006). In the presence of body fluids these materials release alkali ions, and form a Calcium Phosphate layer on their surface which subsequently recrystallizes to form hydroxycarbonate apatite. Cortoss (Orthovita, St Albans, UK) is an example of such a bioactive glass in current clinical use.

Study	Defect/Therapy	Treatments	Endpoints	Conclusions
Randomized Controlled Trial N=55 Damron 2013 (Damron et al., 2013)	Benign cavity lesions, Variety of bones	ß-TCP+BMA (Bone marrow aspirate) vs ß-TCP alone	Clinical, Radiographic Mean follow up 20.2 months.	Improvement in both groups. No significant benefit from BMA
Randomized Controlled Trial N=323 Cassidy 2003 (Cassidy et al., 2003)	Distal radius fractures	Closed reduction vs Closed reduction + Norian (Calcium Phosphate cement) k wiring in some cases	Clinical, Radiographic 1 year follow up	Radiographic and clinical outcomes similar in both groups
Randomized Controlled Trial N=52 Johal 2009 (Johal et al., 2009)	Displaced intra-articular calcaneal fractures	ORIF vs ORIF + ἁ BSM (Calcium phosphate cement)	Clinical, Radiographic 2 years follow up	Less loss of reduction (Bohler's angle) with cement. No clinical difference seen.
Randomized Controlled Trial N=120, Russell 08 (Russell and Leighton, 2008)	Tibial plateau fractures	ORIF + autologous graft vs ORIF + ἁ BSM	Clinical, Radiographic 1-4 years follow up	Subsidence more in autologous group. No clinical difference
Prospective series. N=50 McNamara 2010 (McNamara et al., 2010)	Impaction grafting of acetabulum during arthroplasty surgery	1:1 mixture allograft and Apapore 60 (HA 60% porosity)	Clinical (Harris Hip score) Radiographic Mean follow up 64 months	Mixture allograft and HA comparable to allograft alone in published studies
Retrospective series N=54 Oshima 2012 (Oshima et al., 2012)	Impaction grafting of femur in arthroplasty surgery	Impaction bone grafting with allograft + HA	Clinical, Radiographic scoring. Mean follow up 92 months	Favorable compared to published data of allograft alone
Retrospective series N=43 Whitehouse 2013 (Whitehouse et al., 2013)	Impaction grafting of acetabulum in arthroplasty surgery	Bone Save (80 ß-TCP 20% HA)	Clinical, Radiographic Mean follow up 4 years	Bone save alone reliable material for impaction grafting in medium term
Randomized Controlled Trial N=256, Bae 2012 (Bae et al., 2012)	Vertebral compression fractures	Cortoss (resin+ceramic) vs Poly-methyl methacrylate	Clinical, Radiographic 2 years follow up	Both materials comparable at most time points

Table 1-1 Clinical studies evaluating synthetic bone.

(Gibbs *et al*, Current molecular biology reports

ß-TCP = ß-Tricalciumphosphate, ORIF = Open reduction & internal fixation,

BMA Bone marrow aspirate, HA = Hydroxyapatite

1.10   Application of Tissue engineering to enhance bone healing

The field of tissue engineering and regenerative medicine was born in the 1980s when Eugene Bell embarked on the development of a cell based vascular scaffold. Subsequently Joseph Vacanti and Robert Langer began to develop scaffolds suitable for cell loading for use in clinical practice. At the turn of the century Robert Nareem defined this new field:

'Tissue engineering is the application of the principles and methods of engineering and the life sciences towards the fundamental understanding of structure/function relationships in normal and pathological mammalian tissues and the development of biological substitutes to restore, maintain, or improve functions" described in (Polykandriotis et al., 2010).

The fundamental components of tissue engineering may be conceptualized as: cells, growth factors, and scaffold materials as shown in figure 1-11.
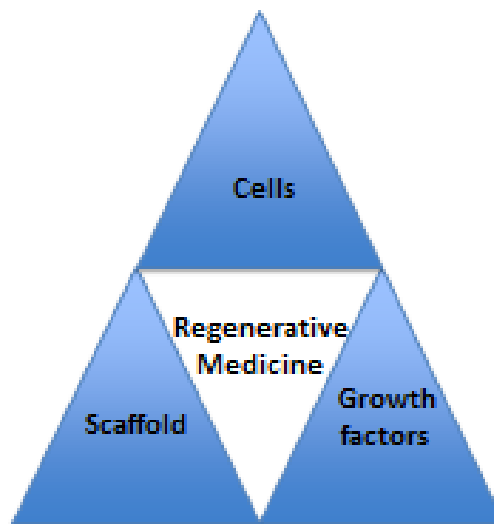
Figure 1-11 Diagrammatic representation of the key components of Tissue Engineering

1.10.1.1 Growth factors used in regenerative medicine to enhance bone healing

While the involvement of literally scores of growth factors have been demonstrated in bone physiology (1-5), only a minority, such as FGF, PDGF, PRP, BMP-2 and BMP-7, have been used in clinical practice, of which only BMP-2 and BMP-7 achieved any degree of widespread clinical use. For this reason, the focus of this thesis was the development of BMP based therapies.

Fibroblast growth factors have affinity for glycosaminoglycan heparin binding sites and are known to be pivotal in angiogenesis, and mitogenesis of mesenchymal cells (Canalis et al., 1989). FGF has been delivered within a gelatin hydrogel in a horse metacarpal defect (Sasaki et al., 2008), and has been evaluated in the treatment of human tibial fractures (Kawaguchi et al., 2010) While an effect of FGF on radiographic union was noted, no clinical difference was observed.

The presence of platelets at fracture sites led to the investigation of platelet-rich plasma (PRP), and platelet derived growth factor (PDGF) for use in fracture healing. The term platelet-rich plasma refers solely to a concentrated solution derived from the fraction of blood containing platelets. This somewhat vague term encompasses formulations that vary in platelet concentration, and also in methods of preparation, which are known to affect efficacy (Perut et al., 2013). Clinical studies using PRP have yet to conclusively demonstrate any benefit (Alsousou et al., 2009). PDGF is commercially available and has shown some success in preclinical models, but this has thus far translated only to the treatment of periodontal defects (Hollinger et al., 2008).

Bone Morphogenetic Protein was initially discovered 5 decades ago when Marshal Urist demonstrated the ability of demineralised bone to induce bone formation in soft tissue (Urist, 1965). Urist identified the protein nature of BMP around 15 years later (Urist et al., 1976). BMP was approved for clinical use by the European Medicines Agency in 2002 and by the Food and Drug Administration in the USA in 2004. While initial results of BMP application were promising (Govender et al., 2002), use subsequently declined following publication of adverse effects (Shields et al., 2006). The adoption of BMP in clinical practice has followed Scott's parabola (Scott, 2001) as shown in figure 1-12.
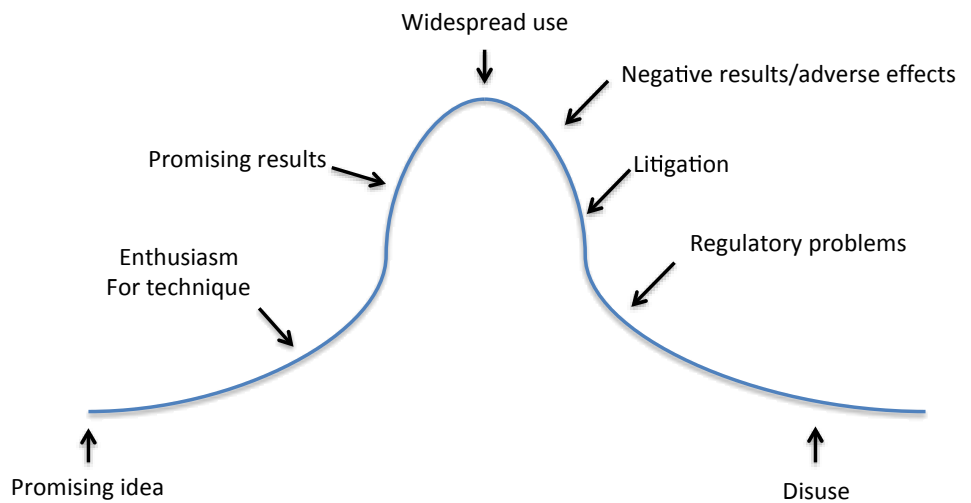
Figure 1-12 The use of BMP in clinical practice

Adapted from Scott's parabola (Scott, 2001).

In the vast majority of clinical cases BMP delivery involved addition of lyophilized BMP to water and application to a collagen sponge (Govender et al., 2002, Klimo Jr and Peelle, 2009, Tumialán et al., 2008), in a minority of cases alternative delivery methods such as Allograft (Buttermann, 2008), PLGA (Katayama et al., 2009) and Gelatin (Johnson et al., 1988) were used.

BMP was shown to enhance spinal arthrodesis, with clinical and radiographic outcomes of posterolateral lumbar fusion using BMP/Collagen/Calcium Phosphate (Dawson et al., 2009) and BMP/PLGA (Katayama et al., 2009) equivalent to those achieved using iliac crest bone graft. A randomised controlled trial of tibial fracture treatment demonstrated greater fracture union with BMP compared to the standard treatment (Govender et al., 2002). However, a number of studies reported significant side effects, including: heterotopic ossification, swelling and osteolysis (Klimo Jr and Peelle, 2009, Shields et al., 2006, Tumialán et al., 2008). Clearly heterotopic ossification and swelling in the cervical spine have enormous potential to cause catastrophe as small volumes of expansion can result in airway compromise or myelopathy. However, heterotopic ossification following BMP use in the treatment of long bone fractures may also result in significant symptoms, such a limitation of movement, swelling, and pain (Axelrad et al., 2008). Tumialán (Tumialán et al., 2008) reported a reduction in side effects with BMP use in cervical spinal fusion when the dose used was reduced from 2.1mg to 0.7mg per cervical spinal level. While Tumialán's findings relate to

cervical surgery it remains of concern that some of the studies describing favourable outcomes with BMP use, at other surgical locations employed doses 20 fold greater than used by Tumialán (Katayama et al., 2009).

1.10.1.2   Methods of Growth factor delivery

Despite eliciting the role of various growth factors in bone physiology, clinical translation has been hindered by lack of efficient delivery vehicles. Thus far, hydrogels, and collagen sponge materials have been utilised in the mainstay for growth factor delivery in clinical practice and *in vivo* studies.

BMPs are water soluble and if delivered in isolation rapidly disperse from the target site; hence there is a need to combine these growth factors with delivery vehicles. Growth factor release from a delivery vehicle is determined by a variety of factors such as: physical entrapment, covalent, electrostatic, or ionic bonding, and receptor mediated binding. Physical entrapment can result if the growth factor (GF) is similar to or larger in size than mesh or material pore size. In addition, rate of release is affected by directness of the pathway within the carrier material, and the rate at which the carrier biodegrades.

A growth factor delivery vehicle must be biocompatible, degrade, and able to convey the active growth factor to the desired site. Additional desirable properties of a GF delivery vehicle are:

> i) optimal GF release rate for target application
>
> ii) an ability to deliver cells
>
> iii) consistent handling properties
>
> iv) ease of growth factor addition
>
> v) permit percutaneous delivery
>
> vi) availability at high purity and low cost.

Hydrogels are hydrated polymer chains, and may be categorized according to the origin of the polymer backbone as natural, synthetic, and semi synthetic. Hydrogels utilized extensively in GF delivery include natural gels: Gelatin, Hyaluronic Acid, and alginate, while Polyethylene Glycol and derivatives represent the predominant synthetic and semisynthetic gels (Gibbs et al., 2014a).

Growth factors have been combined with Gelatin simply through direct addition to freeze dried Gelatin. An initial burst release of GF followed by a sustained release of a minority of GF has been attributed to initial diffusion of free GF, with additional GF only released upon degradation of the Gel (Yamamoto et al., 2001). While the rate of release of GF from gel is proportional to water

content (Yamamoto et al., 2003), burst release of GF remains a problem, with 40% BMP (Asamura et al., 2010) and 60% FGF (Kodama et al., 2009) released from Gelatin gels reported within 24 hours.

Hyaluronic acid can be cross-linked with the use of UV light (Bae et al., 2010) or the use of an aldehyde/hydrazide reaction (Bergman et al., 2009). Addition of gel following cross-linking was found to result in a burst release of BMP (Patterson et al., 2010), while addition of BMP prior to cross linking facilitated a sustained release of BMP over 28 days (Martinez-Sanz et al., 2011). Yeom (Yeom et al., 2010) combined a synthetic bone product (Megagen) formed from biphasic Calcium Phosphate, with 3 hyaluronic acid derived hydrogels which varied in their rate of degradation. Yeom reported that the greatest bone regeneration was mediated by Megagen, combined with the more rapidly degrading gel. It is of note that significant swelling was observed during the experiment. Were this finding replicated in a human study it could have catastrophic consequences (Blackburn and Smyth, 2007).

Polyethylene glycol (PEG) has been developed extensively for the production of hydrogels. Unmodified PEG does not biodegrade, and inflammation following implantation has been reported(Betz et al., 2009). This problem has been overcome with the incorporation of biologically active domains, such as protease-sensitive binding domains. Hoffman 2014 (Hoffman et al., 2014) demonstrated the ability to produce a series of hydrogels with a range of degradation rates by controlling the number of hydrolytically degradable lactide units with PEG-d,l-lactide-methacrylate macromeres. Betz and Lutolf (Betz et al., 2009, Lutolf et al., 2003) developed PEG gels which could physically entrap GF, with release upon degradation of the gel. In the absence of proteolytic enzymes, release was minimal (Lutolf 2003), while presence of these enzymes resulted in a burst release (Lutolf et al., 2003). Alternative approaches include the incorporation of cholesterol modified polysaccharide units (Fujioka-Kobayashi et al., 2012) through which hydrophobic interactions are able to trap GF, which are subsequently released through exchange reactions. More recently synthetic peptide derived gels have been combined with Calcium Phosphate (Matos et al., 2012, Amosi et al., 2012, Lippens et al., 2010). *In vivo* studies demonstrated a random migration of particles resulting in unpredictable osseous conduction, leading the authors to conclude that this approach was not suitable for anatomically non-confined defects (Matos et al., 2012).

Collagen sponge, typically of bovine origin, has been used for many years to deliver BMP and is degraded by collagenases. Typically BMP is applied to the sponge simply by soaking the sponge in

BMP solution for 10-30 minutes (Uludag et al., 2001). The rate at which BMP is released from collagen sponge is independent of BMP concentration within the range of 0.08mg to 2mg/ml (Uludag et al., 1999), indicating that collagen binding to BMP is not saturated within this range. Interestingly, release was found to be affected by the isoelectric point of the BMP (Uludag et al., 1999). Release of BMP from collagen is relatively rapid, with 10-30% lost immediately (Uludag et al., 2001, Uludag et al., 1999), either as a burst release following implantation or during handling, and a further 50% of the growth factor was lost within 3 days (Uludag et al., 2001). Limitations of collagen use include inflammation secondary to the antigenicity of the bovine material, rapid release of the growth factor, and the requirement for open surgery to place the sponge.

1.10.1.3   Limitations of current growth factor delivery methods

There are a number of critical limitations of hydrogels and collagen sponge in GF delivery including:

i) burst release of growth factor

ii) poor localisation of GF

iii) inability to be injected (in some cases)

iv) precipitation of an inflammatory response

Smectite clay is a synthetic, novel biomaterial which offers the potential to overcome the limitations encountered with current hydrogel and collagen sponge materials.

1.11 Smectite clay - a potential growth factor delivery vehicle

Clay minerals are formed from tetrahedral silicate and octahedral hydroxide sheets. Laponite is a synthetic Smectite, clay in which two tetrahedral sheets combine with one octahedral sheet to form each layer (Figure1-13). Smectites possess a net negative charge in pH neutral solutions due to isomorphic cation substitutions which is neutralised during manufacture as Na+ are adsorbed onto the surface of the Laponite crystals. Upon hydration a balance is established between osmotic forces distracting the Na+, and negative surface charge of the Laponite seeking to attract the Na+. Negative surface charges react with the positive edge charges of adjacent clay discs, resulting in a gel (Dawson and Oreffo, 2013). Laponite does not degrade in the presence of ultraviolet light or ethylene oxide, and therefore maybe easily sterilised.

Initial work suggests Laponite is cytocompatible with Human bone marrow stromal cells (HBMSC) (Gaharwar et al., 2013), and upon dispersion results in non-toxic products similar to those of Bioactive glass (Thompson and Butterworth, 1992). Indeed, some evidence has suggested that Laponite may possess an intrinsic osteogenic effect (Wang 2014 ref). The initial objective of this thesis is to investigate if Laponite is cytocompatible with HBMSC, and to assess for intrinsic osteogenic effect on HBMSC.

Laponite is thixotropic, i.e. viscosity decreases as sheer stress increases, this material property has been utilised in industry, where Laponite is frequently used to optimise the rheological properties of products such as cosmetics. The thixotropic properties of Laponite have been shown to be suitable for clinical use, with shear thinning resulting in a gel which passes through a standard gauge needle, followed by gelation at the target site (Dawson et al., 2011). A further objective of this work to seek *in vitro* confirmation that Laponite formulations which could be percutaneously administered can effectively localise growth factor to the surface of bone graft material.

The structural properties of Laponite suggest it offers potential for mediating protein or growth factor delivery as upon hydration broken bonds at the edges of Laponite crystals generate unsatisfied, pH dependent valences which are available for protein binding. These protein binding sites enable Laponite to adsorb and localise growth factors (Dawson et al., 2011). Furthermore, the random arrangement of nano sized crystals adopted by hydrated Laponite results in a torturous path which may also function to retard protein release. Laponite has been shown to adsorb albumin and

lysozyme from solution (Dawson et al., 2011). Laponite gels maybe dried, giving rise to dry Laponite films, which are also able to localise growth factors (Dawson et al., 2011). This thesis will investigate *in vitro* the ability of Laponite in both gel and dry films states to mediate growth factor delivery and localisation. Following the *in vitro* work we will seek to confirm and optimise the use of Laponite as a growth factor deliver vehicle in a small animal model. Subsequently, we aim to evaluate Laponite mediated growth factor delivery in a large animal model.
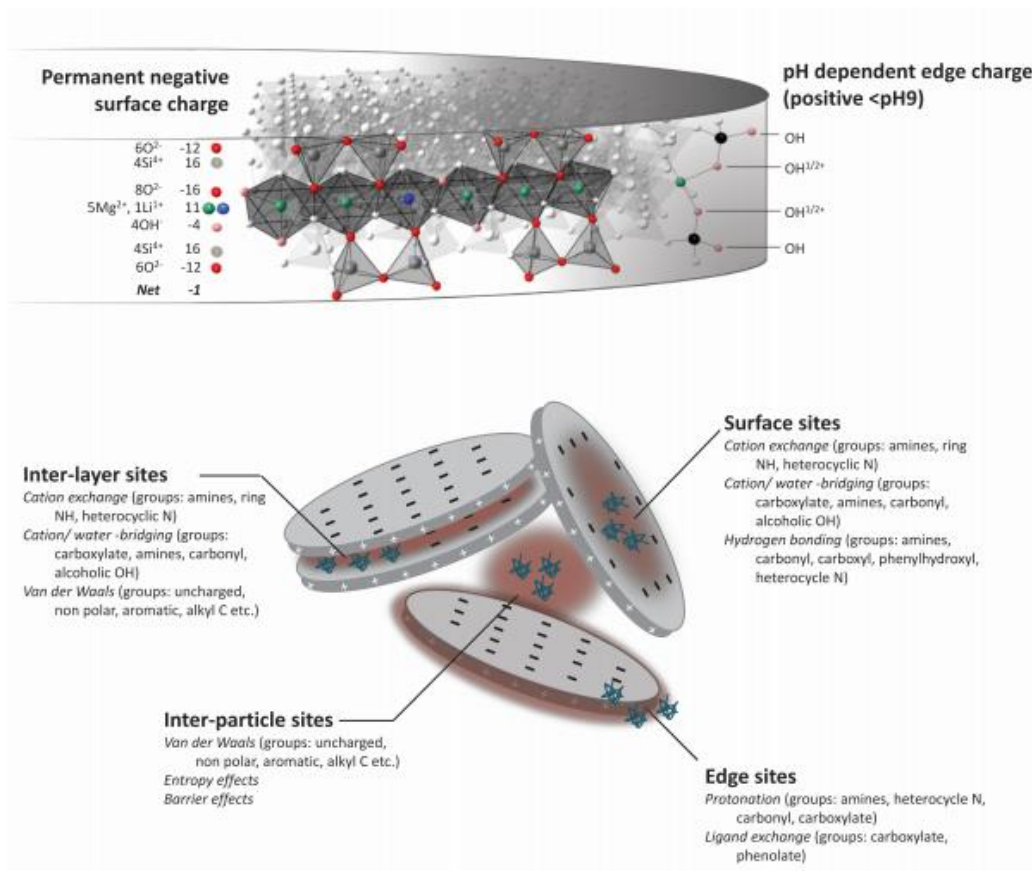
Figure 1-13 Structure of Laponite

This illustration from (Dawson and Oreffo, 2013) demonstrates the bi-tetrahedral, octahedral sandwich of the Smectite group, to which Laponite belongs. Negative charges shown on the disc surface of the Laponite crystals interact with positive charges on edge of adjacent Laponite discs resulting giving rise to the thixotropic property of Laponite.

1.12   Limitations of bone graft materials in current clinical use

Whilst autograft remains the only graft material with significant osteogenic potential, critical limitations of autograft are the limited volume available and donor site morbidity. Allograft use is relatively expensive, offers little or no osteogenic potential, and may result in an inflammatory response. Limitations of synthetic bone products are specifically related to the products used and their method of synthesis.

Calcium Phosphate Cements (CPC) are severely limited by the small pore size, which impedes cell migration, and poor mechanical strength. While porosity can be increased, the size of the pores remains only around 1 µm, furthermore for every 10% increase in porosity the tensile strength maybe reduced by around two-fold (Bohner, 2000). Further challenges in development of CPC are the ability to produce an injectable product which remains cohesive. Limitations of Calcium phosphate derived from thermal treatment include particle migration, and poor degradation. Pertinent clinical trials using CPC and Calcium phosphate products derived from thermal treatment are summarised in Table 1-1.

In addition to the limitations described, Calcium Phosphate compounds and Bioactive glass, while osteoconductive, are not osteoinductive. This feature was highlighted in a recent systematic review of bone graft products for use in spinal surgery, which concluded that whilst materials such as TCP, HA and bioactive glass were of use as osteoconductors, they recommended combining them with additional osteoinductive materials (Fischer et al., 2013).

A key disadvantage with the use of synthetic bone products derived by the processes outlined in 1.9.1.3 is that the porosity, filament size and orientation are determined by chemical processes, and cannot therefore be readily optimized for individual clinical requirements. In contrast, additive manufacture (AM), a new method of material synthesis, is capable of producing materials with tailor made internal architecture. Additionally, some forms of AM can seed growth factors and cells within the materials during production. Therefore it was hypothesized that AM could be used to produce superior synthetic bone graft products for clinical use.

1.13 Additive manufacture - a novel method of bone graft production

Additive Manufacture, commonly referred to as 3D printing, describes computer directed layer by layer deposition of material to form 3D structures. AM processes have been classified by the American Society for Testing and Materials International Committee F42 on Additive Manufacturing Technologies into seven processes in accordance with the method of layers deposition and bonding (Stucker, 2011):

i) Vat photo-polymerisation

ii) Material extrusion

iii) Powder bed fusion

iv) Directed energy deposition

v) Sheet lamination

vi) Material jetting

vii) Binder jetting

The intrinsic advantage of AM over standard material processing are:

i)   ability to directly control filament size

ii)   ability to control pore size, connectively, and spatial formation of composite structures

iii)   possibility of incorporating delivery of living cells and biologically active growth factors during scaffold synthesis

Whilst all forms of AM are capable of producing biomaterials, incorporation of cells or active growth actors limits synthesis to physiologically compatible processes, such as forms of Vat photo-polymerisation, material extrusion, and material jetting as shown in the Table 1-2 (Gibbs et al., 2014b).

AM has been used to produce scaffolds with tailor made fibre alignment, containing bone marrow cells and chondrocytes. These scaffolds subsequently underwent *in vitro* culture and subcutaneous implantation in mice (Fedorovich et al., 2011). Such developments represent a significant step; however a number of limitations must be overcome prior to any possible clinical translation. These

include vascularity, tissue integration, sterilisation and consistency. A more pragmatic approach would appear to be to harness AM to produce a scaffold of optimal material properties for bone, and seed this intra operatively with cells and or growth factor, with localisation facilitated by a hydrogel. Such an approach has shown success in large animal models, in which polycaprolactone scaffolds are produced and seeded intra operatively prior to implantation in ovine tibia (Reichert et al., 2012) and spine (Abbah et al., 2009). This thesis aims to explore the feasibility of employing Additive Manufacture, alone, and in combination with growth factor laden Laponite to produce synthetic bone graft material.

Process	Typical AM techniques	Advantages	Disadvantages	Applications	Living cells and growth factors	Experimental or commercial in medical field
Vat Photo-polymerisation	SL, 2PP	High-dimensional accuracy, offering transparent materials	Only photopolymers, single composition, cytotoxic photo initiator, incomplete conversion thus post-curing required, limited cells for incorporation, non-homogeneous cell distributions,	Printing clinical implants and surgical guides, tissue engineering scaffolds, 3D micro-vasculature networks, biological chips, cell incorporated 3D biological constructs	YES	Experimental
Material extrusion	**Melting extrusion:** FDM, PED, MJS, 3D fibre deposition	Fast, no toxic materials, good material properties	Low dimensional accuracy, delamination, weak bonding between dissimilar polymers	Printing clinical implants, tissue engineering scaffolds	NO	Experimental
	Extrusion without melting: PAM, 3D-bioplotting, Solvent-based extrusion free forming, Robocasting, direct-write assembly, electrospinning	Simple and cheap mechanism, no trapped materials, low material waste, fairly high fabrication speed, cell-friendly environment	Relatively low dimensional accuracy and mechanical strength Solvent is sometimes used Precise control of ink rheology is crucial	Printing tissue engineering scaffolds, cell incorporated 3D biological constructs, organ bio printing	YES	Commercial

Process	Typical AM techniques	Advantages	Disadvantages	Applications	Living cells and growth factors	Experimental or commercial in medical field
Powder bed fusion	SLS, SLM, EBM, SMS	Wide range of materials, good material properties, high material strength	Thermal stress, degradation, accuracy limited by the particle size of materials, require atmosphere control for metals	Printing surgical implants with complex internal and external structure, tissue engineered scaffolds, medical devices	NO	Commercial
Directed energy deposition	LENS, DMD, LC	Wide range of materials, good material properties	Low dimensional accuracy, thermal stress, require atmosphere control, require machining process for finishing the part	Printing orthopaedic implants	NO	Experimental
Sheet lamination	LOM, UC	Low temperature effects	Shrinkage, great amount of waste, delamination	Printing orthopaedic implants	NO	Experimental
Material jetting	DoD Inkjet printing, PJT	Fast process, wide range of biomaterials, use of existing cheap technology, multiple Compositions, multi-cell printing	Nozzle blockage an issue, low viscosity prevents build-up in 3D, low strength	Printing: implants, surgical guides, tissue scaffolds, cell incorporated biological constructs, organ bio printing	YES	Experimental
Binder jetting	3DP	Low temperature process, rapid process, multiple compositions	Requires powder, high porosity, low surface quality, accuracy limited by the particle size of materials, powder entrapment, cell challenging environment	Printing clinical implants and tissue engineering scaffolds	NO	Experimental

Table 1-21-3 Classification and application of additive manufacturing techniques
(Gibbs et al., 2014b)ADD REF

2PP: Two-photon polymerization; 3DP: 3D printing; AM: Additive manufacturing; DMD: Directed metal deposition; DoD: Drop-on-demand; EBM: Electron beam melting; FDM: Fused deposition modelling; LC: Laser cladding; LENS: Laser engineering net shape; LOM: Laminated object manufacturing; MJS: Multiphase jet solidification; PAM: Pressure-assisted microsyringe; PED: Precision extrusion deposition; PJT: PolyJet technology; SL: Stereolithography;

1.14 Use of micro Computed Tomography to assess bone formation

Micro Computed tomography (µCT) has been used extensively to quantify bone formation and absorption in the *in vivo* work of this thesis. For clarity, a synopsis of the principles of µCT is given here.

Quantification of bone formation using µCT is a 3 stage process:

1) Scanning of the target (bone defect or animal) to generate projection images.

2) Reconstruction of the projection images to generate cross sectional images.

3) Analysis of the cross sectional images to quantify parameters such as bone volume, and produce numerical descriptions of the internal bone architecture

The process of µCT scanning is identical to CT scanning performed on patients in hospitals, except the resolution of µCT is far greater. The µCT scanner used in this thesis was Bruker Skyskan 1176 (Bruker, Belgium). This machine contains a bed 6.8cm by 20cm on which the specimen is placed. An x-ray emitter and detector rotate around the bed recording the quantity of x ray beams which penetrate the specimen in hundreds of different projections. The energy of the x-ray beam is controlled by the voltage applied across the x-ray emitter (range 20k-90kV), and a selection of different filters placed in between the x ray emitter and the specimen is used to control the lower energy level of beams projected onto the specimen. Skyskan 1176 is able to perform scans with resolutions of 9, 18 and 36µm, with greater resolutions requiring a longer scan time, and resulting in a larger dataset which requires greater CPU resources to process.

Reconstruction of the projection images to generate cross sectional images was performed using NRecon (v1.6.10 Bruker, Belgium). Key elements of processing to reduce artefacts during transformation from projection to cross sectional data include Smoothing, ring artefact reduction and beam hardening. Smoothing is applied to each pixel, and can be used to delete pixels denoting dense tissue if they are not in contact with a given number of additional neighbouring pixels. This form of processing facilitates reduction in artefacts, however, if applied inappropriately can lead to loss of fine structural detail. Ring artefacts refer to circular artefacts centred on the axis of rotation, and a correction is selected and applied to the images to account for this. Beam hardening is the process by which low energy x-rays are absorbed by dense tissue, the resulting beam which passes through the target then has a higher proportion of high energy photons, which can result in a streaking effect. NRecon permits corrections to reduce artefacts

secondary to the phenomena of beam hardening. Finally, NRecon is used to convert the data from a greyscale of 0-65535 to 8 bits (0.08) resulting in a grey scale of 1-255 to enable processing.

The program CTAn (v1.16 Bruker, Belgium) was used to derive quantitative parameters from the cross sectional images derived using NRecon described above. Processing by CTAn of the cross sectional data sets can be summarised into four steps:

1) Selection from raw images of a region of interest (ROI)

2) Conversion of the 1-255 greyscale images to binary

3) Morphometric analysis of the binary images

4) Additional custom processing

The selection from the raw image of the region of interest is intuitive, and merely describes selection of the volume which is to be analysed, avoiding parts of the specimen which are not relevant to the experiment.

A threshold to convert the greyscale 1-255 output to a binary output maybe arbitrarily selected, or derived from mathematical modelling. Throughout our experiments we used CTAn to calculate the Otsu threshold of each specimen. This is a mathematical process which calculates the threshold which would produce greatest distinction in the object when converting from a greyscale image to a binary output. Mean Otsu thresholds of all specimens in a given experiment were then applied as the threshold to convert the greyscale image into binary.

Morphometric data such as bone volume per tissue volume was subsequently derived from the binary dataset of the region of interest.

Custom processing is a feature of CTAn which automates process such as selection of regions within a region of interest, and subsequent calculation of morphometric data from these additional regions. Alternatively, custom processing can be used to overlay images of a specimen, such as those taken before and after an experiment, permitting calculation of bone formation and bone absorption. Where custom processing has been used, the methodology has been described in the relevant chapter.

Ultimately, as with any form of experimental work, if performed inappropriately, µCT scanning, image reconstruction and subsequent analysis can be abused, and invalidate or introduce bias to the results. In this thesis, µCT scanning, and image processing parameters were optimised using the control specimens, and the same parameters used for all specimens a given study.

1.15   Summary

Fracture healing and bone formation is a complex process mediated by multiple signalling pathways and growth factors which trigger cell differentiation and migration. Of the multiple growth factors identified, only BMP-2 and BMP-7 have reached widespread clinical practice. Whilst efficacy of these growth factors has been demonstrated, lack of an efficient growth factor delivery vehicle necessitated use at supraphysiological doses which resulted in significant side effects and has rendered them clinically and economically non-viable.

Autograft and Allograft are commonly used for bone grafting, despite significant limitations such as donor morbidity and poor osteogenicity respectively. Synthetic graft materials in current use are suboptimal as material properties such as internal architecture is determined by the chemical process employed for synthesis, and cannot be readily enhanced by osteoinductive agents such as BMP.

Material properties of the Smectite Laponite render it potentially uniquely suitable to facilitate a sustained localised release of BMP and stimulate healing. Laponite mediated delivery of growth factors may be capable of enhancing the osteoinductivity of AM derived graft material.

1.16   Aim

Investigate the use of Laponite and Additive Manufacture to facilitate bone regeneration. To develop Laponite for use as a growth factor delivery vehicle to enhance fracture healing, and to assess the suitability of combining Laponite with AM derived products to produce synthetic bone graft.

1.17   Hypothesis

Laponite can be used to facilitate localised, sustained growth factor delivery, and this approach can be used alone and in combination with synthetic bone produced using AM to enhance bone and tissue regeneration.

Objectives

1) To investigate if Laponite is cytocompatible with HBMSC, and to assess for any intrinsic osteogenic effect on HBMSC.

2) To seek *in vitro* confirmation that Laponite formulations which could be percutaneously administered can effectively localise growth factor to the surface of bone graft material.

3) To investigate *in vitro* the ability of Laponite in both gel and dry films states to mediate growth factor delivery and localisation.

4) To confirm and optimise the use of Laponite as a growth factor deliver vehicle in a small animal model.

5) Evaluate the most promising formulation of Laponite and BMP in a large animal bone defect model.

6) Explore the feasibility of Additive Manufacture alone and in combination with Laponite to produce synthetic bone graft material.

Chapter 2: Methods

2.1 Laponite

Laponite is formed through combination of salts of magnesium and lithium with sodium silicate. The resulting precipitate is subjected to high tempatures, resulting in partial crystallization, and is subsequently washed, filtered, dried and milled to produce a fine white powder.

Laponite XLG was obtained from BYK Additives and Instruments, Germany. Suspensions of Laponite were formed as previously described (Dawson et al., 2011). Laponite powder was added to distilled water under agitation sufficient to produce a vortex. Suspensions were stirred at room temperature for 6 hours, sterilized via standard autoclave protocols and stored at room temperature.

Unless otherwise stated, films of dry Laponite for cell culture were formed by pipetting 2.5μl of 1% Laponite individually into 48 well tissue culture plates

2.2 Cell isolation

Bone marrow samples were obtained from patients undergoing elective total hip replacement for osteoarthritis, or arthroplasty following trauma. Only waste material was used in line with ethical approval from Southampton & South West Hampshire Local Research Ethics Committee (LREC 194-99).

Bone marrow stromal cells were isolated as described previously (Oreffo et al., 1998). Marrow samples were washed in α-MEM (Sigma-Aldrich Ltd. Gillingham, UK) and cell pellets formed using centrifugation at 1100rpm. The cells were suspended and plated onto culture flasks, typically 2×10^7 cells would be seeded on an 80cm^2 flask.

Human Umbilical Vein Endothelial Cells (HUVECs) were isolated by Stephanie Inglis from donated umbilical cord tissue from Princess Ann Hospital (the local obstetric facility) with ethical approval (LREC 05/Q1702/102), and donated to me. HUVECs were isolated and cultured as described by (Morgan, 1996) with minor modifications. Cord is incubated with collagenase B; resulting cell

suspension is centrifuged to produce a cell pellet. Pellet is suspended and plated onto culture flasks at appropriate cell densities.

C2C12 cells were purchased from Sigma-Aldrich Ltd. Gillingham, UK.

2.3 Cell culture

All cell culture was performed at 37 degrees Celsius, with 5% CO_2.

Basal culture media

For bone marrow stromal cells α MEM with 10% FCS (Invitrogen, UK) and 1% Penicillin/Streptomycin (Sigma-Aldrich, UK) was used.

HUVECs were cultured in Medium 199 (Sigma-Aldrich, UK) with 10% FCS, 0.02μg/ ml VEGF, 40ng/ml FGF (Sigma-Aldrich, UK, and 0.4μg/ml Endothelial cell growth factor (Sigma-Aldrich, UK).

C2C12 cells were cultured in d-MEM with 10% FCS and 1% Penicillin/Streptomycin, following cell seeding for ALP induction assay FCS concentration was reduced to 2%.

All cell culture was performed at 37° Celsius, with 5% CO_2.

Osteogenic media

To promote osteogenesis bone marrow stromal cells were cultured in α MEM with 10% FCS plus 100nM dexamethasone (Sigma-Aldrich, UK) and 100μM of ascorbic acid (Sigma-Aldrich, UK).

2.4 Cell analysis

Viability assays

Cell viability was assessed using cell tracker green, which labels metabolically active cells, and ethidium homodimer, which labels necrotic cells. 10μl Dimethyl sulfoxide (Sigma-Aldrich, UK) was added to 50μg of cell tracker green and dissolved in 5ml of tissue culture media together with 25μg of ethidium homodimer. This solution was applied to cell cultures, and incubated for 1 hour at 37°C. The media was exchanged with fresh tissue culture media, and incubated for a further

hour. Following a rinse in Phosphate Buffered Saline (Sigma-Aldrich, UK) samples were fixed in 95% ethanol for 10 minutes, and immediately viewed under fluorescent microscopy.

Quantification of specific activity of alkaline phosphatase

Media are removed, cells washed in PBS and fixed in 95% ethanol for 10 minutes. Cells are subsequently washed twice in PBS and air dried. Cells are lysed with use of 0.05% Triton (Sigma-Aldrich, UK) and a cell scraper. Cells are passed through 3 freeze-thaw cycles.

Assay buffer solution (Sigma-Aldrich, UK) and Substrate (Sigma-Aldrich, UK) are made. Five standards are made using serial dilution of 4-nitrophenol (Sigma-Aldrich, UK) and assay buffer solution.

10μl of cell sample lysate and 90μl of substrate are placed in a 96 well plate together with standards. All samples are processed in triplicate.

96 well plate in incubated at 37°C for 30 minutes, and subsequently examined for colour change every 5 minutes. Reaction is terminated with sodium hydroxide, and time of colour change recorded. 96 well plates was analysed using FLx800 Microplate Fluorescence Reader (Biotech Instruments, UK).

ALP activity is derived from comparison with linear regression of the standards, and expressed as nmol pNNP/ml hr^{-1}.

Staining for alkaline phosphatase

Media are removed, cells washed in PBS and fixed in 95% ethanol for 10 minutes. Following a further two PBS washes, cells are dried.

400μl Naphthol AS-MX Phosphate Solution (Sigma-Aldrich, UK) and 2.4mg Fast Violet Salt (Sigma-Aldrich, UK) are dissolved in 9.6 ml distilled water.

Sufficient Naphthol/Violet solution is applied to cover the bottom of the wells and incubated at 37°C for 30 minutes and subsequently examined for colour change every 5 minutes. Reaction is terminated by washing with distilled water, and imaged immediately.

Analysis of staining intensity of alkaline phosphatase

Cells are stained for ALP as described above, and PBS added to cover the cells. Microscopy is performed using Axiovert 200 Inverted Light Microscope (Carl Zeiss, UK) Axiovision Software V4.0 (Carl Zeiss, UK) at x5 magnification. All light settings are kept constant while images are taken of

control and test groups. Staining intensity is subsequently analysed using Cell Profiler image analysis software (Version 2.1.1, Broad Institute, USA).

2.5 *In vivo* surgery

All surgical procedures and animal husbandry were performed at the Biological Research Facility, Southampton General Hospital with consent from Southampton & South West Hampshire Local Research Ethics Committee, and compliant with Home Office Licencing.

Murine studies

Anaesthesia

1ml of Hypnorm (Fentanyl) and 2ml of Hypnoval (Benzodiazepine) were diluted with 3ml and 2 ml respectively of sterile water. Resulting dilutions of Hypnorm and Hypnoval were mixed 1:1 and used for surgical anaesthesia and sedation for both murine studies.

Approximately 0.1ml/10g body weight was given via intra-peritoneal route to achieve surgical anaesthesia; approximately one third of this dose was given for sedation during the CT scans in the second murine study.

Surgery

Surgery was performed by myself and Cameron Black, a licensed veterinary surgeon. Following anaesthesia non-nude mice were shaved. Surgery was performed in a sterile hood with the mouse positioned on a warming blanket. A number 11 scalpel blade was used to make a midline dorsal incision of approximately 3cm. Curved; blunt ended scissors were used to create 6 small subcutaneous pockets, 3 on each side of the midline. Wounds were closed with surgical clips in part 1 of the study. Absorbable sub-cuticular sutures were used to close the wounds of the mice in the second study to reduce the effect of artefact on the CT scanning. Mice were closely monitored and kept in a temperature controlled environment until they had recovered from surgery or sedation.

Animal husbandry

All mice were permitted standard chow and water *ad librium* in cages which complied with Home Office Licensing requirements.

Ovine study

Methodology employed is detailed in chapter 5.

2.6 Micro Computed Tomography

All imaging was performed using SkyScan 1176 micro CT scanner (Bruker, Belgium), and images reconstructed using NRecon (version 1.6.9) (Bruker, Belgium). Scanning and reconstruction settings are detailed in each chapter, and remained constant throughout each experiment.

CT images were viewed and processed using CTVox(version 3.0) (Bruker, Belgium) and Dataviewer (version 1.5.1) (Bruker, Belgium). Quantitative analysis was performed using CT An (version 1.15) (Bruker, Belgium).

2.7 Histology

Embedding of samples

Tissue samples were stored in Paraformaldehyde (PFA) immediately following retrieval.

Allograft samples from the first murine study underwent 24 hours decalcification in Histo decal (Histoline Laboratories, Italy). Collagen sponge samples from the second murine experiment did not undergo decalcification prior to embedding.

Samples were placed in labelled cassettes, and subsequently dehydrated and embedded in wax using Shandon Citadel 2000 (Thermo Fischer, USA) tissue processing machine. Tissue processor was programmed to immerse samples for one hour in: 50%, 90%, 100%, and 100% alcohol, followed by 4 hours in 100% Histoclear, and finally 6 hours in molten wax.

Sectioning of samples

9µm sections were taken using a microtome, and mounted on glass slides.

Alcian Blue and Sirius Red Staining

Slides were de-waxed and rehydrated with Histoclear and serial dilutions of alcohol. Equal amounts of Weigerts Haematoxylin A and B solution were mixed and applied to the slides. Following rinsing in water, immersion in Acid/Alcohol, and a further rinse in water, slides were stained with Alcian Blue. Following a further rinse in water, slides were stained with molybdophosphoric acid, rinsed in water, and stained with Sirius Red. Slides are rinsed again in

water, and dehydrated with use of Histoclear and serial alcohol dilutions prior to mounting cover slides.

Microscopy

Initial microscopy was performed using Axiovert 200 Inverted Light Microscope and Axiovision Software (V4.0 Carl Zeiss Ltd., Cambridge, UK). Further evaluation on selected slides was then performed using the DotSlide Microscope and DotSlide microscope software version 2.1(Olympus, Hamburg, Germany).

2.8 Statistical analysis

All analysis was performed using GraphPad Prism (version 6.05). All experiments were repeated at least three times.

Numerical data

Initial analysis

Comparison of means of 3 or more groups in response to one variable was performed using one-way ANOVA. Comparison of means of 3 or more groups in response to two variables was performed using two-way ANOVA.

Post hoc testing

Tukey's method was used if every mean was compared with every other mean.

Dunnett's method was used when comparing every mean to a control mean.

Sidak's test was used when comparing mean values in at individual concentrations of BMP on Laponite to TCP. P values were adjusted for multiplicity with alpha = 0.05.

Categorical data

Categorical data were analysed using two tailed Fisher's exact test.

Chapter 3:   The potential of Laponite to enhance growth factor delivery *in vitro*

Data from this work have been presented:

China clay enhances activity of Bone Morphogenetic Protein

David M.R. Gibbs, Richard O.C. Oreffo, Jonathan I. Dawson

European Orthopaedic Research Society, Nantes 2014

Clay nanoparticles enhance bone cell osteogenic response to Bone Morphogenetic Protein

David M.R. Gibbs, Richard O.C. Oreffo, Jonathan I. Dawson

Tissue Engineering and Regenerative Medicine European Meeting, Genova 2014

Data from this work have been submitted for publication in Nature Materials:

Clay nanoparticle gels induce bone formation at physiological doses of BMP

D.M.R. Gibbs, C.R.M. Black, G. Hulsart-Billstrom, R.O.C.Oreffo, J.I. Dawson

3.1   Introduction

Chapter one detailed the essential and desirable material properties of a growth factor delivery vehicle. Namely, it must be: biocompatible, biodegradable, and able to convey active growth factor. In addition the material would preferably: permit percutaneous delivery, have a GF release profile optimal for target application, facilitate GF localisation, be able to deliver cells, have consistent handling properties, easy to combine with GF, and is of low cost and high purity.

To establish cell compatibility, unselected bone marrow stromal cells (HBMSC) were cultured on dry Laponite films, consisting of a range of Laponite volumes and concentrations. Cell culture was performed on Laponite gel, including a mixture of Laponite and type 1 collagen gel. As discussed previously, type 1 collagen gels have often been selected for bone tissue engineering as they are formed from the most abundant native bone protein, and can enhance cell migration. Previous studies have suggested that some formulations of Laponite have an osteogenic effect (Wang et al., 2014, Gaharwar et al., 2013). Alkaline phosphatase expression of the HBMSC was assessed to detect any osteogenic effect.

 If Laponite is non-toxic, and has no effect on osteogenesis within the range of concentrations and volumes tested, it should be possible to control these parameters to optimise the rheological properties of the gel, i.e. tailor the concentration of Laponite gel to optimise viscosity for injectable delivery. As the majority of fractures are managed conservatively without recourse to surgery, the ability to percutaneously deliver a growth factor would be a significant clinical advantage.

Percutaneous delivery of a growth factor to a fracture site requires a delicate rheological balance of the delivery vehicle, which must be of sufficiently low viscosity to pass through a relatively narrow gauge needle, and yet of sufficient viscosity and adhesiveness to maintain at, and resist displacement from the fracture site. The thixotropic nature of Laponite renders it potentially uniquely suitable for percutaneous growth factor delivery as shearing reduces viscosity, facilitating delivery through a needle, while viscosity recovers rapidly at 37°C in pH neutral conditions with re-establishment of a gel network (Dawson et al., 2011). Furthermore, the rate of Laponite gelation has been shown to increase with increased electrolyte concentration (Dawson et al., 2011). The thixotropic nature of Laponite, and effect of electrolytes on gelation, are fundamental properties of Laponite which are likely to enhance the ability of Laponite to mediate percutaneous growth factor delivery . In order to assess if the injectable clay gel could persist at a fracture site, Laponite gel of a formulation able to pass through a needle was mixed with fluorescent albumin, a surrogate growth factor, and applied to some bone fragments. These fragments were subsequently washed, and imaging performed to assess protein localisation.

Laponite can be formulated as a hydrogel, the rheological properties of which vary according to the concentration of hydrated Laponite, or as a dry film. Laponite has also been cross-linked within polyethylene glycol based gels (Gaharwar et al., 2011b, Chang et al., 2010). Pristine Laponite formulations were utilised in these studies as these were postulated to be capable of providing the biomechanical properties required to facilitate growth factor delivery and localisation. Formulation of pristine Laponite gels and films is relatively simple, and of low cost, increasing the likelihood of clinical translation.

The clinical requirements of Laponite may include GF localisation to the surface of a synthetic graft, perhaps by a dry Laponite film, or percutaneous delivery of GF to a fracture site, e.g. by a Laponite gel. Therefore the following studies sought to explore the potential use of Laponite in both hydrogel and dry film states for use in GF delivery.

As discussed in 1-7, VEGF is known to be a pivotal mediator of both endochondral bone formation *in utero*, and also of *post-natal* fracture repair. A first approach was to determine if Laponite was capable of delivering this growth factor. While culture of HBMSC on thick Laponite gels is challenging, conversely, Human Umbilical Vein Endothelial cells are readily grown on such films (Dawson et al., 2011). Furthermore, microtubule formation by HUVECs cultured on gels is known to be dependent upon, and highly sensitive to VEGF, with concentrations as low as 10ng/ml observed to induce microtubule formation (Liang et al., 2014). Therefore the response of HUVECs to VEGF contained within, and delivered upon the surface of a Laponite gel was assessed.

BMP is pivotal in bone metabolism, and BMP-2 and BMP-7 remain the only growth factors to have been widely adopted in clinical practice, being used to stimulate fracture healing and spinal arthrodesis respectively (Garrison et al., 2007). C2C12 cells are pre myoblastic mouse cells that are a subclone of C3H muscle myoblasts. In the absence of inducting factors these cells form myotubules and differentiate along a myogenic pathway. However, C2C12 cells undergo osteogenic differentiation in the presence of BMP, and demonstrate a dose dependent increase in ALP activity, and osteocalcin, in response to BMP across the range of 100 to 1000ng/ml (Katagiri et al., 1994). C2C12 cells were used to investigate the ability of dry Laponite films to localise BMP.

3.2   Aim

To assess the suitability of Laponite as a growth factor delivery vehicle for use in fracture healing.

3.3   Null Hypothesis

Laponite is cytotoxic and will be unable to deliver and localise active growth factors.

3.4   Objectives

1) Investigate if Laponite is cytocompatible with HBMSC, and to assess for any intrinsic osteogenic effect on HBMSC

2) To seek *in vitro* confirmation that Laponite formulations capable of percutaneous delivery can effectively localise growth factor to bone graft material.

3) To investigate *in vitro* the ability of Laponite in both gel and dry films states to mediate growth factor delivery and localisation.

3.5 Methods

3.5.1.1 Investigation of the cytocompatibity of Laponite and effect on osteogenicity of HBMSC

3.5.1.1.1 Effect of concentration of Laponite films on HBMSC growth and ALP activity

Dry Laponite films of 2.5 µl Laponite at concentrations of 0.5, 1.0, 2.0 % per unit mass were made as described in chapter 2. HBMSC were seeded at 9×10^4 cells cm^{-2} in basal and osteogenic media as indicated. After 4 and 8 days culture, ALP staining was performed, and at 14 days colourimetric analysis of cell lysate and cell staining with image analysis was performed as described in 2.4.

3.5.1.1.2 Effect of volume of Laponite films on HBMSC growth and ALP activity

Dry Laponite films of 1.25, 2.5, 5, 7.5µl of Laponite were made. HBMSC were seeded at 750 cells cm^{-2}, cultured in basal conditions for 1 week, and subsequently in basal and osteogenic media as indicated for the remainder. ALP staining was performed at 7, 14 and 21 days as described in 2.4.

3.5.1.1.3 Effect of combination of Laponite films with type 1 collagen on HBMSC growth and ALP activity

2.5ml/ml of type 1 collagen in acetic acid was mixed with equal volumes of 2% Laponite to form a Laponite/Collagen mixture, which was subsequently used to form dry Laponite films as previously described. HBMSCs were seeded at 750 cells cm^{-2}, cultured in basal conditions for 1 week, and subsequently in basal and osteogenic media as indicated for the remainder. ALP staining was performed at 7 and 14 days, and after 21 days colourimetric analysis of cell lysate and cell staining with image analysis was performed.

3.5.1.2 Investigation into the ability of Laponite formulations capable of percutaneous delivery to effectively localise growth factor to bone graft material

In order to investigate the feasibility of using Laponite to mediate percutaneous growth factor delivery, Laponite formulations were mixed with labelled proteins and applied to bone specimens using a needle. Itwas established that following shearing 2.5% formulations of Laponite gel are able to pass through a standard 21 gage green needle.

Bone cores were produced from human femoral heads with the use of stoma core drill, subchondral sections were removed, resulting in cylinders 4mm in length and 4mm in diameter. Bone cylinders underwent multiple washes in Hydrogen Peroxide followed by PBS and then dried. To achieve a dry Laponite film, 19µl of 1% Laponite was applied to a group of allograft cylinders which were subsequently dried in a tissue culture hood. 1µl FITC-BSA was mixed with 19µl PBS or 19 µl 2.5% Laponite and was applied to bone cylinders. Following an interval of 20 seconds the bone cylinders were placed in wells containing αMEM. Following 2 hours in the media the cylinders were washed in PBS and fluorescent microscopy performed.

3.5.1.3 *In vitro* investigation of the ability of Laponite in gel and dry films states to mediate growth factor delivery and localisation

3.5.1.3.1 Effect of Laponite gel on the activity of Vascular Endothelial derived Growth factor

0.5ml of 0.5M sucrose and 0.5ml of Fibronectin (1mg/ml) was added to 10ml of sterile 2.5% Laponite, 300µl of this solution was applied alone (L), or VEGF was mixed into the clay (V in L), or VEGF was left at room temperature and added with the media (V on L) in a 24 well plate (table 3-1).

Six microscopic images were systematically taken of each well after 18 hours culture. These images were analysed using Cell Profiler Software. Initially a process was written to count the number of cells, following this a second process was used to quantify the number of microtubule branches (Figure 3-1).

Endpoint was microtubule formation at 18 hours.

0	10	20	40	80	1000
Blank	V on L	V on L	V on L	V on L	V on L
Blank	V on L	V on L	V on L	V on L	V on L
L	V in L	V in L	V in L	V in L	V in L
L	V in L	V in L	V in L	V in L	V in L

Table 3-1 Plate layout of Human Umbilical Vein Endothelial Cell Microtubule Assay.
First row denotes VEGF concentration (ng/ml). V on L = VEGF applied on surface of Laponite. V in L = VEGF mixed into the Laponite. L = culture performed on Laponite in absence of VEGF.
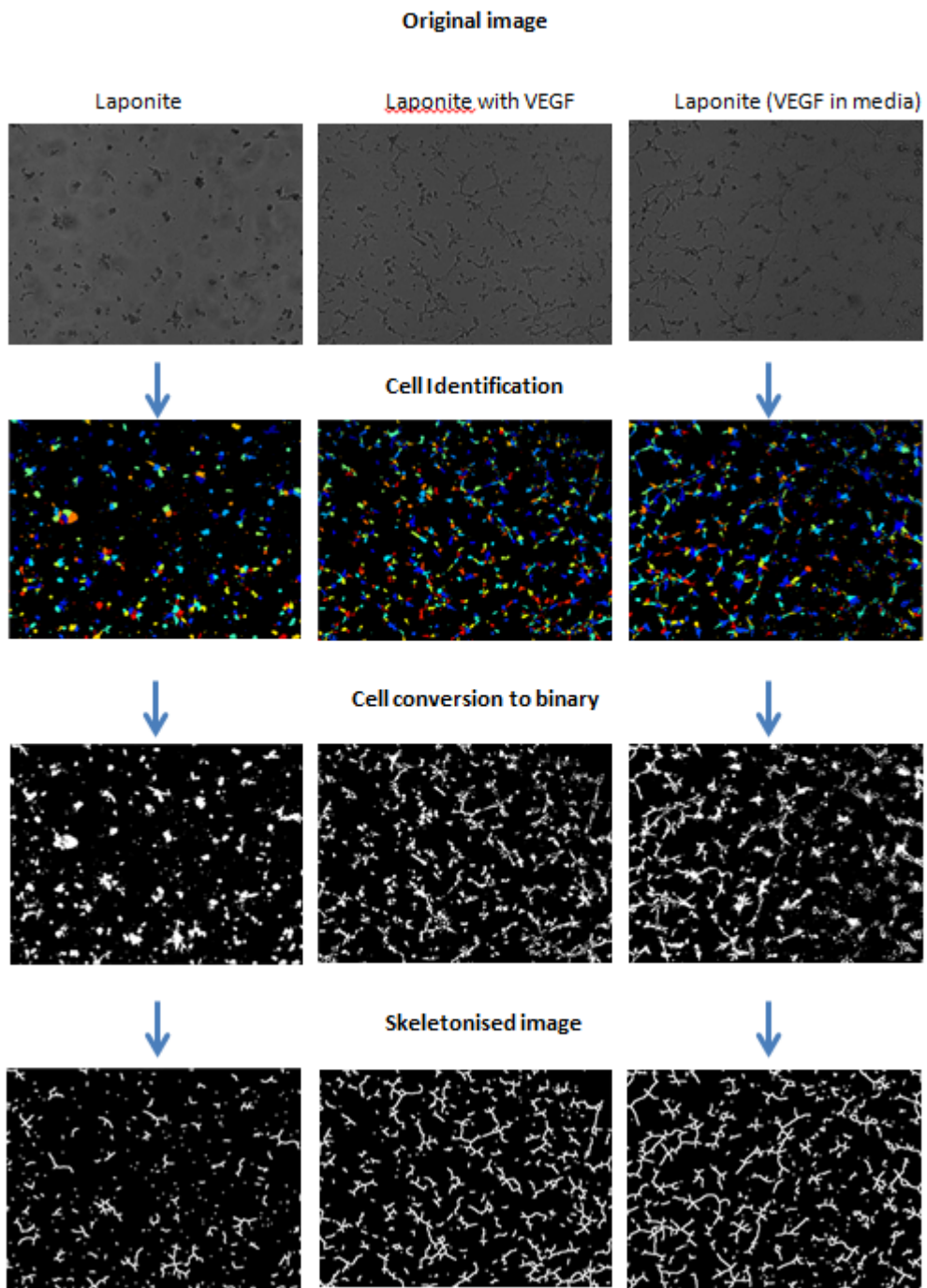
Figure 3-1 Quantification of microtubule formation by HUVEC cells using Cell Profiler software

3.5.1.3.2 Effect of Laponite films on ALP activity in C2C12 cells cultured with variable [BMP]

C2C12 cells in DMEM containing 400, 200, 100, and 0 ng/ml of BMP were seeded at $1x10^5$ per cm^2, in triplicate at each BMP concentration on dry Laponite films and TCP. ALP staining intensity was measured at 72 hours

3.5.1.3.3 Effect of Laponite films on ALP activity in C2C12 cells at variable seeding densities

C2C12 cells in DMEM containing 400ng/ml BMP, were seeded in triplicate at $0.25 x10^4$, $0.5 x10^4$, and $1x10^4$ cells/cm^2 onto dry Laponite films and TCP. ALP staining intensity was measured at 72 hours.

3.5.1.3.4 Effect of Laponite films on ALP activity in C2C12 cells cultured with incubated BMP

DMEM containing 800ng/ml BMP, was placed on dry Laponite films and TCP in triplicate and incubated for 48, 24, 4, 3, and 2 hours prior to seeding C2C12 cells at $1x10^4$/cm^2 (final BMP concentration 400ng/ml). ALP staining intensity was measured at 72 hours.

3.6   Results

The results are presented in three sections corresponding to the three stated objectives of this chapter:

1) Investigate if Laponite is cytocompatible with HBMSC, and to assess for any intrinsic osteogenic effect on HBMSC.

2) To seek *in vitro* confirmation that Laponite formulations capable of percutaneous delivery can effectively localise growth factor to bone graft material.

2) To investigate *in vitro* the ability of Laponite in both gel and dry films states to mediate growth factor delivery and localisation.

I received technical assistance with the use of Cell Profiler software from Dr Jonathan Dawson

3.6.1.1 Cytocompatibility & osteoinductivity of Laponite

To establish if Laponite is cytocompatible with HBMSC, or has any intrinsic osteogenic effect, HBMSC were cultured in basal and osteogenic conditions on Laponite films of various concentrations and volumes, and ALP activity assessed. To explore the effect of type 1 collagen, HBMSC were cultured on collagen, in the presence and absence of Laponite, and ALP activity assessed.

3.6.1.1.1 Effect of concentration of Laponite films on HBMSC growth and ALP activity

No visual difference in HBMSC growth or ALP expression was observed in response to variation in the concentration of Laponite, while an effect on ALP activity was seen in response to basal and osteogenic culture conditions, as shown in figure 3-2.

3.6.1.1.2 Effect of volume of Laponite films on HBMSC growth and ALP activity

No visual difference in HBMSC growth or ALP expression was observed in response to variation in the volume of Laponite, while an effect on ALP activity was seen in response to basal and osteogenic culture conditions, as shown in figure 3-3. Analysis of specific ALP activity correlated with visual inspection as shown in figure 3-4. Linear regression analysis found the gradient not to be significantly different from zero, indicating no detectable effect on ALP in response to Laponite volume in basal or osteogenic conditions.

3.6.1.1.3 Effect of combination of Laponite films with type 1 collagen on HBMSC growth and ALP activity

The addition of type 1 collagen to Laponite had no visual effect on growth or ALP activity of HBMSC seeded and cultured on the collagen/Laponite gels. A clear effect of basal or osteogenic culture conditions on ALP expression was visible as shown in figure 3-5.

No effect on specific ALP activity was seen when Laponite was combined with collagen, compared to Laponite or collagen alone on HBMSC in basal and osteogenic media. A significant increase in specific ALP activity was observed in osteogenic compared to basal conditions ($p = <0.0001$) as shown in Figure 3-6.
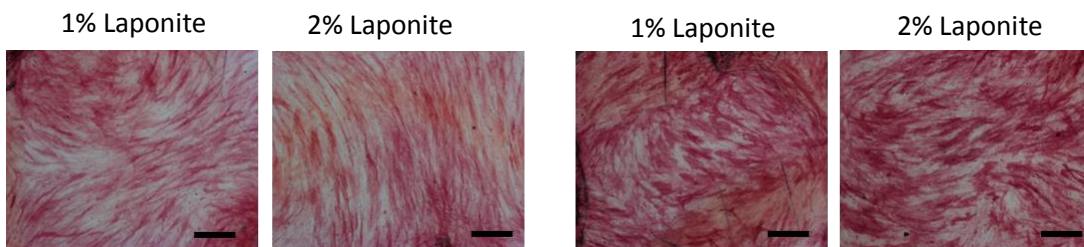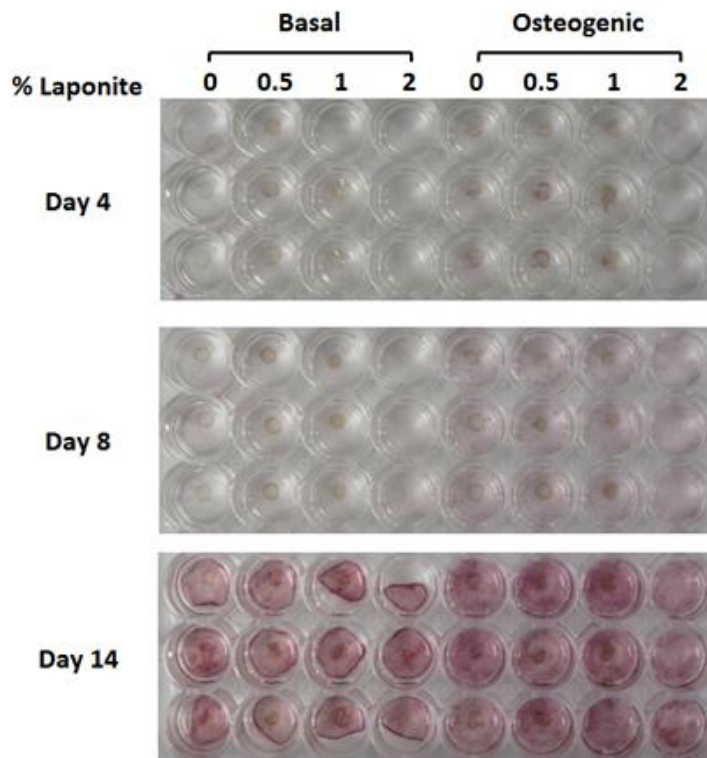
Figure 3-2 Images of HBMSC cultured on films of Laponite at various concentrations and stained for ALP

Images of the cell culture plates at days 4, 8, and 14 are shown above. Lower panel are representative images taken

following 14 days in culture in basal (left) and osteogenic (right) conditions. Scale bar 100μm.
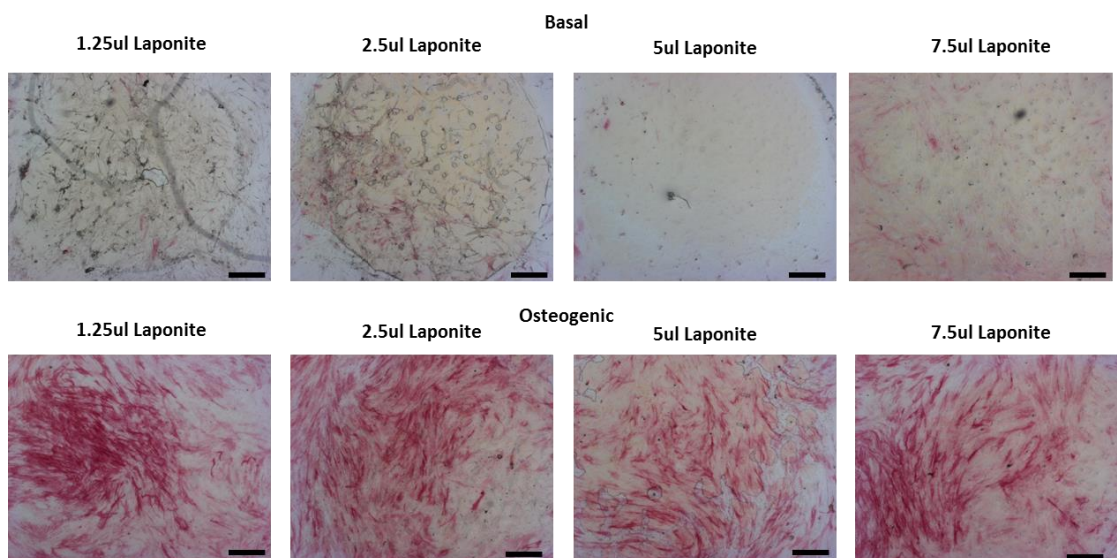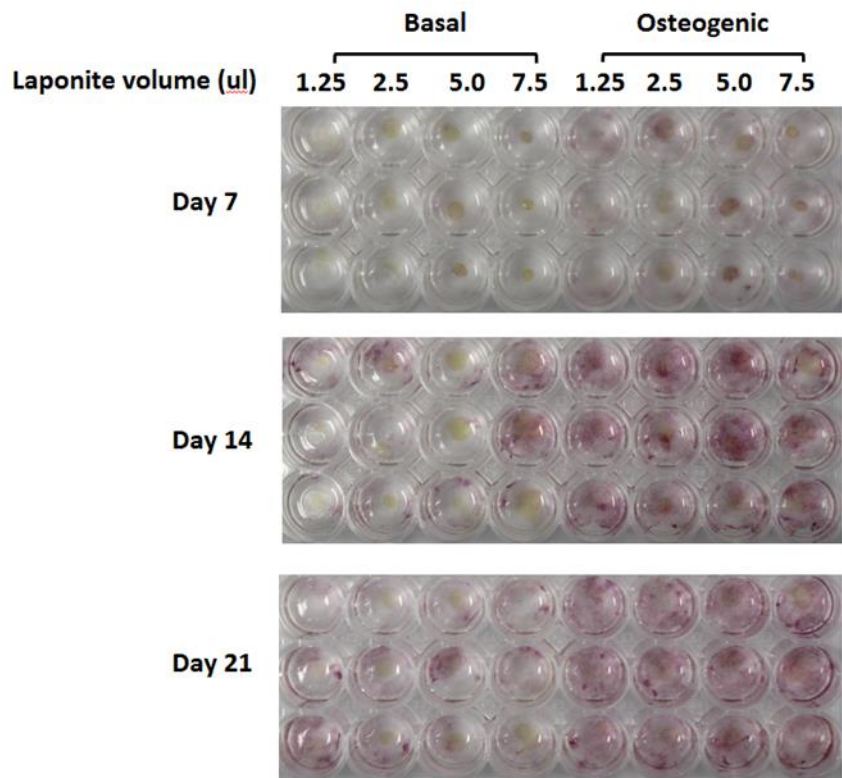
Figure 3-3 Images of HBMSC cultured on Laponite films of various volumes stained for ALP

Images of the cell culture plates at days 7, 14 and 21 are shown above. Lower panels are

representative images taken following 14 days in culture in basal and osteogenic conditions and

stained for ALP. Scale bar is 100μm.
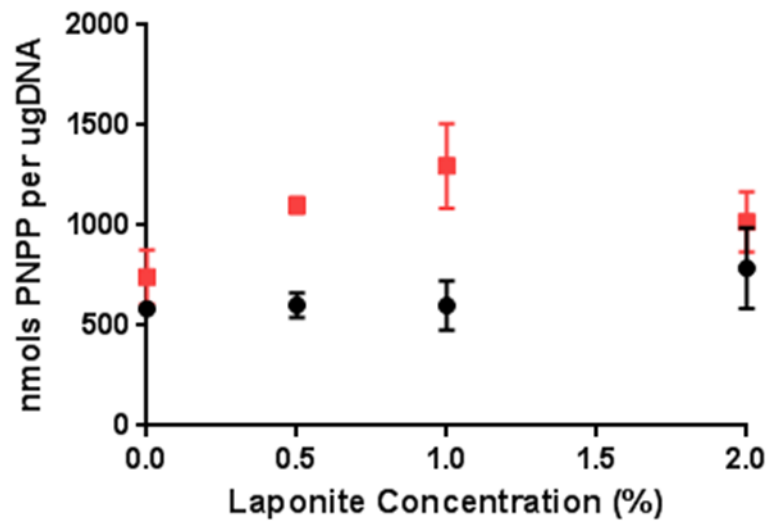
Figure 3-4 Graph of Effect of Laponite concentration on specific ALP activity

ALP staining was performed on HBMSC cultured in basal (black) and osteogenic (red) conditions for 14 days. Graph shows mean ALP activity, error bars show standard deviation. N=3 per group. Error bars show standard deviation.
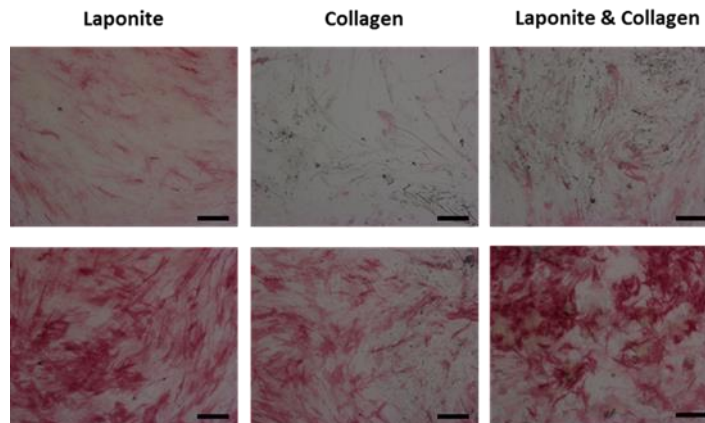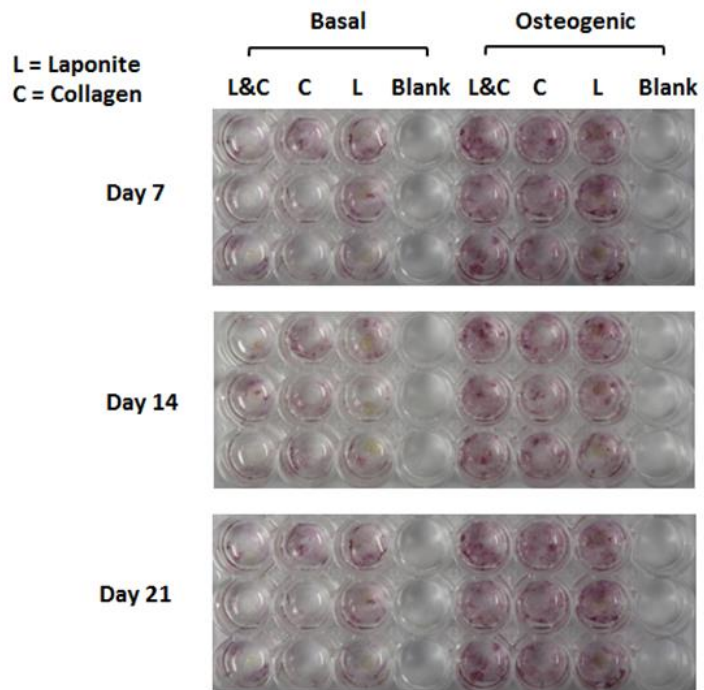
Figure 3-5 Images of HBMSC cultured on films of Laponite and collagen stained for ALP

Images of the cell culture plates at days 7, 14 and 21 are shown above. Lower panels are representative images taken following 21 days in culture in basal (upper row) and osteogenic conditions (lower row) and stained for ALP. Scale bar is 100µm.
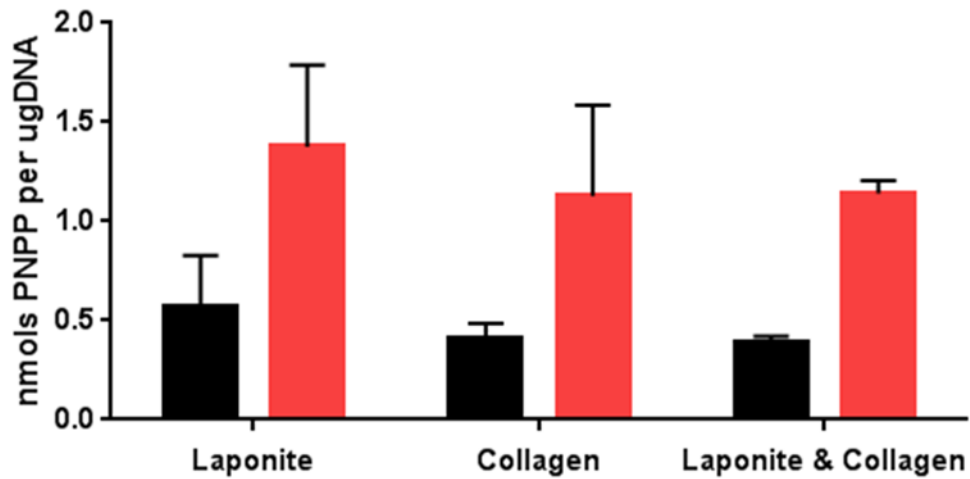
Figure 3-6 Graph showing the effect of Laponite and collagen on ALP activity of HBMSC

ALP stain was performed on HBMSC following 21 days culture in basal (black) and osteogenic (red) conditions. Error bars denote standard deviation. Analysis was performed using two-way ANOVA. No significant difference in specific ALP activity was detected between cultures on Laponite, Collagen or Laponite & Collagen combined. A significant effect of osteogenic versus basal culture conditions was observed (P<0.0001) N=3 per group.

3.6.1.2 Ability of Laponite formulations capable of percutaneous delivery to effectively localise growth factor to bone graft material

In order to assess the ability of percutaneously delivered Laponite to localise growth factor to bone graft, 2.5% Laponite, which is able to pass through a green needle was applied to bone cylinders alone, with fluorescein labelled albumin (FITC) mixed in, or with FITC applied following Laponite administration. Following an interval of 20 seconds the bone cylinders were washed with PBS, and fluorescent microscopy performed. Ability of Laponite gel to localise the surrogate growth factor (fluorescein labelled albumin) was compared with dry Laponite films and a PBS control.

Laponite gel, with FITC mixed into the gel, or applied subsequently, was observed to mediate FITC localisation to the graft surface which remained following PBS wash (figure 3-7). Laponite with FITC mixed in and then dried, also resulted in the persistence of FITC on the graft material. Administration of FITC to graft material coated with dry Laponite was poor at mediating FITC retention.
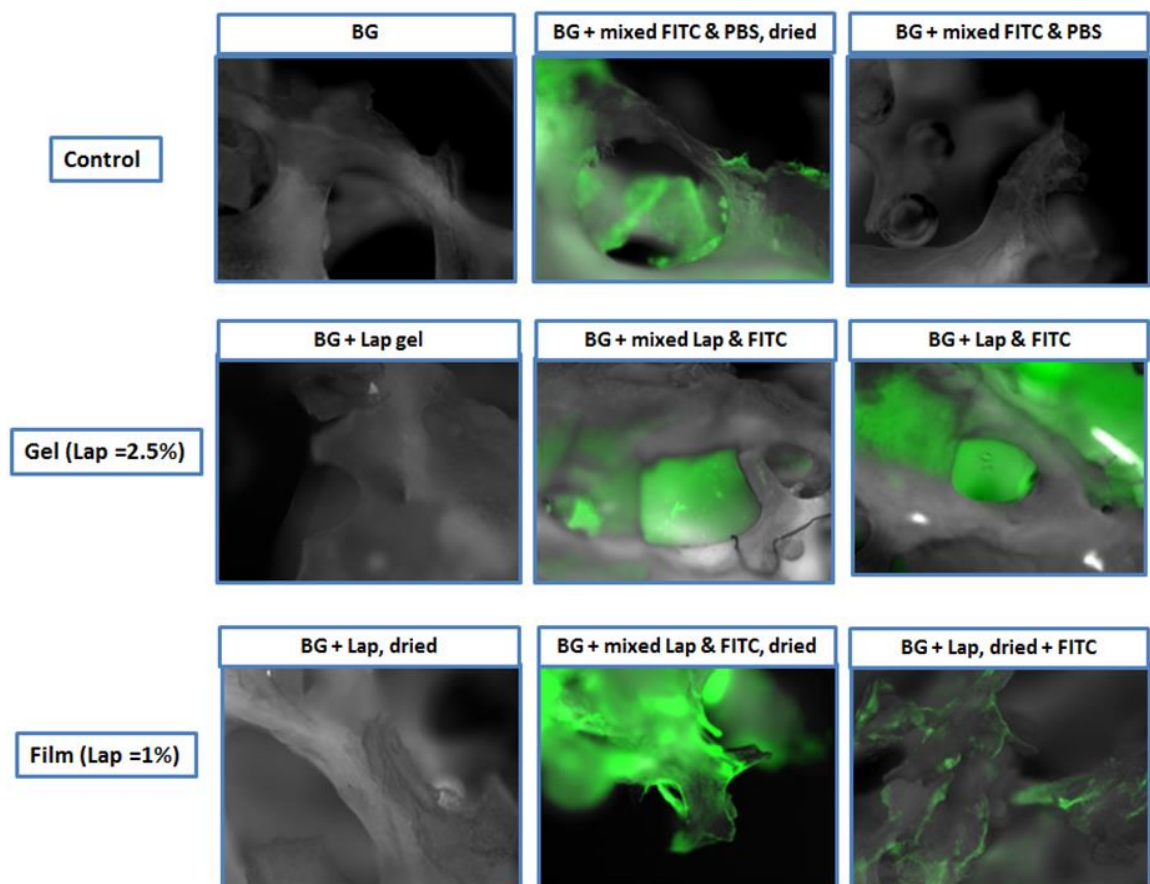
Figure 3-7 Images of graft material and Laponite following protein application

BG= allograft, Lap = Laponite, FITC =fluorescein labelled bovine serum albumin. PBS = phosphate buffered saline

3.6.1.3 Ability of Laponite in gel and dry films states to mediate growth factor delivery and localisation

3.6.1.3.1 Effect of Laponite gel on the activity of VEGF

To assess the ability of Laponite gel to mediate growth factor delivery, VEGF was delivered mixed into, and on the surface of Laponite gel. The endpoint was microtubule formation by HUVEC cells which is known to be proportional to VEGF activity.

VEGF delivered within the Laponite gel, or on the surface of the Laponite gel remained active as demonstrated by the significant increase in microtubule formation compared to HUVEC cultured in the absence of VEGF, as shown in figure 3-8. Maximal microtubule formation was observed with 10ng/ml VEGF when delivered on the surface of Laponite, while the equivalent response was not observed until 1000ng/ml VEGF when mixed into the Laponite.
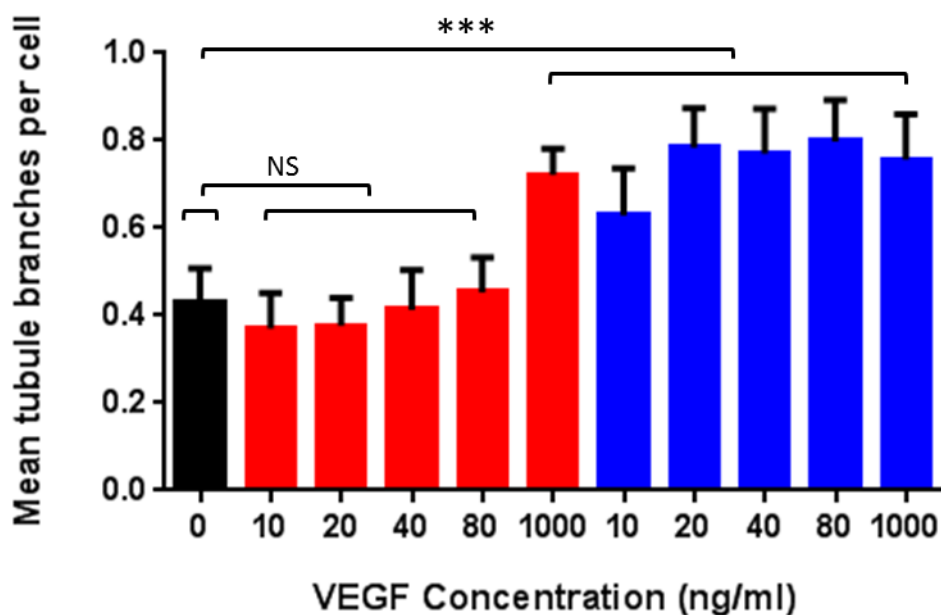
Figure 3-8 Graph of the effect of VEGF in Laponite or media on microtubule formation

Black denotes culture of cells on Laponite in absence of VEGF, red and blue denote presence of VEGF in Laponite gel and media respectively. *** p=<0.0001 for Laponite alone versus: 10-1000ng/ml VEGF in media and 1000ng/ml VEGF in Laponite. NS=No statistically significant difference with Laponite alone versus 10-80ng/ml VEGF in Laponite when subjected to a two way ANOVA test and post hoc testing with Dunnett's multiple comparison test. N=12 per group.

3.6.1.3.2 Effect of Laponite films on ALP activity in C2C12 cells cultured with variable [BMP]

The ability of Laponite in a dry film state to deliver and localise active growth factor was assessed by measurement of ALP activity of C2C12 myoblast cells cultured on dry Laponite films in the presence of exogenous BMP.

On visual inspection an increase in ALP activity of C2C12 cells was observed as BMP concentration increased, with a greater response observed on Laponite compared to TCP as shown in figure 3-8. Quantitive analysis confirmed this with ALP activity shown to be significantly greater on Laponite compared to TCP at 200 and 400ng/ml BMP (p=0.0032 and p=0.006 respectively) as shown in figure 3-9
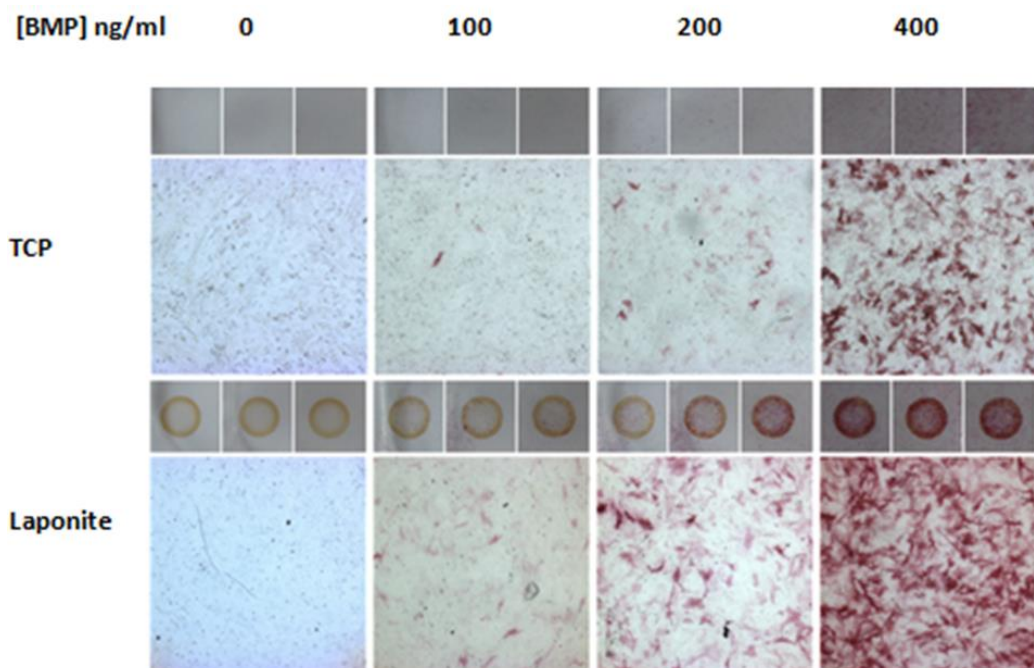
Figure 3-8 Images of C2C12 myoblast cells cultured with BMP on Laponite and TCP.

C2C12 cells were seeded on TCP and dry Laponite films, following 72 hours culture in

media containing a range of BMP concentrations ALP staining was performed. N= 3 per group.
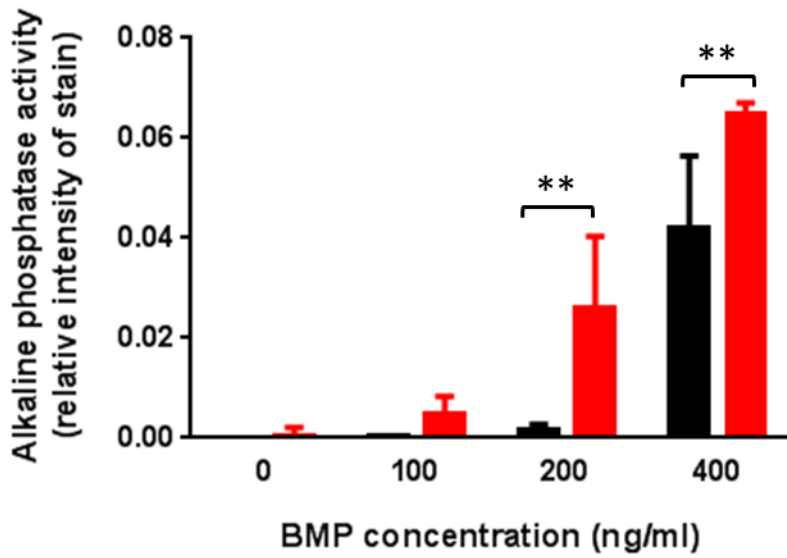
Figure 3-9 Graph showing the effect of Laponite on BMP mediated ALP expression

Graph shows effect of BMP concentration on ALP staining intensity of myoblast cells cultured on Tissue Culture Plastic (black) and Laponite (red). Error bars show standard deviation. ** p=<0.01 Comparison of ALP activity at each BMP concentration on Laponite was with that on TCP was performed with a two way ANOVA test and Sidak's test for post hoc testing. N = 3 per group.

3.6.1.3.3 Effect of Laponite films on ALP activity in C2C12 cells at variable seeding densities

To distinguish between an effect of Laponite on cell seeding density or ALP staining per cell, the effect of Laponite on initial cell seeding density, cell density following culture, and ALP staining intensity per cell were assessed as shown in figures 3-10 to 3-12. At each of the three cell seeding densities tested, greater numbers of cells were present following culture on TCP compared to Laponite. Furthermore, ALP staining per cell was significantly greater on Laponite compared to TCP when seeded at 25, 50 and 100×10^5 per cm^2 (p <0.01, p=<0.001, p<0.01 respectively) as shown in figure 3-12.
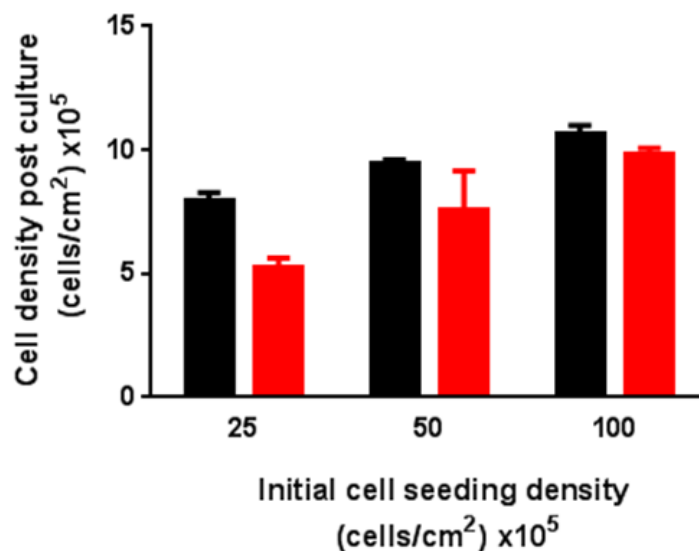
Figure 3-10 Graph of effect of Laponite on cell density

Graph of cell density following 72 hours culture on TCP (black) and Laponite (red) according to initial cell seeding density. Error bars show standard deviation. N = 3 per group.
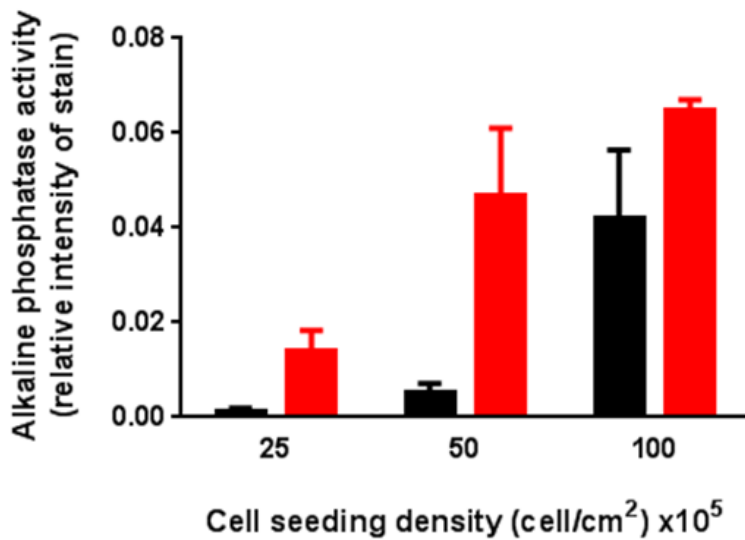
Figure 3-11 Graph of the effect of cell density on ALP activity

Graph of ALP staining intensity following 72 hours culture on TCP (black) and Laponite (red) according to initial cell seeding density. Error bars show standard deviation. N = 3 per group.
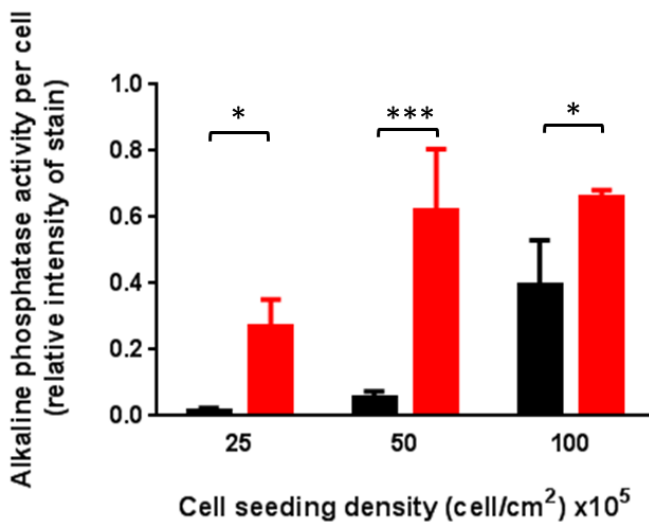
Figure 3-12 Graph demonstrating effect of Laponite on ALP activity per cell

Graph shows ALP staining intensity per cell following culture on TCP (black) and Laponite (red) according to cell density. Error bars show standard deviation. * p=<0.05, *** p=<0.001

Comparison of mean ALP activity on TCP and Laponite was made using a two way ANOVA test and Sidak's test for post hoc testing was. ALP activity per C2C12 cell was significantly was greater on Laponite compared to TCP, with p=0.0286, p<0.001, and p=0.0217 for 25, 50, and 100 x10^5 cells/cm^2 respectively. N = 3 per group.

3.6.1.3.4 Effect of Laponite films on ALP activity in C2C12 cells cultured with incubated BMP

In a further experiment to assess the effect of Laponite film on the activity of BMP over time, BMP was applied to TCP and Laponite, incubated for various time periods, and C2C12 cells were seeded, cultured, and ALP activity assessed.

Greater ALP activity was seen on visual inspection when C2C12 cells were cultured on Laponite films compared to TCP, with BMP incubated for 2, 3, and 4 hours, as shown in figure 3-13. This was confirmed with image analysis and comparison using a two way ANOVA test and Sidak's test for post hoc testing. ALP activity on Laponite was significantly greater than TCP at 2, 3, and 4 hours BMP incubation (p=0.013, p=0.0124 and p=0.0004 respectively) as shown in figure 3-14.
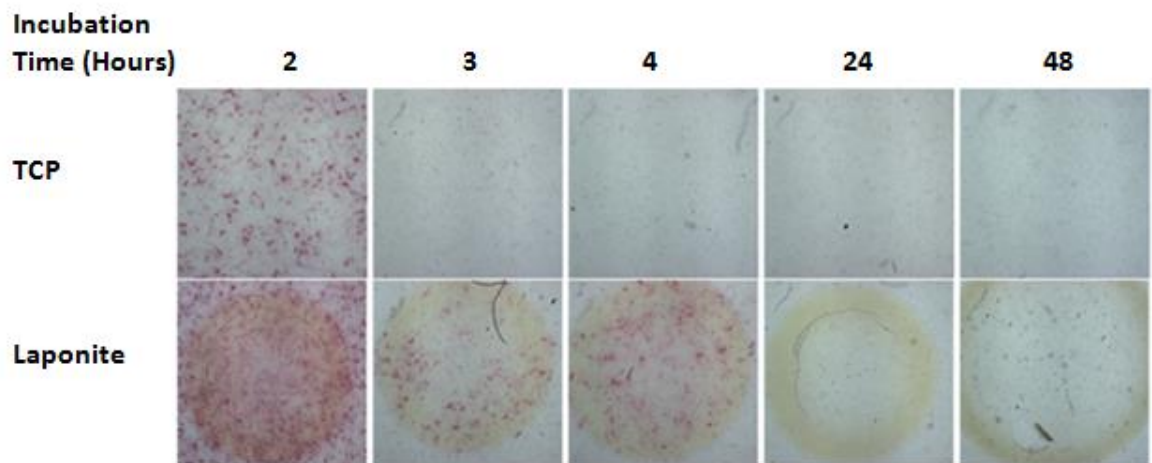
Figure 3-13 Images of C2C12 cells cultured with incubated BMP on Laponite and TCP.
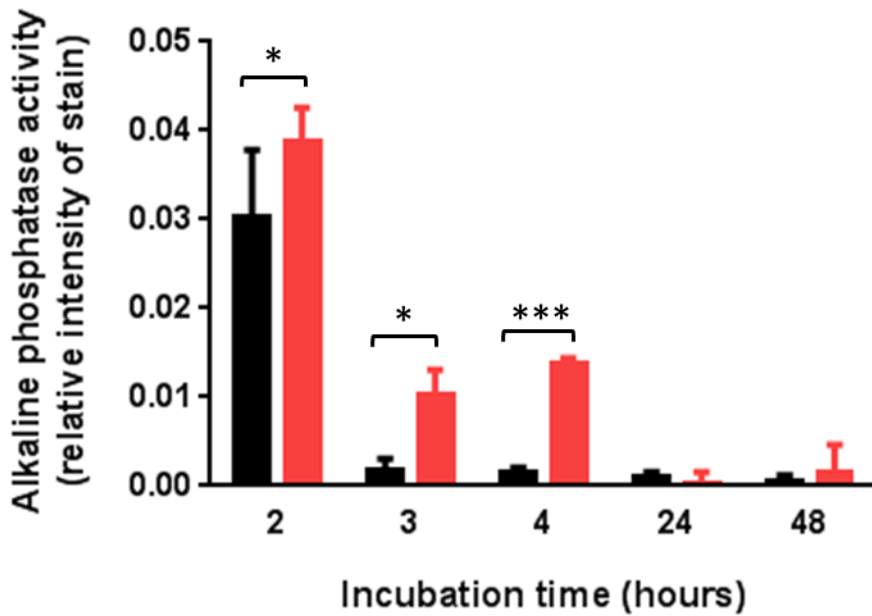
Figure 3-14 Graph of effect of BMP incubation with Laponite on ALP activity

Graph shows ALP staining intensity of C2C12 cells seeded on TCP (black) and Laponite (red) on which BMP has been incubated for various time periods. Error bars show standard deviation. * p=<0.05, *** p=<0.001. Two way ANOVA test and Sidak's test for post hoc testing were performed to analyse ALP activity on Laponite to TCP at 2, 3, and 4 hours BMP incubation with p=0.013, p=0.0124 and p=0.0004 respectively. N=3 per group.

3.7 Discussion

Cytocompatibility of Laponite was tested with HBMSC, the most relevant cell group for clinical translation, over a 3 week period using clinically relevant concentrations of Laponite. Laponite had no effect on cell viability or phenotype. Laponite was found to be cytocompatible with HUVECs and C2C12 cells. Such cellular compatibility has also been observed in previous studies using Laponite (Dawson et al., 2011, Gaharwar et al., 2013, Gaharwar et al., 2011a, Gaharwar et al., 2011b, Chang et al., 2010, Wang et al., 2014, Wang et al., 2012). While these studies provide useful information, Laponite processing, and cell types used varied greatly between these studies rendering direct comparisons impossible. In particular, Gaharwar, Wang (2011), and Chang, (Gaharwar et al., 2011a, Gaharwar et al., 2011b, Wang et al., 2011, Chang et al., 2010) used Laponite as a cross linker in gels based on polymerization of polyethylene glycol, whereas Wang (2014) (Wang et al., 2014) used sintering, to produce Laponite ceramic discs, and Wang 2012 (Wang et al., 2012) used electrospinning to produce PLGA/Laponite fibres. We found HBMSC, C2C12, and HUVEC cells able to grow in the presence of 0.01μg/ml and 6.23μg/ml Laponite in the form of a dry film and gel respectively. Dawson (Dawson et al., 2011) also demonstrated HUVEC viability upon Laponite gel at equivalent Laponite concentrations, and furthermore demonstrated 28 day survival of HBMSC encapsulated in 2.5% Laponite with fibronectin and sucrose as 10% fraction, and applied drop wise to culture media. Wang (Wang et al., 2014) reported good cytocompatibility of Laponite when culturing rat MSC on sintered Laponite discs, however; 8% of RBC haemolysed following contact with un-sintered Laponite. The authors did not directly report the Laponite concentration used in the haemolysis assay, however it is likely to be in the region of 450mg/ml. Chang 2014 (Chang et al., 2010) mixed Laponite with poly(ethylene-glycol) diacrylate and applied ultraviolet light to produce a hydrogel. HBMSC were delivered prior to, and after UV mediated cross linking, with good cell viability in resulting 2D and 3D culture respectively. Similarly, Gaharwar (Gaharwar et al., 2011b) reported excellent cell viability with MCT3-E1 subclone 4 mouse preosteoblast cells cultured on a polyethylene-oxide/Laponite, and also following exposure to Laponite solutions at different concentrations ranging from 0 to 35mg/ml, with viability at 24 hours between 84-92%. In a further study, Gaharwar (Gaharwar et al., 2013) found Laponite in excess of 1mg/ml resulted in a reduction in metabolic activity, with 4mg/ml resulting in a 50% decrease in metabolic activity of HBMSC. No published studies have demonstrated poor cellular compatibility of Laponite in the magnitude of concentrations used in our investigations, i.e. 0.05μg/ml to 6.23μg/ml.

No osteogenic effect of Laponite, as assessed by ALP activity, on HBMSC was found. Wang (Wang et al., 2014) demonstrated a significant increase in specific ALP activity in rat BSC cultured on sintered Laponite compared to TCP. It is likely that the effect of sintered Laponite, a rigid ceramic

is not directly comparable to the Laponite film in our experiments. Gaharwar (Gaharwar et al., 2013) reported no difference in ALP activity of HBMSCs in basal media at 0, 1, 10 and 100µg/ml of Laponite. However, in contrast to our findings, addition of silicate to HBMSCs cultured in osteogenic media, did result in an increase in ALP activity.

This difference in osteoinductivity could be explained by presence of ß-glycerol-phosphate (not used in our experiment, or the manner in which Laponite was applied, directly into the media, compared to presence as a dry film. The standard operating practice within the Bone and Joint Research Group is to use ascorbic acid and dexamethasone as osteoinductive media without addition of ß-glycerol-phosphate, and this reliably results in osteoinduction as shown in the results presented in this manuscript. Addition of ß-glycerol-phosphate alone has been shown to promote osteoinduction (Coelho and Fernandes, 2000); however when used to stimulate osteoinduction typically it is used in combination with ascorbic acid and dexamethasone. ß-glycerol-phosphate promotes mineralisation and/or serves as a local source of inorganic phosphate. As the Osteogenic effect of Laponite was dependent on the presence of ß-glycerol-phosphate this could suggest some form of interaction, this is a distinct possibility as previous studies have used ß-glycerol-phosphate in combination with polymers such as chitosan to modulate hydrogel behaviour (Ding et al., 2013).

Cell viability was not measured directly using a cell metabolic assay such as cell tracker green (CTG) or ethidium homodimer (EH), instead, viability has been derived from ALP staining which is dependent on ALP production, possible only in living cells. Direct measurements of cell viability with methods such as CTG and ET are technically not possible, as the dyes are taken up by the Laponite, resulting in generalized fluorescence (Hagerman et al., 2002) and (Images in Appendix A).

No effect on HBMSC was observed following combination of Laponite with Collagen or addition of type 1 collagen alone. While type 1 collagen is major component of bone, preparation and addition of solubilised in acetic acid resulted in rapid precipitation upon addition to tissue culture media (see figure 3-5). In this form it may be unable to contribute to cell migration or osteogenesis, a result which is supported by published literature (Linsley et al., 2013).

To enable percutaneous delivery in the clinic, the needle must be of sufficiently narrow gage to facilitate injection without inflicting undue distress, and to avoid creating a channel of a magnitude which could increase the risk of infection. Following injection, the delivery vehicle must be capable of maintaining the growth factor at the target site. Thus, Laponite gel at 2.5%, which is able to pass through a 21G green needle was employed. This gage of needle is commonly used in clinical practice for percutaneous administration of medicines, including haematoma

blocks in distal radius fractures. Laponite gel was able to localize and retain FITC labelled albumin to the bone graft surface despite undergoing PBS washes. This mimics the *in vivo* environment, in which bleeding and fluid flows would be expected at the fracture site. This non-quantitative observation of the ability of Laponite gel to remain at the target site is supported by Gaharwar's findings, in which he described the addition of Laponite, in this case to a polymer gel resulted in enhanced adhesiveness (Gaharwar et al., 2011b).

Laponite gel was found to be capable of mediating delivery of active VEGF; however a greater concentration of VEGF was required when mixed into the gel, to produce an effect equivalent to VEGF on the surface of Laponite. From the results of this experiment in isolation it is not possible to define if this effect is due to permanent inactivation of VEGF by the clay, or reversible binding of VEGF by clay, resulting reduction of VEGF available to the cells on the surface of the gel. Dawson and colleagues also found Laponite gel to be capable of mediating VEGF delivery (Dawson et al., 2011).

Laponite in the form of dry films were observed to localise BMP activity. This is of great potential significance to clinical translation, as fractures or in particular synthetic bone graft material could easily be coated with dry Laponite, thus facilitating localisation of BMP to the desired site. C2C12 cells cultured in BMP at 200-400ng/ml on Laponite films expressed greater ALP activity than those cultured on TCP. In addition, when incubated for 2-4 hours, BMP mediated greater ALP expression in C2C12 cells in the presence of Laponite films compared to TCP.

We have demonstrated the ability of Laponite in both a gel and film state to be capable of localising growth factor in an active form. This was achieved without recourse to techniques involving growth factor binding, which through an effect on molecular weight and charge of the BMP molecule could themselves alter the results. Assays used to detect BMP and VEGF activity, namely ALP expression by C2C12 cells and microtubule formation by HUVECs, respectively are validated and widely accepted methods (Liang et al., 2014, Katagiri et al., 1994).

A limitation of this study is that in cases where ALP staining intensity was shown to be greater on Laponite, the exact cause cannot be fully determined. Whether the effect of Laponite is mediated via localization of BMP, an effect on BMP activity or degradation rate of BMP remains unknown.

Whilst we tested the ability of Laponite to deliver and localise two growth factors which are pivotal in bone formation and fracture healing, the molecular weight and isoelectric points of VEGF (28kDa IE 8.5) and BMP-2 (32kDa IE 8.5) are almost identical, thus it could be that a growth factor of differing molecular weight and isoelectric point may not be amenable to localisation and delivery by Laponite. This would however seem unlikely, as a previous study (Dawson et al., 2011)

found identical protein adsorption and release profiles from Laponite of albumin (65kDa IE 4.7) and lysozyme (14.3kDa, IE 11), two proteins which differ substantially in molecular weight and isoelectric points .

Null Hypothesis

Laponite is cytotoxic and will be unable to deliver and localise active growth factors

3.8   Conclusion

We have demonstrated that Laponite is cytocompatible within the range of concentrations tested, and these findings are supported in the literature. In our study Laponite alone was not shown to be capable of mediating osteoinduction of HBMSC cultured in basal conditions, nor was an additional effect of Laponite on HBMSC cultured in osteogenic conditions observed. While our results of Laponite on HBMSC in basal conditions are supported in the literature, our result in osteogenic media contrasted to published results. Laponite gel (2.5%), capable of percutaneous delivery, did localise protein on bone graft material. Our results demonstrated that Laponite, in the form of a gel, and a dry film is capable of delivering and localising VEGF and BMP respectively

In summary, Laponite is biocompatible, able to deliver and localise active growth factors, and may or may not have some intrinsic effect on osteoinduction of HBMSC in osteogenic conditions. These *in vitro* findings suggest Laponite shows potential as a growth factor delivery vehicle, however, the degree to which these results translate to the *in vivo* environment, in which fluid flows and mechanical stimulation are present, must be investigated.

The null hypothesis can therefore be rejected.

Chapter 4: The potential of Laponite to enhance BMP mediated bone formation *in vivo*

4.1   Introduction

As detailed in the introduction (1.10.1.2), an injectable growth factor delivery vehicle could be applied to stimulate fracture healing without requirement for open surgery which current delivery methods require. Laponite exists as a thixotropic hydrogel up to concentrations of around 2.5%, beyond which Laponite becomes relatively solid. With sheering, Laponite hydrogel can pass through a standard 21 gage needle, and gels upon exit from the needle, rendering it potentially suitable for percutaneous clinical application.

A number of studies have explored methods such as application of bone marrow aspirate (Fischer et al., 2013), or BMP (Buttermann, 2008)to enhance the osteogenicity of allograft and synthetic bone graft substitutes. Laponite in the form of a dry clay film applied to the graft may facilitate greater growth factor localisation, and hence osteogenicity, than a Laponite gel, as such a composition is likely to produce a more even distribution of growth factor. Furthermore, following application, dry Laponite film is stable. Thus graft material coated with a dry Laponite film during manufacture could be readily transported and stored, offering potential development as an off the shelf product, ready for use with minimal additional preparation.

As noted in the introduction (1.10.1.1), lack of an efficient method of delivering BMP has necessitated the use of large doses in clinical practice which have resulted in severe adverse effects (Chrastil et al., 2013).

In vitro studies presented in chapter 3 demonstrated the ability of Laponite, in the form hydrogel or dry film, to mediate growth factor delivery. The effect of fluid flows and application of mechanical force *in vivo* upon the Laponite film and gel is unknown. As such it remains unclear whether Laponite presented as a gel or dry film would offer superior growth factor delivery, or if there would be any difference between application of a gel or film.

In this chapter the primary aim was to establish if Laponite in the form of a hydrogel or a dry film is capable of enhancing BMP-mediated bone formation, and if there is any difference between the two approaches. The secondary aim was to investigate if use of Laponite gel could reduce the dose of BMP required to stimulate bone formation *in vivo*. In the following sections the experimental methodology to investigate these aims is described:

An ectopic murine model was selected as such models have been firmly established in the investigation of hydrogel mediated growth factor delivery, and bone formation (Gibbs et al.,

2014a). Acellular allograft material was selected as the scaffold material given the clinical relevance and ready availability.

Selection of an appropriate dose of BMP to test is crucial because in humans high doses have been associated with significant side effects (Tumialán et al., 2008). Furthermore, high doses of BMP could result in saturation, thereby masking any effect mediated by Laponite. In a previous subcutaneous murine study Yamamoto (Yamamoto et al., 2003) applied BMP-2 in the range of 0.5 to 5μg per mouse, and found 1μg to be as effective as 5μg in mediating bone formation. Both 1 and 5μg resulted in greater bone formation than smaller doses. In clinical practice BMP has been used at 6-12mg per patient in treatment of tibial fractures (Govender et al., 2002). When these doses are adjusted per kg, assuming the average mouse and human weight 0.025kg and 75kg respectively, BMP given was 0.04-0.2mg/kg in the murine study, and 0.08-0.16mg/kg in human study. We therefore decided to apply a dose of 1μg per allograft, equating to approximately 0.1mg/kg, which is within the range of the doses used experimentally in mice, and in clinical practice. This equates to a dose per volume of allograft of approximately 20μg/ml.

In order to perform a sample size calculation data were selected from a study reporting bone mineral density following intra muscular injection of a BMP-2 laden hydrogel in rats (Hulsart-Billström et al., 2011). Mean bone mineral density of ectopic bone formed was 350mg/cm^3, with a Standard Deviation of 32. A useful clinical effect was postulated to be the doubling of the effect when BMP was delivered in the presence of Laponite. Such an effect of Laponite on BMP has been described for other hydrogels (Boerckel et al., 2011).

A sample size calculation was performed assuming: standard deviation (σ)=32 and means of 350 and 700 for control treatment group respectively, adjusted for 80% power ($Z_{ß}$=0.84), and significance at 95% ($Z_{\alpha/2}$=1.96) using the standard equation:

$$\text{Sample size (n)} = 2\ \sigma^2\ (Z_{ß}+Z_{\alpha/2})^2 / = (\text{difference in mean})^2$$

On this basis a sample size of 6 samples per group was determined.

In order to investigate the ability of Laponite gel to reduce the dose of BMP required to stimulate ectopic bone formation *in vivo,* a subcutaneous murine model was also used; however Collagen sponge was used in place of Allograft. The reason for this was two-fold; firstly, collagen sponge is

used in current clinical practice to deliver BMP. Secondly, determination of bone formation in Allograft is complex, as the total bone volume, which is easily derived from micro CT, is the net of both bone formation and bone absorption, differentiation of the contribution of these two processes is technically challenging., whereas total bone within the collagen sponge represents the volume of new bone formed.

This study was intended to investigate if BMP dose required to mediate bone formation *in vivo* was reduced in the presence of Laponite. To achieve this it was critical that BMP was applied at sufficient quantity to produce a response, but below the levels at which the response to BMP was saturated. A number of studies (Luca et al., 2010, Kim et al., 2014, Pelaez et al., 2014, Wang et al., 1990, Boerckel et al., 2011) reporting bone formation following BMP delivery *in vivo* were reviewed, and doses of BMP described were translated into dose per defect volume to permit comparison. Boerckel (Boerckel et al., 2011) reported an almost linear increase in bone formation when BMP was increased from 0.6μg/ml to 6μg/ml and delivered in a collagen sponge. BMP dose used in this study was based on the data from Boerckel (Boerckel et al., 2011), and the results of our Allograft/BMP/Laponite study in Part 1 of this chapter.

For the sample size calculation we used data from the first part of this experiment. Mean bone volumes were 20mm^3 and 12mm^3, in Laponite/BMP group and Allograft respectively with a Standard Deviation of 11. With α =0.05, and 80% power, a sample size of 19 per group was determined as adequate to detect any significant difference. In order for the experiment to be sufficiently powered and account for mice not completing the study we used 24 for each test group. A single mouse was used as a blank control (n=6) as it is widely accepted that subcutaneous implantation of a collagen sponge does not result in bone formation in the absence of osteoinductive agents.

4.2   Aim

To assess the ability of Laponite to enhance BMP-2 mediated bone formation *in vivo*.

4.3   Null Hypothesis

Use of Laponite to deliver BMP will not result in greater bone formation compared to BMP applied alone or with an alternative growth factor delivery vehicle.

4.4   Objectives

1) To establish if Laponite in the form of a hydrogel or a dry film is capable of enhancing BMP-mediated bone formation *in vivo*.

2) To investigate if Laponite gel can reduce the dose of BMP required to stimulate ectopic bone formation *in vivo*.

4.5   Methods

4.5.1.1   Part 1: To establish if Laponite in the form of a hydrogel or a dry film is capable of enhancing BMP-mediated bone formation *in vivo*.

Outline

Acellular allograft cylinders were prepared; and Allograft bone volume measured using micro CT. Laponite was applied to the acellular allograft cylinders as a dry film or hydrogel, with and without BMP as shown in figure 4-1 . Allograft was subcutaneously implanted into nude mice; bone volume was assessed at 4 weeks by micro CT, and histological analysis performed.

Experimental Groups (n=6 per group)

Control groups   **Laponite dry film groups**

Allograft alone   Allograft + dry Laponite

Allograft + BMP   Allograft + dry Laponite + BMP

Laponite hydrogel groups

Allograft + Laponite gel

Allograft + Laponite gel/bmp mix

Allograft + Laponite gel + BMP
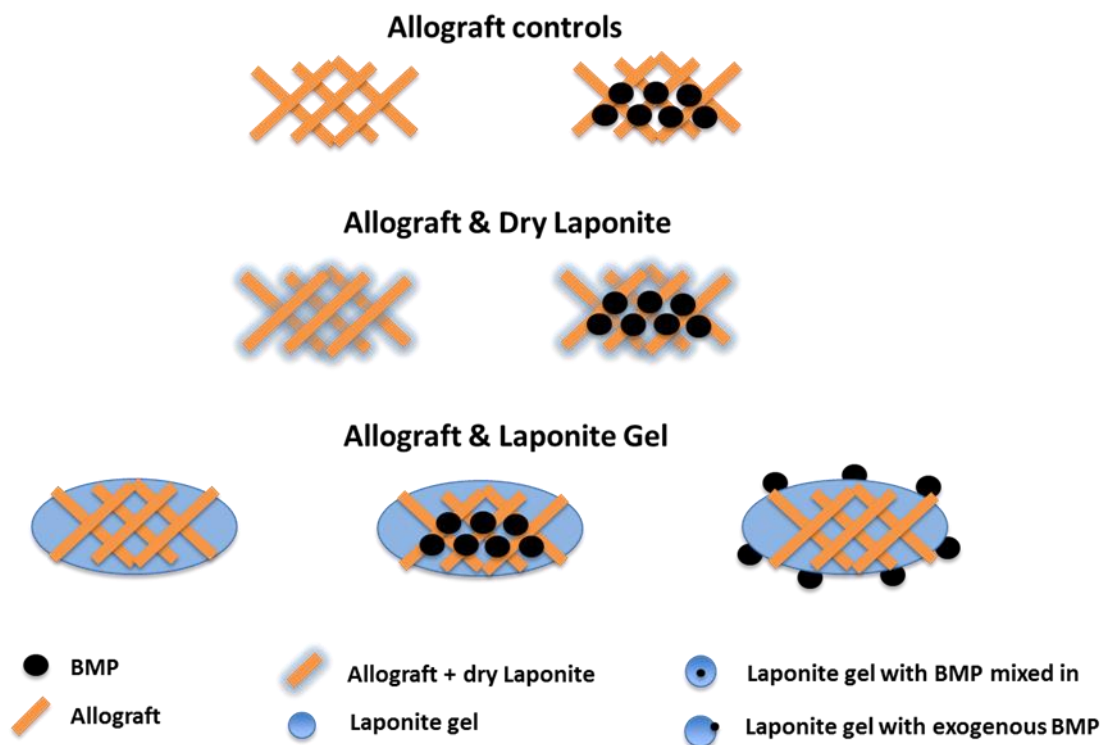
Figure 4-1 Diagram of allograft preparations

BMP dose

When BMP was applied a dose of 1μg per allograft cylinder was used.

Allograft preparation

Allograft cylinders were prepared from donated human femoral heads. A hollow drill piece with internal diameter of 4mm was used to produce 42 cylindrical bone segments.

Bone cylinders were 6-7mm long, a scalpel was used to remove all subchondral bone and produce cylinders approximately equal in length. Cylinders were subsequently immersed in hydrogen peroxide (10%) in a falcon tube, and rotated for 48 hours. During this period hydrogen peroxide was changed 4 times, following this the allograft cylinders were washed 4 times in PBS, and dried in a tissue culture hood. Subsequent preparation from the experimental groups was as follows:

Allograft alone

No additional preparation prior to implantation.

Allograft + BMP

For BMP application: 7.5μl BMP (1μg/μl) mixed with 142.5ul PBS in an Eppendorf, and 20μl applied to each allograft immediately prior to *in vivo* implantation.

Allograft + Dry Laponite film

20μl 1% Laponite was applied to each allograft cylinder with a pipette; allograft was then dried in a tissue culture hood.

Allograft + dry Laponite + BMP

Allograft and dry Laponite films were produced as for allograft + dry Laponite, and then BMP applied *in vivo* as for allograft + BMP.

Allograft + Laponite gel

20μl 2.5% Laponite gel was applied to each allograft cylinder *in vivo* immediately prior to implantation.

Allograft + Laponite gel/bmp mix

7.5μl BMP (1μg/μl) was mixed with 142.5μl 2.5% Laponite gel in an Eppendorf, and 20μl applied to each allograft cylinder with a pipette *in vivo* immediately prior to implantation. BMP is considered endogenous to the Laponite.

Allograft + Laponite gel + *in vivo* **BMP**

7.5µl BMP (1µg/µl) was mixed with 30µl PBS. 20ul 2.5% Laponite was applied to each allograft *in vivo* immediately prior to implantation, following this 5µl of BMP/PBS solution was applied to each allograft. BMP is considered exogenous to the Laponite.

Surgical procedure

Full details are found in chapter 2. Briefly, a dorsal midline incision was made, and blunt subcutaneous dissection used to create 6 pockets. Three allograft cylinders of the same experimental group were implanted on the left side, and three cylinders from another experimental group were implanted on the contralateral side. Following implantation wounds were closed with surgical clips.

Micro Computed Tomography scanning

Micro CT of the allograft cylinders was performed prior to implantation, with the following parameters: 0.5mm Aluminium filter, voltage 50kV, current 500μA, and pixel size 9μm. At the 4 week endpoint following euthanasia allografts were removed and scanned again with the same settings.

Micro Computed Tomography image reconstruction

Reconstruction of the images was performed using NRecon. Global settings were: Smoothing 2, Ring artefact reduction 5, beam hardening 40%, and output data 0 to 0.08.

Two methods of Quantitative analysis of micro CT reconstructions were performed:

1) Calculation of the difference between allograft bone volume prior to and after implantation

This method produces the mean change in bone volume and is derived directly from the initial CT dataset.

2) Automated co registration of 3D images of allograft pre and post implantation, and calculation of volume of bone formed and absorbed.

Two Dataviewer programs are opened simultaneously. Sagittal, coronal and trans axial images of allograft pre and post implantation are loaded as shown in figure (4-2). The allograft in subsequently rotated in 3 planes to match alignment in pre and post implantation images as shown in figure 4-3.

Following orientation in Dataviewer, pre and post implantation images are loaded using 3D co registration feature (Figure 4-4 left). Initially the images are manipulated manually to obtain approximate matching of pre and post implantation images, followed by manipulation by Dataviewer software, resulting in matching of pre and post implantation images (Figure 4-4 right).
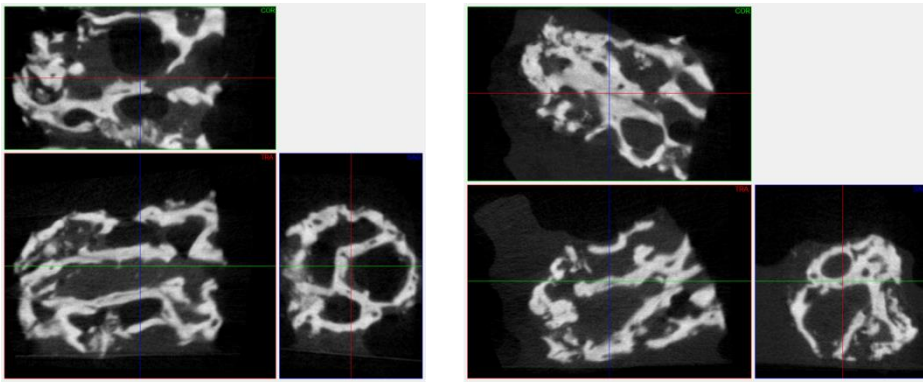
Figure 4-2 Sagittal, coronal and trans axial images of allograft pre (left) and post (right) implantation
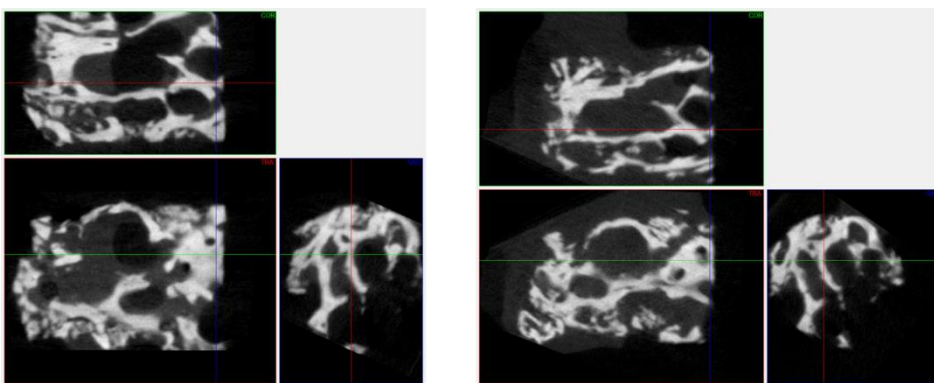
Figure 4-3 Sagittal, coronal and trans axial images of allograft pre (left) and post (right) implantation, following orientation in Dataviewer.
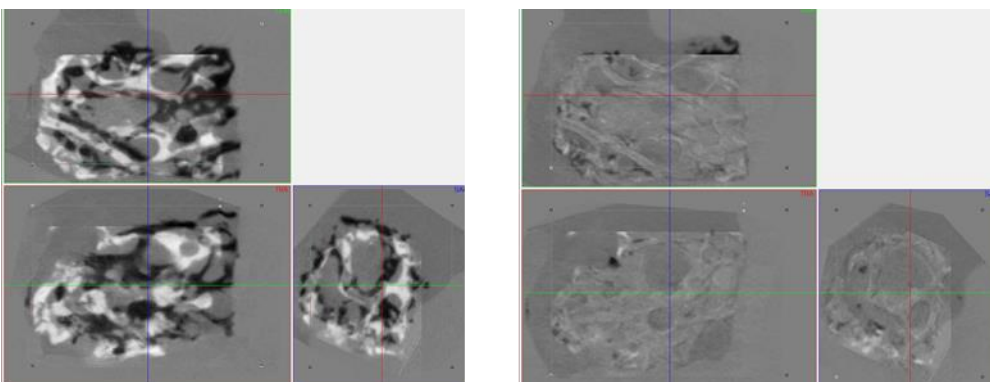
Figure 4-4 Sagittal, coronal and trans axial images of allograft during coregistration

Pre implantation images are loaded as the reference, and post implantation as target images (left). Pre implantation allograft is white, post implantation scaffold is black. Areas of overlap are coloured grey. Corresponding images on the right are taken following manual and automated co registration.

At this stage the co registered images are loaded into CT An. Region of interest is drawn selecting the co registered image, but avoiding artefacts resulting from the image of adjacent grafts .
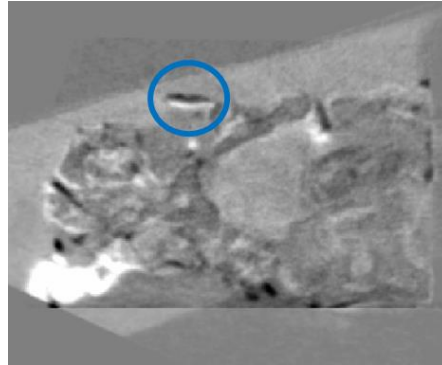
Figure 4-5 Movement artefact on coregistered image

Coregistered images following loading into CT An. A movement artefact is seen(circled).

Finally analysis was performed in CT An with the thresholds 238-255, to quantify volume of new bone formed, visualised as white, and 1-62, to quantify bone resorption visualised as black. A further analysis was performed on the same region with thresholds 100-255, on the reference (pre implantation) allograft to quantify initial allograft bone volume. Subsequently, results were expressed as: bone absorption and formation as a percentage of initial allograft bone volume, and as a ratio of bone formation to bone absorption.

Histology

Following euthanasia, allograft material blocks were removed from the nude mice and placed in 4% Paraformaldehyde (PFA). Blocks were then embedded in wax, sectioned using a microtome, and stained as described in chapter 2. Following slide mounting microscopy was performed.

4.5.1.2   Part 2: Investigation into the ability of Laponite gel to reduce the dose of BMP required to stimulate ectopic bone formation *in vivo*.

Outline

Alginate and Laponite hydrogels containing BMP at high and low concentrations was applied to Collagen sponge cylinders and implanted subcutaneously in mice. Micro CT was performed on day 0 and at 1, 2, 4, and 6 weeks *in vivo*. At 8 weeks the mice were culled, a final micro CT scan was performed, samples removed and histological analysis performed.

Experimental Groups (5) (n=24 per group, except for control where n=6)

1) Laponite and high dose bmp (0.35µg per sponge)   (7µg/ml per volume of sponge)

2) Laponite and low dose bmp   (0.0286µg per sponge)   (0.5µg/ml per volume of sponge)

3) Alginate and high dose bmp (0.35µg per sponge)   (7µg/ml per volume of sponge)

4) Alginate low dose bmp   (0.0286µg per sponge)   (0.5µg/ml per volume of sponge)

5) Collagen scaffold only

Sponge and gel preparation

Type 1 collagen sponge sheet was purchased from Medtronic (InductOS kit). A skin biopsy punch was used to produce 102 identical collagen cylinders 4mm diameter and 4mm depth.

500µl and 450µl of 2% Laponite and 2% alginate was transferred to 4 separate Eppendorf's under sterile conditions. 3.5ul of BMP (1ug/1ul) was added to the 500µl of Laponite and 500µl of Alginate and mixed using a vortex. 40µl of the gel/BMP mix was transferred to the 450µl of the respective Laponite and Alginate gels. This produced 460µl and 490µl of Laponite and Alginate gels containing BMP at high (7µg/ml) and low (0.57µg/ml) concentration.

Each mouse received 3 high dose and 3 low dose scaffolds (except the control mouse). For each mouse the gel was made separately whilst the mouse underwent anaesthesia, with BMP kept on dry ice throughout the experiment.

140µl of each gel was transferred into individual wells in a 96 well plate, for each mouse 3 wells of gel at a high dose and low dose were filled. Collagen sponges were compressed and placed separately into the individual wells. A period of 5 minutes was permitted to allow the sponge to absorb the BMP laden gels.

Residual gel measurement

Following implantation of the collagen sponge, volume of gel remaining in the 96 well plates which had not been absorbed by the collagen sponge was measured, and recorded.

Surgical procedure

Full details are found in chapter 2. A dorsal midline incision was made, and blunt subcutaneous dissection used to create 6 pockets. Each mouse received 6 Laponite or six alginate loaded scaffolds, with 3 containing high dose BMP on the left side, and 3 containing low dose BMP, on the right side. The control mouse received 6 blank collagen sponges.

Micro Computed Tomography scanning

Mice were scanned *in vivo* and post mortem, a full description of the scanning parameters is located in the appendix. In summary, 0.5mm Aluminium filter was used, voltage 50kV, current 500μA, and scans performed with a pixel size of 18μm.

Micro Computed Tomography image reconstruction

Reconstruction of the images was performed using NRecon. Global settings were: Smoothing 2, Ring artefact reduction 5, beam hardening 40%, and data output range set to 0 to 0.08.

4.6   Results

The results of this chapter are presented in two parts corresponding to the objectives set in the introduction:

1) Ability of Laponite in the form of a hydrogel or a dry film to enhance BMP-mediated bone formation *in vivo*.

2) Ability of Laponite gel to reduce the dose of BMP required to stimulate ectopic bone formation *in vivo*.

I would like to acknowledge specific help I received during the course of the experimental work as outlined below:

Assistance received during experiments performed in Part 1

I received assistance performing the micro CT scans from Dr Janos Kanczler.

Cameron Black and I alternated between providing anaesthesia or performing surgery.

I received advice, and help reconstructing the micro CT scans from Gry Hulsart-Billstrom

I received help performing the imaging of the histological sections from Julia Wells.

Assistance received during experiments performed in Part 2

While the experimental protocols were designed by myself, due to the time dependant nature of the work, the experimental work was performed simultaneously by myself, Dr Jonathon Dawson, Cameron Black, and Gry Hulsart-Billstrom.

Scaffolds were perfused with gel by Dr Dawson according to my protocol, while Cameron and I performed surgery and anaesthesia. Following implantation, while the animals remained sedated, micro CT was performed by Gry. Micro CT scanning performed following the day of surgery was performed jointly by myself and Gry. I performed the reconstructions of the micro CT scans, however, this was only possible with the guidance and advice from Gry.

I received help performing the imaging of the histological sections from Julia Wells.

Results Part 1: Ability of Laponite in the form of a hydrogel and dry film to enhance BMP-mediated bone formation *in vivo*

4.6.1.1.1   Micro Computed Tomography Results

In vitro work in the previous chapter demonstrated that Laponite in a gel (3.6.1.3.1) or dry film (3.6.1.3.2) state was able to localise active growth factors. It is noteworthy that growth factor administered endogenously, i.e. mixed within the gel, required a greater dose to produce an equivalent effect with growth actor administered on the surface of the gel (3.6.1.3.1). The manner in which these results may translate to the *in vivo* environment is unknown, in particular, fluid flows or mechanical stimulation would be expected to have an effect on the Laponite gel or film itself.

To elicit if Laponite may be more efficient as a growth factor delivery vehicle for BMP in a gel or dry film state *in vivo* we employed a subcutaneous murine model. Acellular allograft cylinders were coated with Laponite gel or dry film, and BMP was applied either following coating with clay, or mixed within the gel itself. Allograft/BMP/Laponite cylinders were subsequently implanted in nude mice, and bone formation assessed at 4 weeks with the use of micro CT and Histological analysis.

The change in mean allograft bone volume was significantly greater when BMP was delivered either mixed into Laponite gel, or administered onto Laponite gel, compared to Allograft with BMP alone, as shown in Table 4-1 and Figure 4-6. No significant difference was detected between the other groups.

The results of change in mean bone volume were supported by the coregistration analysis (see Table 4-2), which demonstrated that bone formation, and ratio of bone formation to absorption was greatest with Allograft and Laponite gel with BMP mixed into the gel or applied exogenously as shown in Figures 4-7 and 4-8 respectively. However, statistical significance was only achieved when BMP was applied exogenously to Allograft and Laponite gel (Figures 4-7 and 4-8).

Allograft Number	Bone volume (mm^3)		Difference (mm^3)	Difference (%)
	Pre	Post		
Allograft				
1	18.39	20.37	1.98	10.78
2	19.75	21.78	2.03	10.29
3	20.88	22.45	1.57	7.52
4	14.09	16.19	2.11	14.96
5	26.42	29.54	3.13	11.84
6	12.58	14.72	2.14	17.01
		Mean	**2.16**	**12.06**
Allograft + BMP				
1	18.92	19.74	0.82	4.34
2	15.24	16.40	1.15	7.56
3	16.56	18.26	1.70	10.26
4	12.95	13.43	0.49	3.75
5	22.37	24.14	1.76	7.89
6	16.81	17.03	0.23	1.35
		Mean	**1.02**	**5.86**
Allograft + dry Laponite				
1	18.91	18.39	-0.51	-2.72
2	18.09	20.42	2.33	12.88
3	12.48	14.01	1.54	12.31
4	22.40	24.70	2.31	10.30
5	13.51	15.33	1.82	13.47
6	14.64	16.83	2.19	14.93
		Mean	**1.61**	**10.19**
Allograft + dry Laponite +BMP				
1	22.43	24.09	1.66	7.42
2	11.75	14.03	2.28	19.44
3	13.12	14.29	1.17	8.95
4	11.83	13.97	2.14	18.08
5	14.47	17.26	2.79	19.28
6	15.95	18.11	2.15	13.50
		Mean	**2.03**	**14.44**

Table 4 1 Bone volume of allograft/Laponite/BMP combinations pre and post implantation

Allograft number	Bone volume (mm^3)		Difference (mm^3)	Difference (%)
	Pre	Post		
Allograft + Laponite gel				
1	14.89	16.37	1.49	9.98
2	23.37	25.12	1.75	7.49
3	20.50	23.04	2.54	12.39
4	13.46	15.76	2.30	17.05
5	12.54	12.90	0.36	2.90
6	14.02	15.85	1.83	13.08
		Mean	**1.71**	**10.48**
Allograft + Laponite gel/BMP mix				
1	11.15	12.73	1.58	14.17
2	14.16	16.42	2.26	15.98
3	20.35	23.15	2.80	13.77
4	13.53	15.26	1.74	12.83
5	9.09	13.03	3.94	43.34
6	11.63	13.96	2.33	20.07
		Mean	**2.44**	**20.03**
Allograft + Laponite gel + BMP				
1	16.94	18.31	1.37	8.11
2	19.77	22.92	3.15	15.93
3	10.12	14.42	4.29	42.42
4	12.81	15.34	2.53	19.76
5	13.76	17.29	3.53	25.63
6	12.57	15.06	2.50	19.88
		Mean	**2.90**	**21.95**

Table 4-1 Bone volume of allograft/Laponite/BMP combinations pre and post implantation
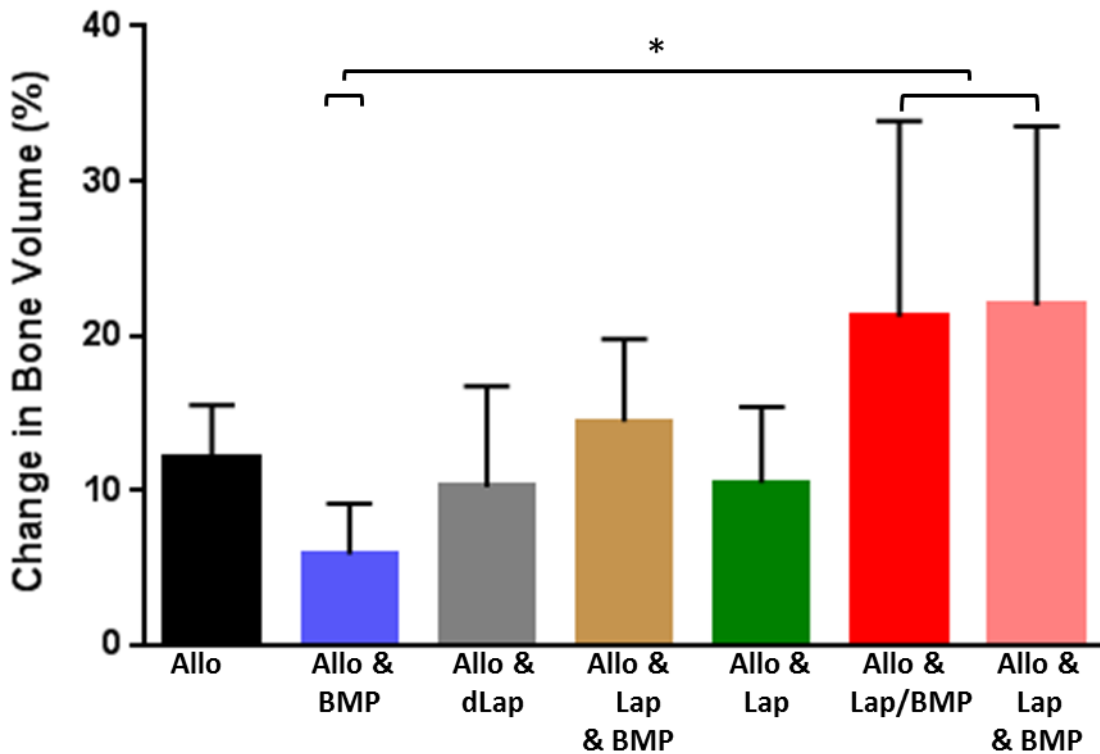
Figure 4-6 Graph of change in allograft bone volume following implantation

Allo = allograft, dLAP = dry Laponite, Lap/BMP = BMP is mixed into Laponite gel, Lap & BMP =
BMP is applied exogenously onto Laponite gel. Graph shows change in mean allograft bone
volume of Allograft/Laponite/BMP preparations as a percentage of initial allograft bone volume.
Error bars show standard deviation. * p<0.05, NS = not statistically significant. N = 6 per group.

Comparison of percentage change in mean volume was performed using a one way-ANOVA test
and Tukey's test for post hoc testing, with P values adjusted for multiple comparisons with
alpha=0.05. A significant difference was detected between Allograft & BMP with
Allograft/Laponite gel with BMP mixed in, and Allograft/Laponite gel and exogenous BMP ,
P=0.0268 and p=0.0112 respectively. There was no statistically significant difference in change in
mean bone volume between any other groups.

| Allograft number | Bone volume (mm^3) | | Formation/ absorption | Initial bone volume | % Bone | |
	Absorption	Formation			Absorption	Formation
Allograft						
1	0.13	0.10	0.78	15.53	0.82	0.64
2	0.05	0.06	1.29	17.26	0.29	0.37
3	0.67	0.37	0.56	17.02	3.92	2.18
4	0.32	0.35	1.07	10.79	3.00	3.21
5	0.09	0.06	0.67	19.92	0.48	0.32
6	0.13	0.15	1.12	7.27	1.80	2.02
		Mean	**0.91**	**14.63**	**1.72**	**1.46**
Allograft + BMP						
1	0.34	0.22	0.63	16.25	2.11	1.32
2	0.18	0.37	2.03	14.17	1.28	2.61
3	0.44	0.26	0.60	10.71	4.07	2.42
4	0.33	0.29	0.89	18.69	1.75	1.56
5	0.38	0.23	0.61	14.11	2.67	1.62
		Mean	**0.95**	**14.79**	**2.37**	**1.91**
Allograft + Laponite						
1	0.17	0.16	0.93	11.63	1.50	1.40
2	0.17	0.11	0.63	20.16	0.83	0.52
3	0.21	0.20	0.94	17.24	1.20	1.13
4	0.22	0.24	1.09	11.41	1.93	2.10
5	0.17	0.20	1.20	9.19	1.84	2.21
6	0.25	0.31	1.26	11.68	2.12	2.68
		Mean	**1.01**	**13.55**	**1.57**	**1.73**
Allograft + Laponite/BMP mix						
1	0.15	0.25	1.67	8.17	1.82	3.03
2	0.19	0.37	1.89	11.44	1.70	3.21
3	0.06	0.18	3.00	17.47	0.34	1.02
4	0.21	0.83	4.05	7.13	2.88	11.65
5	0.22	0.46	2.13	9.21	2.36	5.03
		Mean	**2.55**	**10.68**	**1.82**	**4.79**
Allograft + Laponite exogenous BMP						
1	0.27	0.42	1.53	14.18	1.93	2.96
2	0.19	1.01	5.28	8.19	2.34	12.36
3	0.25	0.55	2.17	9.87	2.58	5.61
4	0.13	0.79	5.95	11.39	1.16	6.89
5	0.31	0.35	1.13	10.65	2.93	3.32
		Mean	**3.21**	**10.86**	**2.19**	**6.23**

Table 4-2 Results of Allograft bone formation & absorption
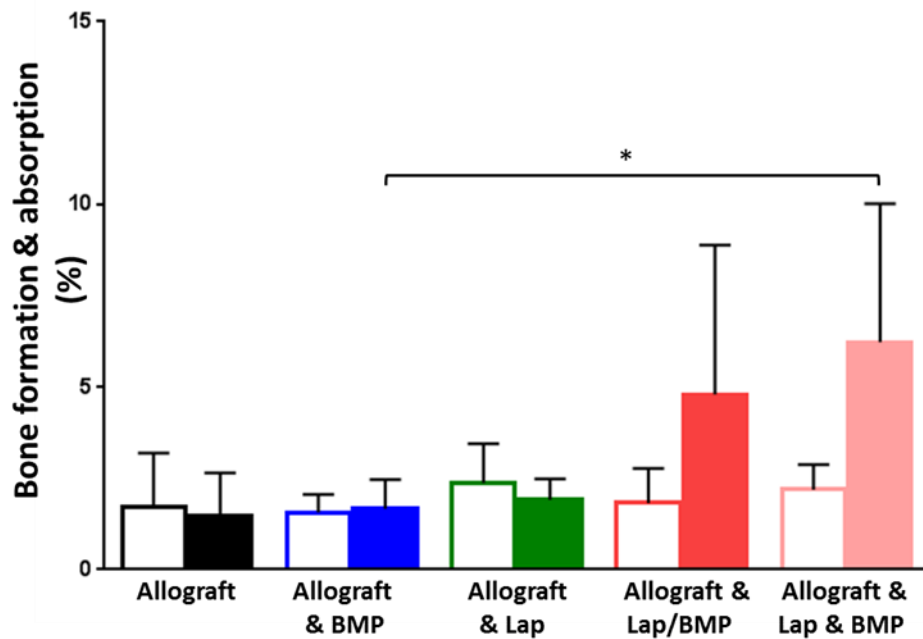
Figure 4-7 Percentage Bone formation and absorption of Allograft, Laponite & BMP formulations

Graph shows mean bone absorption (unfilled bars) and formation (Filled bars) as a percentage of the initial bone volume, error bars show standard deviation. * p<0.005; N =6 per group.

A one way ANOVA test was performed to compare the mean bone absorption and mean bone formation. No statistically significant differences were detected in mean bone absorption. A significant difference in mean bone formation was detected (p=0.0141). Tukey's test was used for post hoc testing, with P values adjusted for multiple comparisons with alpha=0.05. Bone formation was found to be significantly greater with Allograft & Laponite with exogenous compared to Allograft with BMP (P= 0.0322).
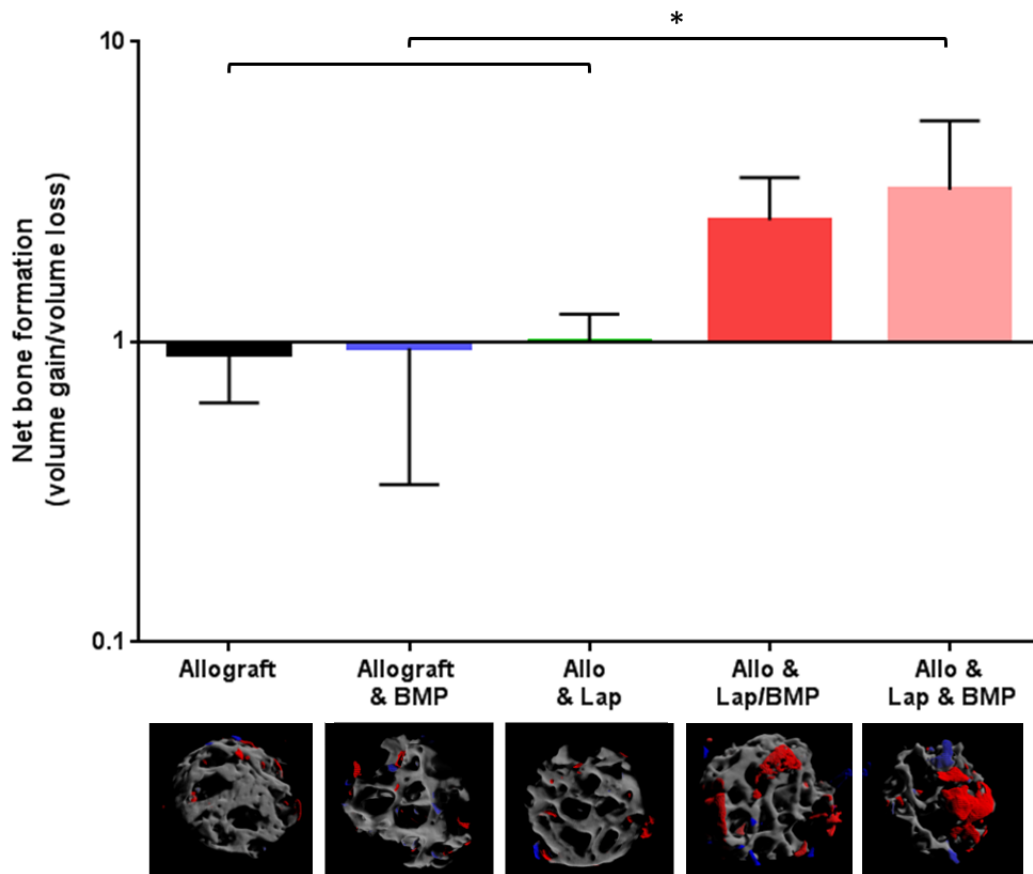
Figure 4-8 Net bone formation Allograft, Laponite & BMP formulations

Allo = Allograft, Lap = Laponite gel, Lap/BMP = Laponite BMP mix, Lap & BMP = Laponite and BMP applied separately. Mean Net bone formation is shown as the ratio of net bone formation observed in Allograft & BMP control, error bars show standard deviation. * p<0.05 Images below are 3D reconstructions of coregistered images with red and blue denoting bone formation and resorption respectively.

A one way ANOVA test was performed to compare the ratio of bone formation to bone absorption (p=0.0044). Tukey's test was used for post hoc testing, with P values adjusted for multiple comparisons with alpha=0.05. Bone formation was found to be significantly greater with Allograft & Laponite with exogenous BMP compared to Allograft (p=0.0159), Allograft with BMP (p=0.0251), and Allograft with Laponite (P= 0.022).

4.6.1.1.2 Histological analysis of ability of Laponite gel and dry film to enhance BMP mediated bone formation *in vivo*

Following 4 weeks subcutaneous implantation and micro CT analysis, allograft samples were decalcified, embedded in wax and sectioned at 9μms. Representative sections were stained with Alcian blue and Sirius red, and viewed under light microscopy. In addition, polarised light microscopy was used in specific cases to differentiate between newly formed and mature bone.

Parallel lamellae encompassing cells typical in nature of osteocytes, representing the mature allograft bone were readily identified in all the specimens as shown in figures 4-10 to 4-15, and confirmed with polarised light microscopy (figure 4-15). Laponite gel is stained bright blue as shown in figures 4-12, 4-13, 4-14, whilst Laponite dried onto the allograft was not readily identified on the sections (figure 4-11)

No new bone formation was observed with Allograft (figure 4-9),or Allograft & Laponite gel (figure 4-12). Minimal new bone formation was observed on Allograft with BMP (figure 4-10 , and Allograft coated with dry Laponite and BMP (figure 4-11).

New bone formation was evident adjacent to Allograft with Laponite gel and exogenous BMP (figure 4-14). Multiple areas of new bone were observed adjacent to hypertrophic chondrocytes within the gel, on sections of allograft which received Laponite and endogenous BMP as shown in figure 4-13.

BMP delivered within the Laponite gel appeared to result in endochondral bone formation within the Laponite gel, while exogenous BMP application appeared to show appositional bone formation on the periphery of gel as shown in figure 4-16.
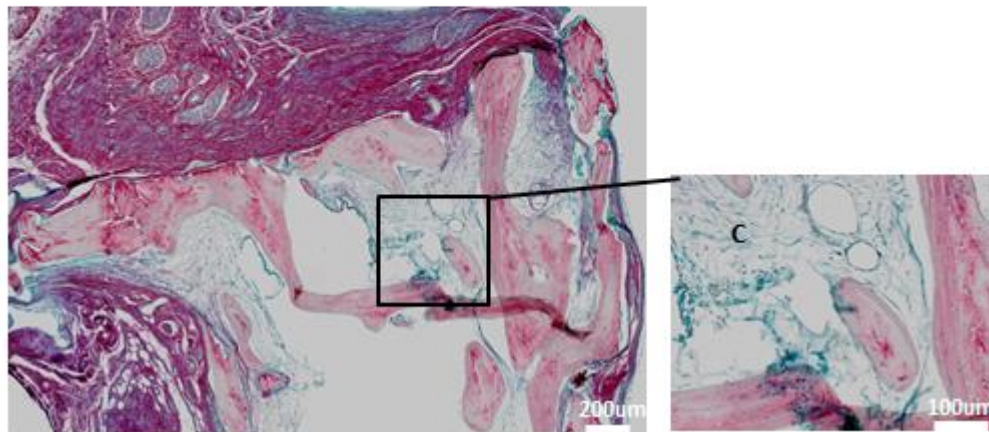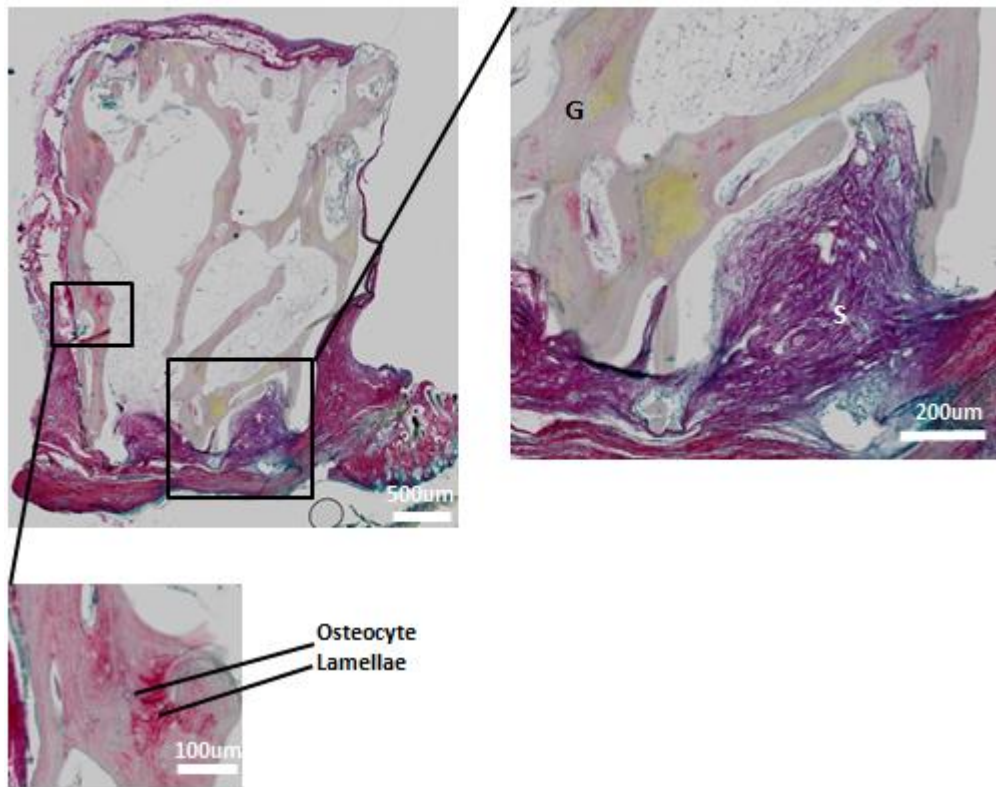
Figure 4-9 Histology of Allograft control

Mature allograft bone seen with parallel lamellae and osteocytes. Skin covering part of allograft material, and connective tissue invasion of allograft visualised. No endochondral bone formation is seen. G = allograft,   S = skin, C = connective tissue
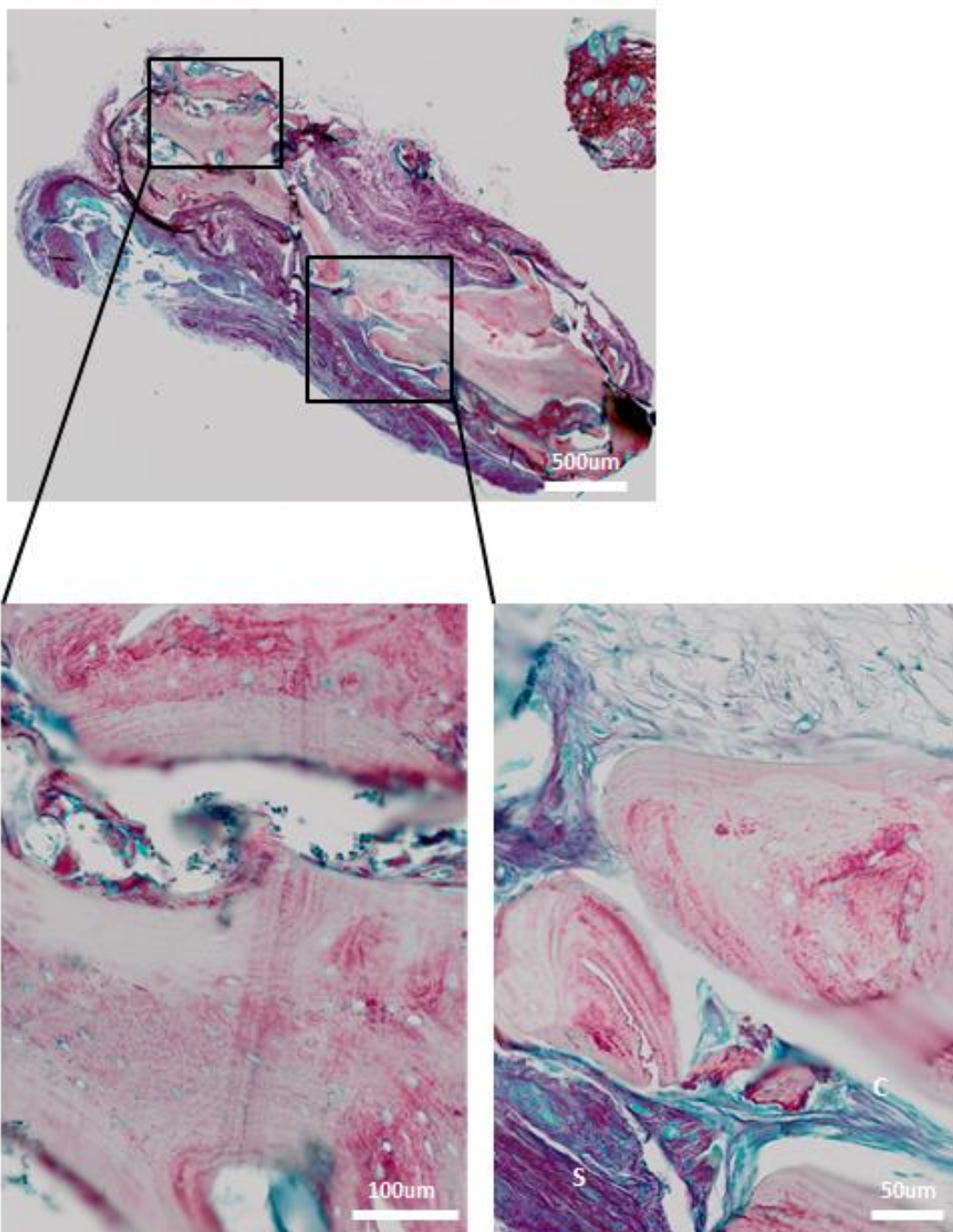
Figure 4-10 Histological sections of allograft with BMP

Regions demonstrating blue staining are shown at higher magnification below. Skin and

connective tissue are identified, no hypertrophic chondrocytes are seen.

 S = skin,   C = connective tissue
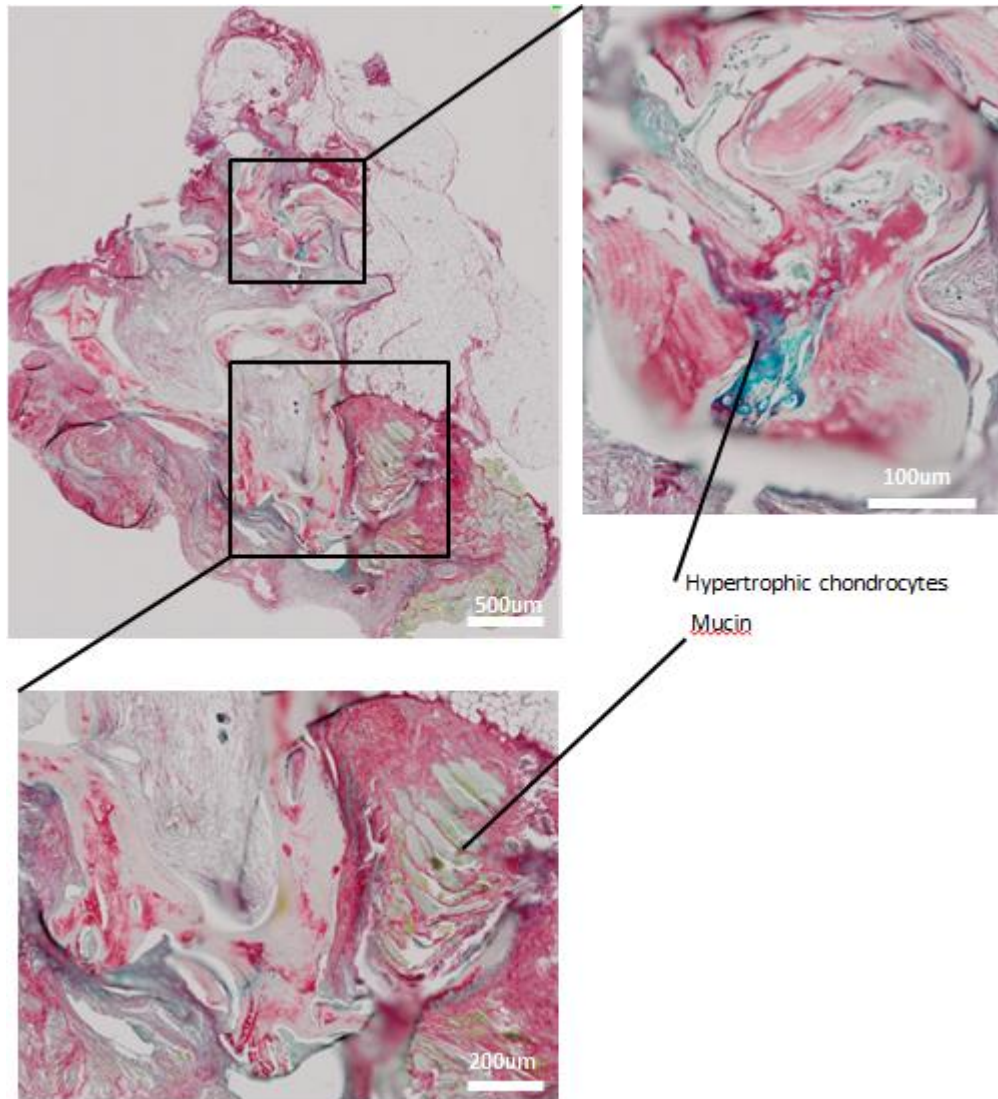
Figure 4-11 Histological sections of Allograft coated with dry Laponite film & BMP

Hypertrophic chondrocytes seen in one area of the section as demonstrated in top right panel.

Mucin from dermis attached to the sample is shown in bottom left panel.
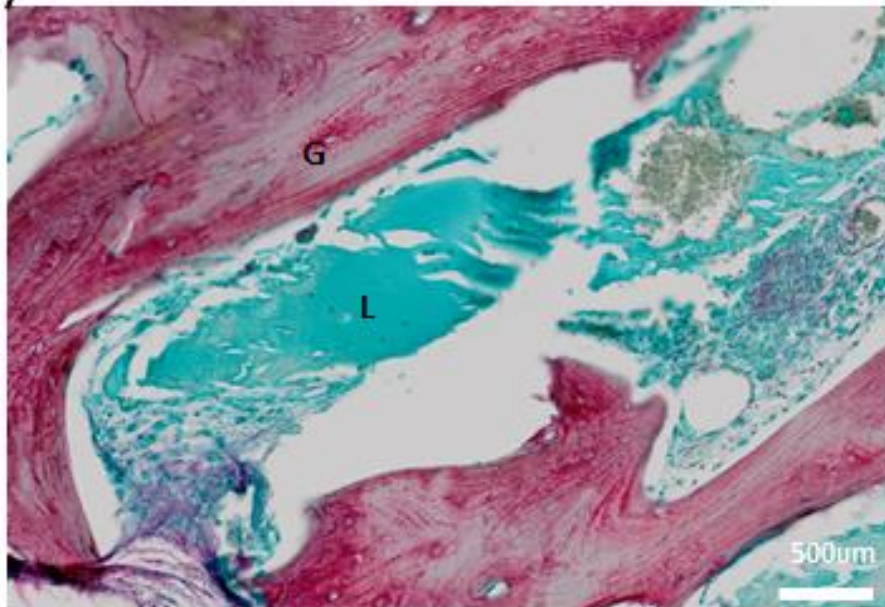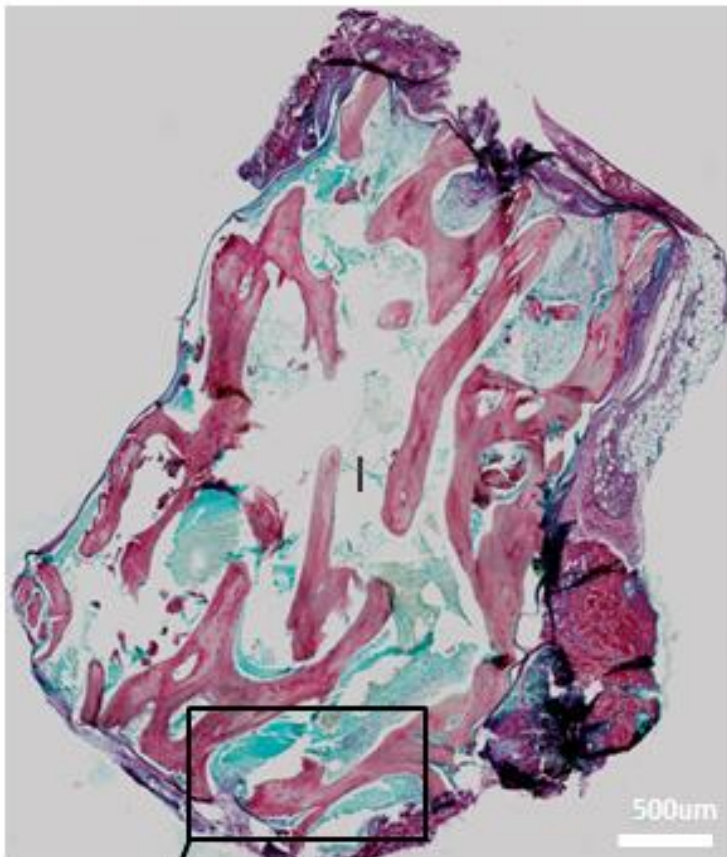
Figure 4-12 Histological sections of Allograft coated with Laponite gel

Laponite gel and allograft are clearly visualised. No evidence of new bone formation is seen

 L = Laponite G = allograft
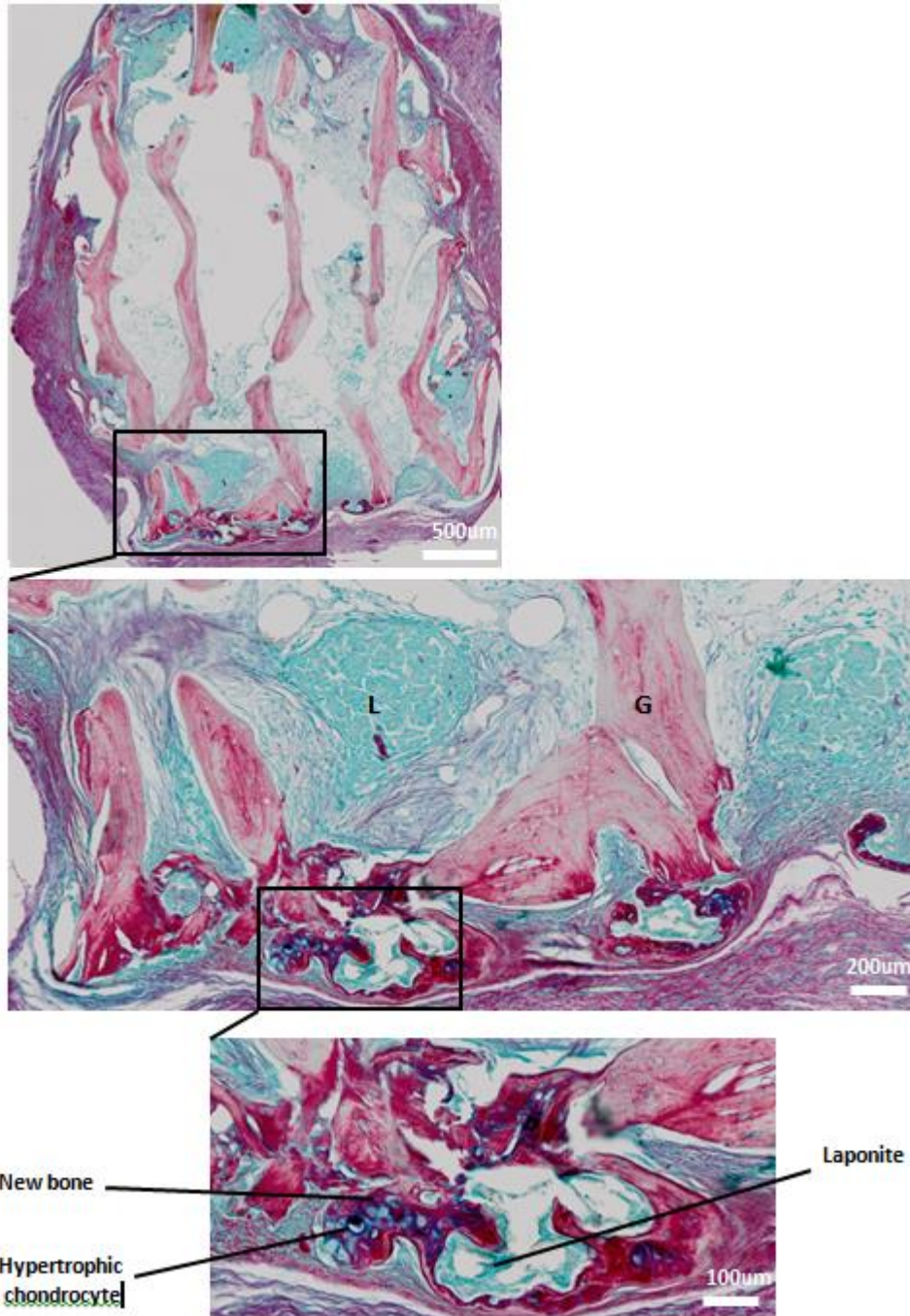
Figure 4-13 Histological sections of Allograft coated with Laponite gel/BMP mix

Endochondral bone formation by hypertrophic chondrocytes is visualised in close proximity to Laponite gel.
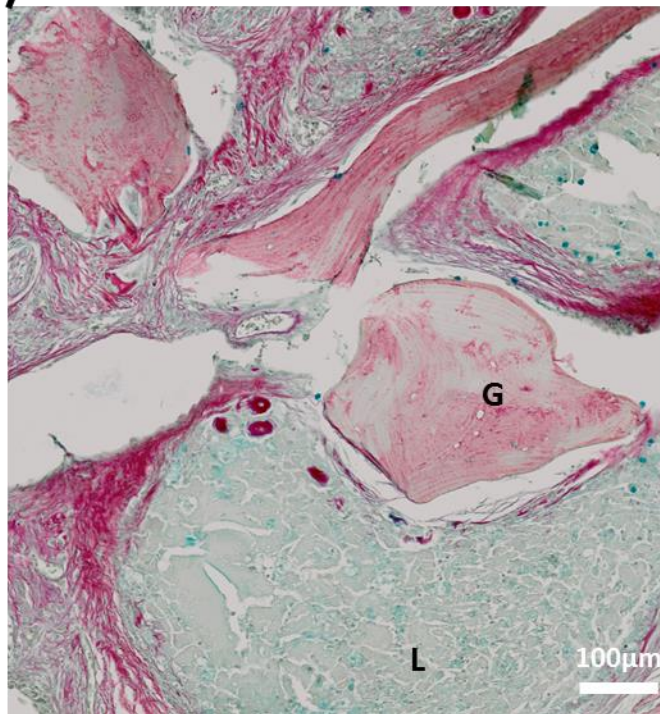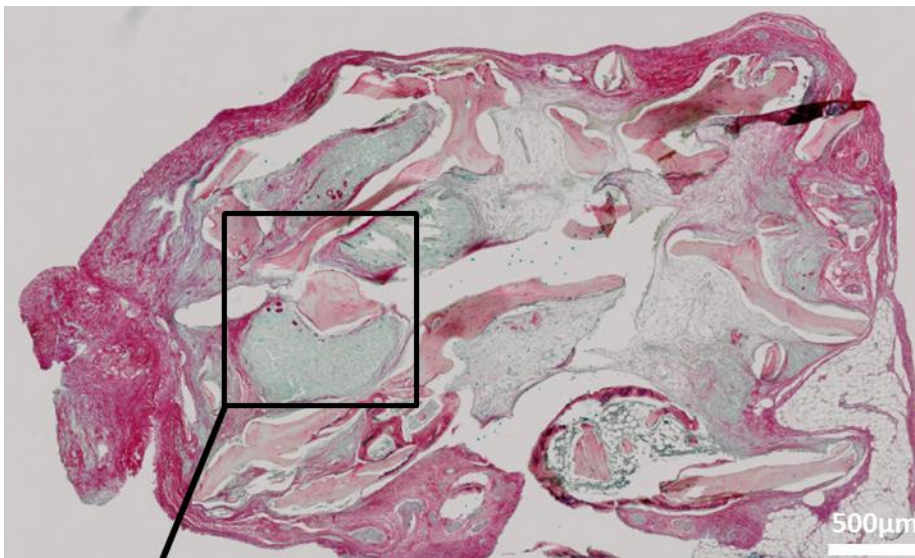
Figure 4-14 Histological sections of Allograft coated with Laponite gel and exogenous BMP

Areas of new bone are seen on the periphery of the gel adjacent to the Allograft.
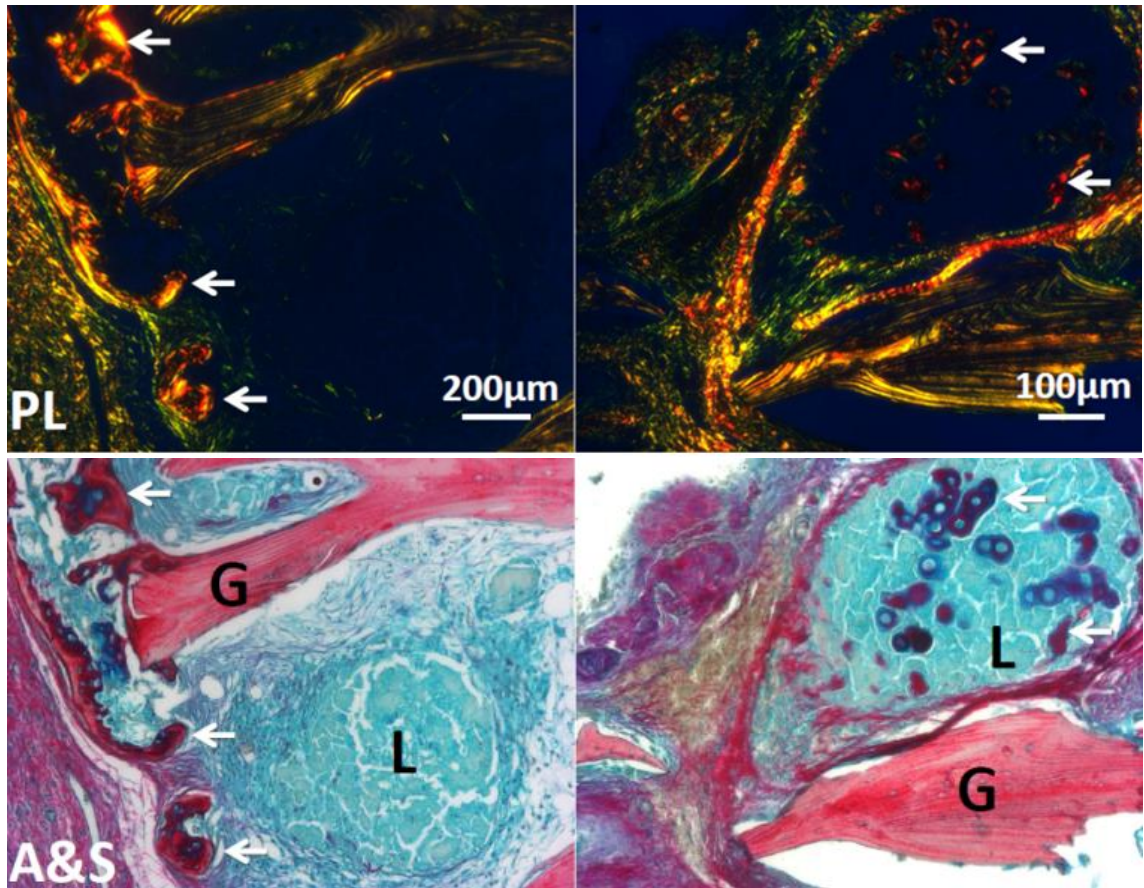
Figure 4-15 Polarised light microscopy of Allograft with Laponite gel/BMP mix

Top panels show A&S staining, bottom panels represent the same sections imaged under polarised light microscopy. Arrows identify areas of bone seen adjacent to hypertrophic chondrocytes. Polarised light microscopy demonstrates parallel lamellae in mature bone (allograft), and lack of such fibre organisation in the bone adjacent to chondrocytes confirms that this is newly formed bone rather than allograft. L = Laponite, G = allograft, PL = polarised light, A&S= Alcian blue & Sirius red
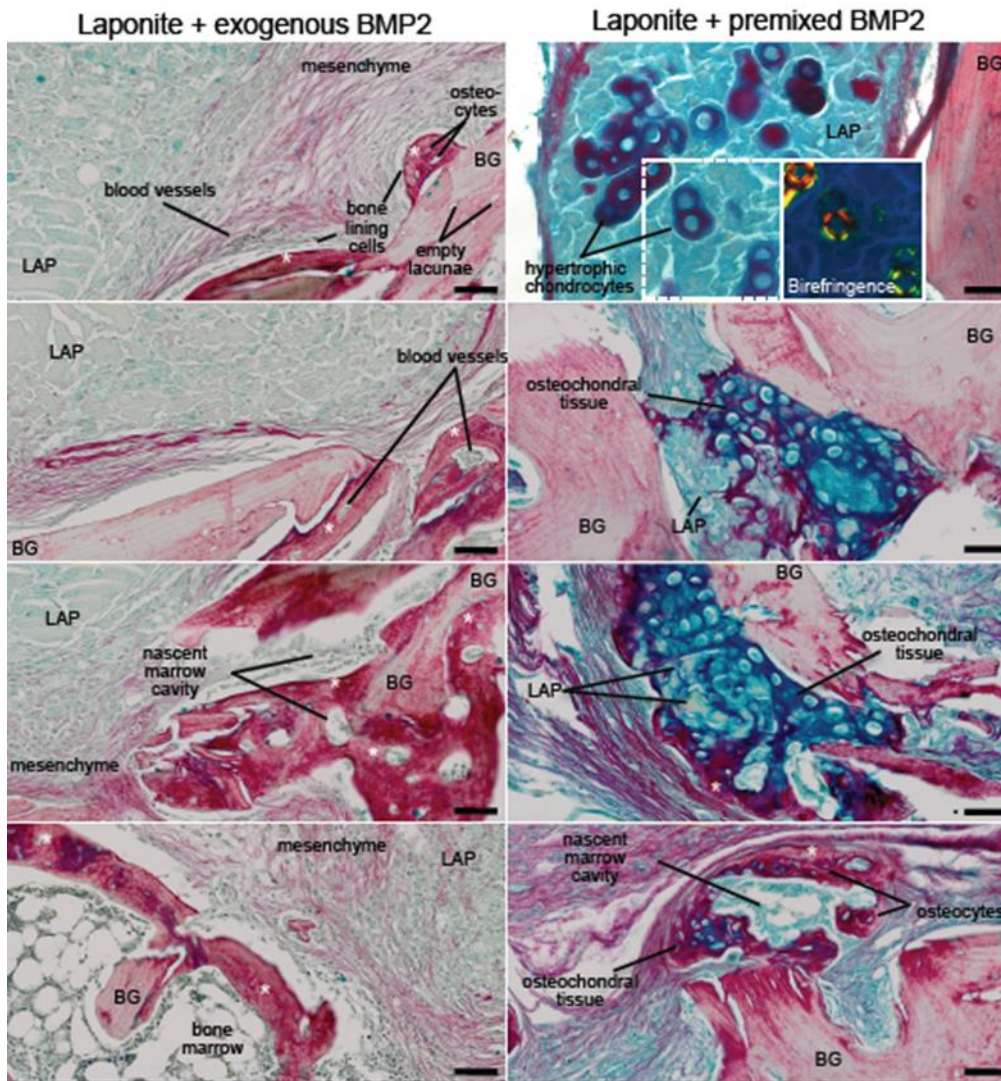
Figure 4-16 Histological analysis of bone formation mediated by Laponite with endogenous and exogenous BMP

Appositional bone formation was observed on bone graft surfaces (and enhanced by Laponite gel) in response to exogenously applied BMP (Left panel of images). This is in contrast to endochondral bone formation observed when BMP was delivered endogenously, within the Laponite gel (right panel of images). Scale bar is 50μm.

Results Part 2: Ability of Laponite gel to reduce the dose of BMP required to mediate ectopic bone formation

4.6.1.1.3   Micro Computed Tomography Results

To investigation the ability of Laponite to reduce the effective dose of BMP collagen sponge cylinders were soaked in Laponite and Alginate gels laden with BMP. Sponge cylinders were implanted in mice, and bone formation assessed using micro CT and histology.

Micro CT reconstructions were performed in which colour representative of the attenuation of the material, hard tissue, such as cortical bone is blue, while material equal in density to cartilage, such as the anterior aspect of the murine rib cage are represented by green (figure 4-17).

Representative reconstructions a of control mouse which received blank collagen sponge, and receiving collagen with BMP laden Laponite and Alginate gels, at high dose (left flank) and low dose (right flank) are shown (figure 4-17). Following 2 weeks implantation some tissue equal in density to cartilage is observed in the test groups in the region in which the collagen was implanted. The density of this new tissue is observed to increase over the subsequent weeks (figure 4-17).

CT reconstructions of each mouse at 8 weeks are shown in figure 4-18. It is noteworthy that while Laponite and Alginate groups both demonstrated formation of hard tissue at the higher doses of BMP (left flank), hard tissue formation was only observed with Laponite when BMP was applied at the lower dose. Categorical analysis of the presence or absence of hard tissue, visible on the micro CT reconstruction at 8 weeks was performed. At high dose BMP, hard tissue formation was observed in a significantly greater number of scaffolds in Alginate compared to Laponite (P=0.0192). Conversely, hard tissue formation at low dose BMP was significantly greater in Laponite compared to Alginate (P<0.0001), as shown in table 4-3 and figure 4-19.

Micro CT was used to quantify the volume of new bone formed within the collagen scaffolds as shown in tables 4-4, 4-5, and 4-6. Volume of bone formed within the collagen scaffold was significantly greater with Alginate and high dose BMP compared to Alginate and low dose BMP and Laponite with high or low dose BMP, as shown in figure 4-20.

Volume of gel remaining in each well following absorption by the collagen sponge was recorded as shown in table 4-7. A significantly greater volume of Laponite remained following loading of the collagen sponge compared to Laponite, as shown in figure 4-21. Subsequently, Bone volume

formed per volume of gel loaded was calculated, and also found to be greatest with Alginate and high dose BMP compared to Alginate and low dose BMP, or Laponite and BMP, however this was not found to be statistically significant.

When bone volume formed was quantified as bone volume per unit BMP, bone formation was found to be significantly greater with Laponite and low dose BMP compared to Laponite and high dose BMP, and Alginate with high or low dose BMP, as shown in figure 4-23. Subsequent analysis was unable to demonstrate a correlation was found between volume of gel loaded and volume of bone formed as shown in figure 4-24.

4.6.1.2   Micro CT reconstructions of bone formation within collagen sponge
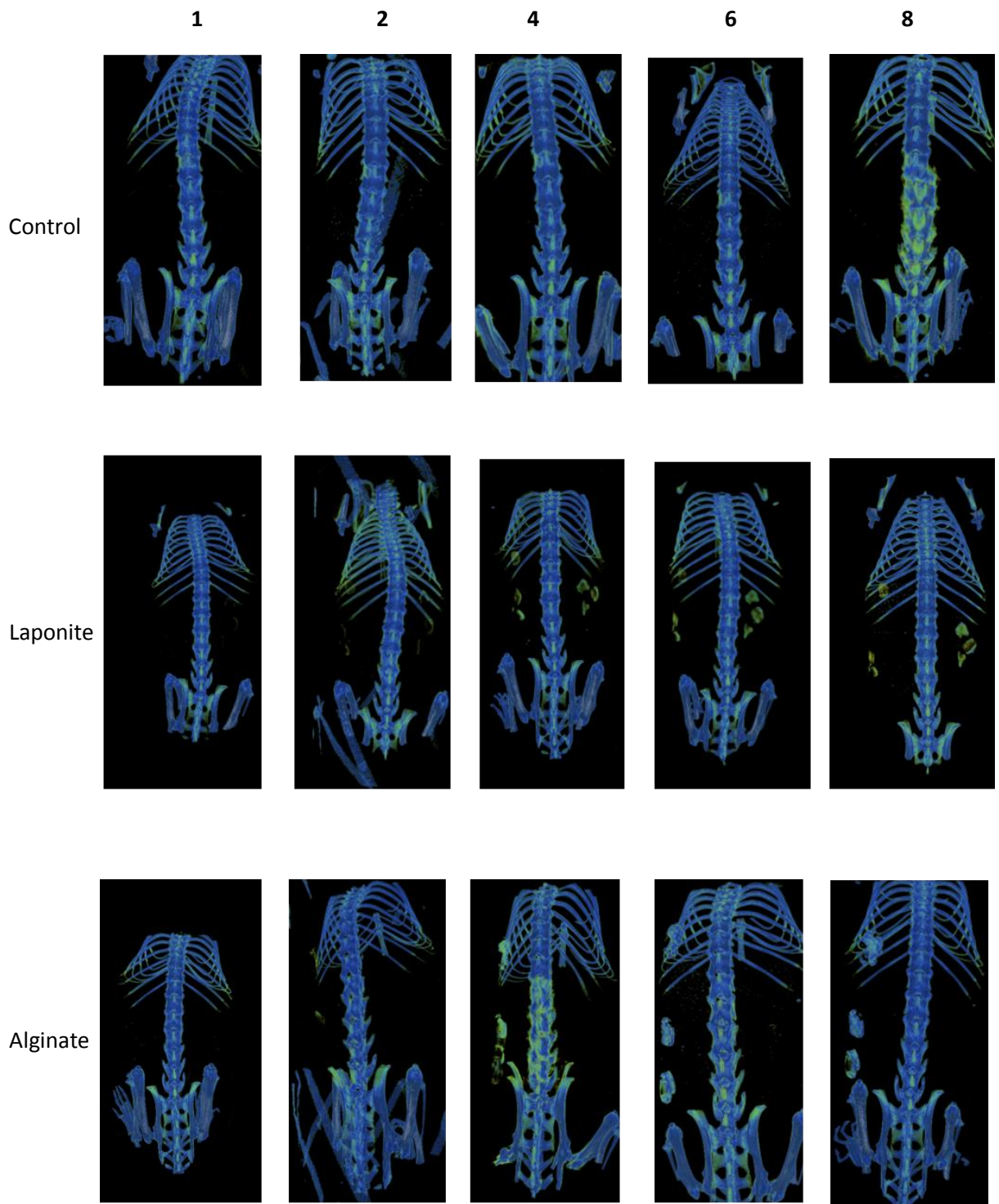
Figure 4-17 3D Micro CT reconstructions of bone formation mediated by Laponite and Alginate gels containing BMP
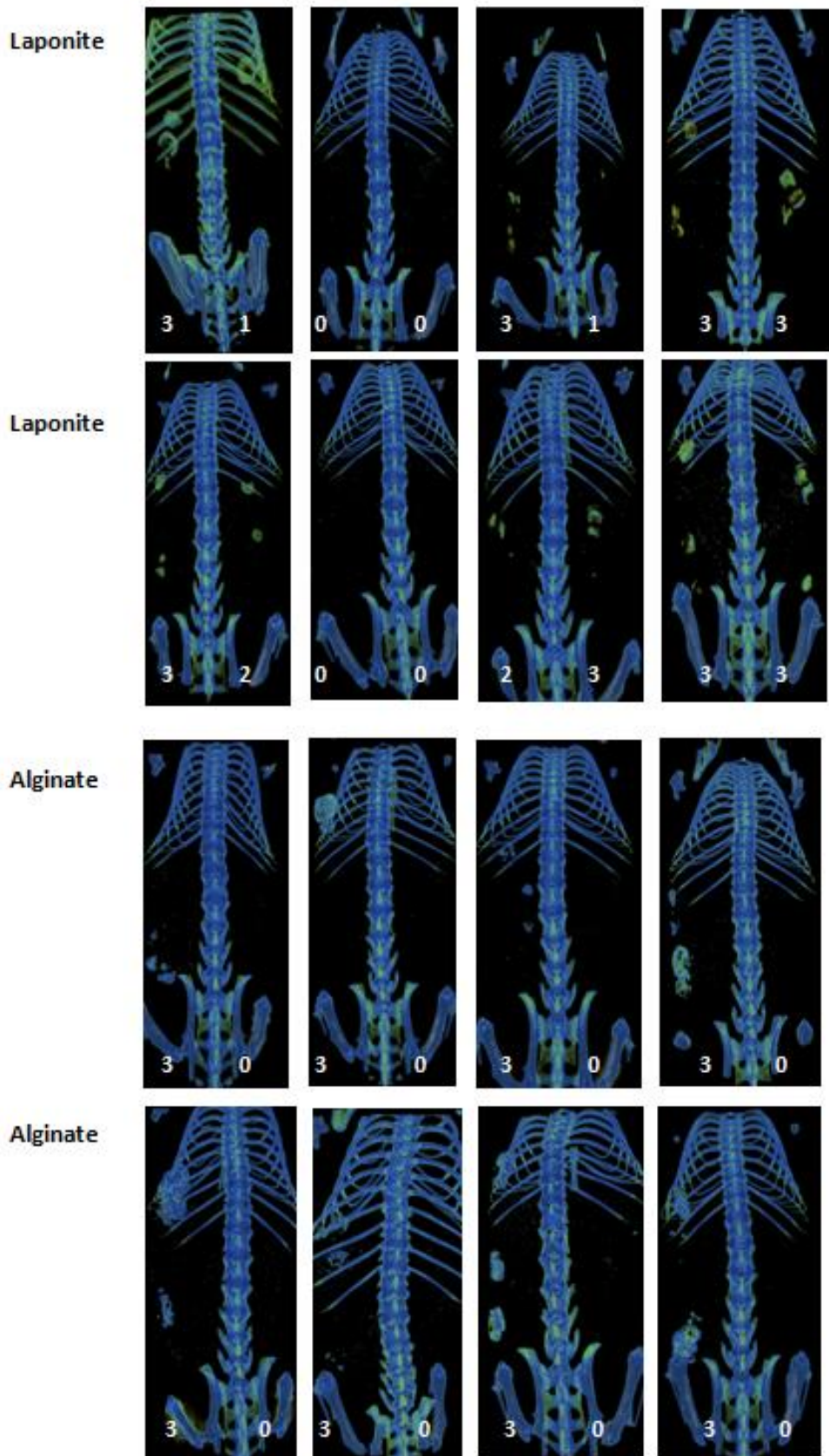
Figure 4-18 CT images of bone formation mediated by Laponite/BMP & Alginate/BMP

All scans were performed at 6 weeks. Number of scaffolds demonstrating hard tissue formation at

high (left side) and low (right side) BMP are shown.

Collagen Sponge & Laponite

Mouse	High dose	Low dose
R cut C1	3	1
R1 C1	0	0
LE2 C1	3	1
R low C1	3	3
L1 C2	3	2
no mk C2	0	0
R1 C2	2	3
R1 L2 C2	3	3
Total with Bone	**17**	**13**
Total with no bone	**7**	**11**

Collagen Sponge & Alginate

Mouse	High dose	Low dose
L1 C3	3	0
no mk C3	3	0
R1 C3	3	0
R1 L1 C3	3	0
L1 C4	3	0
R cen C4	3	0
R1 cut C4	3	0
R1L1 C4	3	0
Total with Bone	**24**	**0**
Total with no bone	**0**	**24**

Table 4-3 Bone formation mediated by BMP laden Laponite and Alginate gels

The tables displays the number of collagen scaffolds receiving high and low dose BMP in Laponite (upper table) and Alginate (lower table) which were visible on the micro CT images shown on the previous page. Collagen sponge scaffolds are only visible reconstructed micro CT images shown on the previous page when hard tissue has formed, and thus this was taken to represent bone formation. Letters entered into the table describe the ear markings of the mice and which cage they were in, thereby identifying which treatment the mouse received.
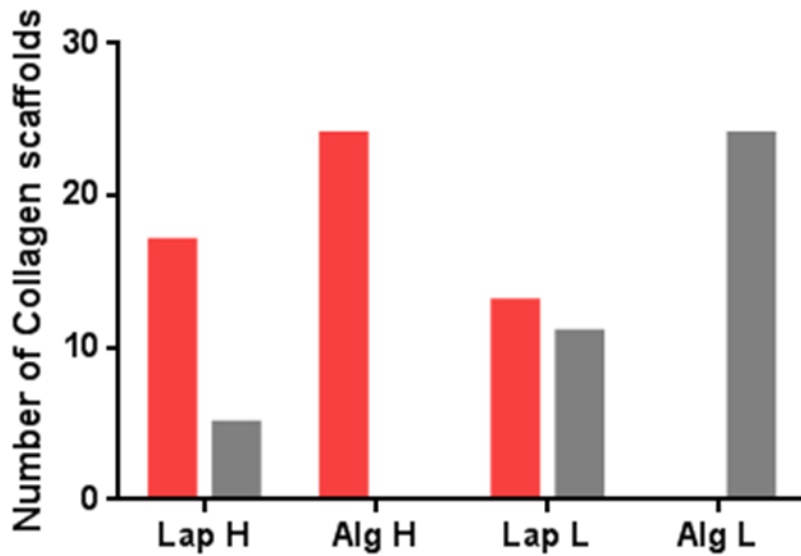
Figure 4-19 Graph of number of scaffolds showing bone formation

Graph shows the number of collagen scaffolds which demonstrated bone formation following application of BMP delivered at high and low dose, by Laponite and Alginate hydrogels. Red denotes presence of bone within the scaffold, grey denotes absence of bone on micro CT.
Lap = Laponite, Alg =Alginate, H = high dose, L = Low dose BMP.

Fisher's exact test was performed to compare the number of scaffolds demonstrating bone formation with Low dose and high dose BMP delivered in Laponite with Low dose and high dose BMP delivered in Alginate.

Bone formation in collagen scaffolds receiving high dose BMP was observed in a significantly greater number of scaffolds in Alginate compared to Laponite (P=0.0192). Conversely, bone formation in collagen scaffolds receiving low dose BMP was observed in a significantly greater number of scaffolds in Laponite compared to Alginate (P<0.0001).

Bone volume formed with Laponite and High dose BMP

Scaffold (n=17)	TV (mm^3)	BV (mm^3)	BV/TV (%)
R cut C1D1	19	1	7
R cut C1D2	75	5	7
R cut C1D3	55	4	8
LE2 C1 D1	149	5	3
LE2 C1 D2	81	2	3
LE2 C1 D3	215	3	2
R low C1D1	61	2	4
R low C1D2	125	4	4
R low C1D3	41	4	11
L1 C2 D1	38	2	5
L1 C2 D2	56	1	2
L1 C2 D3	65	4	7
R1 C2 D1	53	2	4
R1 C2 D2	80	2	3
R1L1 C2 D1	65	1	1
R1L1 C2 D2	66	3	5
R1L1 C2 D3	98	7	7
Mean	**79**	**3**	**5**
Standard Deviation	47	2	3

Table 4-4 Volume of bone formed by Laponite and high dose BMP

Letters and numbers in the first column identify each mouse and the position of the scaffold within the mouse. TV = tissue volume, BV = bone volume.

Bone volume formed by Alginate and High dose BMP

Scaffold (n=14)	TV (mm^3)	BV (mm^3)	BV/TV (%)
R1 C3 D1	30	1	2
R1 C3 D2	51	1	2
R1 C3 D3	108	2	2
R1 L1 C3D1	447	23	5
R1 L1 C3D2	35	2	5
R1 L1 C3D3	71	5	8
L1 C4 D1	231	7	3
RCENC4D1	271	1	0
RCEN C4D2	83	2	2
RCEN C4D3	149	3	2
RCUT C4D1	354	18	5
RCUT C4D2	315	14	4
RCUT C4D3	475	20	4
R1 L1 C4D3	425	14	3
Mean	**218**	**8**	**3**
Standard Deviation	163	8	2

Table 4-5 Volume of bone formed by Alginate and high dose BMP

Letters and numbers in the first column identify each mouse and the position of the scaffold within the mouse. TV = tissue volume, BV = bone volume.

Bone volume formed by Laponite and Low dose BMP

Scaffold (n=12)	TV (mm^3)	BV (mm^3)	BV/TV (%)
R cut C1	77	7	9
LE2 C1 E1	80	1	1
R low C1E1	28	2	8
R low C1E2	51	4	8
R low C1E3	42	3	8
L1 C2 E1	32	2	6
L1 C2 E2	38	3	7
R1 C2 E1	34	2	4
R1 C2 E2	36	3	8
R1L1 C2 E1	72	4	5
R1L1 C2 E2	59	3	5
R1L1 C2 E3	42	4	9
Mean	**49**	**3**	**6**
Standard Deviation	18	2	2

Table 4-6 Volume of bone formed by Laponite and high dose BMP

Letters and numbers in the first column identify each mouse and the position of the scaffold within the mouse. TV = tissue volume, BV = bone volume.

Collagen sponge + Alginate and low dose BMP

None of the collagen sponges receiving Alginate and low dose BMP produced bone.
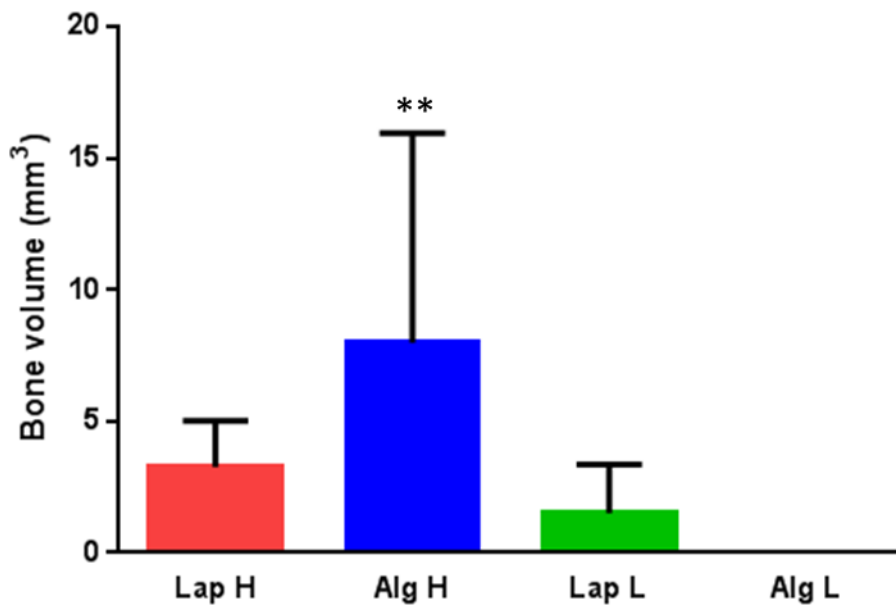
Figure 4-20 Graph of bone volume formed by BMP laden Laponite and Alginate gels

Graph shows mean bone volume and Standard Deviation formed within collagen scaffolds receiving BMP at high and low dose, delivered by Laponite and Alginate hydrogels. No detectable bone was formed with Alginate and low dose BMP. Lap = Laponite, Alg =Alginate, H = high dose, L = Low dose BMP.

One- way ANOVA test was performed initially and a significant difference in mean bone volume between the four groups (P<0.0001) was detected. Each mean was subsequently compared with every other mean using Tukey's multiple comparison test. Alginate and high dose BMP resulted in significantly greater bone volume than Alginate with low dose BMP (p<0.0001), Laponite with High dose BMP (p=0.0025)and Laponite with low dose BMP (P<0.0001). No significance in bone volume was detected between Laponite with high and low dose BMP.

	Volume of gel NOT loaded onto collagen				% Gel NOT loaded onto collagen			
	Lap high (µl)	Lap low (µl)	Alg high (µl)	Alg low (µl)	Lap high (%)	Lap low (%)	Alg high (%)	Alg low (%)
	81	86	54	54	58	61	39	39
	72	89	66	88	51	64	47	63
	89	81	38	50	64	58	27	36
	90	75	54	61	64	54	39	44
	72	64	54	54	51	46	39	39
	81	62	57	58	58	44	41	41
	69	81	58	66	49	58	41	47
	78	76	52	63	56	54	37	45
	66	74	45	58	47	53	32	41
	51	70	84	95	36	50	60	68
	70	61	58	64	50	44	41	46
	75	58	50	63	54	41	36	45
	82	94	66	64	59	67	47	46
	81	84	56	63	58	60	40	45
	84	78	47	76	60	56	34	54
	81	79	61	54	58	56	44	39
	69	84	52	58	49	60	37	41
	74	81	86	62	53	58	61	44
	84	71	59	56	60	51	42	40
	69	70	53	60	49	50	38	43
	74	88	64	68	53	63	46	49
	89	77	66	52	64	55	47	37
	86	72	61	51	61	51	44	36
	76	78	60	65	54	56	43	46
Mean	77	76	58	63	55	55	42	45
SD	9	9	11	11	6	7	8	8

Table 4-7 Volume of gel NOT loaded onto the collagen

Table showing the volume (µl) and % of the 140µl of gel which remained in each well following

adsorption by the collagen sponge.
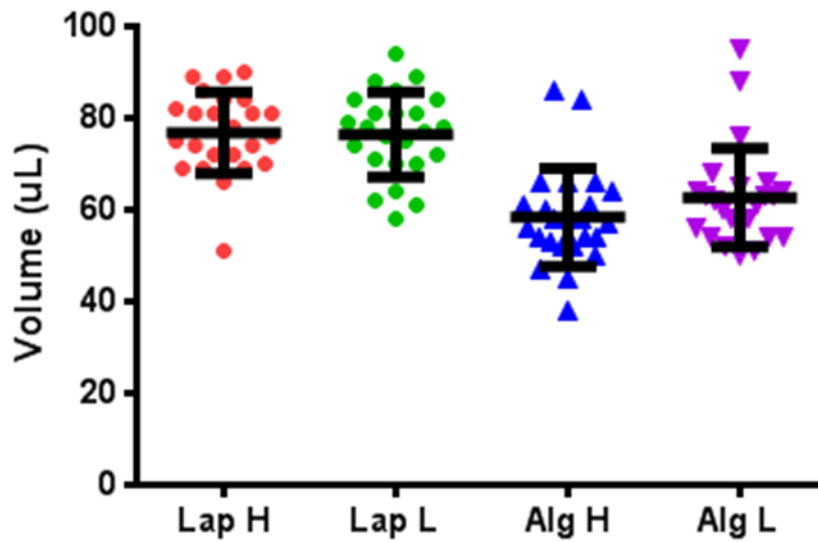
Figure 4-21 Scatter dot plot of the volume of gel remaining adsorption by collagen

Graph shows mean volume of gel remaining and Standard Deviation following adsorption by collagen sponge. Lap = Laponite, Alg =Alginate, H = high dose, L = Low dose BMP.

Volume of Laponite gel at high and low concentration BMP remaining in the 96 well plate following loading onto the collagen scaffold was significantly greater than volume of Alginate gels (P<0.0001). There was no significant difference of volume of gel remaining between Laponite gels at different BMP concentrations or between Alginate gels at different BMP concentrations.
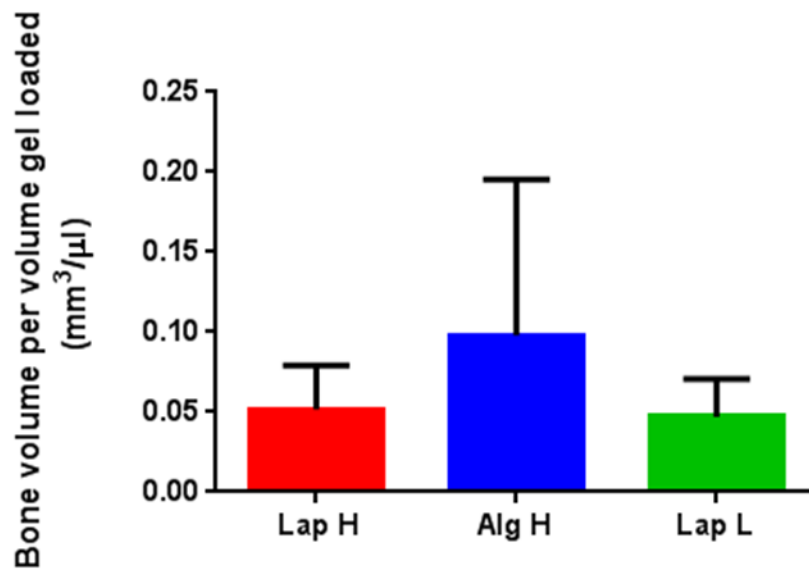
Figure 4-22 Graph of bone volume per volume of BMP laden Laponite & Alginate gels

Graph shows mean volume of bone formed within collagen sponge scaffolds per volume of gel. Error bars show standard deviation. Lap = Laponite, Alg =Alginate, H = high dose, L = Low dose BMP.

A one-way ANOVA test was performed and determined that there was no significant difference between the mean bone volume per μl gel loaded for Laponite with high and low dose BMP and Alginate with high dose BMP (P=0.0564)
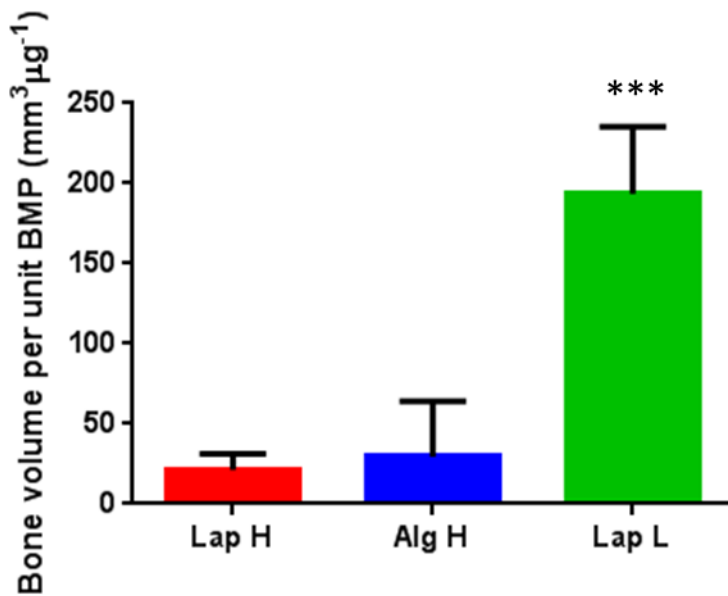
Figure 4-23 Graph of Bone volume formed per µg BMP

Graph shows mean bone volume formed within the collagen scaffolds and standard deviation.

Lap = Laponite, Alg =Alginate, H = high dose, L = Low dose BMP.

Bone volume per µg BMP was significantly greater with Laponite and low dose BMP compared to Alginate and Laponite with high dose BMP (p<0.0001). There was no significant difference between mean bone volume per µg BMP with gels Alginate and Laponite gels containing high dose BMP.
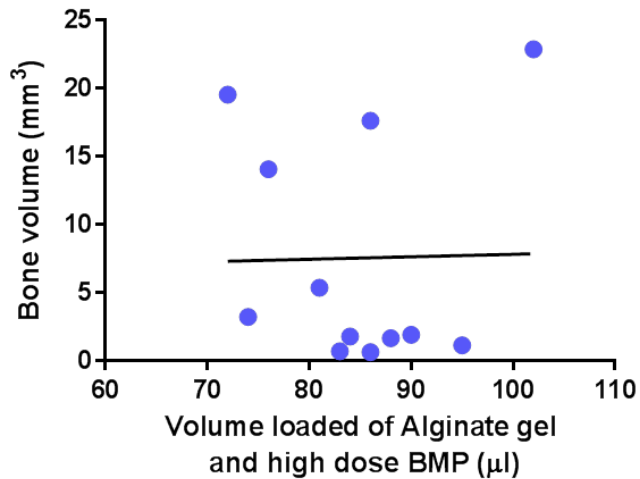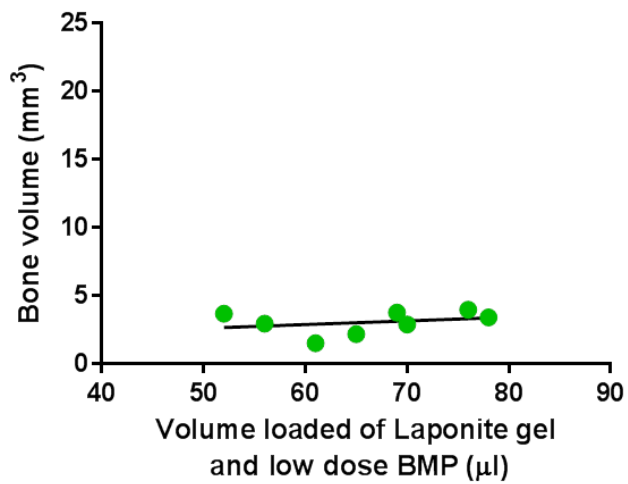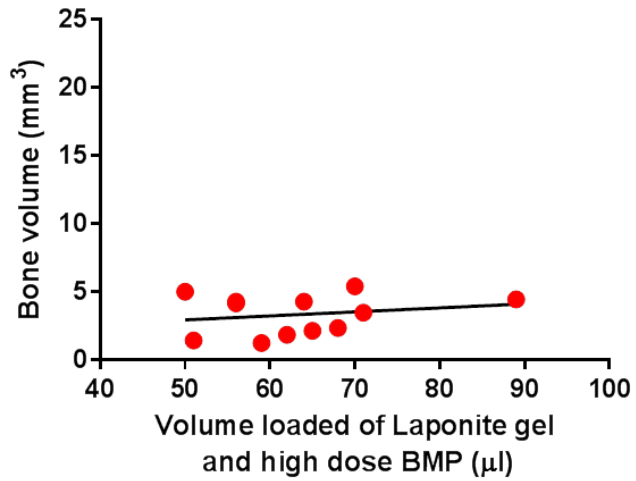
Figure 4-24 Graphs showing individual scaffold bone volume per volume of gel loaded

Graphs show volume of bone formed within collagen scaffolds per µl of: Laponite & High dose BMP (upper graph), Alginate & High dose BMP (middle graph), and Laponite & Low dose BMP (lower graph). No correlation was found between bone volume and BMP dose when analysed using linear regression.

4.6.1.2.1 Histological analysis of bone formation within collagen sponge mediated by BMP laden Laponite & Alginate gels

To investigate the ability of Laponite to reduce the effective dose of BMP collagen sponge cylinders were soaked in Laponite and Alginate gels laden with BMP at two doses and implanted in mice. Following 8 weeks subcutaneous implantation and micro CT analysis, collagen sponge samples were embedded in wax and sectioned at 9µms. Representative sections were stained with Alcian blue and Sirius red, and viewed under light microscopy.

Laponite gel was stained light blue as shown in figure 4-25 and 4-27. Alginate also appear blue, however the staining was of a greater intensity, as seen in 4-26 and 4-27.Collagen sponge appeared as a grey/blue structure following staining.

Bone formation was most obvious with Alginate and high dose BMP (4-26), but was also seen to a lesser extent with Laponite and high (4-25) and low (4-27) dose BMP as a red stained structure.
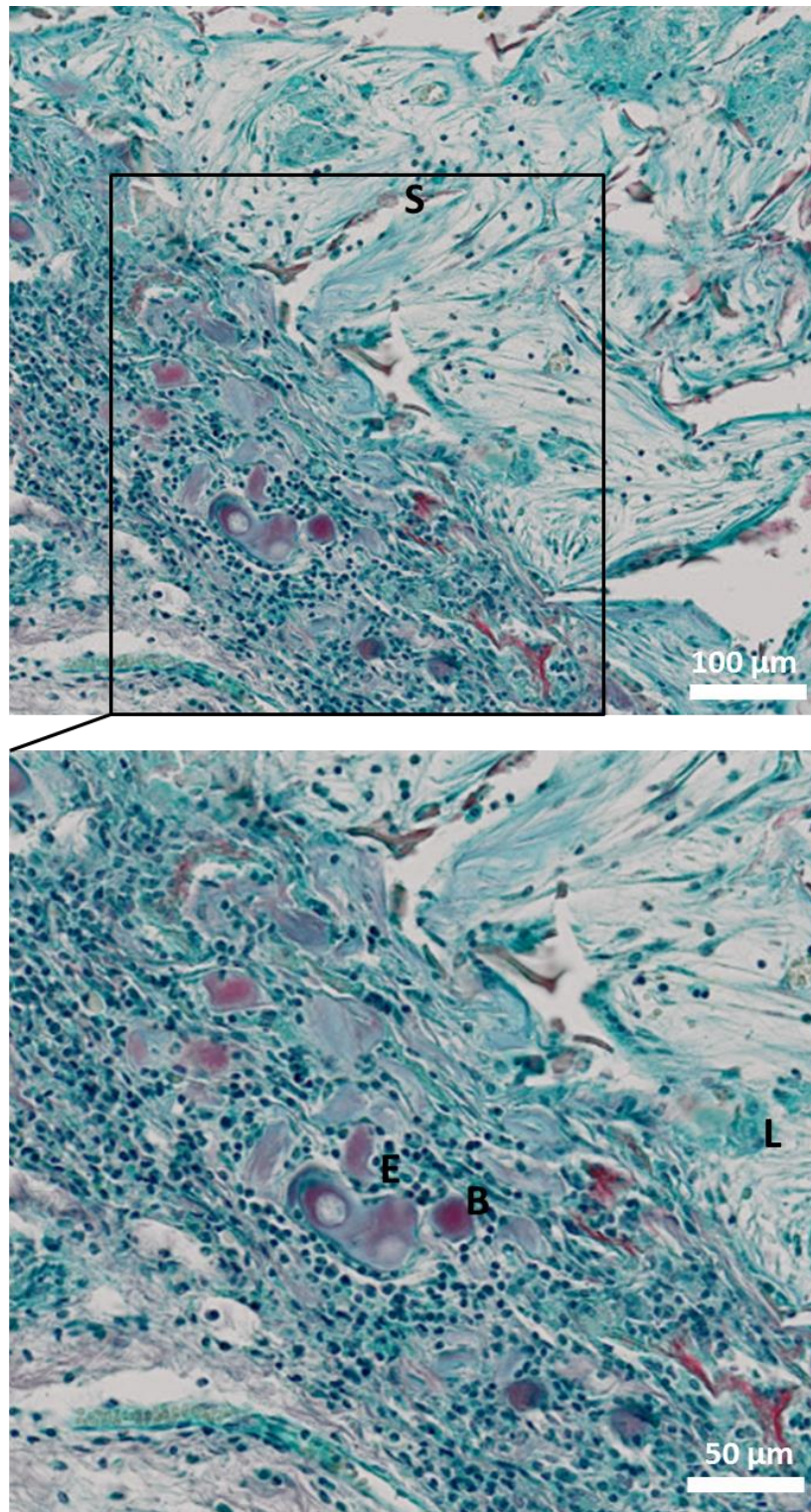
Figure 4-25 Histological sections of Collagen with Laponite & High dose BMP

Red strands represent remains of collagen sponge, labelled S. Bone formation within the sponge is seen at higher power (B). Laponite gel (L) is difficult to differentiate from cartilage. Potential endochondral bone formation observed bottom left of lower image, labelled E.
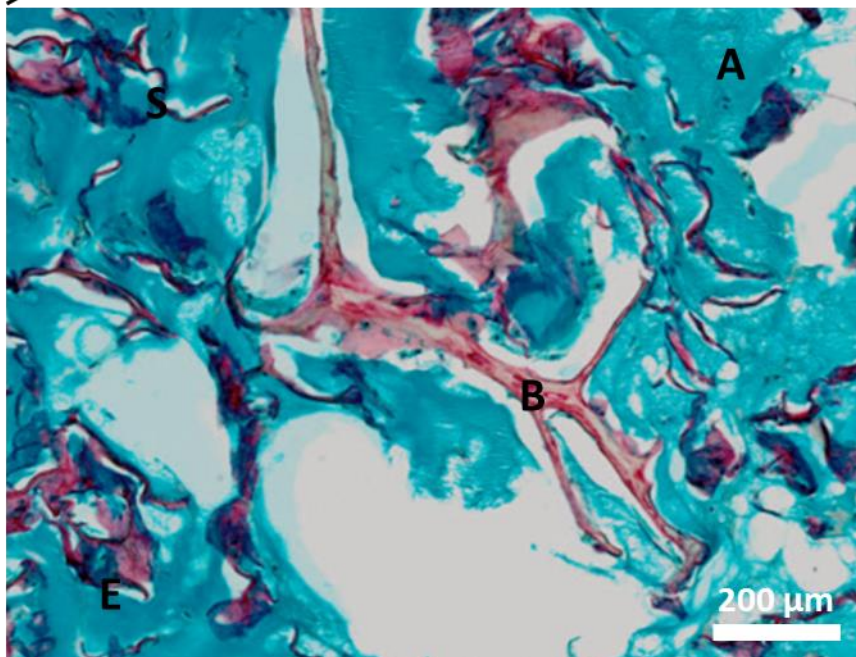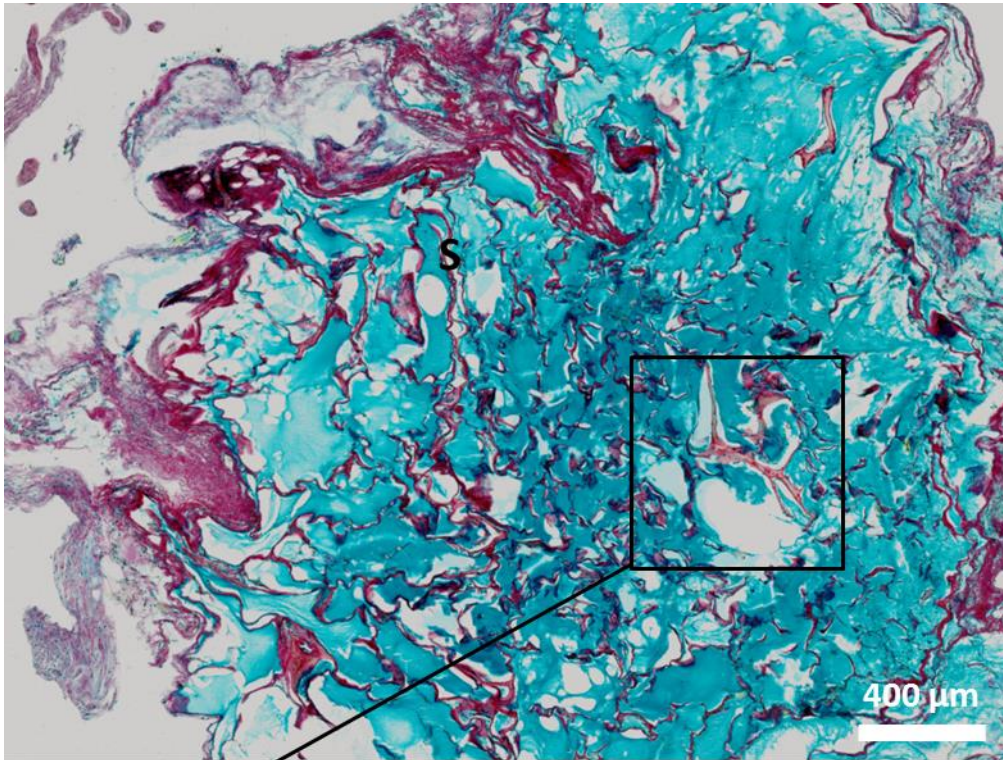
Figure 4-26 Histological sections of Collagen with Alginate & High dose BMP

Red strands represent remains of collagen sponge, labelled S. Bone formation within the sponge is seen at higher power (B) Alginate gel (A) is difficult to differentiate from cartilage. Potential endochondral bone formation observed bottom left of lower image, labelled E
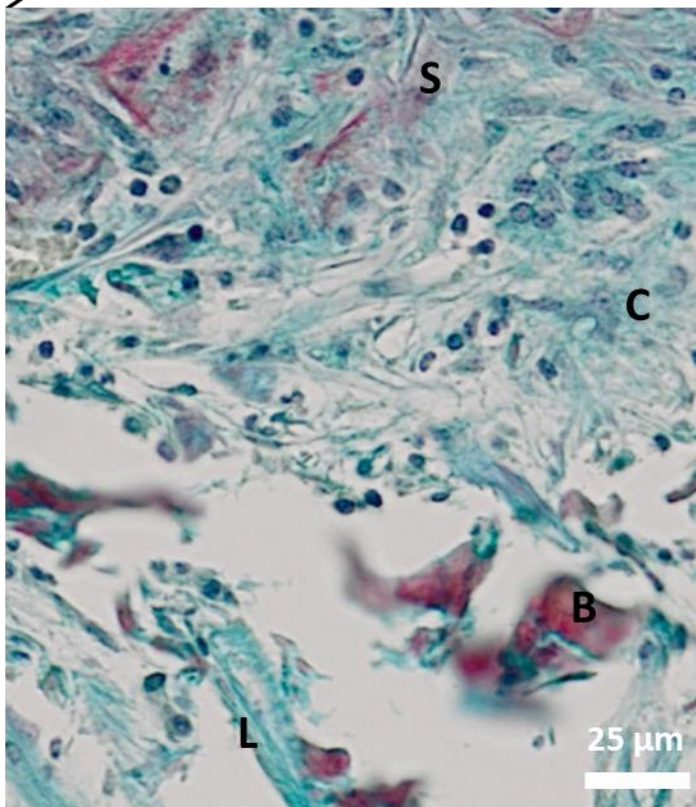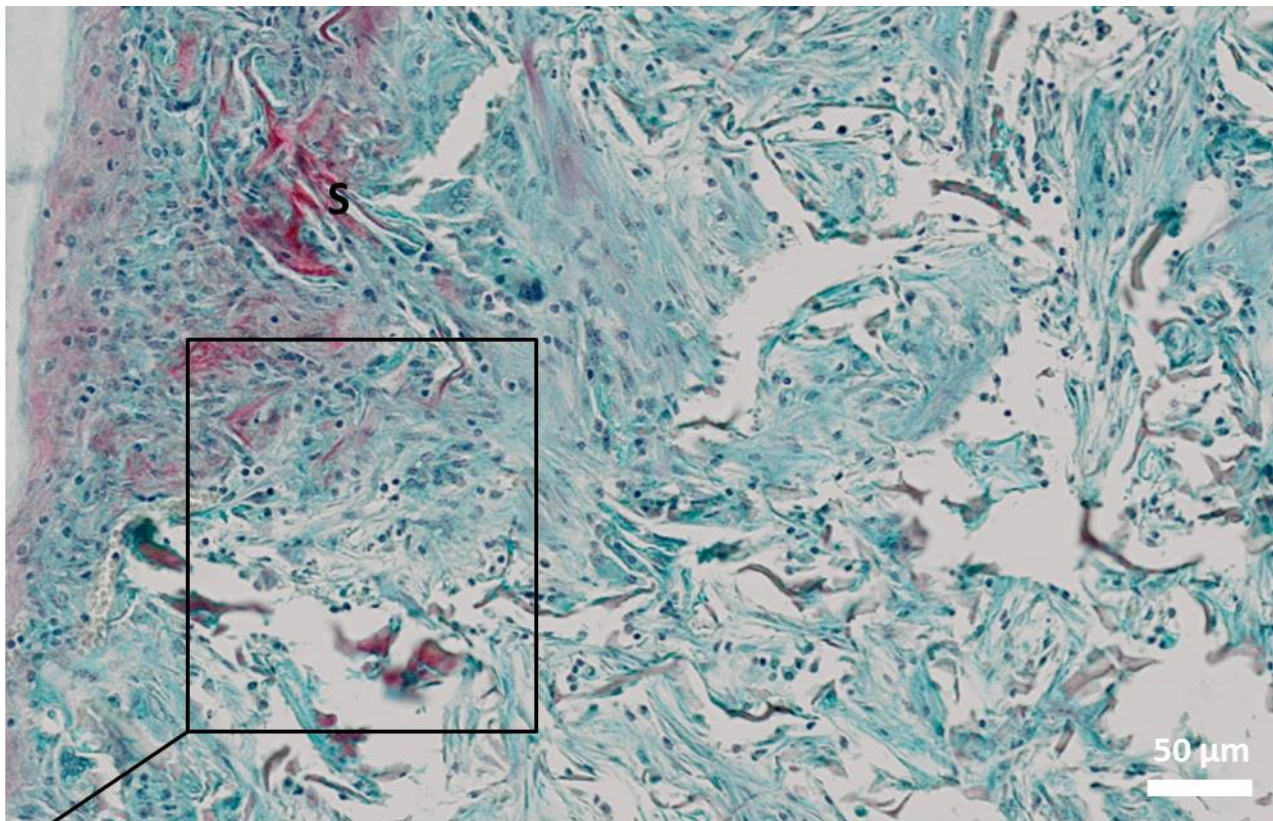
Figure 4-27 Histological sections of Collagen with Laponite & low dose BMP

2Red strands represent remains of collagen sponge, labelled S. Bone formation within the sponge is seen at higher power (B) Laponite gel (L) is difficult to differentiate from cartilage (C). Potential endochondral bone formation observed bottom left of lower image
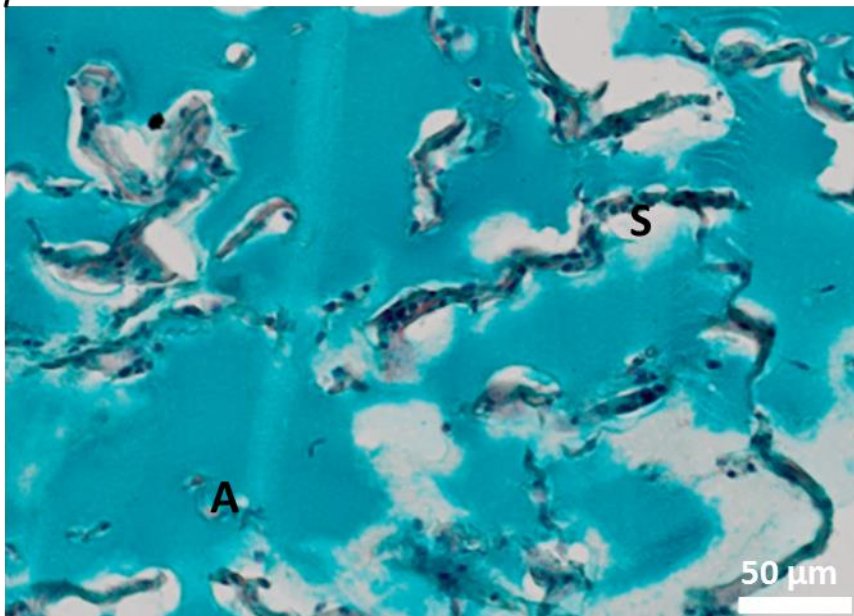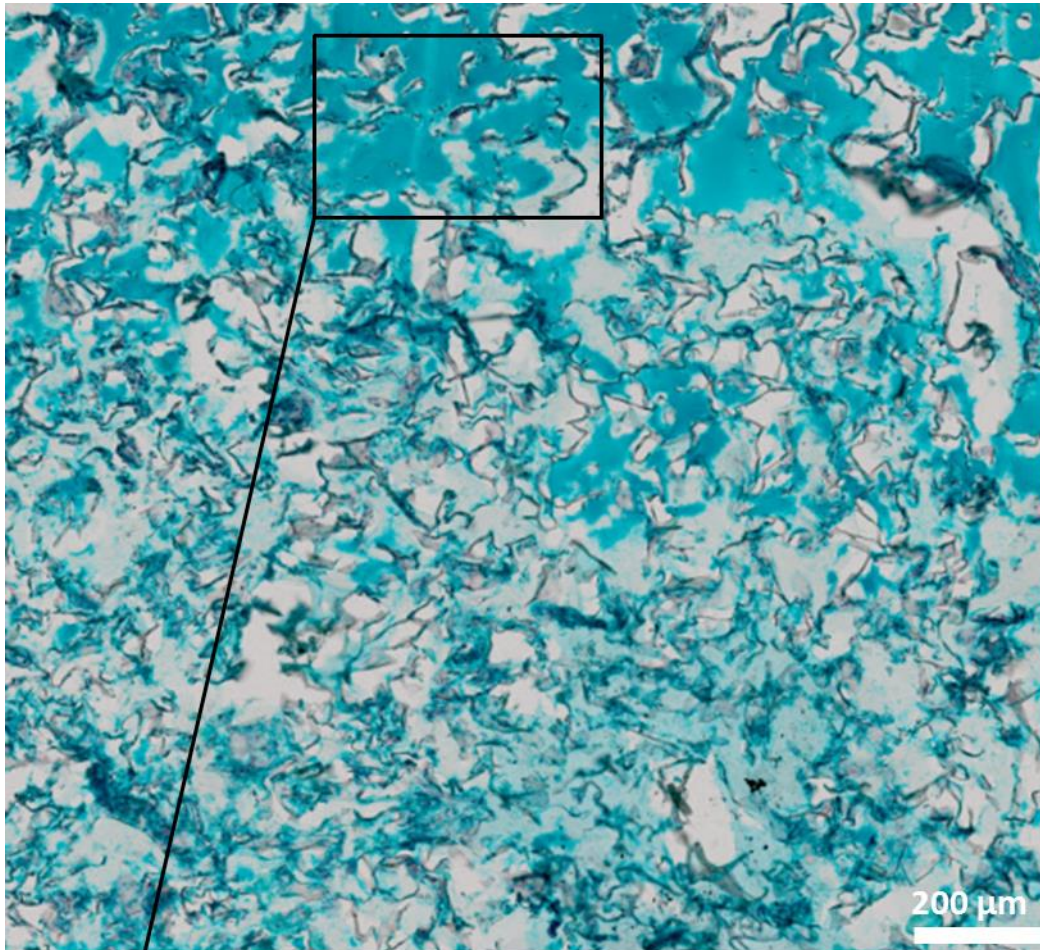
Figure 4-28 Histological sections of Collagen with Alginate & low dose BMP

Red strands represent remains of collagen sponge, labelled S. A= Alginate gel

4.7 Discussion

This study sought **t**o establish if Laponite in the form of a hydrogel or a dry film is capable of enhancing BMP-mediated bone formation *in vivo.* BMP was localised by Laponite gel and dry film to allograft cylinders and implanted subcutaneously in mice as shown in figure 4-1. Micro CT analysis was used to calculate change in total bone volume, volume of bone formed and volume absorbed, and correlated with histology.

Increase in total bone volume was lower in Allograft with BMP compared to Allograft alone. BMP has catabolic and anabolic effects through stimulation of osteoclasts and osteoblasts respectively. In this study BMP applied in absence of Laponite may have exerted a net catabolic effect. Belfrage (Belfrage et al., 2011) also found application of BMP-7 to Allograft material in rats resulted in a reduction in bone volume compared to saline control. Furthermore, co-application of BMP-7 and Zoledronate, an osteoclast inhibitor resulted in greater bone formation compared to control (Belfrage et al., 2011). However, our study, analysis of co-registered images did not demonstrate increased bone absorption in Allograft and BMP, and this correlates with the lack of statistical difference compared to bone formation observed in allograft alone.

BMP applied to Allograft in the presence of Laponite gel resulted in significantly greater increase in total Allograft bone volume compared to Allograft with BMP alone, whilst BMP applied to allograft coated with a dry Laponite film did not mediate a significant increase in total bone volume compared to BMP with Allograft. Of the five groups (allograft, allograft+BMP, allograft + Laponite, allograft + endogenous or exogenous BMP) in which co registration analysis was performed, no significant difference in absorption was seen, however bone formation was significantly greater with Laponite gel + exogenous BMP compared to the other groups. Results of the coregistration analysis broadly concur with the analysis of mean bone volume in that Laponite receiving both exogenous and endogenous BMP demonstrated greater bone formation than the other groups. While bone formation observed with allograft receiving Laponite and endogenous BMP was not statistically different from other groups this may be a result of the experiment being marginally underpowered. Allograft with Laponite and endogenous BMP contained only 5 samples, as one was not amenable to co-registration analysis, which is below the n=6 calculated in our power study.

Histological analysis correlated with micro CT results, with multiple areas of bone formation seen in close proximity to Laponite in the Laponite gel /BMP groups, only one area of area of bone formation was observed in the Laponite dry film/BMP group. The current study attempted to

explore if osteolysis stimulated by BMP had resulted in reduced bone volume observed in Allograft with BMP group by performing Tartrate-resistant acid phosphatase staining (TRAP) to quantify presence of osteoclasts. This was unsuccessful, and the technical failure of this analysis is likely to be secondary to the acid based decalcification process which was performed prior to sectioning.

No statistical difference in bone volume increase was detected when BMP was mixed into the Laponite gel or applied exogenously onto the gel *in vivo*. This similarity, and the similarity in bone absorption and formation implies that the effective dose of BMP was similar in these two cases. Laponite has been shown to adsorb proteins (Dawson et al., 2011) and therefore, adsorption of BMP applied onto the gel may ultimately result in a similar dose of BMP to that resulting from application of Laponite with BMP mixed prior to application.

It is of significant interest that while no significant difference in increase in allograft bone volume with Laponite and premixed BMP-2 and Laponite with exogenous BMP-2 was observed on micro CT; histological analysis appeared to show that Laponite and exogenous BMP promoted appositional bone formation, whereas Laponite gel and premixed BMP mediated endochondral bone formation. Our *in vitro* results suggest premixing results in BMP localisation within the gel, if this is replicated *in vivo* only osteoprogenitor cells present within the gel may be activated by the BMP, in contrast to exogenous BMP which is available to stimulate cells on the surface of the gel. The difference in biomechanical and biological environments within the gel and on the gel surface may explain the stimulation of endochondral and appositional osteogenesis observed in Laponite with premixed and exogenously applied BMP, respectively.

The choice of Allograft as a test scaffold to investigate Laponite mediated BMP delivery is a clinically relevant approach as Allograft is in widespread clinical use as a bone graft (Kurien et al., 2013a), and BMP has been applied to allograft and ceramic bone graft in clinical practice to increase osteogenicity (Buttermann, 2008, Dawson et al., 2009). However, assessment of bone formation on allograft is complex, as total bone volume, which is readily quantified on micro CT is the net result of bone absorption and bone formation. The additional coregistration analysis of micro CT data required to differentiate bone absorption and formation is a relatively complex process. Even with computational processing, there is inevitably some movement artefact between the pre and post implantation images as shown in figure 4-5. The expression of net bone formation, ratio of bone formation to bone absorption mitigates movement artefacts.

Furthermore, there was correlation between change in total bone volume, ratio of bone formation/absorption, and histological analysis.

While a detailed sample size calculation was performed prior to the first experiment, the data used for this process were derived from an intramuscular murine model (Hulsart-Billstrom et al., 2011). Volume of bone formed during that experiment (Hulsart-Billstrom et al., 2011) was directly measured, without requirement to account for bone absorption; possibly as a consequence there was less variation in the data set than observed in this study. As a result, while this study did produce some statistically significant outcomes, it may have been marginally underpowered, and selection of data from a publication in which Allograft material was used may have advantageous. In the second part of this study, data from Part 1 was used to perform the power calculation, increasing the number per group, and reducing the number of experimental groups.

When reporting micro CT data some publications express bone volume per unit tissue volume (Gao et al., 2013) or as bone mineral density. As the 3D reconstruction images demonstrate the volume of tissue surrounding the scaffolds varied considerably in this experiment, and therefore expression of bone volume in terms of total tissue volume would confound the results. Threshold setting applied during the reconstruction of the micro CT images effectively removed soft tissue, permitting recording of bone volume identified within variable volumes of tissue. This methodology has been widely applied in the literature (Boerckel et al., 2011, Pelaez et al., 2014, Bhakta et al., 2012).

While every effort was made to standardise the Allograft cylinders, such as harvest from a single patient, removal of subchondral bone, and sectioning to achieve uniform length and volume, a considerable degree of heterogeneity remained between the cylinders in terms of total volume and bone density of the allograft cylinders. Use of collagen sponge as a scaffold material in the second experiment facilitated data analysis as all bone identified within the collagen was newly formed, and the sponges were of identical length and density.

Ectopic murine studies are clearly not as comparable to clinical practice as orthotopic models in large animals. However, the ectopic models utilised permitted implantation of 6 allografts or collagen sponges per animal, enabling a reduction in the number of animal required, whilst still permitting investigation of the key research aim, ability of Laponite gel and dry film to deliver BMP *in vivo*.

In relation to the first objective, we conclude that Laponite gel is more effective at mediating BMP induced bone formation on allograft material than a dry Laponite film. Pre-mixing BMP into Laponite or exogenous application on Laponite appear to be equally effective in volume of bone formed; however the pathway of bone regeneration maybe different, i.e. endochondral and appositional.

Bone formation in collagen scaffolds receiving low dose BMP was observed in a significantly greater number of scaffolds with Laponite compared to Alginate, in which no bone formation was observed on micro CT. Conversely bone formation in collagen scaffolds receiving high dose BMP was observed in a significantly greater number of scaffolds in Alginate compared to Laponite. None of the 12 collagen scaffolds in two mice receiving Laponite/BMP group demonstrated any bone formation. The complete failure to induce bone even at the higher dose, which was present in 41 of the 42 other scaffolds leads to speculation that BMP may not have been mixed into the gel during the experiment. As the methodology involved diluting the high concentration of BMP/gel to produce lower concentration of BMP/Gel this would appear plausible. The possibility of failure to load BMP in 6 high dose and 6 low dose BMP sponges in the Laponite group may have reduced the effect seen. Whilst at present this is mere speculation, such a possibility may be confirmed were it to be possible to perform an Antibody mediated assay for BMP presence on the remaining gel samples which remain frozen following the experiment.

Histological results were only weakly supportive of the micro CT results. Collagen sponge, Alginate and Laponite gels were identifiable, with very small areas of possible bone tissue observed. In many cases tissue adjacent to areas of apparent bone formation was missing. Hard tissue may have been shed during sectioning as samples did not undergo decalcification.

Bone volume formed per µg BMP was significantly greater with Laponite and low dose BMP compared to Alginate and Laponite with high dose BMP. Previous work has established the ability of hydrogels to enhance growth factor delivery. Boerckel (Boerckel et al., 2011) reported that use of a mesh/Alginate hydrogel delivery system for BMP resulted in significantly greater bone volume than Collagen/BMP, and Dawson (Dawson et al., 2011) reported increased angiogenesis when VEGF was delivered in Laponite and applied to a collagen sponge.

A critical consideration is if Laponite is capable of reducing the dose of BMP required to stimulate bone formation compared to other methods of BMP delivery. Inter-study comparison of BMP dosing is inherently challenging due to variation in BMP preparation, and the plethora of species and *in vivo* models employed. To facilitate comparison of BMP doses used in our study we have

expressed BMP doses as µg BMP per volume of defect (cm^3) of some key publications in Table 4-8, and graphically in figure 4-29.

Author	BMP carrier	Species	Model	Defect volume (µL)	Dose BMP (µg/cm^3)	Min. effect dose BMP (µg/cm^3)
(Lee et al., 2015)	Heparin based hydrogel	Rat	Postero-lateral spinal fusion	200	0.5	0.5
	Heparin based hydrogel	mouse	Ectopic (muscle)	20	50	50
Gibbs 2015	ACS/ Laponite	mouse	Ectopic (subcutaneous)	63	0.57-6.97	0.57
(Boerckel et al., 2011)	PCL mesh + Alginate	Rat	Femoral defect	157	0.64-31.83	6.37
	ACS	Rat	Femoral defect	157	0.63-15.91	6.37
(Wang et al., 1990)	None	Rat	Ectopic (subcutaneous)	50	9.2	9.2
(Pelaez et al., 2014)	ACS	Rat	Calvarial	50	24.87-397.89	24.87
(Ben-David et al., 2013)	PEG/fibrinogen hydrogel	Nude mice	Ectopic (subcutaneous)	30	33.95	33.95
(Govender et al., 2002)	ACS	human	Tibial fracture		750-1500	750

Table 4-8 Range of dose of BMP employed in previous in vivo and clinical studies

ACS = collagen sponge, PCL = Polycaprolactone
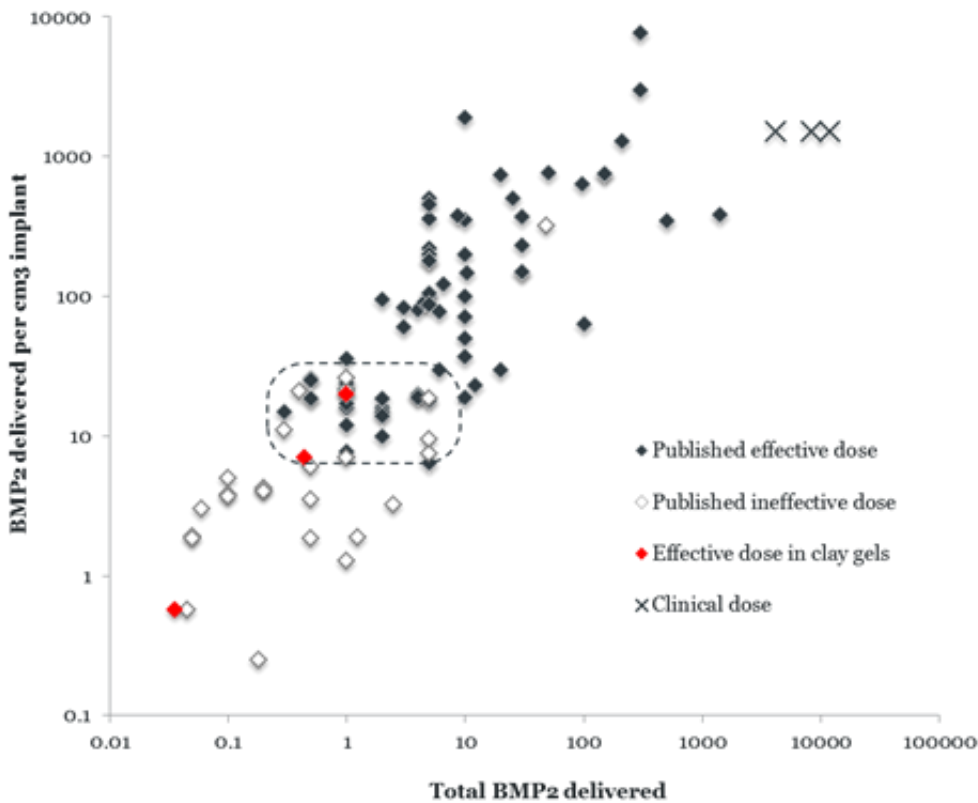
Figure 4-29 Comparison of BMP doses (µg) used in previous ectopic in vivo studies

This figure is included in a manuscript which has been submitted for publication:

Clay nanoparticle gels induce bone formation at physiological doses of BMP
D.M.R. Gibbs, C.R.M. Black, G. Hulsart-Billstrom, Richard O.C. Oreffo, Jonathan I. Dawson

In this study BMP doses of 0.57µg/cm^3 delivered in Laponite mediated ectopic bone formation. This is the lowest recorded BMP dose to stimulate ectopic bone formation in the published literature. It is noteworthy that the ectopic environment is considerably less osteogenic that orthotopic or spinal fusion models (Lee et al., 2015), in which the defect is adjacent to bleeding bone.

The collagen sponge utilised in this study is used clinically to mediate BMP-2 delivery (Infuse, Medtronic) and (InductOS, Medtronic) to stimulate fracture healing and spinal fusion respectively. BMP was delivered within Alginate gel as a control, rather than water, as this permitted comparison of Laponite with another hydrogel, rather than water. Furthermore, alginate is widely used in tissue engineering as a scaffold material, and delivery vehicle for growth factors and drugs (Augst et al., 2006, Gibbs et al., 2014a). Alginate and Laponite concentrations, and experimental

methodology were optimised prior to experimentation to provide consistent gel loading of the Allograft and collagen sponges. Relatively low Standard Deviation of volumes of gel remaining following loading of the collagen sponges demonstrates consistent loading was achieved.

As described previously, in clinical practice, lyophilised BMP is used, and use of this product here may have produced data more representative of clinical practice, compared to laboratory grade BMP, which is less stable. However, clinical grade lyophilised BMP is combined with additional products, the nature of which is commercially secret, and therefore could not be used in this study. Degradation of BMP was minimised with use of dry ice, and individual preparation of BMP/Gel for each mouse as anaesthesia was induced.

Volume of sponge was relatively small, around $1/10^{th}$ of the volume which may require stimulation of bone formation. The volume of sponge was limited by thickness of the sponge used in clinical practice to deliver BMP, and the diameter of skin biopsy punch. It may be advantageous to either use a thicker collagen sponge or a larger punch biopsy.

We were only able to precisely correlate individual gel loading and bone volume for 8 Laponite and low dose BMP samples, 17 Laponite and High dose samples, and 12 Alginate and high dose BMP samples. This was due to the fact that only 2 of 3 scaffolds on one side of some mice were visible on micro CT rendering it impossible to correlate initial gel loading and bone volume with individual scaffolds.

The results of this study have significant implications for orthopaedic practice. We have demonstrated that Laponite gel is able to reduce the dose of BMP required to stimulate bone formation by several orders of magnitude, and is a more effective delivery vehicle than current gold standards of collagen or Alginate. This offers the potential to harness the powerful osteogenic effect of BMP at doses sufficiently low to mitigate serious side effects, and to drastically reduce the cost of treatment. The reduction in dose of BMP may reduce the cost sufficiently to alter the cost benefit analysis of BMP thearapy performed by Garrison (Garrison et al., 2007), rendering them economically viable. Influence of delivery of BMP with Laponite on rate of fracture healing was beyod the scope of this investigation. Should further investigations demonstrate acceleration of fracture healing, and therefore earlier return to work, the economic rational for BMP use would be overwhelming.

Null Hypothesis

Use of Laponite to deliver BMP will not result in greater bone formation compared to BMP applied alone or with an alternative growth factor delivery vehicle.

4.8   Conclusions

It has been demonstrated that Laponite gel is capable of delivering BMP *in vivo,* and is superior to dry Laponite film as a growth factor delivery vehicle. The dose of BMP required to stimulate endochondral bone formation *in vivo* was significantly reduced when delivered with Laponite compared to Alginate gel.

The null hypothesis can therefore be rejected.

Chapter 5:   The ability of Laponite gel mediated BMP delivery and allograft to enhance healing in an ovine femoral cortical defect.

I am grateful to Cameron Black, a veterinary surgeon who developed this animal model.

Within the experimental design I selected the BMP dose, and performed the power study. Control and test groups were determined jointly by myself and Cameron.

I performed the animal surgery jointly with Cameron, and assisted by Janos Kanczler and David Gothard.

CT scanning was performed by myself, Cameron and Gry Hulsart-Billstrom.

Method of CT analysis was designed and performed by myself, with guidance and assistance from Gry Hulsart-Billstrom.

5.1 Introduction

The over-arching aim of this thesis is to explore the potential of Laponite for use as a growth factor delivery vehicle to enhance fracture healing, and to assess the suitability of combining Laponite with AM to produce synthetic bone graft material. In chapter 3 dry Laponite films and Laponite gels were shown to localise and deliver active BMP *in vitro*. Subsequently in chapter 4 Laponite gel, rather than a dry film was found to be more effective in mediating BMP delivery on allograft material, and was shown to reduce the dose of BMP required to induce bone formation in an ectopic murine model.

While ultimately we seek to harness Laponite to localise BMP to AM derived bone, as an initial step the effect of Laponite gel and BMP application to allograft, on healing within a bone defect was assessed. Allograft was chosen as it is commonly used in clinical practice and *in vivo* studies, thus aiding comparison of data, and if allograft function were to be enhanced by Laponite gel/BMP preparations, this result could, potentially, directly translate into clinical practice. Furthermore, due to technical challenges, the scaffolds produced by AM were not of suitable biomechanical properties for further *in vivo* investigation as described in appendix A.

An ovine model was chosen to evaluate Laponite/BMP/Allograft material. As described in the introduction (1-4), bone formation and architecture is determined by the forces exerted upon them. Notwithstanding their quadrupedal nature, sheep biomechanics bear closer resemblance to human biomechanics (Nunamaker, 1998) and thus provide a model that is more representative to humans than small animal models. Adequate perfusion throughout a scaffold material is critical to avoid necrosis, defects and scaffold material of sufficient dimensions to take account of limitations of perfusion is only possible in large animal models. Furthermore, sheep are more docile in nature, than canine or feline species (Nunamaker, 1998).

In order to reduce the number of animals required, bilateral defects were planned in the distal medial femoral condyle. The technique closely resembles that described by Malhotra (Malhotra et al., 2014). Previously, Nuss (Nuss et al., 2006) used an equivalent technique on the distal lateral femoral condyle. Other studies have sought to further reduce the number of animals required by increasing the number of defects per animal, in some cases by forming defects not only in the femur, but also in the humerus (Nuss et al., 2006). This model was not selected in this study as a higher risk of fracture was seen with humeral defects, and there is a greater physiological and nociceptive insult to the animal.

Previous ovine bone defect studies have utilised BMP at doses ranging from 0.22mg/cm^3 (Cipitria et al., 2013) to 54mg/cm^3(Liu et al., 2013) as shown in Table 5-1. In the previous chapter Laponite gel adsorbed onto collagen was combined with of 0.57-6.97µg BMP per cm^3 of collagen. Laponite gel was found to decrease the effective dose of BMP by an order of magnitude compared to Alginate. On this basis we reduced the dose applied to an ovine tibial defect by Cipitria (Cipitria et al., 2013) by approximately twenty fold, selecting 0.01mg /cm^3 as the dose of BMP for this experiment.

Author	BMP carrier	Species Of Sheep	Mean weight (kg)	Model	Defect volume (cm³)	Dose BMP (mg/cm³)	Min. effect dose BMP (µg/cm³)
Cipitria	PCL & ß-TCP	Merino	43.3	Tibial defect	As hollow tube 7.9	0.22-0.44	0.22
Donati	Allograft Collagen putty	Alpine	65	metatarsal	2.4[1]	1.46	Did not increase BV
Liu	DBB & Calcium phosphate	Australia	45	Cortical defect Humerus/femur	0.65	54	54

Table 5-1 Dose of BMP used in previous ovine studies

1: Assuming metatarsal is 1cm in diameter and solid.

DBB deproteinated bovine bone, BV = Bone volume, PCL = polycaprolactone,

ß-TCP = ß-tricalcium phosphate

The primary endpoint was bone volume formed within the defect, assessed using micro CT.

The fourth stage of secondary fracture healing, remodelling was described in the introduction. Remodelling involves not only deposition of bone, but also resorption of bone. Thus in addition to volume of bone formed the current study will assess bone morphology within the defect as a secondary endpoint, specifically, the alignment bone architecture, trabecular number, thickness and separation.

A sample size calculation was performed using data from Van der Pol (van der Pol et al., 2010), in which bone volume formation within femoral and tibial defects of 5mm diameter and 15mm depth was assessed. This paper was selected as the defect size is similar in size to the defect planned in our study. A standard endpoint was utilised (Bone Volume/Tissue Volume) and a relatively large number of defects were reported (n=150). The mean standard deviation of Bone Volume per Tissue Volume was 9%, and effect size of treatment was 15%. In this study (van der

Pol et al., 2010) the bone defect was treated using a bio-composite scaffold and compared to an empty bone defect. Using the equation: Sample size (n) = $2 \sigma^2 (Z_\beta + Z_{\alpha/2})^2 /=$ (difference in mean)^2, selecting for 80% power and 0.05% level of significance, 6 samples per group are required. Previous published work on a comparable ovine femoral defects has also used 6 samples per group (Liu et al., 2013).

5.2 Aim

Assess the ability of Laponite to enhance bone healing mediated by allograft and BMP in a large animal bone defect.

Null Hypothesis

The use of Laponite to deliver BMP will not result in greater bone defect healing by allograft compared to BMP applied to allograft material with an alternative growth factor delivery vehicle or use of allograft alone.

Objectives

1) To investigate the biocompatibility of Laponite gel combined with BMP and allograft material in a large animal model.

2) To investigate the ability of Laponite gel to increase bone formation mediated by BMP and allograft.

3) To evaluate morphometric parameters of newly formed bone within a large animal bone defect mediated by allograft alone and in the presence of BMP, delivered alone or with Laponite.

5.3   Methodology

Peri operative care

Sheep selection

Adult sheep of an upland hill breed (Welsh Lynn), weighing between 65-75kg and of similar age were selected. All sheep underwent a health inspection prior to surgery by a veterinary surgeon, and received a minimum of 7 days acclimation at the BRF prior to the procedure.

Anaesthesia

Sheep were starved for 12 hours prior to surgery, and did not receive water for 1 hour prior to surgery.

Pre-medication

Midazolam 0.2mg/kg was administered intra-muscularly 20 minutes prior to anaesthetic induction.

Induction

A 21G iv catheter was sited in the cephalic vein, and Propofol 3-5mg/kg was given intra-venously. Following induction Lidocaine spray was applied to the larynx. An endotracheal tube (ET) was inserted and the cuff inflated as appropriate. Tube was secured with tape and connected to the anaesthetic circuit.

Maintenance

Isoflurane 2-4% was used to maintain anaesthesia.

Monitoring

Heart rate, respiration rate, arterial oxygen saturation was monitored throughout the procedure. In addition, mucous membrane colour, capillary refill time, and palpebral reflex were monitored throughout surgery.

Post operative analgesia

Following the surgical procedure, 1% Lidocaine was infiltrated subcutaneously around the surgical site. A forelimb was shaved, and a Fentanyl Patch was applied to the skin and secured with a bandage.

Recovery

Each animal was supervised on recovery. Sheep were placed in sternal recovery position and the ET tube removed once the swallowing reflex had returned. Animals were monitored until conscious, able to stand and maintain posture independently, and pass a post-operative clinical exam which involved examination of nervous responses, vital parameters, and ruminal integrity.

Surgery

The operative procedure was developed by Cameron Black and subsequent photographs were taken by Cameron Black.

5.3.1.1 Preparation

The anaesthetised sheep was placed supine on the operating table with the head rotated as shown in Figure 5-2. The pelvis and hind limbs were secured using foam blocks as shown in Figure 5-3. The operative site was shaved. Following application of 2% Chlorhexidine, the surgical site was draped as shown in Figure 5-4.

Figure 5-1 Positioning the head

Figure 5-2 Positioning the hind legs

Figure 5-3 Draping of operative site

5.3.1.2 Operative procedure

Incision

The bony prominences of the patella, medial femoral epicondyle and the tibial tuberosity were identified by palpation. Together these 3 landmarks form a triangle through the middle of which a 5cm incision was made through the skin.

Approach

Typically virtually no subcutaneous fat was encountered during the procedure. Following incision through the skin and subcutaneous fascia, blunt dissection was used to split the underlying muscle in the direction of its fibres. Soft tissues were retracted with the use of a retractor or an assistant with 2 Langenbeck retractors (Figure 5-5).
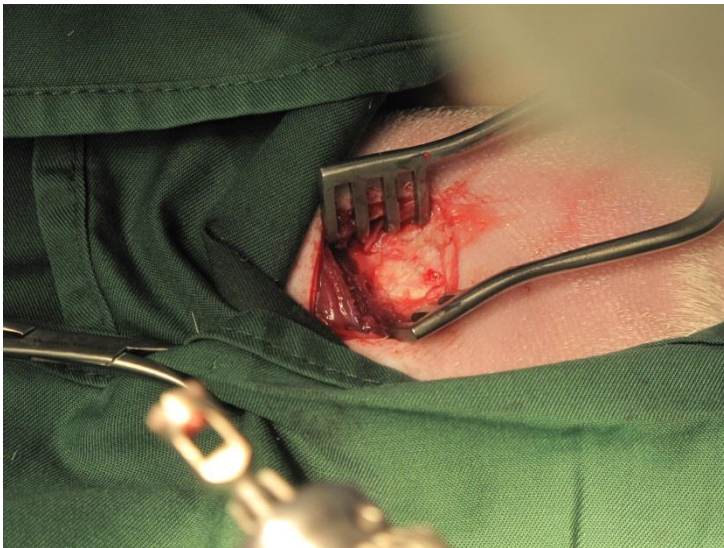
Figure 5-4 Visualisation of the medial femoral condyle

Drilling of the condyle defect

A defect was made using an 8mm diameter hollow trephine. Initial entry was made using a guide, with subsequent drilling freehand. 10mm depth was clearly marked on the drill bit to facilitate consistent depth drilling. Throughout the procedure the site was irrigated with sterile saline to avoid thermal necrosis (Figure 5-6). Following drilling the 8mmx10mm core was removed with a custom made trephine as shown in Figure 5-7, leaving an empty defect (Figure 5-8).

Figure 5-5 Drilling the defect

Figure 5-6 Removal of bone core
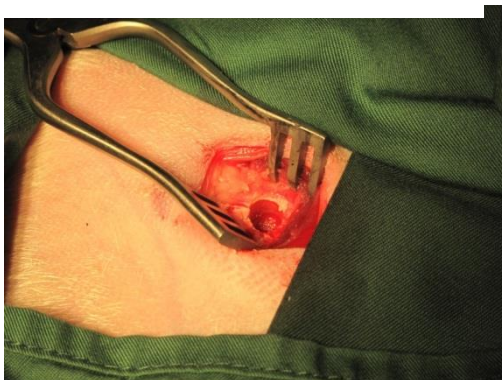
Figure 5-7 Empty bone defect

Graft preparation

Allograft material was harvested from the femoral condyle of a single sheep, following milling, graft material underwent multiple washes in hydrogen peroxide, followed by saline. 5μg BMP were applied to 120μl of 2.5% Laponite (or 2.5% Alginate), subsequently this was mixed with 540mg of allograft material, and applied to the defect.

Control defects were left completely blank.

Autologous bone defects received fresh bone graft from the femoral condyle, which was not weighed prior to implantation.

Sample retrieval

Ten weeks following the initial surgery sheep were euthanized with iv Sodium Thiopentone. Medial distal femoral condyles were removed with the use of a bone saw and preserved in 4% Paraformaldehyde in PBS.

CT Scanning and image reconstruction

Samples were removed from the specimen pots and wrapped in cling film to prevent desiccation. Wrapped samples were placed centrally in the CT and scanned at 90kV, 278uA, with a 0.1mm Cu filter and a pixel size of 18μm.

The Otsu method, a mathematical method which identifies the optimal greyscale level to differentiate objects was performed on each sample (Otsu, 1975). Images were subsequently reconstructed with the mean Otsu threshold used for the lower greyscale level (118). Corrections were made to account for beam hardening and ring artefacts. The same reconstruction protocol was used for all scans.

In order to minimise the effect of inter-sheep variation in bone mineral density on our primary endpoint, volume of bone formed within the defect site was standardised to bone volume per tissue volume in a region of bone adjacent to, but distinct from the defect. This methodology is discussed in 5.3.1.3 to 5.3.1.3 summarised in figure 5-10. A similar methodology was described by Berner (Berner et al., 2013), who standardised volume of bone formed within an ovine tibial segmental defect to the bone volume of the corresponding region on the contralateral limb.

CT analysis

5.3.1.3   Enclosed defect Region of Interest (ROI)

Images were rotated in Data Viewer to obtain a view centred on the defect. Due to the spherical nature of the condyle the initial part of the defect is often not fully enclosed as shown in Figure 5-9. We manually selected the top of the enclosed defect ROI as the first slice which was fully enclosed by bone. The bottom slice was taken to be 58 slices (1mm) above the first slice at which the trabecular pattern was unbroken when moving from the defect to the surrounding bone. This was named the enclosed defect ROI (See figure 5-12).
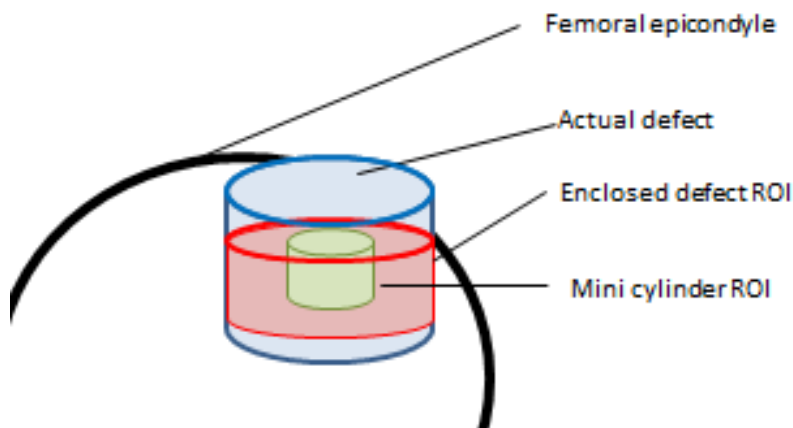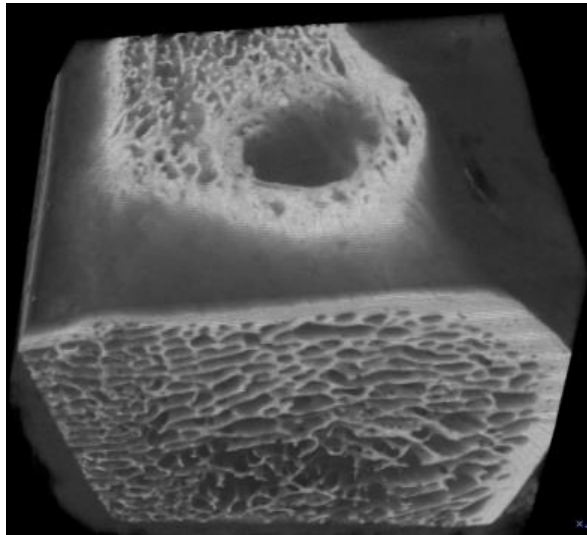
Figure 5-8 Selection of Regions of Interest for CT analysis

3D reconstruction of the bone defect formed within the femoral condyle and diagrammatic representation of the regions of interest.

5.3.1.4 Mini cylinder

The length of the cylinder of all samples was reduced to 4mm, and the customised image profiler was then used to shrink the diameter from 8 to 4mm in centre of defect. This produced a cylinder 4mm in diameter and 4mm in length. This was termed the mini cylinder ROI.

5.3.1.5 Outer Standardisation region

In order to normalise bone formation to adjacent bone to take account of inevitable variation in sheep bone volume per tissue volume, a region of native bone adjacent to the defect was identified. The enclosed defect ROI was reduced from the top slice by 100 slices, to permit dilation of the ROI without extending out of the condyle (Figure 5-11). The customised profiler was used to form a donut shaped ROI with an outer diameter of 12mm, and an inner diameter of 10mm as shown in Figure 5-10. In cases in which this technique resulted in selection of a region within the medulla or cortex the length of the cylinder was further reduced to avoid this. This region was termed the outer standardisation region (figure 5-12).

5.3.1.6 Inner standardisation region

A second doughnut was selected using the same technique as described for the standardisation ROI, with the exception that the outer and inner diameters were 10 and 8mm respectively. This ROI was formed to quantify bone immediately adjacent to the enclosed defects, this was termed the inner standardisation region (figure5-12).
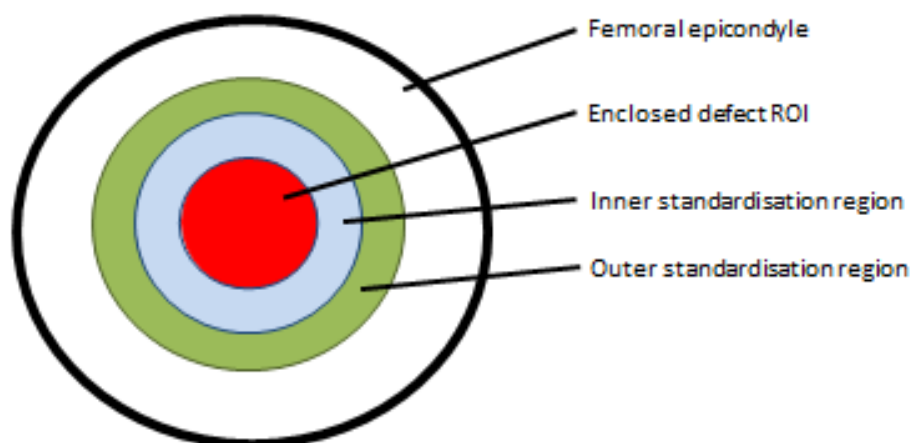
Figure 5-9 Diagrammatic representation of Regions of Interest surrounding the defect.
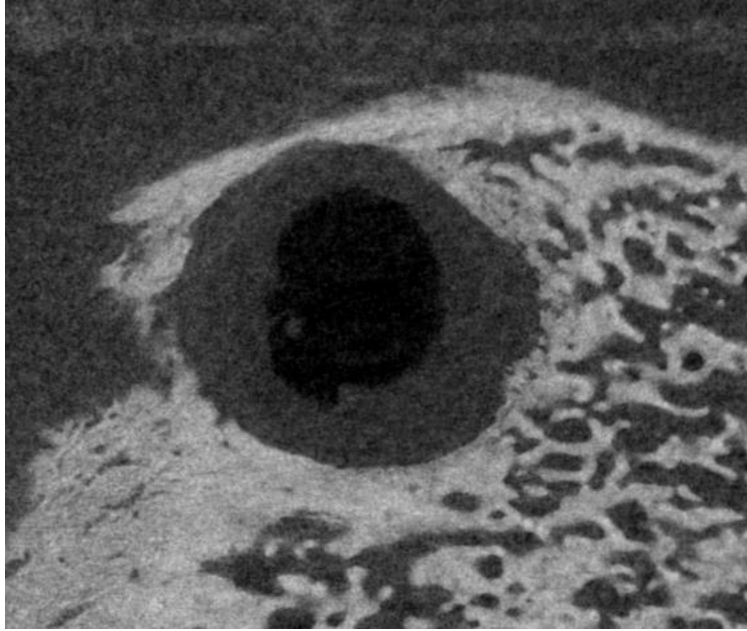
Figure 5-10 CT image demonstrating thickness of bone surrounding the

defect

Transverse section of sheep 6 at the top of the enclosed defect ROI,

demonstrating that any selection of volume surrounding the defect at this

level would have enclosed air rather than bone
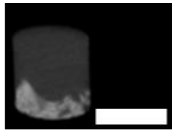
Mini cylinder
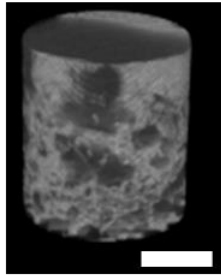
Enclosed defect region
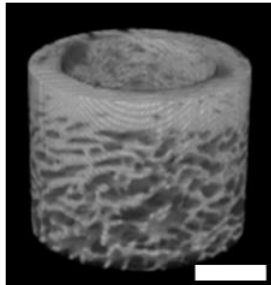
Inner standardisation region
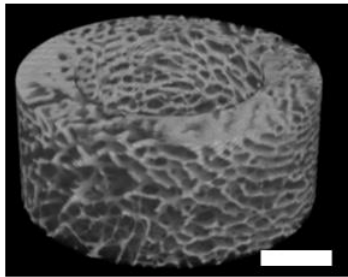
Outer standardisation region
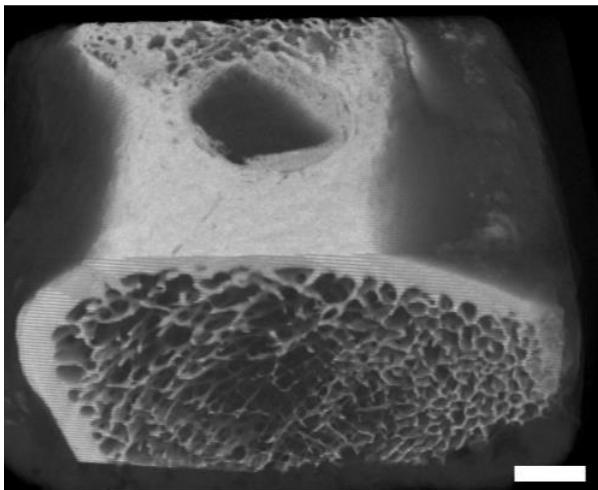
Femoral condyle

Figure 5-11 Regions of interest defined within the femoral condyle

Scale bar shown is 4mm.

5.3.1.7   Assessment of the secondary endpoint, bone morphometry

As Wolff so eloquently described cancellous bone has a "well motivated architecture, which is closely related to its statics and mechanics." Indeed, in mature cancellous bone, the trabeculae are aligned, whilst in fracture callus a random alignment of fibres is observed. Previous ovine work has reported a decrease in bone volume within a fracture during this stage of fracture healing (Donati et al., 2008), or failed to detect a difference in bone volume formed by different treatment groups, while a difference in bone morphology at the defect was detected (Ding et al., 2013).

In this thesis we will use Bone Morphometric terminology defined by Parfitt (Parfitt et al., 1987) and adopted by SkyScan. Isotropy and anisotropy are measures of the tendency of fibres to align in 3D within an object. If an object is isotropic, a line passing through the object will intercept a similar number of fibres in any plane. The number of intercepts of a line passing through an anisotropic object will depend upon the orientation of the line as shown in figure 5-12.
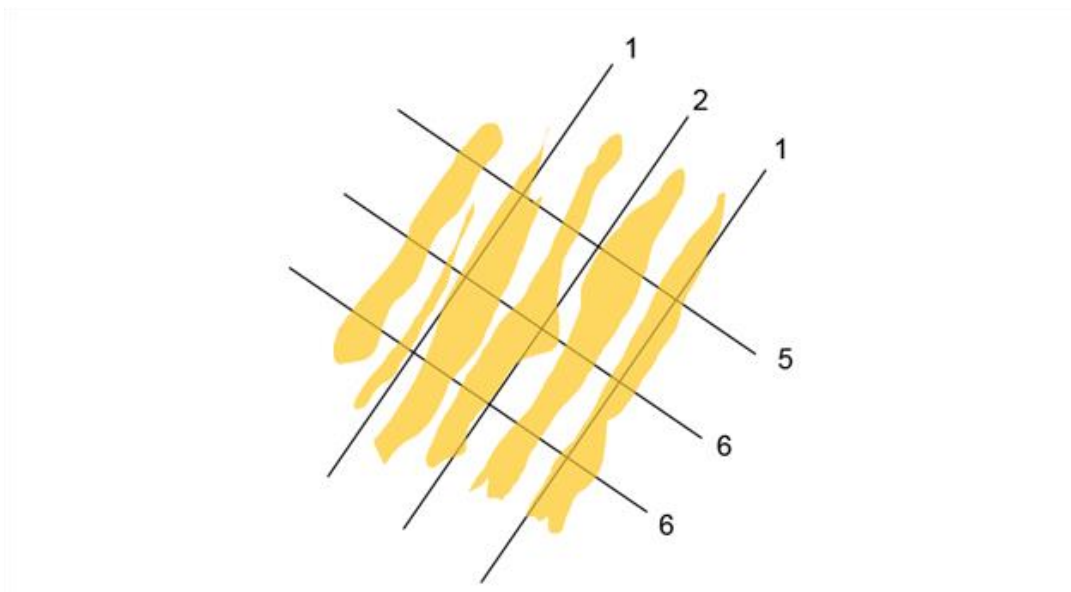
Figure 5-12 Diagrammatic representation of anisotropy

This figure is taken from the Manual for Bruker-micro CT Analyser (Bruker, 2014). Aligned structures such as that demonstrated are highly anisotropic. Test lines make few intercepts in the long axis, but lines perpendicular to the structure make many more intercepts. The number of intercepts for each line is shown.

Mean intercept length (MIL) is a measurement of anisotropy, it is found by drawing lines through an object, and dividing the number of times the line intercepts solid phase. Typically MIL is

measured in three vectors, known as Eigen values. Anisotropy of an object is a continuum from zero, completely isotropic, to infinity, completely anisotropic. CT Analyser software translates 3 Eigen values into a single output, Degrees of anisotropy, in which 0 represents total isotropy, and 1, represents total anisotropy, in lieu of a range from 0 to infinity to facilitate comparison and analysis.

$$DA = \left(1 - \left[\frac{\min eigenvalue}{\max eigenvalue} \right] \right)$$

Equation 1 Calculation of Degrees of anisotropy with CT

For bone morphometric analysis the top 50 slices of the inner standardisation region which did not include any soft tissue were used. Reduction in ROI volume was necessary morphometric analysis of larger ROI volumes exceeded the computational capacity of the computer. In addition to the alignment of the internal bone architecture we will also measure the trabecular number, thickness and separation.

5.4   Results

This study was intended to assess the biocompatibility and efficacy of Laponite to enhance bone healing mediated by allograft and BMP in a large animal bone defect. A medial femoral cortical bone defect was made in sheep and filled with allograft, Laponite and BMP. Healing was assessed using the primary endpoint of bone volume formed within the defect, and secondary endpoints related to bone morphometry. Comparison was made with control groups: autograft, allograft, and allograft combined with Alginate and BMP.

None of the sheep suffered any apparent adverse effects related to surgery, or from the implantation of allograft material combined with Alginate or Laponite and BMP. All sheep began standing and weight bearing on the operated limb within hours of the surgery. No cases of wound infection or wound inflammation were observed.

While all sheep completed the study, inadvertently, the second sample, which received allograft material alone, was sawed through during retrieval, and thus could not be included in the study. Of the 27 samples, 26 were analysed.

Bone volume, and bone volume per tissue volume formed within the enclosed defect was greatest with allograft, and least with empty defects, however this was not statistically significant (figures 5-13 & 5-14). Bone volume per tissue volume within the mini cylinder, the central area within the defect was significantly greater with allograft compared to the blank defect (P=0.013), as shown in table 5-2 and figure 5-15, with no other significant difference detected between other groups (autograft, allograft/BMP/Alginate, allograft/BMP/Laponite).

There was no significant difference in bone volume per tissue volume of the inner and outer standardisation regions of bone surrounding the defect (5-18 & 5-19), indicating minimal inter sheep variation in bone mineral density.

Standardisation of bone volume per tissue volume of the mini cylinder with the outer (5-18) or inner (5-19) standardisation region adjacent to the defect did not alter the result, with BV/TV significantly greater with allograft compared to blank defects, and no other significant difference detected.

Bone morphometry, in the form of trabecular thickness, separation and number, and anisotropy was also assessed. Trabecular thickness was significantly greater with allograft compared to blank defects (P=0.0181), with no significant difference detected with autograft, allograft/BMP/Alginate, allograft/BMP/Laponite. No significant difference in trabecular separation

or number was observed. Degrees of anisotropy, a measure of structural alignment, was greatest with allograft/BMP/Laponite, however this was not statistically significant.

Quantitative analysis of bone formation
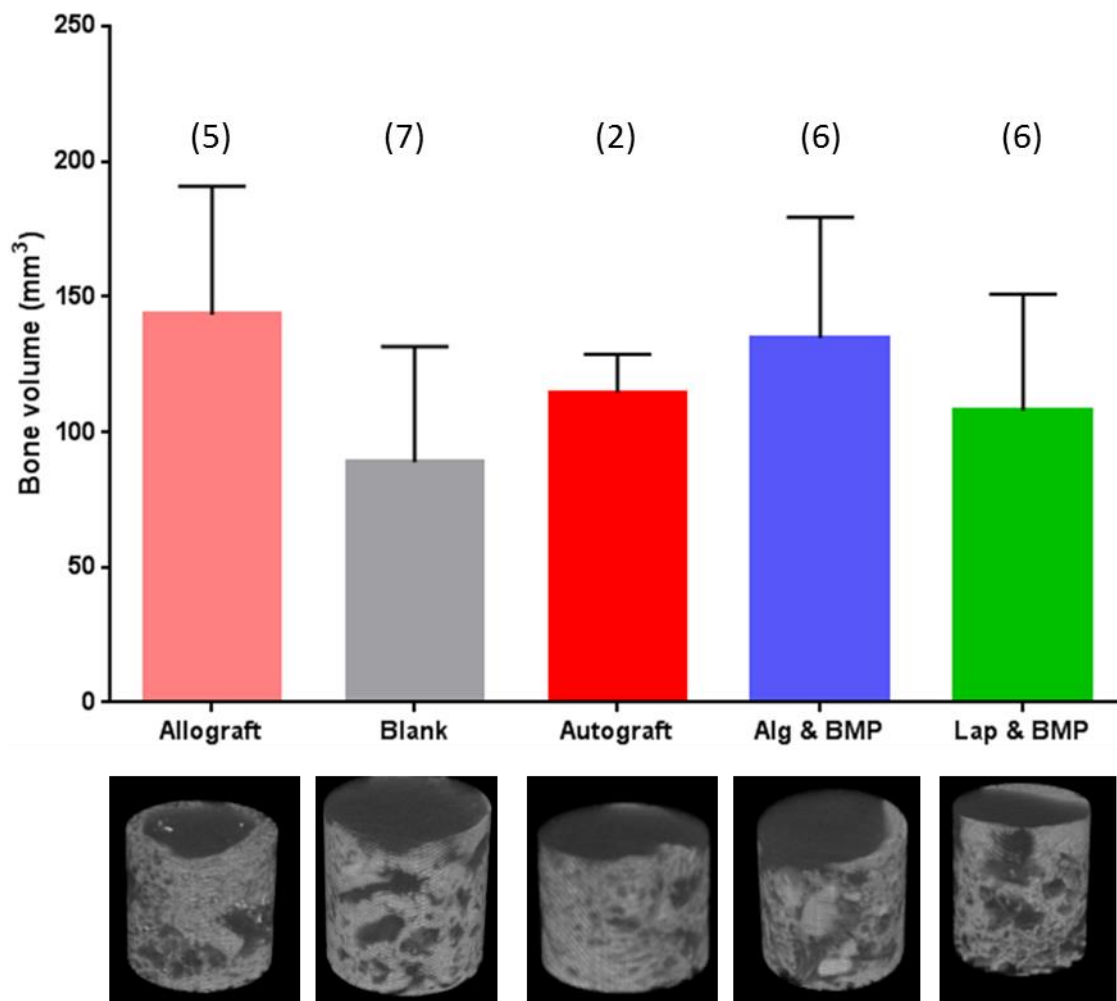
Figure 5-13 Graph of Bone volume formed within the enclosed defect

Graph shows mean bone volume formed within the enclosed defects with corresponding representative 3D reconstructions shown below. Error bars show standard deviation. Number of samples is shown in brackets. Analysis with one-way ANOVA did not detect any significant difference between the groups.
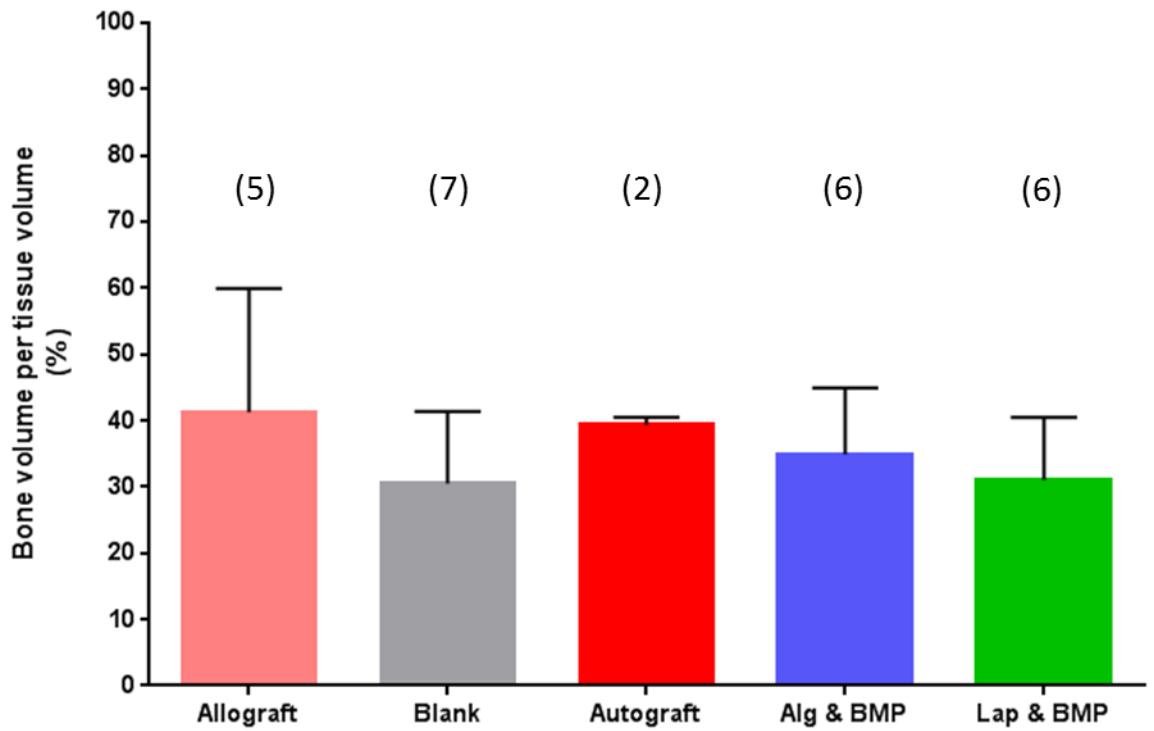
Figure 5-14 Graph of Bone volume per tissue volume formed within the enclosed defects

Graph illustrates mean bone volume per tissue volume of the enclosed defects. Error bars show standard deviation. Number of samples is shown in brackets. Analysis with one-way ANOVA did not detect any significant difference between the groups.

	Alginate & BMP BV/TV (%)	Allograft BV/TV (%)	Autograft BV/TV (%)	Blank BV/TV (%)	Laponite & BMP BV/TV (%)
	16.04	38.72	24.15	6.28	24.61
	13.31	6.48	19.35	22.53	2.25
	34.61	37.53		4.61	35.73
	20.22	22.33		7.42	0.94
	35.94	51.57		0.00	11.35
	18.02			4.99	16.06
				5.82	
Mean	23.02	29.48	21.75	7.56	15.16
SD	9.77	17.33	3.39	7.08	13.39
N	6	5	2	7	6

Table 5-2 Bone volume per tissue volume formed within mini cylinder

BV = Bone volume, TV = Tissue volume, SD = standard deviation, N = number of samples
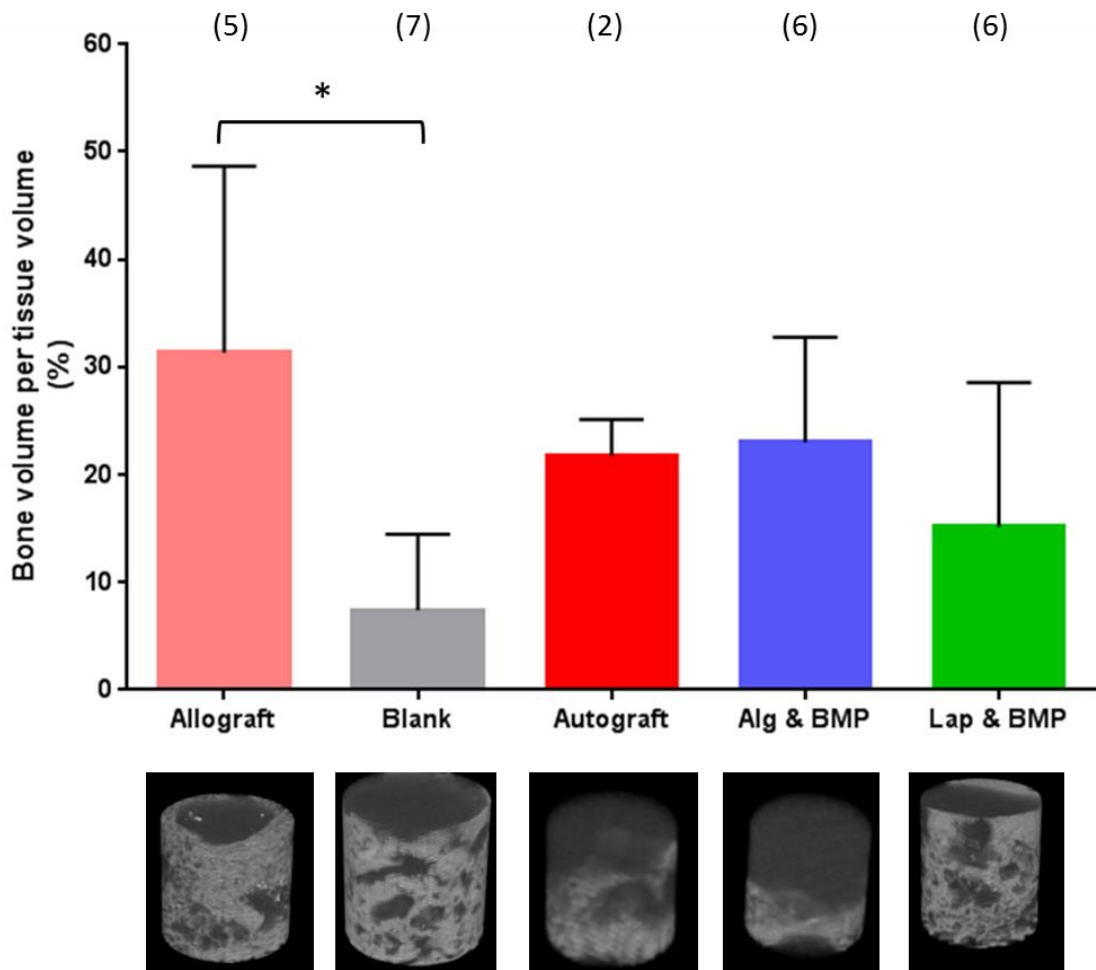
Figure 5-15 Graph of Bone volume per tissue volume formed within the mini cylinder

Graph shows mean bone volume formed within the enclosed defects with corresponding representative 3D reconstructions shown below. Allograft material resulted in significantly greater volume of bone formed within the mini cylinder compared to blank defects. Bone volumes formed within the defects of all groups were analysed using a one way ANOVA test, with P=0.026. Post hoc testing was performed using Turkey's test and p values adjusted to account for multiple comparisons. P=0.017 for Allograft compared to blank defect, with no significant difference detected between any of the other groups. Error bars show standard deviation. Number of samples is shown in brackets. * p<0.05
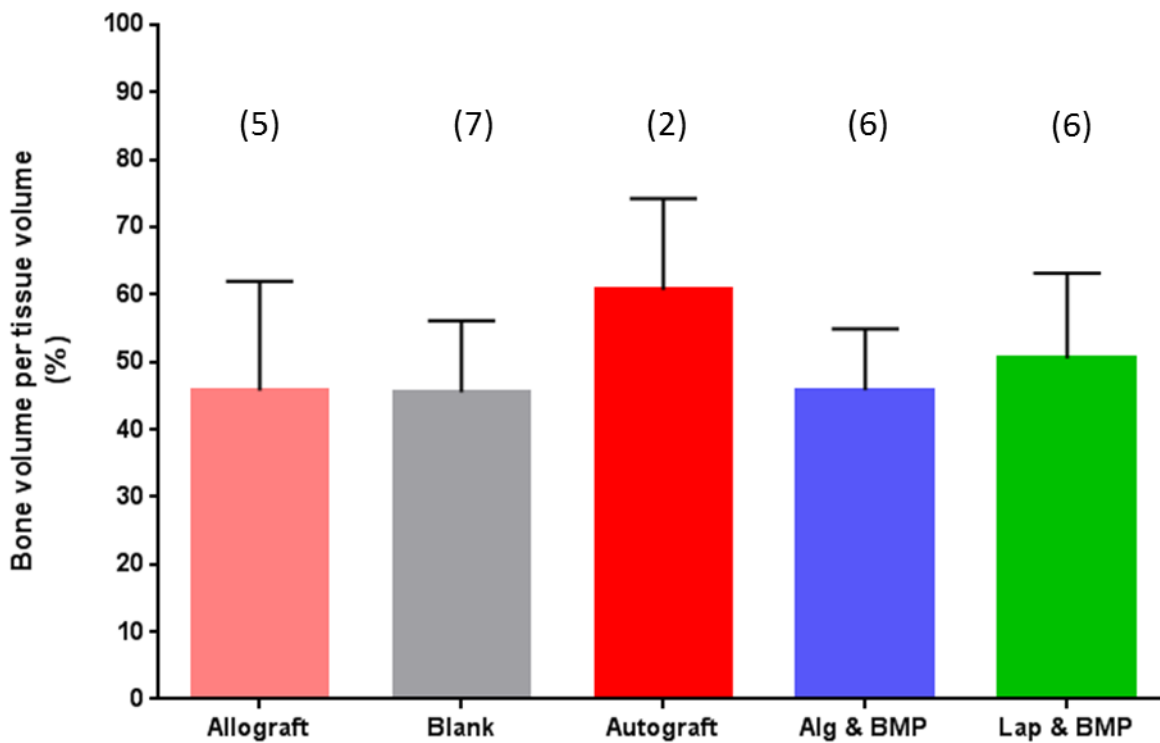
Figure 5-16 Graph of Bone volume per tissue volume of outer standardisation region

Graph shows mean bone volume formed within the outer standardisation region per tissue volume. Error bars show standard deviation. Number of samples is shown in brackets.

No significant difference in bone volume per tissue volume within outer standardisation region was demonstrated when analysed using ANOVA.
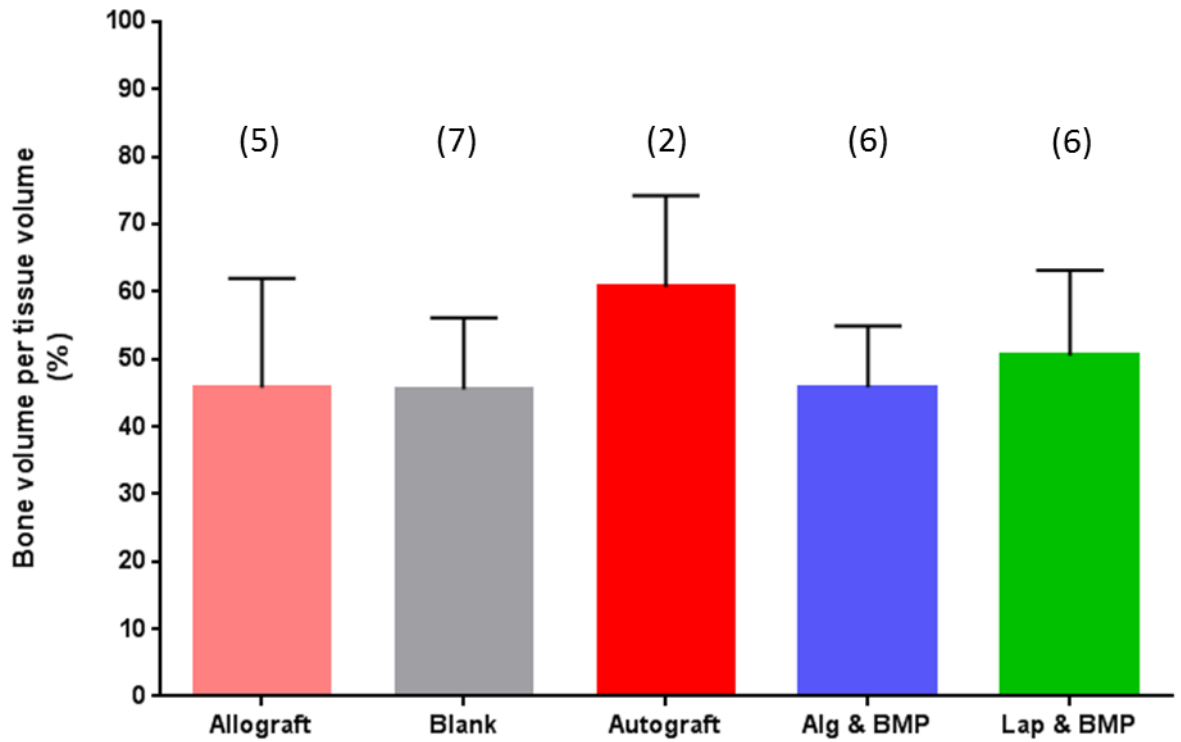
Figure 5-17 Graph of Bone volume per tissue volume of inner standardisation region

Graph illustrates mean bone volume per tissue volume of the inner standardisation region, error bars show standard deviation. Number of samples is shown in brackets

No significant difference in bone volume per tissue volume within inner standardisation region was demonstrated when analysed using ANOVA.

Graph 5-6 Bone formation within mini cylinder compared to bone within the outer standardisation region
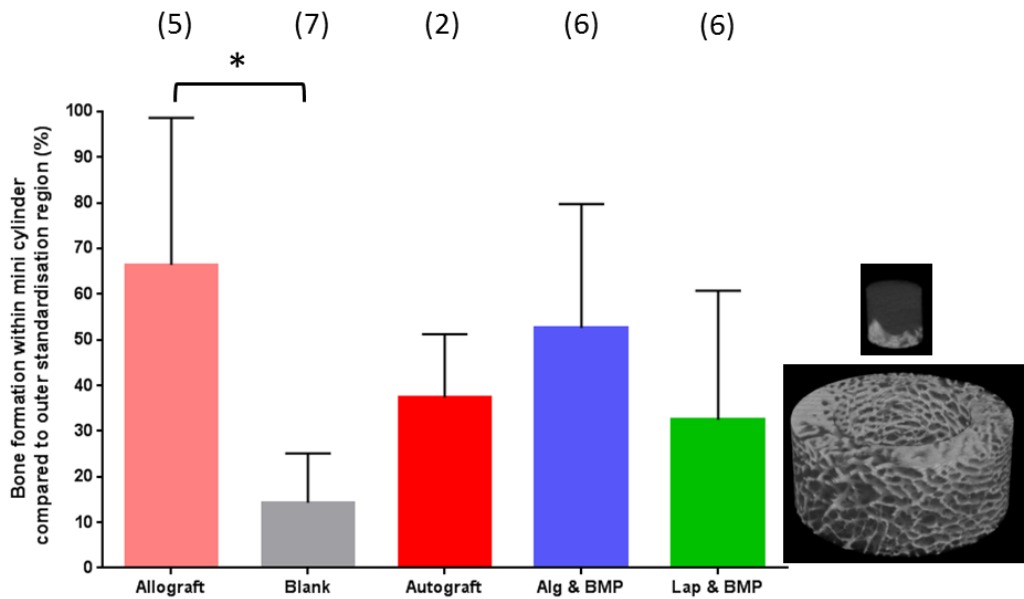
Figure 5-18 Graph of bone formation within mini cylinder compared to outer standardisation region

Graph illustrates Percentage Bone volume per tissue volume within the mini cylinder divided by the percentage bone volume per tissue volume in the outer standardisation region. Representative 3D reconstructions of the mini cylinder and outer standardisation region are shown on the right.

Allograft material resulted in significantly greater volume of bone formed within the mini cylinder compared to blank defects when normalised to the standard region each sample. Bone volumes per tissue volume formed within the defects and compared to standard regions of all groups were analysed using one way ANOVA (P=0.017). Post hoc testing was performed using Turkey's test and p values adjusted to account for multiple comparisons. P=0.013 for Allograft compared to blank defect, with no significant difference detected between the other groups. Error bars show standard deviation. * p <0.05. Sample numbers are shown above in brackets.
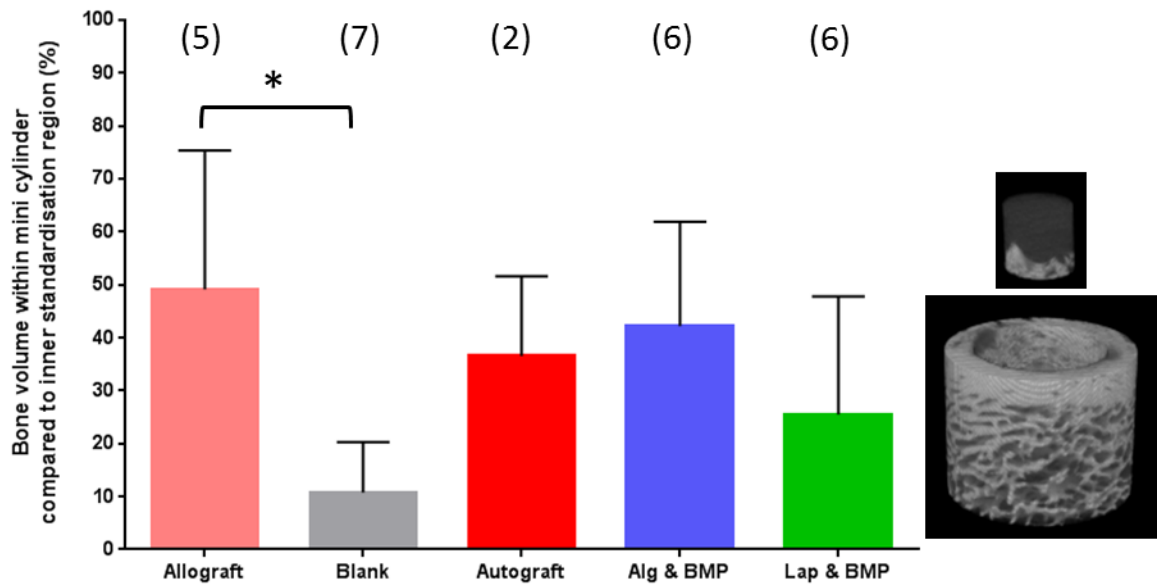
Figure 5-19 Graph of Bone formation per tissue volume within mini cylinder compared to inner standardisation region

Graph illustrates Percentage Bone volume per tissue volume within the mini cylinder divided by the percentage bone volume per tissue volume in the inner standardisation region. Representative 3D reconstructions of the mini cylinder and inner standardisation region are shown on the right.

Allograft material resulted in significantly greater volume of bone formed within the mini cylinder compared to blank defects when normalised to the standard donut for each sample. Bone volumes formed within the defects of all groups were analysed using one way ANOVA (P=0.021) Post hoc testing was performed using Turkey's test and p values adjusted to account for multiple comparison. P=0.022 for Allograft compared to blank defect, with no significant difference detected between the other groups. Error bars show standard deviation. *p<0.05. Sample numbers are shown above in brackets.

Morphometric analysis of bone formation
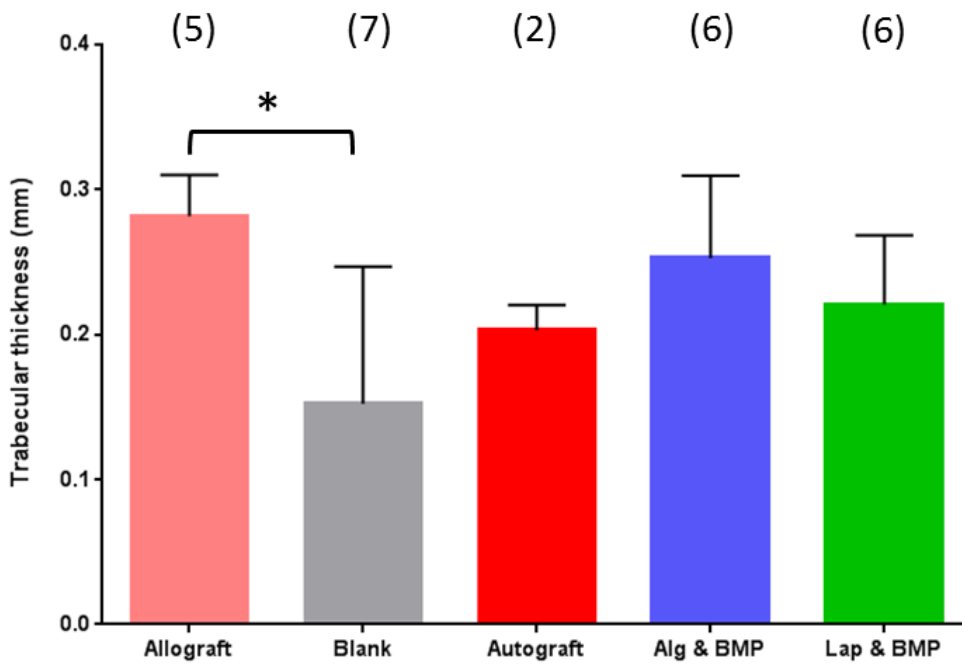
Figure 5-20 Graph of mean trabecular thickness of bone within mini cylinder

Graph illustrates shows mean trabecular thickness of bone formed within the mini cylinder.

The means of the different groups were compared with each other using one way ANOVA. Trabecular thickness of bone formed with the mini-cylinder was significantly greater in the Allograft group compared to the blank defect group P=0.0181. Error bars show standard deviation. Sample numbers are shown below in brackets. * p<0.05
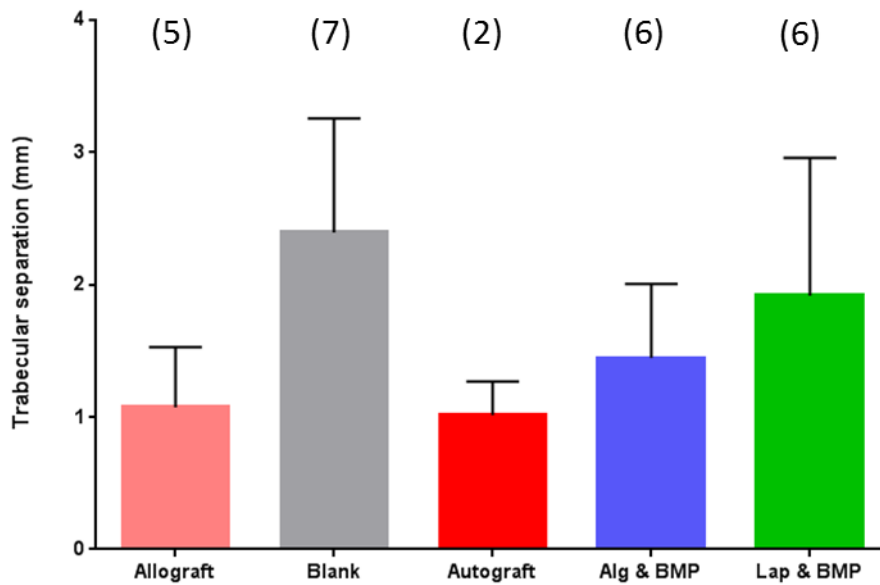
Figure 5-21 Graph of Trabecular separation of bone within the mini cylinder

Graph shows mean trabecular separation. No significant difference was detected when subject to one-way ANOVA. Error bars show standard deviation. Sample numbers are shown in brackets.
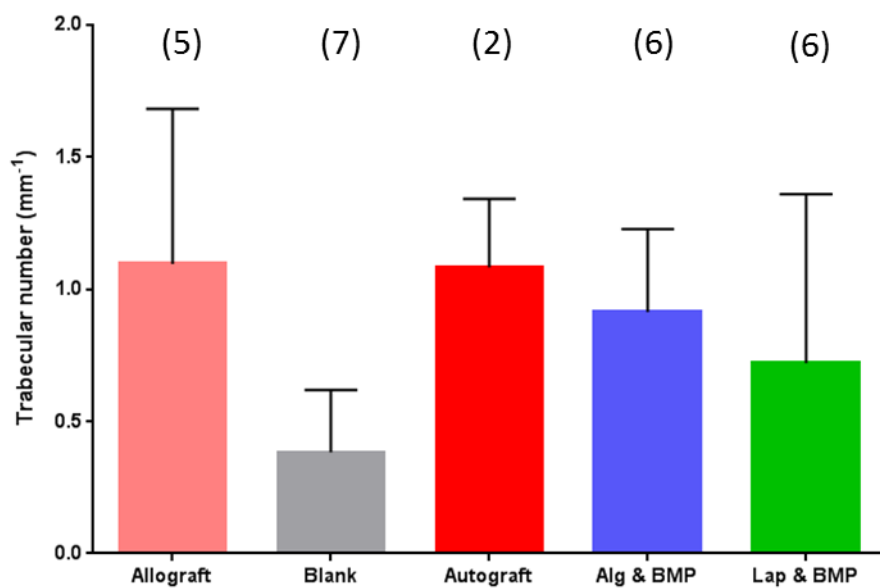
Figure 5-22 Graph of trabecular number of bone formed within mini cylinder

Graph shows mean trabecular number per mm of bone formed within the mini cylinder. No significant difference was detected when subject to one-way ANOVA. Error bars show standard deviation. Sample numbers are shown in brackets. error bars show standard deviation. Sample numbers are shown in brackets
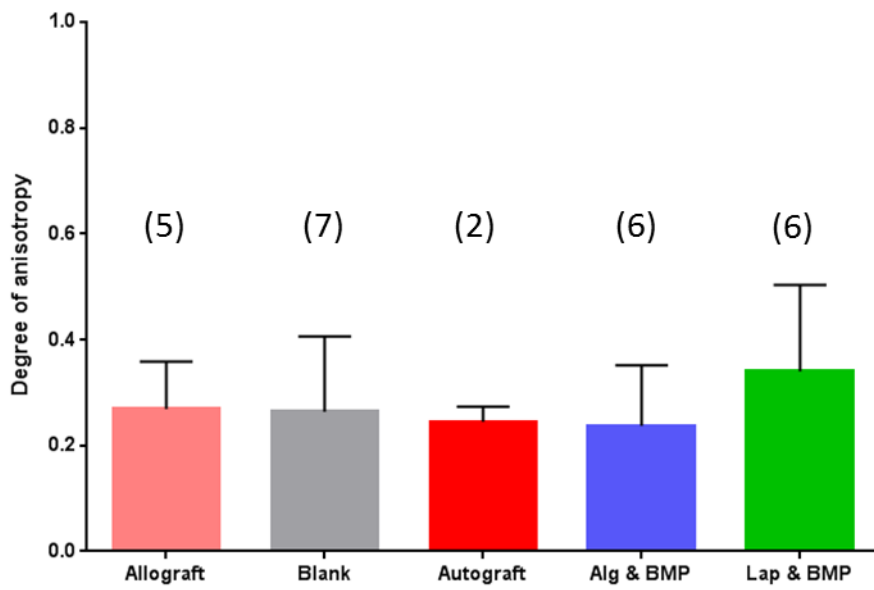
Figure 5-23 Graph showing anisotropy of bone formed within mini cylinder

Graph shows mean degree of anisotropy of bone formed within the mini cylinder. No significant difference was detected when subject to one-way ANOVA. error bars show standard deviation. Sample numbers are shown in brackets.

5.5 Discussion

This study endeavoured to examine the biocompatibility and efficacy of bone formation mediated by allograft and BMP delivered by a Laponite hydrogel.

No adverse effects of Laponite were manifest in the form of local inflammation, or systemic toxicity. This finding concurs with the *in vitro* and *in vivo* work performed in chapters 3 and 4 respectively, and is supported by published literature (dawson ? gahawar).

No significant differences between the groups: allograft, blank, autograft, allograft/BMP/Alginate and allograft/BMP/Laponite in bone volume or bone volume per tissue volume were observed within the enclosed defect. Allograft alone and the blank defect mediated the greatest and least bone formation respectively. Inspection of the 3D reconstructions revealed healing in all groups and this is reflected quantitatively in bone volume per tissue volume analysis which demonstrated 30-40% in all groups including the blank control. Direct comparison of this result with published work is challenging due to multiple permutations of defect model, breed of sheep, endpoint and study duration (Malhotra et al., 2014, Nuss et al., 2006, Berner et al., 2013, Cipitria et al., 2013, Donati et al., 2008). Some ovine studies seem comparable to this study on the basis of defect dimensions and endpoints, however, results of defects performed in the tibia and femur are presented collectively (van der Pol et al., 2010, Liu et al., 2013, Malhotra et al., 2014). Thus limiting the value of such a comparison. Malhotra (Malhotra et al., 2014), investigated healing of blank defects 8, 11, and 14mm in diameter, and 25mm depth in femur, and tibia, of aged and young sheep. The defects most comparable to the current study, 8mm x 25mm, showed BV/TV of 26% at 1 month. Van der Pol (van der Pol et al., 2010) and Liu (Liu et al., 2013) reported BV/TV of blank femoral cancellous defects of 5 x15mm at 2 months and 8 x13mm at 1 month respectively, finding 6.1% and 1% BV/TV respectively. It would appear that the considerable variation in study methodology of cancellous ovine models is reflected in the range of results described. While accepting differences between the study by Malhotra (Malhotra et al., 2014) and the current study, in terms of pooling tibial and femoral data, an earlier time point, deeper defect, and different breed of sheep, results from (Malhotra et al., 2014) are broadly comparable with this study.

It is possible that were our analysis performed at an earlier time point a significant difference in bone formation may have been present between our experimental groups. However, the ten week duration of this study was based on results from (van der Pol et al., 2010). As our micro CT scanner cannot accommodate living sheep, investigation of an additional earlier timepoint would have necessitated the use of more sheep, for which we did not have ethical approval.

Given the large amount of bone formation within the enclosed defect in the control group (30-40%) the inability to distinguish to a statistical degree of certainty, an effect between the different groups is unsurprising. As would be expected from bone formation via creeping substitution (Nuss et al., 2006), bone formation was observed on micro CT at the edges and base of the defects, with the central area appearing to demonstrate the least amount of bone. The methodology of subdividing bone into various regions for micro CT analysis has been utilised in a previous peer-reviewed ovine work (Cipitria et al., 2013). On this basis the central, superior region, termed the mini-cylinder was analysed, and bone volume formed by the allograft alone was determined to be significantly greater than the blank defect control. No significant difference in bone volume was observed between Autograft, allograft/BMP/Laponite and allograft/BMP/alginate, and the blank and allograft controls. This result remained consistent when BV/TV was normalised to BV/TV of inner standard region or outer standard region. Superiority of allograft compared to the blank defect was further validated by morphometric analysis in which allograft demonstrated significantly greater thickness in trabecular thickness than the blank control.

In contrast to our findings, autograft would in general terms be expected to mediate greater bone volume than allograft (Kurien et al., 2013a), and this effect has been observed in ovine cancellous defect work (Liu et al., 2013) A number of factors may have resulted in allograft mediating greater bone formation compared to autograft in the current study:

1) Only 2 autograft samples were performed and these two samples may not be truly representative. Additional autograph samples are planned to be performed in the future to address this issue.

2) The volume of autograft material was not measured prior to implantation, as no further material was available, and sterility was required. Hence it is possible the autograft samples received less bone than the allograft group.

3) While autograft has been shown to be more effective than allograft, in some ovine studies (Liu et al., 2013, Leniz et al., 2004) the differential effect between autograft and allograft with sheep is not as apparent as that observed in humans. This maybe due to the lack of a immunogenic inflammatory reaction in the sheep in response to allograft.

4) Despite the multiple washes of allograft material with hydrogen peroxide it is likely that osteogenic proteins remained viable and present within allograft material.

In this study application of BMP in Alginate or Laponite hydrogel to the allograft material resulted in a non-significant reduction of BV/TV within the mini-cylinder compared to allograft alone. Given that BMP has been applied to allograft in clinical practice to enhance bone formation (Murena et al., 2014) the observed reduction in bone formation with BMP observed here is not clear, or conclusive. It is possible that the dose of BMP employed in this study was sub-therapeutic. While lower doses of BMP were observed to stimulate ectopic bone formation in the second murine study in chapter 4, interaction of Laponite with the collagen sponge in that case may have been pivotal to results observed. Similarly, in the first murine study, in which a dose similar to the ovine study was employed ($20\mu g/cm^3$), while allograft was used, the graft was in the form of a single scaffold, perfused with BMP laden Laponite gel, rather than multiple allograft granules mixed with Laponite/BMP gel.

As described in the introduction during the remodelling phase of bone healing net bone volume may actually decrease. In an ovine metatarsal model Donati (Donati et al., 2008) reported an increase in bone formation between months 2-4 with allograft treatment while application of BMP with allograft material mediated a reduction in bone volume during this time period. Remodelling stimulated by the presence of BMP was postulated to account for this, and this was supported by biomechanical testing and greater bone formation at earlier time points in the allograft and BMP group. In the current study it is conceivable that the lower volume of bone formed with allograft in presence of BMP & Alginate or BMP & Laponite may represent remodelling. If this is case, given the weight bearing location of the defect, and effect of 3 months of quadrupedal mobilisation by the sheep, increased remodelling may be anticipated to manifest in anisotropic analysis. A non-significant increase in anisotropy was observed with allograft/BMP/Laponite was seen. It is possible our experiment was not significantly powered to detect any difference in anisotropy with micro CT analysis, or alternatively no difference in internal architecture may exist. Graphically a clear reduction in degrees of anisotropy is observed in the mini-cylinder compared to the inner standardisation region, which is consistent with the *in vivo* model. Literature searches of PubMed and google scholar fail to reveal descriptive statistics of structural indices of bone healing within a healing ovine cancellous bone defect. Interestingly, Degrees of Anisotropy in the calcaneum and femoral head have been reported to be virtually identical 1.74 and 173, respectively. Given the description of anisotropy of the entire defect region, by a single number, and lack of comparative data, any numerical statistical significance could not be viewed as biologically significant in the absence of additional quantitative and qualitative data.

Micro CT scanning at an earlier time point could also have contributed useful information. However, aside from the morbidity and difficult of anaesthetising the sheep to perform additional scans the micro CT scanner is unable to accommodate them *in vivo*, and thus more sheep would have been required to investigate the outcome at earlier time points. Future histological analysis following decalcification should be capable of resolving this question. Similarly, biomechanical investigation would provide information on the degree of remodelling present within the bone defect. Given the limited numbers of animals performed in this study, the fact that the power calculation was derived using BV/TV as the endpoint rather than anisotropy, and the difficulty of comparing biomechanical testing to an operated contralateral limb, there are insufficient samples with which to perform biomechanical analysis capable of sufficient statistical power to provide robust data.

To account for inter sheep variation, BV/TV in the mini-cylinder was standardised to the BV/TV of inner standard region and outer standard region. The inner standard region was selected as the region formed enclosed bone and no soft tissue or air (Figure 5-9). A potential disadvantage of this region is that, it may in some way be affect by formation and healing of the defect. Drilling of a defect with a fluted drill can result in displacement of bone material from the defect into the surrounding bone, which in this case would be the inner standardisation area. While the use of a hollow trephine device will have minimised the effect of bone movement into the adjacent area, the adjacent bone may still be affected by the defect. In particular, bone surrounding the defect would be subject to greater stress, and thus this would be anticipated to stimulate greater bone formation in this region. A disadvantage of the outer standardisation region is that some amounts of soft tissue rather than bone are likely to be included despite attempting to avoid this. Furthermore, to avoid inclusion of air or soft tissue in the region the lengths of the donut shaped varied. To accommodate for the limitations of both these standardisation regions BV/TV within the mini-cylinder was compared to both these regions. Nevertheless, throughout this process the findings, that allograft alone mediated greater bone formation than the blank defect, remained consistent.

Allograft mediated a significantly greater volume of bone within the mini-cylinder area analysed within the defect compared to the blank control. Furthermore, the results were consistent with published data, and bone morphometry, in particular trabecular thickness of bone formed in the mini cylinder correlated with these results. No significant difference in bone volume per tissue volume of the standardisation regions was identified between the sheep. On the basis of these results the ovine femoral defect employed in this study remains a valid technique.

Null Hypothesis

The use of Laponite to deliver BMP will not result in greater bone defect healing by allograft compared to BMP applied to allograft material with an alternative growth factor delivery vehicle or use of allograft alone.

5.6   Conclusion

Allograft alone resulted in greater bone formation within the ovine defect model compared to the blank control, with no significant difference in bone formation observed with autograft or allograft with BMP delivered with alginate or Laponite.

On the assessment solely of the primary and secondary endpoints of bone volume formation and bone morphometry assessed using micro CT the Null hypothesis should be accepted. Use of Laponite to deliver BMP to allograft material did not result in greater bone formation. However, bone formation mediated by Laponite/BMP/Allograft material was equivalent to that mediated by Alginate/BMP/Allograft. Furthermore, in the absence of histological analysis it is possible that the reduced bone volume identified in the Laponite group may be a result of greater remodelling. Future studies to increase the number of autograft samples to facilitate adequate statistical power, and evaluation of collagen with Laponite and BMP would be of great interest. Sample decalcification, a process which requires several months has commenced, following which histological analysis will be performed.

Chapter 6:   Final Discussion

Every year in the UK over 2 million people suffer a broken bone (van Staa et al., 2001). Typically fractures heal, however incapacity during the healing process, which may last months, has a huge effect on patient morbidity, and a great economic impact both for the patient and society. At present, patients do not routinely receive any growth factor based therapy to accelerate fracture healing or increase likelihood of healing, due to the lack of effective delivery mechanisms (Garrison et al., 2007). The economic argument is even stronger in the case of high energy fractures, in which 40% may fail to unite following initial treatment (Lack et al., 2014). Annually 2.2 million people worldwide receive some form of bone graft. Synthetic graft products offer the potential to avoid limitations associated with autograft and allograft use, however, at present synthetic materials lack sufficient osteoinduction (Fischer et al., 2013). Laponite offers the potential to mediate effective delivery of BMP to accelerate fracture healing and enhance the osteoinductivity of synthetic graft material.

Laponite was observed to be cyto-compatible with HBMSC, mouse myoblast cells, and HUVEC cells. Furthermore, no adverse or inflammatory reactions were observed following subcutaneous implantation in nude mice, MF-1 mice, or orthotopic implantation in sheep. Collectively these results, in combination with other published investigations (Gaharwar et al., 2011a, Gaharwar et al., 2011b, Dawson et al., 2011, Wang et al., 2012) provide evidence for the biocompatibility of Laponite. Whilst these results are encouraging, Lithium and Silicate nanoparticles will remain *in vivo* following application, and the long term effect of these is unknown. The potential effect of metallic particles is of particular concern within the orthopaedic community, following the morbidity associated with Colbalt and Chromium ions and their associated alloys through stimulation of an immune based reaction (Langton et al., 2011). Lithium, in contrast to Nickel, Colbalt and Chromium, is not known as a metal sensitizer (Hallab et al., 2001), and is distinct from known metal sensitizers in terms of molecular weight, electric charge and periodic group. While these material properties, and the results presented in this thesis are encouraging, in terms of biocompatibility, long term biocompatibility of Laponite can only be proved following analysis after long term human implantation.

Dry Laponite films were shown to be capable of localising exogenously applied BMP, and to enhance the response to incubated BMP in myoblast cell assays (figure 3-13). In isolation, it is not possible to differentiate if the latter results from a reduced rate of BMP degradation mediated by the Laponite, or solely an effect on BMP localisation. Activity of VEGF determined by HUVEC assay, was shown to decrease when VEGF was mixed within Laponite hydrogel, compared to exogenous application of VEGF on the surface of the Laponite gel (figure 3-8). Similarly, in isolation, the reduced response seen with endogenous VEGF, could result from an effect on VEGF degradation, or localisation of VEGF within the gel, thus reducing the quantity available on the gel

surface to stimulate microtubule formation. Conversely, dry Laponite films were not shown to enhance bone formation mediated by BMP exogenously applied to allograft *in vivo*, whereas, Laponite hydrogel was observed to increase the response to exogenous and endogenous BMP (figure 4-6) *in vivo*. Collective interpretation of these results requires the appreciation that osteoblast cells require a relatively rigid culture surface, not afforded by hydrogels, while microtubule formation is only possible on gels, furthermore, *in vitro* and *in vivo* observations are not directly equivalent. It is postulated that the effects observed by Laponite films and hydrogels *in vitro*, result from growth factor binding and localisation rather than an effect on GF degradation. Similarly, superiority of Laponite hydrogel, as opposed to a dry film in the murine study, is postulated to result from binding of BMP within the gel, BMP becomes available to osteoblasts only as the gel breaks down due to mechanical forces and fluid flows exerted within the *in vivo* environment.

In this thesis Laponite has been shown be capable of localising the effect of BMP. Of the multitude of potential binding mechanisms possessed by Laponite described (1.11), the exact nature of the BMP/Laponite interaction remains unknown. Previous studies have shown Laponite to be capable of adsorbing albumin and Lysozyme, which differ in molecular weight and isoelectric point (Dawson et al., 2011) and localising VEGF (Dawson et al., 2011). Therefore, it is likely that the interaction of Laponite with these proteins is non-specific in nature, thus potentially rendering Laponite capable of delivering a range of growth factors in other tissue regeneration strategies.

The second subcutaneous murine experiment demonstrated the ability of Laponite hydrogel to reduce the dose of BMP required to stimulate ectopic bone formation within collagen sponge (4-23). While this result offers evidence for the efficacy of Laponite hydrogel as a growth factor delivery vehicle, various experimental limitations must be considered in order to realistically evaluate the implications. Such limitations include the small volume of sponge within which bone formation was evaluated, at around 50μl, which is at least tenfold smaller than a clinically relevant volume. In the absence of an active perfusion system, such as a functional vascular system, cell migration and diffusion of nutrients is proportional to the surface and volume ratio, thus 50μl of collagen sponge may not be representative of the clinical scenario. Furthermore, Laponite and Alginate were adsorbed in significantly different volumes by collagen (Figure 4-21), expression of bone formation per unit BMP does not entirely mitigate this discrepancy as volume of hydrogel could itself have an effect. Differential gel adsorption by the collagen is dependent upon the relative viscosity of Alginate and Laponite, both of which are temperature dependent, and in the case of Laponite shear dependent (thixotropic). Thus, in all likelihood, it would not be possible to obtain equal Laponite and Alginate adsorption even with experimental repetition and

alteration of gel concentrations, which themselves could affect osmolality and therefore cellular response.

The ovine femoral defect model employed in chapter 5 is comparable to models published in peer reviewed journals (Malhotra et al., 2014, Nuss et al., 2006), and demonstrated statistically significant difference in volume of bone within the defect between blank defects and those filled with allograft. Bone formation mediated by allograft and Laponite/BMP or Alginate/BMP was in-between that mediated by allograft alone and blank defects. Paradoxically, volume of bone formed is not equivalent to degree of healing. As illustrated in Figure 1-9, the final stage of secondary fracture healing, the process by which the ovine femoral defect heals, is remodelling, which actually involves a decrease in bone volume. Given the inability to demonstrate a statistically significant difference with morphometric analysis of the micro CT data, firm conclusions may only be drawn from this study following histological analysis.

The current study applied Laponite in conjunction with allograft. Allograft has limitations and thus future approaches may be explored such as application of Laponite/BMP to synthetic material derived from Additive Manufacture. Theoretically, AM offers the potential to produce bone graft material of superior biomechanical properties compared to conventional material processing as it permits greater control of topography, porosity, filament size, and internal architecture (Gibbs et al., 2014b). Paradoxically, the potentially infinite number of biomaterial patterns and material combinations is strictly limited according to the form of AM processing (Table 1-2). During the initial studies evaluating extrusion free forming (figure 6-2) attempts at blending pure hydroxyapatite with a polymer (poly lactic acid). In the second form of AM investigated in this thesis, electro spraying, it was not possible to readily demonstrate the viability of cells encapsulated within Laponite, due to dye adsorption by the Laponite (figure 6-10). Due to these technical limitations, and the absence of published work utilising electro spraying in production of hard tissue, the experimental focus of this thesis was the development of Laponite as a growth factor delivery vehicle rather than use of AM to produce synthetic graft material.

In conclusion the *in vitro* and *in vivo* studies presented in this thesis demonstrate that Laponite offers great potential as a growth factor delivery vehicle, thus potentially accelerating fracture healing through delivery of BMP, and may enhance osteoinductivity of bone graft material.

Future directions

Laponite has been used in the cosmetic and pharmaceutical industry without reported adverse effects. Similarly, in these *in vivo* and *in vitro* studies Laponite has been shown to be

biocompatible. However, these studies are not sufficient to permit human clinical studies. Formal toxicity testing of Laponite in a facility accredited by the Medical and Healthcare products Regulatory Agency (MRHA) should be undertaken as soon as funding permits. This testing is mandatory prior to application to the MHRA and ethics committee for investigation of Laponite as an investigational medicinal product, the first step to use in clinical practice.

Development and assessment of Laponite in an animal model specific to fracture healing, rather than ectopic bone formation, or healing of a bone defect would be of great value. In particular, a study in which rate of fracture healing was the primary endpoint, rather than bone formation. A potential candidate model is a Lapine ulnar fracture model. I have been involved in developing such a model, and have applied to the Home Office for permission to undertake this experimental work. The fracture could be made with a bone saw irrigated with saline to avoid heat necrosis. Synostosis of the forearm in rabbits renders operative fixation unnecessary. Furthermore, the subcutaneous nature renders per cutaneous administration of a Laponite/BMP gel at 1-2 days following initial fracture feasible. This would mimic the potential application of Laponite/BMP in clinical practice in treatment of conservatively managed fractures. A further benefit of this model is that in addition to assessment of fracture healing with micro CT, rabbit forearms may be readily subjected to biomechanical analysis. Investigation and optimisation of an injectable Laponite/BMP preparation would facilitate clinical translation of this therapy, with potential application to millions of patients who annually suffer fractures which are managed conservatively without recourse to open surgery. If rate of healing of fractures could be increased by merely 10-15% this would have an enormous effect for patients and society.

Given the control AM processes permit on internal architecture of material, it is only a matter of time until this form of manufacturing produces synthetic bone products of greater efficacy to those currently derived from conventional processing. Laponite, as a potent, non toxic growth factor delivery vehicle would readily be combined with AM in the future to produce synthetic bone of efficacy approaching that of autologous bone graft.

As discussed earlier, the non specific nature of the interaction of Laponite and proteins enables potential delivery of a whole range of growth factors. Within Orthopaedic surgery, tendinopathy, a relatively common pathology, (Maffulli et al., 2003), in which hypo vascularity has been implicated in the pathophysiology (Maffulli et al., 2004) could be suitable for application of Laponite mediated VEGF delivery. Further afield, Laponite could be harnessed to delivery growth factors associated with angiogenesis for treatment in peripheral vascular disease, or delivery of neurotrophins to enhance recovery following peripheral nerve injury.

Whilst, Laponite offers great potential to enhance fracture healing in the medium term, and potentially a host of other therapies in the long term, key challenges remain to be overcome prior to clinical translation. Namely, optimisation growth factor dose, and timing of delivery. Critically, delivery and localisation of growth factors, such as VEGF, which is known to be pivotal in tumour growth, could result in adverse effects or death. Systematic, well planned and implemented trials will be required prior to widespread clinical application in order to prevent the trajectory of Laponite based therapies following Scott's parabola.

Appendices

Appendix A

Use of Laponite and AM to produce bone graft

6.1   Introduction

As outlined in the introduction (1.9), demand for bone graft has prompted development of synthetic graft materials to overcome the limitations of autograft use, namely limited availability and donor morbidity. Optimal bone graft characteristics depend upon the exact clinical application, however key properties include osteoconductivity, osteogenicity, osteoinductivity, porosity, rate of degradation and ability to avoid displacement form the target site (figure 6-1).
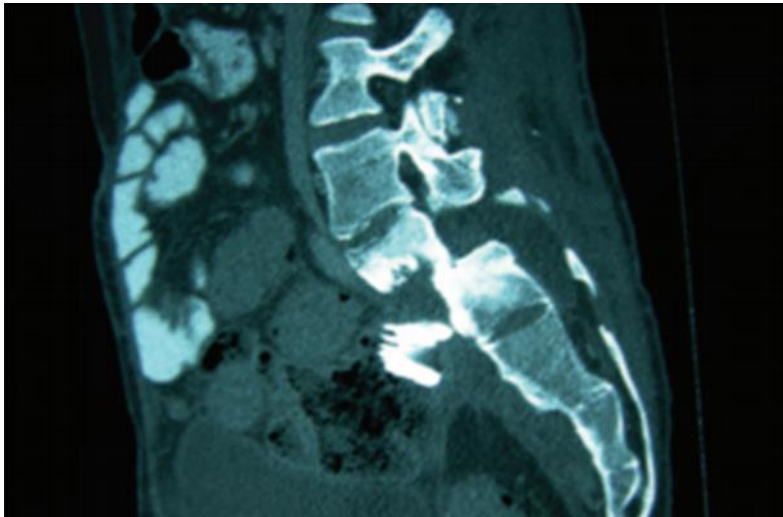
Figure 6-1 CT scan demonstrating a complication of graft migration

A rare but devastating complication of bone graft migration Atıl et al

Components of bone themselves, such as hydroxyapatite have frequently been used to produce synthetic graft bone, however, due to their relatively poor osteoinductive properties combination with additional osteoinductive materials has been recommended (Fischer et al., 2013). Additive Manufacture offers a distinct advantage current fabrication processes used to produce bone graft, in particular, internal architecture, porosity and filament size can be directly controlled. IS also permits control of graft topography offering the potential to produce graft material which could integrate with a fixation system thereby resisting graft migration as shown in figure 6-2.
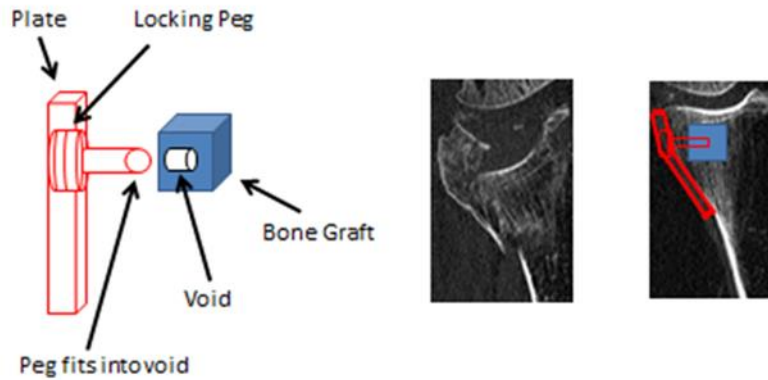
Figure 6-2 Integration of AM dervied graft material with a fracture fixation system

Extrusion free forming (Yang et al., 2006), a form of AM, involves the extrusion of material dissolved in a solvent, following deposition the solvent evaporates resulting in a transition from a liquid to a solid state (figure 6-3). Extrusion free forming permits control of porosity with resolutions less than 100μm, and has been used to produce rigid scaffolds derived from Hydroxyapatite (Yang et al., 2008a).

Electro spinning describes application of an electric field to accelerate particles towards a target, upon deposition a state transition from aerosol to solid takes place. Electro-spinning has been shown to be capable of producing fibres containing living cells with resolutions in the nanometre range (Gibbs et al., 2014b). A first step towards electro spinning is electro spraying, production of a jet of liquid material through application of an electrical field without transition to a solid state.

Extrusion free forming and electrospinning offer distinct advantages to production of bone graft material. Namely, extrusion free forming is known to be capable of producing rigid scaffolds with control of internal architecture, however processing is not compatible living cells or growth factors. Conversely, electro spinning, whilst highly compatible with living cells and growth factors, has not been shown to be capable of production of rigid scaffolds. These two AM processes, with their complementary advantages and limitations were therefore selected for investigation into the feasibility of combination with Laponite and BMP to produce synthetic bone graft material.

6.2   Aim

Explore the feasibility of Additive Manufacture alone and in combination with Laponite to produce synthetic bone graft material.

6.3   Null Hypothesis

It will not be possible to combine AM techniques with Laponite to produce synthetic bone graft material.

6.4   Objectives

1) Investigate the ability of extrusion free forming to produce bone graft material of optimal porosity, which is biocompatible with HBMSC, and capable of *in vivo* degradation.

2) Develop extrusion free forming to produce bone graft material capable of integrating with a fracture fixation system, thereby resisting graft migration.

3) Assess the effect of electro spraying on viability of HBMSC.

4) Assess the ability of electro spraying to facilitate deposition of HBMSC or growth factors encapsulated within Laponite.

6.5 Methods

6.5.1.1 Extrusion free forming

Extrusion free forming device was built by Mohammad Vaezi and Shoufeng Yang, Faculty of engineering, University of Southampton. The method of extrusion free forming has been described in great detail in previously (Yang et al., 2008b) and is summarised in figure 6-2. Hydroxyapatite powder, poly-vinylbutyral and polyethylene glycol were dissolved in propan-2-ol. Resulting paste was extruded, and solidified as the solvent evaporated. Resulting material was then sintered at 1300°C for 2 hours.
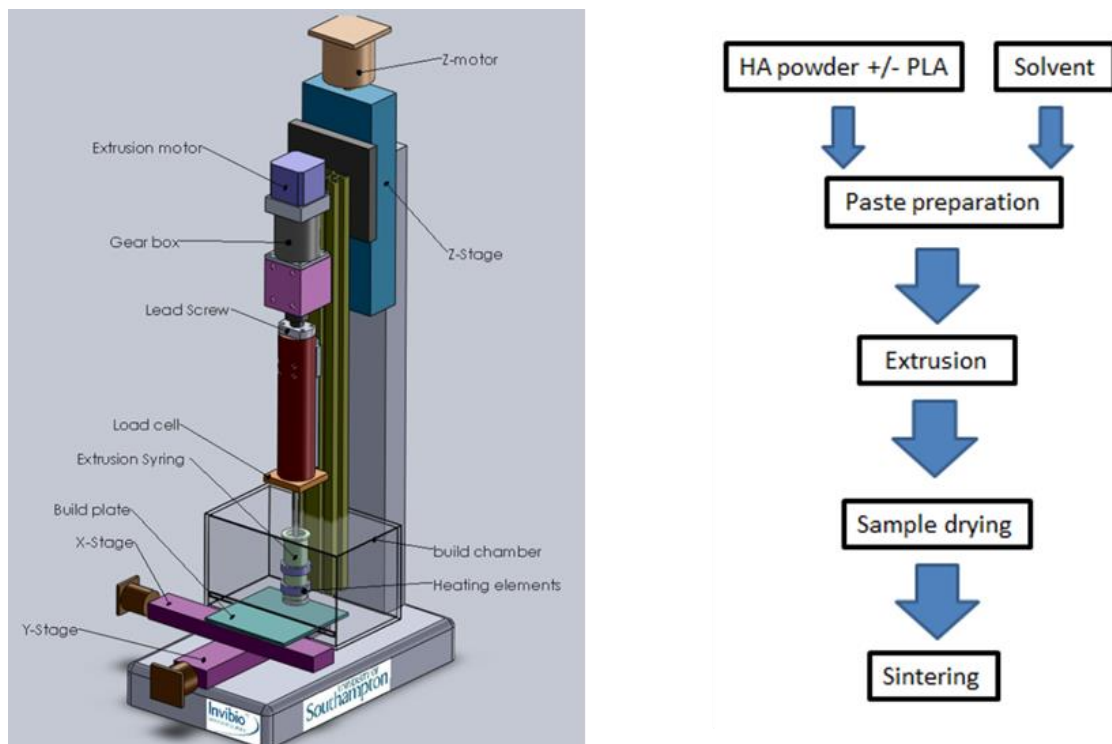
Figure 6-3 Diagram of extrusion free forming

Diagrammatic representation (Left) of the experimental apparatus used to produce the scaffolds (courtesy of Mohammad Vaezi), and Flow diagram (right) outlining the process of extrusion free forming. HA = hydroxyapatite, PLA = Polylactic Acid

6.5.1.1.1 Use of extrusion free forming to produce bone graft material biocompatible with HBMSC

Hydroxyapatite scaffolds produced using extrusion free forming were seeded with Unselected HBMSC. Following 7 days culture in basal conditions, staining with Cell Tracker Green and Ethidium Homodimer was performed to assess cell viability.

6.5.1.1.2 Use of extrusion free forming to produce bone graft of optimal porosity

Alterations in nozzle diameter, rate of extrusion, and platform motion were made by Mohammad Vaezi to ascertain if alteration in these parameters permitted consistent control of porosity and filament size of scaffold material.

6.5.1.1.3 Use of extrusion free forming to produce bone graft capable of integration with a fracture fixation system

To evaluate the feasibility of using extrusion free forming to produce graft material which would integrate directly with a fracture fixation system, graft material was produced with a central circular defect. A segment of a Chick femur was removed, and replaced with the graft material. Graft material was subsequently stabilised within the bone defect with an intra-medullary device, as shown in figure 6-4. Resulting construct was implanted subcutaneously in a nude mouse, at 4 weeks the mouse was culled and device imaged using micro CT.
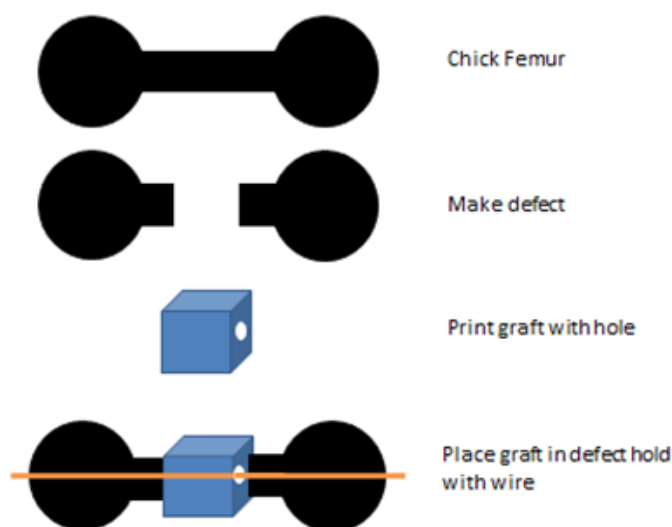
Figure 6-4 Diagrammatic representation of integration of bone with fracture fixation system

6.5.1.2   Electro-spraying

Electro spraying apparatus as depicted in Figure 6-5 was built by Suwan Jayasinge, Department of Mechanical Engineering, University College London. The methodology of electro spraying and electro spinning has been describe in detail (Townsend-Nicholson and Jayasinghe, 2006). Biomaterial was dispensed at 20ml/hour and subject to an electrical potential of 11kV.
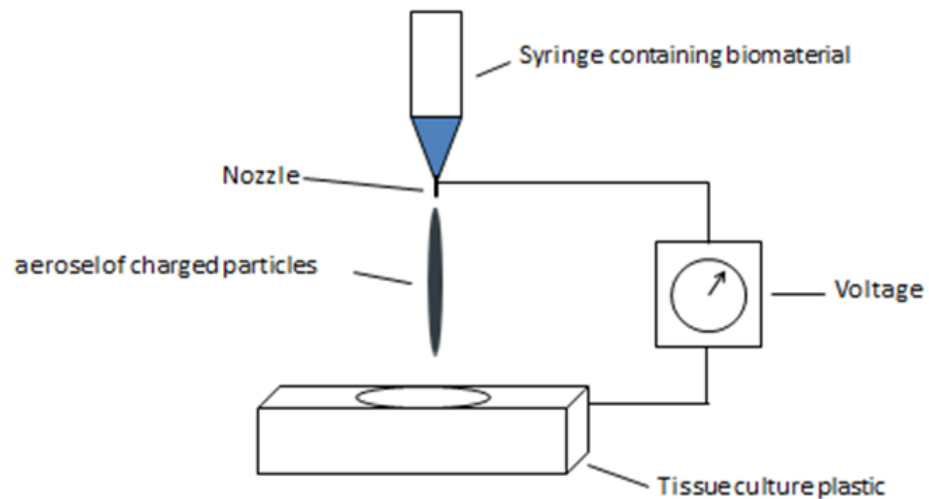
Figure 6-5 Diagrammatic representation of electro spraying

6.5.1.2.1   Effect of electro spraying on viability of HBMSC

Unselected Human bone marrow stromal cells were delivered onto TCP with electro spraying technique described above. Following 72 hours culture in basal conditions staining with Cell Tracker Green and Ethidium Homodimer was performed to assess cell viability.

6.5.1.2.2   Ability electro spraying to facilitate deposition of living cells or growth factors encapsulated within Laponite

Unselected Human bone marrow stromal cells were encapsulated in Laponite gel and delivered onto TCP with electro spraying technique described in 11. Following 72 hours culture in basal conditions staining with Cell Tracker Green and Ethidium Homodimer was performed to assess cell viability.

6.6   Results

Results are presented in two parts, firstly the results of the extrusion free forming experiments, and secondly, the results of the electro spraying experiments.

All extrusion free forming was performed by Mohammad Vaezi and Shoufeng Yang, at Faculty of Engineering, University of Southampton. I designed and performed the experiments to assess the scaffold material with HBMSC. I designed and performed the *in vivo* proof of concept study to assess the production of graft material which integrates with a fracture fixation system.

I designed the electro spraying experiments with Suwan Jayasinge. I produced the solutions of HBMSC cells in media and encapsulated in Laponite. Suwan Jayasinge performed the electro spraying of the cell solutions in my presence at the faculty of Engineering, University College London. I performed the subsequent cell culture and viability assays.

Bone graft material produced using extrusion free forming was biocompatible with HBMSC as demonstrated by the viability of HBMSC cultured on the surface of the graft material as shown in (figure 6-6). Extrusion free forming was shown to be capable of controlling porosity (figure 6-7), and producing graft material which was able to integrate with a fixation device (6-8).

Electro spraying was found to be compatible with HBMSC, as demonstrated by the viability assay performed following electro spraying (6-9). Viability assays performed on HBMSC encapsulated within Laponite were unable to demonstrate cell viability due to fluorescence of the Laponite itself (6-10).

6.6.1.1 Extrusion free forming

6.6.1.1.1 Use of extrusion free forming to produce bone graft compatible with HBMSC

Hydroxyapatite scaffolds produced using extrusion free forming were cytocompatible. Unselected Human bone marrow stromal cells were shown to be viable following culture on the graft material as shown in figure 6-6.
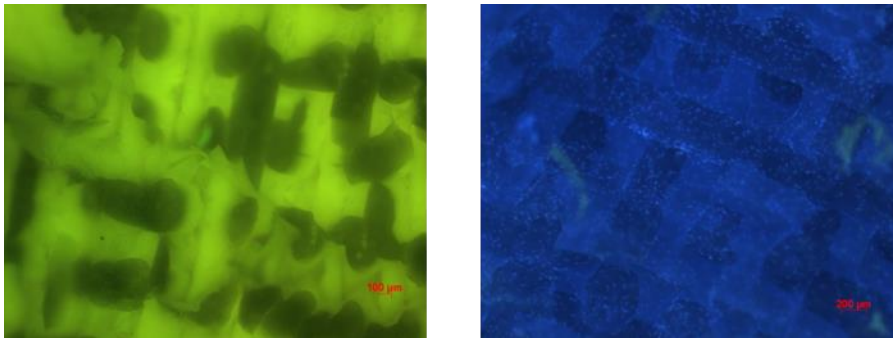
Figure 6-6 Viability of cells cultured on extruded graft material

Assessment of cells cultured on graft material was performed with use of Cell Tracker Green (left) and DAPI (right).

6.6.1.1.2 Use of extrusion free forming to produce bone graft of optimal porosity
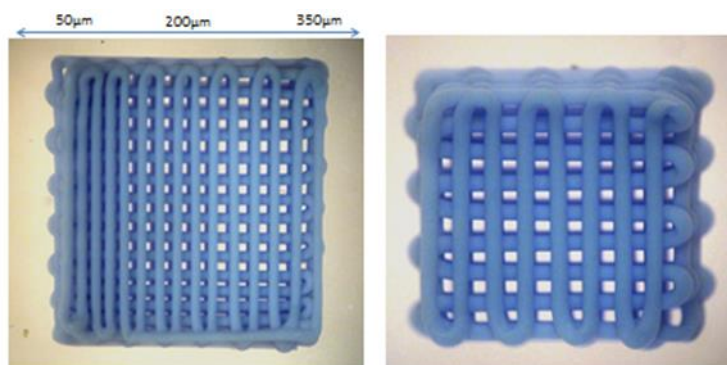
Figure 6-7 Porosity control with extrusion free forming

Photographs show graft material produced by extrusion free forming.
 Left: 1cmx1cm diameter, 3mm depth. Pore size: 50-350µm Right 300µm fixed pore size

6.6.1.1.3 Use of extrusion free forming to produce bone graft capable of integration with a fracture fixation system

Graft material held within the Chick femur defect through a customised void formed within the graft material remained in position following 28 days subcutaneous implantation in a mouse, as shown in figure 6-8.

Figure 6-8 Prototype graft material integrating with fracture fixation system

Photograph on the left is of the graft formed using extrusion free forming, with central defect shown, through with intra medullary fixation device was passed. Central photograph and 3D reconstruction of micro CT were taken following 28 days subcutaneous implantation in the mouse, and demonstrate the graft material did not migrate

6.6.1.2 Electro-spraying

6.6.1.2.1 Effect of electro spraying on viability of HBMSC

Electro spraying was not found to have an effect on viability of unselected Human Bone Marrow Stromal cells as shown in figure 6-9.
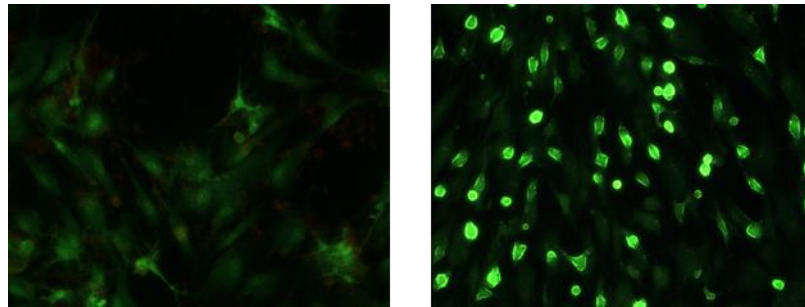
Figure 6-9 Effect of electro spaying on viability of HBMSC

6.6.1.2.2 Effect of electro spraying on viability of or growth factors encapsulated within Laponite

Due to the fluorescence of Laponite, it was not possible to demonstrate viability of HBSC following encapsulation with Laponite and electro spraying as shown in figure 6-10.
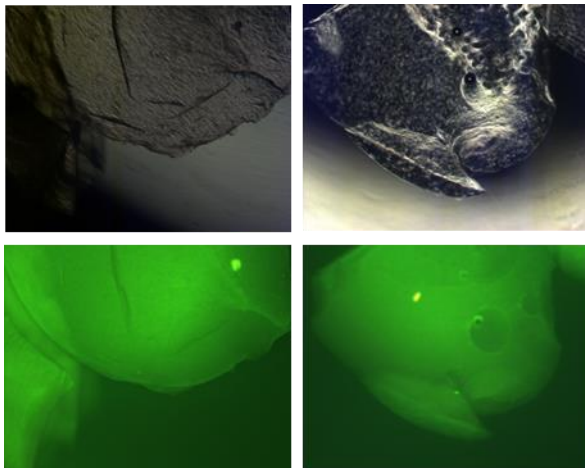
Figure 6-10 Effect of cell encapsulation within Laponite and electro spraying on cell viability

Images show cells encapsulated in Laponite viewed under light (upper) and fluorescent (lower) microscopy post 72 hours culture in basal conditions following encapsulation with Laponite and electro spraying.

6.7   Discussion

The results demonstrated that the hydroxyapatite scaffolds produced were cytocompatible, and furthermore, extrusion free forming was capable of controlling the porosity, and producing a void which could integrate with a fracture fixation system. Critically, the pure hydroxyapatite scaffolds derived by this process are highly crystalline, thus effectively non-absorbable, and brittle. These material properties render the graft unsuitable for application in bone regeneration.

Following cytocompatibility and initial proof of concept evaluation we sought to blend the hydroxyapatite powder with poly lactic acid, to produce a bio absorbable scaffold of superior bio mechanical properties. As described in the introduction, a key limitation of extrusion free forming is the requirement that the material processed can be adequately dissolved in a solvent which will subsequently evaporate. It was not possible to produce HA PLA blended scaffold material as the solvents capable of dissolving HA and PLA were highly volatile; consequently the variable evaporation resulted in gross inconsistency in scaffolds, rendering the scaffolds completely unsuitable for use as synthetic bone graft material. Given the inability to produce graft material of suitable biomechanical properties for bone regeneration, we did not explore the effect of Laponite and BMP on the extrusion free formed scaffolds.

The method of electro spraying was shown to be compatible with HBMSC, and this is consistent with previous published work (Townsend-Nicholson and Jayasinghe, 2006). It was not possible to demonstrate viability of cells encapsulated in Laponite following electro spraying using Cell Tracker Green as the Laponite adsorbs the dye. The electro spraying experiments required relatively large volumes of encapsulated cells in order to fill the tubing connecting the syringe and pump to the electro spraying nozzle. Furthermore as the electro spraying was performed in London, transportation of cells was also required. Further evaluation of cell viability could have been performed using alternative techniques, such as culture of Laponite encapsulated electro sprayed HBMSC in chondrogenic conditions, and staining to demonstrate formation of cartilage. Electro spraying is the initial step towards electro spinning, a process capable of producing solid scaffold material. While electro spinning has been applied to produce a range of soft tissues (Huang et al., 2003) this form of material processing is less well suited to production of hard tissue such as bone as it is dependent on liquid polymers which solidify at room temperature following dispersal from the nozzle. Given the technical challenges encountered during the initial experiments and the realisation that this form of AM is not optimal for production of hard tissue further experimental evaluation of electro spraying with Laponite was not pursued.

Despite the inability to develop AM to produce synthetic graft material of superior biomechanical properties to bone graft products in current use, it is highly likely that, such products will be developed and enter widespread clinical use in the near future. In-particular, development of scaffolds consisting of medical grade polycaprolactone and Tri calcium phosphate are very promising (Cipitria et al., 2015). The osteoinductivity of scaffolds such as this may be potentially enhanced with intra-operative delivery of Laponite gel laden with BMP. Indeed, "low tech" approaches in which graft material is perfused intra-operatively with growth factors or bone marrow aspirate have shown success in clinical studies (Fischer et al., 2013) and permit use of AM processes which are not compatible with living cells.

As additive manufacturing technologies develop rapidly the regulatory frame work appears to lag behind, and indeed this also presents a potential barrier to clinical translation. An interesting paradox is that current regulation of medical technologies and pharmaceutical products revolves around maintaining consistency of the products. Conversely, AM could result in production of patient and site specific bone graft, of which no two products are ever the same. Relatively small changes in material properties such as porosity or filament size could result in radicle changes in rate of biodegradation, and mechanical strength, which at weight bearing locations could have critical results in clinical practice.

Null Hypothesis

It will not be possible to combine AM techniques with Laponite to produce synthetic bone graft material.

6.8   Conclusion

Extrusion free forming was capable of producing bone graft material which was biocompatible, optimised porosity, and able to integrate with a fracture fixation system. However, it was not possible to optimise the biomechanical properties of the material, thus the study did not progress to combing extrusion free formed products with Laponite. Electro spraying was biocompatible with HBMSC, however it was not possible to the viability of HBMSC encapsulated in Laponite.

These experiments were unable to demonstrate the ability of AM techniques combined with Laponite to produce synthetic graft material, therefore the null hypothesis therefore the null hypothesis should be accepted.

Bibliography

Abbah, S. A., Lam, C. X. L., Hutmacher, D. W., Goh, J. C. H. & Wong, H.-K. (2009). Biological performance of a polycaprolactone-based scaffold used as fusion cage device in a large animal model of spinal reconstructive surgery. *Biomaterials,* 30**,** 5086-5093.

Alsousou, J., Thompson, M., Hulley, P., Noble, A. & Willett, K. (2009). The biology of platelet-rich plasma and its application in trauma and orthopaedic surgery: a review of the literature. *J Bone Joint Surg Br,* 91**,** 987-96.

Amosi, N., Zarzhitsky, S., Gilsohn, E., Salnikov, O., Monsonego-Ornan, E., Shahar, R. & Rapaport, H. (2012). Acidic peptide hydrogel scaffolds enhance calcium phosphate mineral turnover into bone tissue. *Acta Biomater,* 8**,** 2466-75.

Asamura, S., Mochizuki, Y., Yamamoto, M., Tabata, Y. & Isogai, N. (2010). Bone regeneration using a bone morphogenetic protein-2 saturated slow-release gelatin hydrogel sheet: evaluation in a canine orbital floor fracture model. *Ann Plast Surg,* 64**,** 496-502.

Axelrad, T., Steen, B., Lowenberg, D., Creevy, W. & Einhorn, T. (2008). Heterotopic ossification after the use of commercially available recombinant human bone morphogenetic proteins in four patients. *Journal of Bone & Joint Surgery, British Volume,* 90**,** 1617-1622.

Bae, H., Hatten Jr, H. P., Linovitz, R., Tahernia, A. D., Schaufele, M. K., McCollom, V., Gilula, L., Maurer, P., Benyamin, R. & Mathis, J. M. (2012). A prospective randomized FDA-IDE trial comparing Cortoss with PMMA for vertebroplasty: a comparative effectiveness research study with 24-month follow-up. *Spine,* 37**,** 544-550.

Bae, H., Shen, M., Maurer, P., Peppelman, W., Beutler, W., Linovitz, R., Westerlund, E., Peppers, T., Lieberman, I. & Kim, C. (2010). Clinical experience using Cortoss for treating vertebral compression fractures with vertebroplasty and kyphoplasty: twenty four-month follow-up. *Spine,* 35**,** E1030-E1036.

Barak, M. M., Lieberman, D. E. & Hublin, J.-J. (2011). A Wolff in sheep's clothing: trabecular bone adaptation in response to changes in joint loading orientation. *Bone,* 49**,** 1141-1151.

Ben-David, D., Srouji, S., Shapira-Schweitzer, K., Kossover, O., Ivanir, E., Kuhn, G., Müller, R., Seliktar, D. & Livne, E. (2013). Low dose BMP-2 treatment for bone repair using a PEGylated fibrinogen hydrogel matrix. *Biomaterials,* 34**,** 2902-2910.

Bergman, K., Engstrand, T., Hilborn, J., Ossipov, D., Piskounova, S. & Bowden, T. (2009). Injectable cell-free template for bone-tissue formation. *Journal of Biomedical Materials Research Part A,* 91A**,** 1111-1118.

Berner, A., Reichert, J., Woodruff, M. A., Saifzadeh, S., Morris, A., Epari, D., Nerlich, M., Schuetz, M. & Hutmacher, D. (2013). Autologous vs. allogenic mesenchymal progenitor cells for the reconstruction of critical sized segmental tibial bone defects in aged sheep. *Acta Biomaterialia,* 9**,** 7874-7884.

Betz, M. W., Caccamese, J. F., Coletti, D. P., Sauk, J. J. & Fisher, J. P. (2009). Tissue response and orbital floor regeneration using cyclic acetal hydrogels. *J Biomed Mater Res A,* 90**,** 819-29.

Bianco, P., Robey, P. G. & Simmons, P. J. (2008). Mesenchymal stem cells: revisiting history, concepts, and assays. *Cell stem cell,* 2**,** 313-319.

Blackburn, S. l. & Smyth, M. D. (2007). Hydrogel-induced cervicomedullary compression after posterior fossa decompression for Chiari malformation: case report. *Journal of Neurosurgery: Pediatrics,* 106**,** 302-304.

Boerckel, J. D., Kolambkar, Y. M., Dupont, K. M., Uhrig, B. A., Phelps, E. A., Stevens, H. Y., García, A. J. & Guldberg, R. E. (2011). Effects of protein dose and delivery system on BMP-mediated bone regeneration. *Biomaterials,* 32**,** 5241-5251.

Bohner, M. (2000). Calcium orthophosphates in medicine: from ceramics to calcium phosphate cements. *Injury,* 31**,** D37-D47.

Boyce, B. F. (2013). Advances in osteoclast biology reveal potential new drug targets and new roles for osteoclasts. *Journal of Bone and Mineral Research,* 28**,** 711-722.

Brown, W. E. & Chow, L. C. (1986). Combinations of sparingly soluble calcium phosphates in slurries and pastes as mineralizers and cements. Google Patents.

Bruker (2014). Manual for Bruker-microCT CT-Analyser v.1.13.

Buttermann, G. R. (2008). Prospective nonrandomized comparison of an allograft with bone morphogenic protein versus an iliac-crest autograft in anterior cervical discectomy and fusion. *The Spine Journal,* 8**,** 426-435.

Canalis, E., McCarthy, T. L. & Centrella, M. (1989). Effects of platelet-derived growth factor on bone formation in vitro. *Journal of cellular physiology,* 140**,** 530-537.

Caplan, A. I. (1991). Mesenchymal stem cells. *Journal of Orthopaedic Research,* 9**,** 641-650.

Cassidy, C., Jupiter, J. B., Cohen, M., Delli-Santi, M., Fennell, C., Leinberry, C., Husband, J., Ladd, A., Seitz, W. R. & Constanz, B. (2003). Norian SRS cement compared with conventional fixation in distal radial fracturesA randomized study. *The Journal of Bone & Joint Surgery,* 85**,** 2127-2137.

Chang, C.-W., van Spreeuwel, A., Zhang, C. & Varghese, S. (2010). PEG/clay nanocomposite hydrogel: a mechanically robust tissue engineering scaffold. *Soft Matter,* 6**,** 5157.

Chrastil, J., Low, J. B., Whang, P. G. & Patel, A. A. (2013). Complications associated with the use of the recombinant human bone morphogenetic proteins for posterior interbody fusions of the lumbar spine. *Spine,* 38**,** E1020-E1027.

Cipitria, A., Reichert, J. C., Epari, D. R., Saifzadeh, S., Berner, A., Schell, H., Mehta, M., Schuetz, M. A., Duda, G. N. & Hutmacher, D. W. (2013). Polycaprolactone scaffold and reduced rhBMP-7 dose for the regeneration of critical-sized defects in sheep tibiae. *Biomaterials,* 34**,** 9960-9968.

Cipitria, A., Wagermaier, W., Zaslansky, P., Schell, H., Reichert, J., Fratzl, P., Hutmacher, D. & Duda, G. (2015). BMP delivery complements the guiding effect of scaffold architecture without altering bone microstructure in critical-sized long bone defects: A multiscale analysis. *Acta Biomaterialia*.

Coelho, M. J. & Fernandes, M. H. (2000). Human bone cell cultures in biocompatibility testing. Part II: effect of ascorbic acid, β-glycerophosphate and dexamethasone on osteoblastic differentiation. *Biomaterials,* 21**,** 1095-1102.

D'Este, M. & Eglin, D. (2013). Hydrogels in calcium phosphate moldable and injectable bone substitutes: Sticky excipients or advanced 3-D carriers? *Acta Biomaterialia,* 9**,** 5421-5430.

Daculsi, G., Uzel, A. P., Weiss, P., Goyenvalle, E. & Aguado, E. (2010). Developments in injectable multiphasic biomaterials. The performance of microporous biphasic calcium phosphate granules and hydrogels. *J Mater Sci Mater Med,* 21**,** 855-61.

Damron, T. A., Lisle, J., Craig, T., Wade, M., Silbert, W. & Cohen, H. (2013). Ultraporous beta-tricalcium phosphate alone or combined with bone marrow aspirate for benign cavitary lesions: comparison in a prospective randomized clinical trial. *J Bone Joint Surg Am,* 95**,** 158-66.

Dawson, E., Bae, H. W., Burkus, J. K., Stambough, J. L. & Glassman, S. D. (2009). Recombinant Human Bone Morphogenetic Protein-2 on an Absorbable Collagen Sponge with an Osteoconductive Bulking Agent in Posterolateral Arthrodesis with InstrumentationA Prospective Randomized Trial. *The Journal of Bone & Joint Surgery,* 91**,** 1604-1613.

Dawson, J. I., Kanczler, J. M., Yang, X. B., Attard, G. S. & Oreffo, R. O. (2011). Clay gels for the delivery of regenerative microenvironments. *Adv Mater,* 23**,** 3304-8.

Dawson, J. I. & Oreffo, R. O. (2013). Clay: New opportunities for tissue regeneration and biomaterial design. *Advanced Materials,* 25**,** 4069-4086.

Day, T. F., Guo, X., Garrett-Beal, L. & Yang, Y. (2005). Wnt/beta-catenin signaling in mesenchymal progenitors controls osteoblast and chondrocyte differentiation during vertebrate skeletogenesis. *Dev Cell,* 8**,** 739-50.

Delloye, C., Cornu, O., Druez, V. & Barbier, O. (2007). Bone allografts: What they can offer and what they cannot. *J Bone Joint Surg Br,* 89**,** 574-9.

Ding, K., Yang, Z., Zhang, Y. L. & Xu, J. Z. (2013). Injectable thermosensitive chitosan/β-glycerophosphate/collagen hydrogel maintains the plasticity of skeletal muscle satellite cells and supports their in vivo viability. *Cell Biology International,* 37**,** 977-987.

Donati, D., Di Bella, C., Lucarelli, E., Dozza, B., Frisoni, T., Aldini, N. N. & Giardino, R. (2008). OP-1 application in bone allograft integration: preliminary results in sheep experimental surgery. *Injury,* 39**,** S65-S72.

Egol, K., Dolan, R. & Koval, K. (2000). Functional outcome of surgery for fractures of the ankle A PROSPECTIVE, RANDOMISED COMPARISON OF MANAGEMENT IN A CAST OR A FUNCTIONAL BRACE. *Journal of Bone & Joint Surgery, British Volume,* 82**,** 246-249.

Einhorn, T. A. (1998). The cell and molecular biology of fracture healing. *Clinical Orthopaedics and Related Research,* 355**,** S7-S21.

Even, J., Eskander, M. & Kang, J. (2012). Bone morphogenetic protein in spine surgery: current and future uses. *Journal of the American Academy of Orthopaedic Surgeons,* 20**,** 547-552.

Fedorovich, N. E., Schuurman, W., Wijnberg, H. M., Prins, H.-J., van Weeren, P. R., Malda, J., Alblas, J. & Dhert, W. J. (2011). Biofabrication of osteochondral tissue equivalents by printing topologically defined, cell-laden hydrogel scaffolds. *Tissue Engineering Part C: Methods,* 18**,** 33-44.

Fischer, C. R., Cassilly, R., Cantor, W., Edusei, E., Hammouri, Q. & Errico, T. (2013). A systematic review of comparative studies on bone graft alternatives for common spine fusion procedures. *European Spine Journal***,** 1-13.

Fujioka-Kobayashi, M., Ota, M. S., Shimoda, A., Nakahama, K., Akiyoshi, K., Miyamoto, Y. & Iseki, S. (2012). Cholesteryl group- and acryloyl group-bearing pullulan nanogel to deliver BMP2 and FGF18 for bone tissue engineering. *Biomaterials,* 33**,** 7613-20.

Gaharwar, A. K., Mihaila, S. M., Swami, A., Patel, A., Sant, S., Reis, R. L., Marques, A. P., Gomes, M. E. & Khademhosseini, A. (2013). Bioactive silicate nanoplatelets for osteogenic differentiation of human mesenchymal stem cells. *Adv Mater,* 25**,** 3329-36.

Gaharwar, A. K., Rivera, C. P., Wu, C. J. & Schmidt, G. (2011a). Transparent, elastomeric and tough hydrogels from poly(ethylene glycol) and silicate nanoparticles. *Acta Biomater,* 7**,** 4139-48.

Gaharwar, A. K., Schexnailder, P. J., Kline, B. P. & Schmidt, G. (2011b). Assessment of using laponite cross-linked poly(ethylene oxide) for controlled cell adhesion and mineralization. *Acta Biomater,* 7**,** 568-77.

Garrison, K. R., Donell, S., Ryder, J., Shemilt, I., Mugford, M., Harvey, I. & Song, F. (2007). Clinical effectiveness and cost-effectiveness of bone morphogenetic proteins in the non-healing of fractures and spinal fusion: a systematic review. *Health Technol Assess,* 11**,** 1-150.

Gibbs, D. M., Black, C. R., Dawson, J. I. & Oreffo, R. O. (2014a). A review of hydrogel use in fracture healing and bone regeneration. *Journal of tissue engineering and regenerative medicine*.

Gibbs, D. M. R., Vaezi, M., Yang, S. & Oreffo, Richard O. (2014b). Hope versus hype: what can additive manufacturing realistically offer trauma and orthopedic surgery? *Regenerative Medicine,* 9**,** 535-549.

Govender, S., Csimma, C., Genant, H. K., Valentin-Opran, A., Amit, Y., Arbel, R., Aro, H., Atar, D., Bishay, M. & Börner, M. G. (2002). Recombinant human bone morphogenetic protein-2 for treatment of open tibial fractures a prospective, controlled, randomized study of four hundred and fifty patients. *The Journal of Bone & Joint Surgery,* 84**,** 2123-2134.

Granero-Moltó, F., Weis, J. A., Miga, M. I., Landis, B., Myers, T. J., O'Rear, L., Longobardi, L., Jansen, E. D., Mortlock, D. P. & Spagnoli, A. (2009). Regenerative Effects of Transplanted Mesenchymal Stem Cells in Fracture Healing. *Stem Cells,* 27**,** 1887-1898.

Green, E., Lubahn, J. & Evans, J. (2004). Risk factors, treatment, and outcomes associated with nonunion of the midshaft humerus fracture. *Journal of surgical orthopaedic advances,* 14**,** 64-72.

Gronthos, S., Zannettino, A. C., Hay, S. J., Shi, S., Graves, S. E., Kortesidis, A. & Simmons, P. J. (2003). Molecular and cellular characterisation of highly purified stromal stem cells derived from human bone marrow. *Journal of Cell Science,* 116**,** 1827-1835.

Hagerman, M. E., Salamone, S. J., Herbst, R. W. & Payeur, A. L. (2002). Tris(2,2'-bipyridine)ruthenium(II) Cations as Photoprobes of Clay Tactoid Architecture within Hectorite and Laponite Films. *Chemistry of Materials,* 15**,** 443-450.

Hallab, N., Merritt, K. & Jacobs, J. J. (2001). Metal sensitivity in patients with orthopaedic implants. *JOURNAL OF BONE AND JOINT SURGERY-AMERICAN VOLUME-,* 83**,** 428-437.

Hoffman, M. D., Van Hove, A. H. & Benoit, D. S. (2014). Degradable hydrogels for spatiotemporal control of mesenchymal stem cells localized at decellularized bone allografts. *Acta biomaterialia*.

Hollinger, J. O., Hart, C. E., Hirsch, S. N., Lynch, S. & Friedlaender, G. E. (2008). Recombinant human platelet-derived growth factor: biology and clinical applications. *The Journal of Bone & Joint Surgery,* 90**,** 48-54.

Hooper, G. J., Keddell, R. G. & Penny, I. D. (1991). Conservative management or closed nailing for tibial shaft fractures. A randomised prospective trial. *Journal of Bone & Joint Surgery, British Volume,* 73**,** 83-85.

Huang, W., Yang, S., Shao, J. & Li, Y.-P. (2007). Signaling and transcriptional regulation in osteoblast commitment and differentiation. *Frontiers in bioscience: a journal and virtual library,* 12**,** 3068.

Huang, Z.-M., Zhang, Y.-Z., Kotaki, M. & Ramakrishna, S. (2003). A review on polymer nanofibers by electrospinning and their applications in nanocomposites. *Composites Science and Technology,* 63**,** 2223-2253.

Hulsart-Billstrom, G., Hu, Q., Bergman, K., Jonsson, K. B., Aberg, J., Tang, R., Larsson, S. & Hilborn, J. (2011). Calcium phosphates compounds in conjunction with hydrogel as carrier for BMP-2: a study on ectopic bone formation in rats. *Acta Biomater,* 7**,** 3042-9.

Hulsart-Billström, G., Hu, Q., Bergman, K., Jonsson, K. B., Åberg, J., Tang, R., Larsson, S. & Hilborn, J. (2011). Calcium phosphates compounds in conjunction with hydrogel as carrier for BMP-2: A study on ectopic bone formation in rats. *Acta Biomaterialia,* 7**,** 3042-3049.

Hynes, R. O. (2009). The Extracellular Matrix: Not Just Pretty Fibrils. *Science,* 326**,** 1216-1219.

Johal, H. S., Buckley, R. E., Le, I. L. & Leighton, R. K. (2009). A Prospective Randomized Controlled Trial of a Bioresorbable Calcium Phosphate Paste ([alpha]-BSM) in Treatment of Displaced Intra-Articular Calcaneal Fractures. *The Journal of Trauma and Acute Care Surgery,* 67**,** 875-882.

Johnson, E. E., Urist, M. R. & AM FINERMAN, G. (1988). Bone morphogenetic protein augmentation grafting of resistant femoral nonunions: a preliminary report. *Clinical Orthopaedics and Related Research,* 230**,** 257-265.

Kaderly, R. (Year) Published. Primary bone healing. Seminars in veterinary medicine and surgery (small animal), 1991. 21.

Katagiri, T., Yamaguchi, A., Komaki, M., Abe, E., Takahashi, N., Ikeda, T., Rosen, V., Wozney, J. M., Fujisawa-Sehara, A. & Suda, T. (1994). Bone morphogenetic protein-2 converts the differentiation pathway of C2C12 myoblasts into the osteoblast lineage. *The Journal of Cell Biology,* 127**,** 1755-1766.

Katayama, Y., Matsuyama, Y., Yoshihara, H., Sakai, Y., Nakamura, H., Imagama, S., Ito, Z., Wakao, N., Kamiya, M. & Yukawa, Y. (2009). Clinical and radiographic outcomes of posterolateral lumbar spine fusion in humans using recombinant human bone morphogenetic protein-2: an average five-year follow-up study. *International orthopaedics,* 33**,** 1061-1067.

Kawaguchi, H., Oka, H., Jingushi, S., Izumi, T., Fukunaga, M., Sato, K., Matsushita, T. & Nakamura, K. (2010). A local application of recombinant human fibroblast growth factor 2 for tibial shaft fractures: A randomized, placebo-controlled trial. *Journal of Bone and Mineral Research,* 25**,** 2735-2743.

Kim, R. Y., Oh, J. H., Lee, B. S., Seo, Y.-K., Hwang, S. J. & Kim, I. S. (2014). The effect of dose on rhBMP-2 signaling, delivered via collagen sponge, on osteoclast activation and in vivo bone resorption. *Biomaterials,* 35**,** 1869-1881.

Klimo Jr, P. & Peelle, M. W. (2009). Use of polyetheretherketone spacer and recombinant human bone morphogenetic protein-2 in the cervical spine: a radiographic analysis. *The Spine Journal,* 9**,** 959-966.

Kodama, N., Nagata, M., Tabata, Y., Ozeki, M., Ninomiya, T. & Takagi, R. (2009). A local bone anabolic effect of rhFGF2-impregnated gelatin hydrogel by promoting cell proliferation and coordinating osteoblastic differentiation. *Bone,* 44**,** 699-707.

Kurien, T., Pearson, R. & Scammell, B. (2013a). Bone graft substitutes currently available in orthopaedic practice The evidence for their use. *Bone & Joint Journal,* 95**,** 583-597.

Kurien, T., Pearson, R. G. & Scammell, B. E. (2013b). Bone graft substitutes currently available in orthopaedic practice: the evidence for their use. *Bone Joint J***,** 30286.

Lack, W. D., Starman, J. S., Seymour, R., Bosse, M., Karunakar, M., Sims, S. & Kellam, J. (2014). *Any Cortical Bridging Predicts Healing of Tibial Shaft Fractures*.

Langton, D. J., Joyce, T. J., Jameson, S. S., Lord, J., Van Orsouw, M., Holland, J. P., Nargol, A. V. & De Smet, K. A. (2011). Adverse reaction to metal debris following hip resurfacing: the influence of component type, orientation and volumetric wear. *J Bone Joint Surg Br,* 93**,** 164-71.

Lee, S. S., Hsu, E. L., Mendoza, M., Ghodasra, J., Nickoli, M. S., Ashtekar, A., Polavarapu, M., Babu, J., Riaz, R. M. & Nicolas, J. D. (2015). Gel Scaffolds of BMP-2-Binding Peptide Amphiphile Nanofibers for Spinal Arthrodesis. *Advanced healthcare materials,* 4**,** 131-141.

Leniz, P., Ripalda, P. & Forriol, F. (2004). The incorporation of different sorts of cancellous bone graft and the reaction of the host bone. A histomorphometric study in sheep. *International orthopaedics,* 28**,** 2-6.

Liang, Z.-w., Wang, Z., Chen, H., Li, C., Zhou, T., Yang, Z., Yang, X., Yang, Y., Gao, G. & Cai, W. (2014). *Nestin-Mediated Cytoskeleton Remodeling in Endothelial Cells: a Novel Mechanistic Insight into VEGF-Induced Cell Migration in Angiogenesis*.

Linsley, C., Wu, B. & Tawil, B. (2013). The effect of fibrinogen, collagen type I, and fibronectin on mesenchymal stem cell growth and differentiation into osteoblasts. *Tissue Eng Part A,* 19**,** 1416-23.

Lippens, E., Vertenten, G., Girones, J., Declercq, H., Saunders, J., Luyten, J., Duchateau, L., Schacht, E., Vlaminck, L., Gasthuys, F. & Cornelissen, M. (2010). Evaluation of bone regeneration with an injectable, in situ polymerizable Pluronic F127 hydrogel derivative combined with autologous mesenchymal stem cells in a goat tibia defect model. *Tissue Eng Part A,* 16**,** 617-27.

Liu, T., Wu, G., Wismeijer, D., Gu, Z. & Liu, Y. (2013). Deproteinized bovine bone functionalized with the slow delivery of BMP-2 for the repair of critical-sized bone defects in sheep. *Bone,* 56**,** 110-118.

Luca, L., Rougemont, A.-L., Walpoth, B. H., Gurny, R. & Jordan, O. (2010). The effects of carrier nature and pH on rhBMP-2-induced ectopic bone formation. *Journal of Controlled Release,* 147**,** 38-44.

Lutolf, M. P., Lauer-Fields, J. L., Schmoekel, H. G., Metters, A. T., Weber, F. E., Fields, G. B. & Hubbell, J. A. (2003). Synthetic matrix metalloproteinase-sensitive hydrogels for the conduction of tissue regeneration: engineering cell-invasion characteristics. *Proc Natl Acad Sci U S A,* 100**,** 5413-8.

Mackie, E., Ahmed, Y., Tatarczuch, L., Chen, K.-S. & Mirams, M. (2008). Endochondral ossification: how cartilage is converted into bone in the developing skeleton. *The international journal of biochemistry & cell biology,* 40**,** 46-62.

Maffulli, N., Sharma, P. & Luscombe, K. L. (2004). Achilles tendinopathy: aetiology and management. *Journal of the Royal Society of Medicine,* 97**,** 472-476.

Maffulli, N., Wong, J. & Almekinders, L. C. (2003). Types and epidemiology of tendinopathy. *Clinics in sports medicine,* 22**,** 675-692.

Malhotra, A., Pelletier, M. H., Yu, Y., Christou, C. & Walsh, W. R. (2014). A sheep model for cancellous bone healing. *Frontiers in surgery,* 1.

Marsell, R. & Einhorn, T. A. (2011). The biology of fracture healing. *Injury,* 42**,** 551-555.

Martinez-Sanz, E., Ossipov, D. A., Hilborn, J., Larsson, S., Jonsson, K. B. & Varghese, O. P. (2011). Bone reservoir: Injectable hyaluronic acid hydrogel for minimal invasive bone augmentation. *J Control Release,* 152**,** 232-40.

Matos, S., Guerra, F., Krauser, J. T., Figueiredo, H., Marcelino, J. P. & Sanz, M. (2012). Evaluation of an anorganic bovine-derived mineral with P-15 hydrogel bone graft: preliminary study in a rabbit cranial bone model. *Clin Oral Implants Res,* 23**,** 698-705.

Mattsson, J. P., Skyman, C., Palokangas, H., Väänänen, K. H. & Keeling, D. J. (1997). Characterization and Cellular Distribution of the Osteoclast Ruffled Membrane Vacuolar H+-ATPase B-Subunit Using Isoform-Specific Antibodies. *Journal of Bone and Mineral Research,* 12**,** 753-760.

McNamara, I., Deshpande, S. & Porteous, M. (2010). Impaction grafting of the acetabulum with a mixture of frozen, ground irradiated bone graft and porous synthetic bone substitute (Apapore 60). *Journal of Bone & Joint Surgery, British Volume,* 92**,** 617-623.

Medici, D., Shore, E. M., Lounev, V. Y., Kaplan, F. S., Kalluri, R. & Olsen, B. R. (2010). Conversion of vascular endothelial cells into multipotent stem-like cells. *Nat Med,* 16**,** 1400-1406.

Morgan, D. M. (1996). Isolation and culture of human umbilical vein endothelial cells. *Methods Mol Med,* 2**,** 101-9.

Murena, L., Canton, G., Vulcano, E., Surace, M. F. & Cherubino, P. (2014). Treatment of Humeral Shaft Aseptic Nonunions in Elderly Patients With Opposite Structural Allograft, BMP-7, and Mesenchymal Stem Cells. *Orthopedics,* 37**,** e201-e206.

Nunamaker, D. (1998). Experimental models of fracture repair. *Clinical Orthopaedics and Related Research,* 355**,** S56-S65.

Nuss, K. M., Auer, J. A., Boos, A. & Von Rechenberg, B. (2006). An animal model in sheep for biocompatibility testing of biomaterials in cancellous bones. *BMC Musculoskeletal Disorders,* 7**,** 67.

Oreffo, R. O., Driessens, F., Planell, J. A. & Triffitt, J. T. (1998). Growth and differentiation of human bone marrow osteoprogenitors on novel calcium phosphate cements. *Biomaterials,* 19**,** 1845-1854.

Oryan, A., Monazzah, S. & Bigham-Sadegh, A. (2015). Bone Injury and Fracture Healing Biology. *Biomedical and Environmental Sciences,* 28**,** 57-71.

Oshima, S., Yasunaga, Y., Yamasaki, T., Yoshida, T., Hori, J. & Ochi, M. (2012). Midterm results of Femoral impaction bone grafting with an allograft combined with hydroxyapatite in revision total hip arthroplasty. *The Journal of arthroplasty,* 27**,** 470-476.

Otsu, N. (1975). A threshold selection method from gray-level histograms. *Automatica,* 11**,** 23-27.

Parfitt, A. M., Drezner, M. K., Glorieux, F. H., Kanis, J. A., Malluche, H., Meunier, P. J., Ott, S. M. & Recker, R. R. (1987). Bone histomorphometry: standardization of nomenclature, symbols, and units: report of the ASBMR Histomorphometry Nomenclature Committee. *Journal of Bone and Mineral Research,* 2**,** 595-610.

Patterson, J., Siew, R., Herring, S. W., Lin, A. S., Guldberg, R. & Stayton, P. S. (2010). Hyaluronic acid hydrogels with controlled degradation properties for oriented bone regeneration. *Biomaterials,* 31**,** 6772-81.

Pelaez, M., Susin, C., Lee, J., Fiorini, T., Bisch, F. C., Dixon, D. R., McPherson, J. C., Buxton, A. N. & Wikesjö, U. M. (2014). Effect of rhBMP-2 dose on bone formation/maturation in a rat critical-size calvarial defect model. *Journal of clinical periodontology*.

Perut, F., Filardo, G., Mariani, E., Cenacchi, A., Pratelli, L., Devescovi, V., Kon, E., Marcacci, M., Facchini, A. & Baldini, N. (2013). Preparation method and growth factor content of platelet concentrate influence the osteogenic differentiation of bone marrow stromal cells. *Cytotherapy,* 15**,** 830-839.

Peters, C. L., Hines, J. L., Bachus, K. N., Craig, M. A. & Bloebaum, R. D. (2006). Biological effects of calcium sulfate as a bone graft substitute in ovine metaphyseal defects. *Journal of Biomedical Materials Research Part A,* 76**,** 456-462.

Pittenger, M. F., Mackay, A. M., Beck, S. C., Jaiswal, R. K., Douglas, R., Mosca, J. D., Moorman, M. A., Simonetti, D. W., Craig, S. & Marshak, D. R. (1999). Multilineage potential of adult human mesenchymal stem cells. *science,* 284**,** 143-147.

Polykandriotis, E., Popescu, L. & Horch, R. (2010). Regenerative medicine: then and now–an update of recent history into future possibilities. *Journal of Cellular and Molecular Medicine,* 14**,** 2350-2358.

Reichert, J. C., Cipitria, A., Epari, D. R., Saifzadeh, S., Krishnakanth, P., Berner, A., Woodruff, M. A., Schell, H., Mehta, M. & Schuetz, M. A. (2012). A tissue engineering solution for segmental defect regeneration in load-bearing long bones. *Science Translational Medicine,* 4**,** 141ra93-141ra93.

Rogers, G. F. & Greene, A. K. (2012). Autogenous Bone Graft: Basic Science and Clinical Implications. *Journal of Craniofacial Surgery,* 23**,** 323-327 10.1097/SCS.0b013e318241dcba.

Russell, T. A. & Leighton, R. K. (2008). Comparison of autogenous bone graft and endothermic calcium phosphate cement for defect augmentation in tibial plateau fracturesA multicenter, prospective, randomized study. *The Journal of Bone & Joint Surgery,* 90**,** 2057-2061.

Sacchetti, B., Funari, A., Michienzi, S., Di Cesare, S., Piersanti, S., Saggio, I., Tagliafico, E., Ferrari, S., Robey, P. G. & Riminucci, M. (2007). Self-renewing osteoprogenitors in bone marrow sinusoids can organize a hematopoietic microenvironment. *Cell,* 131**,** 324-336.

Sasaki, N., Minami, T., Yamada, K., Yamada, H., Inoue, Y., Kobayashi, M. & Tabata, Y. (2008). In vivo effects of intra-articular injection of gelatin hydrogen microspheres containing basic

fibroblast growth factor on experimentally induced defects in third metacarpal bones of horses. *Am J Vet Res,* 69**,** 1555-9.

Scott, J. (2001). Scott's parabola. *BMJ,* 323**,** 1477.

Settembre, C., Arteaga-Solis, E., McKee, M. D., de Pablo, R., Al Awqati, Q., Ballabio, A. & Karsenty, G. (2008). Proteoglycan desulfation determines the efficiency of chondrocyte autophagy and the extent of FGF signaling during endochondral ossification. *Genes & Development,* 22**,** 2645-2650.

Shapiro, F. (1988). Cortical bone repair. The relationship of the lacunar-canalicular system and intercellular gap junctions to the repair process. *The Journal of Bone & Joint Surgery,* 70**,** 1067-1081.

Shields, L. B., Raque, G. H., Glassman, S. D., Campbell, M., Vitaz, T., Harpring, J. & Shields, C. B. (2006). Adverse effects associated with high-dose recombinant human bone morphogenetic protein-2 use in anterior cervical spine fusion. *Spine,* 31**,** 542-547.

Simmons, P. & Torok-Storb, B. (1991). *Identification of stromal cell precursors in human bone marrow by a novel monoclonal antibody, STRO-1*.

Sroga, G. E., Karim, L., Colón, W. & Vashishth, D. (2011). Biochemical characterization of major bone-matrix proteins using nanoscale-size bone samples and proteomics methodology. *Molecular & Cellular Proteomics,* 10**,** M110. 006718.

Stucker, B. (Year) Published. Additive manufacturing technologies: technology introduction and business implications. Frontiers of Engineering: Reports on Leading-Edge Engineering from the 2011 Symposium, 2011. 5-14.

Takeuchi, Y., Kodama, Y. & Matsumoto, T. (1994). Bone matrix decorin binds transforming growth factor-beta and enhances its bioactivity. *Journal of Biological Chemistry,* 269**,** 32634-32638.

Thompson, D. W. & Butterworth, J. T. (1992). The nature of laponite and its aqueous dispersions. *Journal of Colloid and Interface Science,* 151**,** 236-243.

Thurner, P. J., Chen, C. G., Ionova-Martin, S., Sun, L., Harman, A., Porter, A., Ager Iii, J. W., Ritchie, R. O. & Alliston, T. (2010). Osteopontin deficiency increases bone fragility but preserves bone mass. *Bone,* 46**,** 1564-1573.

Townsend-Nicholson, A. & Jayasinghe, S. N. (2006). Cell electrospinning: a unique biotechnique for encapsulating living organisms for generating active biological microthreads/scaffolds. *Biomacromolecules,* 7**,** 3364-3369.

Tumialán, L. M., Pan, J., Rodts Jr, G. E. & Mummaneni, P. V. (2008). The safety and efficacy of anterior cervical discectomy and fusion with polyetheretherketone spacer and recombinant human bone morphogenetic protein–2: a review of 200 patients.

Uludag, H., D'Augusta, D., Palmer, R., Timony, G. & Wozney, J. (1999). Characterization of rhBMP-2 pharmacokinetics implanted with biomaterial carriers in the rat ectopic model. *Journal of Biomedical Materials Research,* 46**,** 193-202.

Uludag, H., Gao, T., Porter, T. J., Friess, W. & Wozney, J. M. (2001). *Delivery Systems for BMPs: Factors Contributing to Protein Retention at an Application Site*.

Urist, M., Nogami, H. & Mikulski, A. (1976). A bone morphogenetic polypeptide. *Calcified Tissues 1975.* Springer.

Urist, M. R. (1965). Bone: formation by autoinduction. *Science,* 150**,** 893-899.

van der Pol, U., Mathieu, L., Zeiter, S., Bourban, P.-E., Zambelli, P.-Y., Pearce, S. G., Bouré, L. & Pioletti, D. P. (2010). Augmentation of bone defect healing using a new biocomposite scaffold: an in vivo study in sheep. *Acta Biomaterialia,* 6**,** 3755-3762.

Van der Stok, J., Van Lieshout, E. M. M., El-Massoudi, Y., Van Kralingen, G. H. & Patka, P. (2011). Bone substitutes in the Netherlands – A systematic literature review. *Acta Biomaterialia,* 7**,** 739-750.

van Staa, T. P., Dennison, E. M., Leufkens, H. G. M. & Cooper, C. (2001). <Epidemiology of fractures in England and Wales.pdf>. *Bone,* 29**,** 517-522.

Veeman, M. T., Axelrod, J. D. & Moon, R. T. (2003). A second canon. Functions and mechanisms of beta-catenin-independent Wnt signaling. *Dev Cell,* 5**,** 367-77.

Wang, C., Wang, S., Li, K., Ju, Y., Li, J., Zhang, Y., Li, J., Liu, X., Shi, X. & Zhao, Q. (2014). Preparation of Laponite Bioceramics for Potential Bone Tissue Engineering Applications. *PloS one,* 9**,** e99585.

Wang, E. A., Rosen, V., D'Alessandro, J. S., Bauduy, M., Cordes, P., Harada, T., Israel, D. I., Hewick, R. M., Kerns, K. M. & LaPan, P. (1990). Recombinant human bone morphogenetic protein induces bone formation. *Proceedings of the National Academy of Sciences,* 87**,** 2220-2224.

Wang, S., Castro, R., An, X., Song, C., Luo, Y., Shen, M., Tomas, H., Zhu, M. & Shi, X. (2012). Electrospun laponite-doped poly(lactic-co-glycolic acid) nanofibers for osteogenic differentiation of human mesenchymal stem cells. *Journal of Materials Chemistry,* 22**,** 23357-23367.

Wang, T., Liu, D., Lian, C., Zheng, S., Liu, X., Wang, C. & Tong, Z. (2011). Rapid cell sheet detachment from alginate semi-interpenetrating nanocomposite hydrogels of PNIPAm and hectorite clay. *Reactive and Functional Polymers,* 71**,** 447-454.

Weiner, S. & Wagner, H. D. (1998). The material bone: structure-mechanical function relations. *Annual Review of Materials Science,* 28**,** 271-298.

Whitehouse, M. R., Dacombe, P. J., Webb, J. C. & Blom, A. W. (2013). Impaction grafting of the acetabulum with ceramic bone graft substitute: high survivorship in 43 patients with a mean follow-up period of 4 years. *Acta Orthop,* 84**,** 371-6.

Yamamoto, M., Ikada, Y. & Tabata, Y. (2001). Controlled release of growth factors based on biodegradation of gelatin hydrogel. *Journal of Biomaterials Science, Polymer Edition,* 12**,** 77-88.

Yamamoto, M., Takahashi, Y. & Tabata, Y. (2003). Controlled release by biodegradable hydrogels enhances the ectopic bone formation of bone morphogenetic protein. *Biomaterials,* 24**,** 4375-4383.

Yang, H., Thompson, I., Yang, S., Chi, X., Evans, J. & Cook, R. (2008a). Dissolution characteristics of extrusion freeformed hydroxyapatite–tricalcium phosphate scaffolds. *Journal of Materials Science: Materials in Medicine,* 19**,** 3345-3353.

Yang, H., Yang, S., Chi, X. & Evans, J. R. (2006). Fine ceramic lattices prepared by extrusion freeforming. *Journal of Biomedical Materials Research Part B: Applied Biomaterials,* 79**,** 116-121.

Yang, S., Yang, H., Chi, X., Evans, J. R., Thompson, I., Cook, R. J. & Robinson, P. (2008b). Rapid prototyping of ceramic lattices for hard tissue scaffolds. *Materials & Design,* 29**,** 1802-1809.

Yeom, J., Chang, S., Park, J. K., Je, J. H., Yang, D. J., Choi, S. K., Shin, H. I., Lee, S. J., Shim, J. H., Cho, D. W. & Hahn, S. K. (2010). Synchrotron X-ray bioimaging of bone regeneration by artificial bone substitute of MegaGen Synthetic Bone and hyaluronate hydrogels. *Tissue Eng Part C Methods,* 16**,** 1059-68.

Younger, E. M. & Chapman, M. W. (1989). Morbidity at bone graft donor sites. *J Orthop Trauma,* 3**,** 192-5.